Applied Optics

March
1962

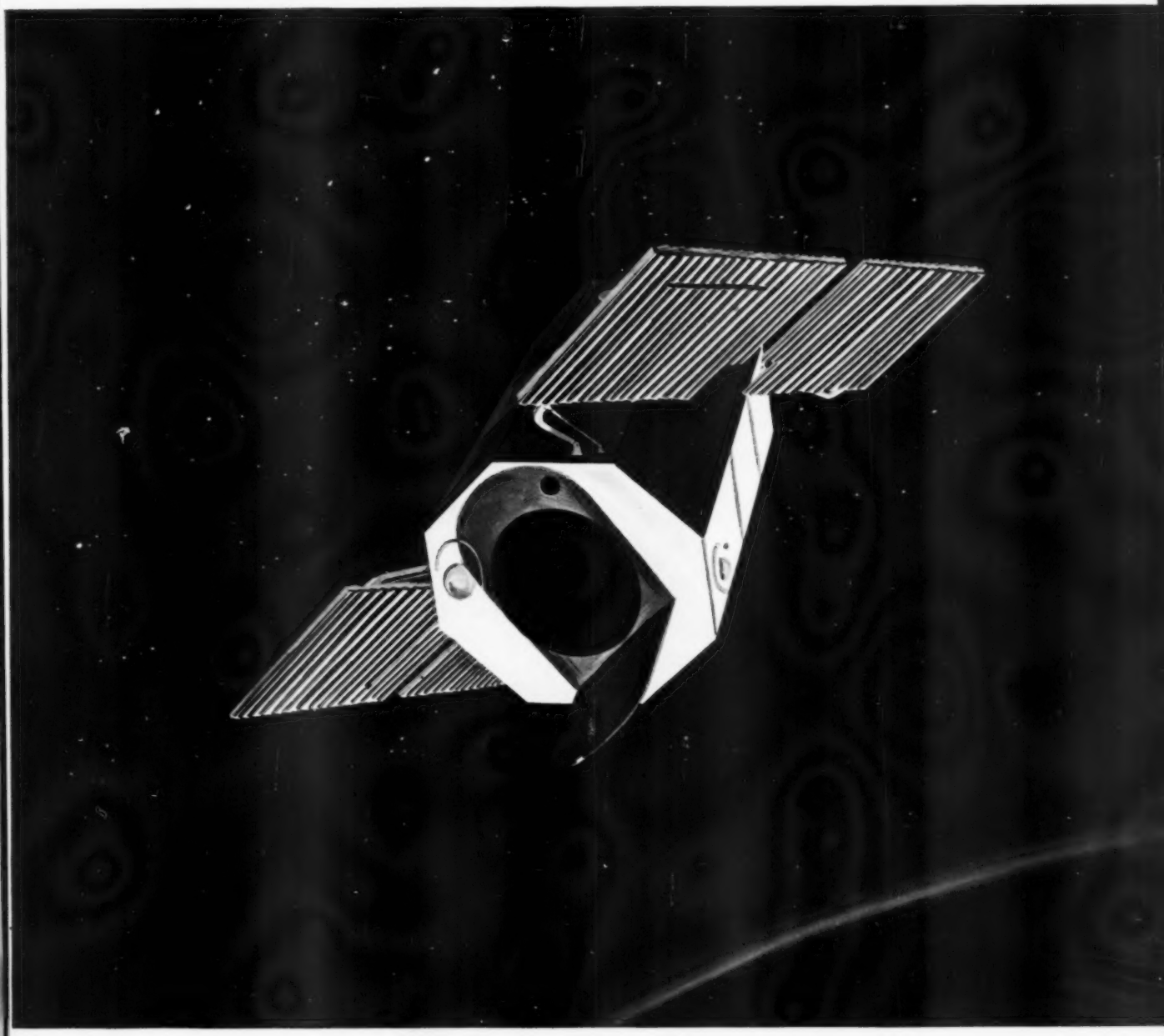

SPACE OPTICS

Effective Jan. 1, 1965. All back issues and single copies are sold at $3.00 per copy.

ENGINEERS

ELECTRO-OPTICAL SYSTEMS

explore your Future in

SATELLITE AND SPACE VEHICLE DEVELOPMENT

at RCA's new Space Center in Princeton, N. J.

Here is an opportunity to let your imagination soar with the team that created Tiros. Now at this rapidly growing division of RCA, a number of challenging opportunities are available for electronic engineers.

To qualify Supervisory Engineers must have 5 to 10 years experience . . . Engineers, 3 to 5 years experience in the following fields:

TELEVISION CAMERA DESIGN and EVALUATION
SOLID STATE CIRCUIT DESIGN EXPERIENCE
KNOWLEDGE OF ELECTRO-OPTICAL SYSTEMS and OPTICAL SYSTEMS

Work to be performed must conform to stringent operational and environmental specifications.

FOR A CONFIDENTIAL INTERVIEW call collect:

MR. D. D. BRODHEAD
609-448-3400 or write:

MR. D. D. BRODHEAD, DEPT. #PE-566
ASTRO-ELECTRONICS DIVISION
PRINCETON, NEW JERSEY

An Equal Opportunity Employer

The Most Trusted Name in Electronics

RADIO CORPORATION OF AMERICA

Applied Optics

VOLUME 1
NUMBER 2

March
1962

A bimonthly publication of the
Optical Society of America

John N. Howard, Editor

Lloyd G. Mundie, Feature Editor

Patricia R. Wakeling, Managing Editor

COVER: The NASA-Grumman OAO is a 1500 kg (3300 lb) optical satellite. Large-aperture photoelectric astronomical telescopes for ultraviolet spectrophotometry are carried in the central core. Solar sensors, star trackers, and a television camera are mounted in the basic spacecraft for use in attitude determination and control. Extended fixed solar cell paddles and a large sun shield for the main optics are prominent external features. The cover is reproduced in color thanks to the generosity of the Grumman Aircraft Engineering Corporation.

Published bimonthly by the Optical Society of America, Inc., in cooperation with the American Institute of Physics, at 20th and Northampton Streets, Easton, Pa. Editorial offices: 1155 16th St. N.W., Washington 6, D.C. Supported in part by a grant from the National Science Foundation. Advertising Office: 55 West 16th Street, New York 11, N.Y. A. P. Oppenheim–Chelsea 2-1311. Subscription rates: $6.00 to OSA members, $8.00 other AIP Societies' members; nonmembers and libraries: $10.00 per year. Single copies $2.00. Application to mail at second class postage rates is pending at Easton, Pa.

© Copyright 1962 by the Optical Society of America.

87 **The Radiation Environment of Interplanetary Space**—John H. Shaw

97 **Infrared Satellite Radiometry**—F. F. Hall, Jr. and C. V. Stanley

105 **Infrared Spectroscopy of Planets and Stars**—William M. Sinton

111 **The Elimination of Scattered Light in Solar Spectrographs**—J. W. Evans and J. Waddell

115 **Rocket Exhaust Radiation Measurements in the Upper Atmosphere**—N. W. Rosenberg, W. M. Hamilton, and D. J. Lovell

121 **Optical Measurements from High Altitude Balloons**—D. G. Murcray, J. N. Brooks, N. J. Sible, and H. C. Westdahl

129 **High Altitude Atmospheric Transmission Measurements**—F. Stauffer and J. Strong

131 **Ultraviolet Instrumentation for Celescope**—Robert J. Davis and Om P. Rustgi

139 **Optical Instrumentation for TIROS**—Marvin H. Harper, Jr.

147 **Inside-Out Horizon Scanner**—Joseph Killpatrick

155 **Optics in the Orbiting Astronomical Observatory**—H. B. Hallock

165 **Threshold and Stability of a Simplified Model Optical Maser**—E. J. Post

169 **Physical Optics of Coherent Radiation Systems**—J. E. Rosenthal

173 **High Efficiency Optical Maser Parameters**—Stanley J. Sage

DEPARTMENTS

179 **Letters to the Editor**

A More Complete Description for α/ϵ—Lucien M. Biberman

The Visibility of Flashbulbs and Their Application to Rocket Tracking—G. B. Spindler

A Continuously Operating Ruby Optical Maser—D. F. Nelson and W. S. Boyle

96 **Optical Activities in the Universities**

138 **Meetings Calendar**

154 **From the Editor**

164 **Books**

184 **Patents**

184 **Meeting Reports**

188 **Of Optics and Opticists**

Power Supplies, Light Pumps and Accessories

for OPTICAL MASER RESEARCH

From the beginning of Maser research, Electro Powerpacs, Inc. has supplied leading laboratories* with the essential equipment for their investigation of laser/maser technology. Because our engineers are in direct contact with this field, we are in a position to continually update equipment as the state of the art develops.

The Optical Maser Light Pump (Model 275) includes a basic power supply with voltages up to 5KV, capacitor banks and light pump. We can also provide Power Supplies with voltages up to 10KV and various accessories for mounting ruby or other types of material within the energy field of flash lamp sources. All of these units have been specially designed to provide the most practical and flexible research tools available.

Power Supply

The Power Supply, for example, provides continuously variable voltages up to 5,000 volts to operate Xenon or other types of gas-filled tubes as Light Pumps. It can be furnished with energy storage banks to 20,000 joules and its modular design and construction allows for the addition of energy storage banks as needed.

Trigger voltage capable of firing gas-filled tubes is contained within the Power Source, where Thyratron circuitry isolates workers from all contact with dangerous high voltages.

Capacitor Banks

Capacitor Banks are supplied from 1,000 to 20,000 watt seconds, in increments of 1,000 watt seconds. They are built for stacking and mount conveniently on wheeled dollies. Any bank of capacitors may be connected or disconnected as desired and each capacitor is separately fused so that if one fails, the capacitor bank in which it is located will continue to operate. An individual indicator light shows which capacitor fuse has blown. For worker safety, interlocks and built-in automatic discharge are included in Capacitor Banks and in the Power Supply.

To maintain the standards of reliability and performance which scientists look for in this type of research equipment, Electro Powerpacs units operate well below the full capabilities of their components. For example, the capacitors are designed for 6KV and operate at 5KV; transformers insulated for 20KV operate at 5KV; all high voltages are isolated from cases by insulation rated at 20KV.

Light Pumps

Light Pumps are designed to provide researchers with a convenient means for mounting various types of rod (ruby crystal or other material) 3mm to ⅝" in diameter and up to 6" long within the energy field. They can be used with either helical or straight arc flash tubes at a wide range of voltages, repetition rates and powers. Provision has been made for convenient interchange of rods of different size. For many types of laser crystals, airblast cooling is sufficient to maintain safe operating temperatures. Where liquid nitrogen temperatures are required in order to achieve cryogenic results, a liquid cooled mount is furnished. This mount provides airblast as well as cryogenic cooling to give the equipment maximum flexibility.

Ruby Crystals

Ruby Crystals and other materials used to achieve laser action can be supplied in rods of the sizes most commonly used, 3mm to ⅝" in diameter and up to 6" in length. Various end configurations and reflecting coatings are available.

Electro Powerpac engineers are well qualified to recommend the types of equipment required for laser/maser research and to develop necessary accessories and hardware for special projects.

*** Partial list of laboratories using Electro Powerpac equipment:**

American Optical Company
Bell Telephone Laboratories
General Telephone & Electronics
Lincoln Laboratory of M.I.T.
National Aeronautics & Space Adm.
Perkin-Elmer Corporation
Westinghouse Air Arm Division
International Bus. Machines
Radio Corporation of America
Avco Corporation
Harvard University
McMasters University
University of Dayton
University of Virginia

Requests for further information and detailed specifications invited

ELECTRO POWERPACS, INC.

A Subsidiary of Hydra-Power Corporation

5 HADLEY STREET, CAMBRIDGE 40, MASS.

POLAROID ®

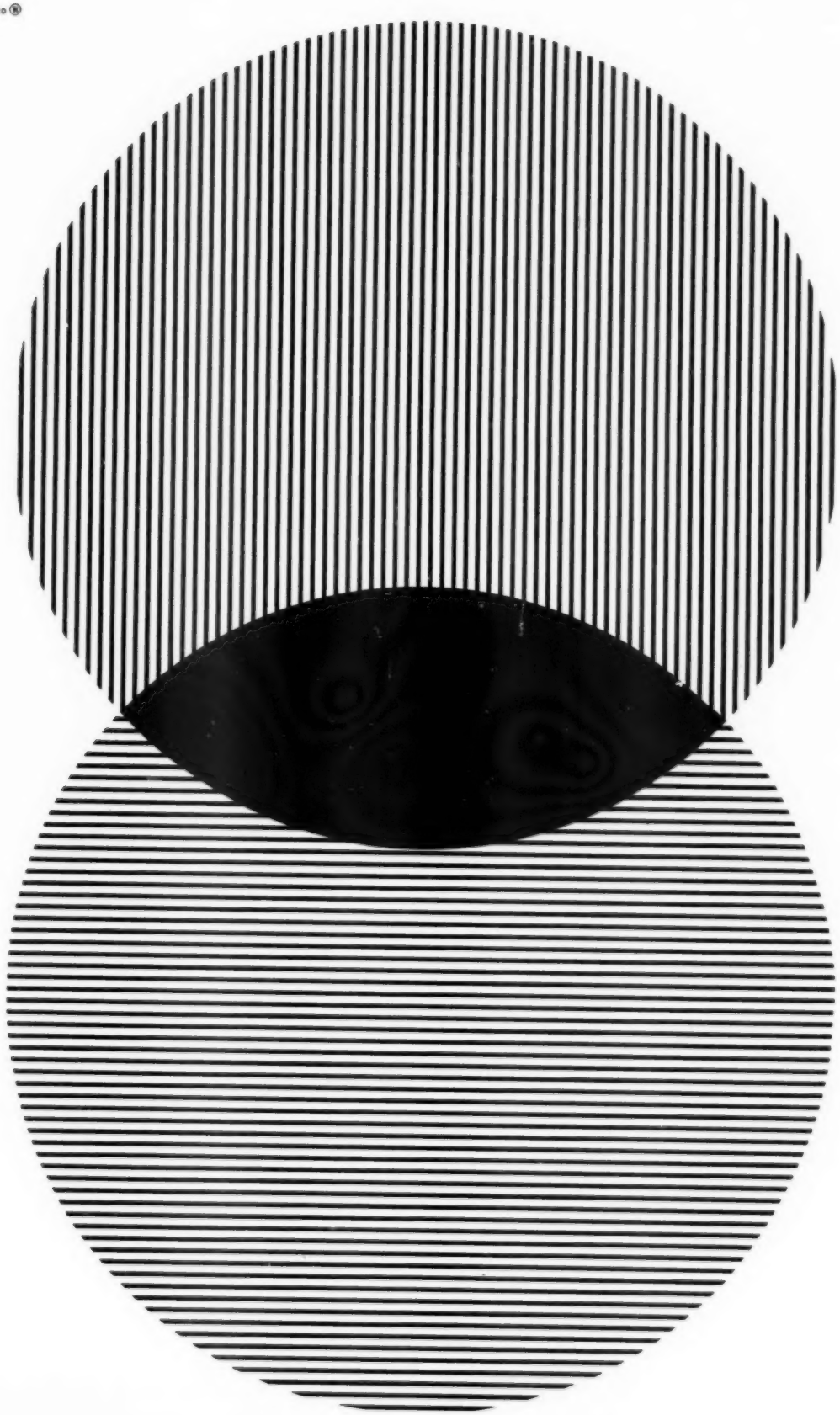

For information on polarizers for use in optical systems, write Polaroid Corporation, Cambridge 39, Massachusetts, attention: Polarizer Division.

TIFFEN OPTICAL FACILITIES FOR SCIENCE AND INDUSTRY

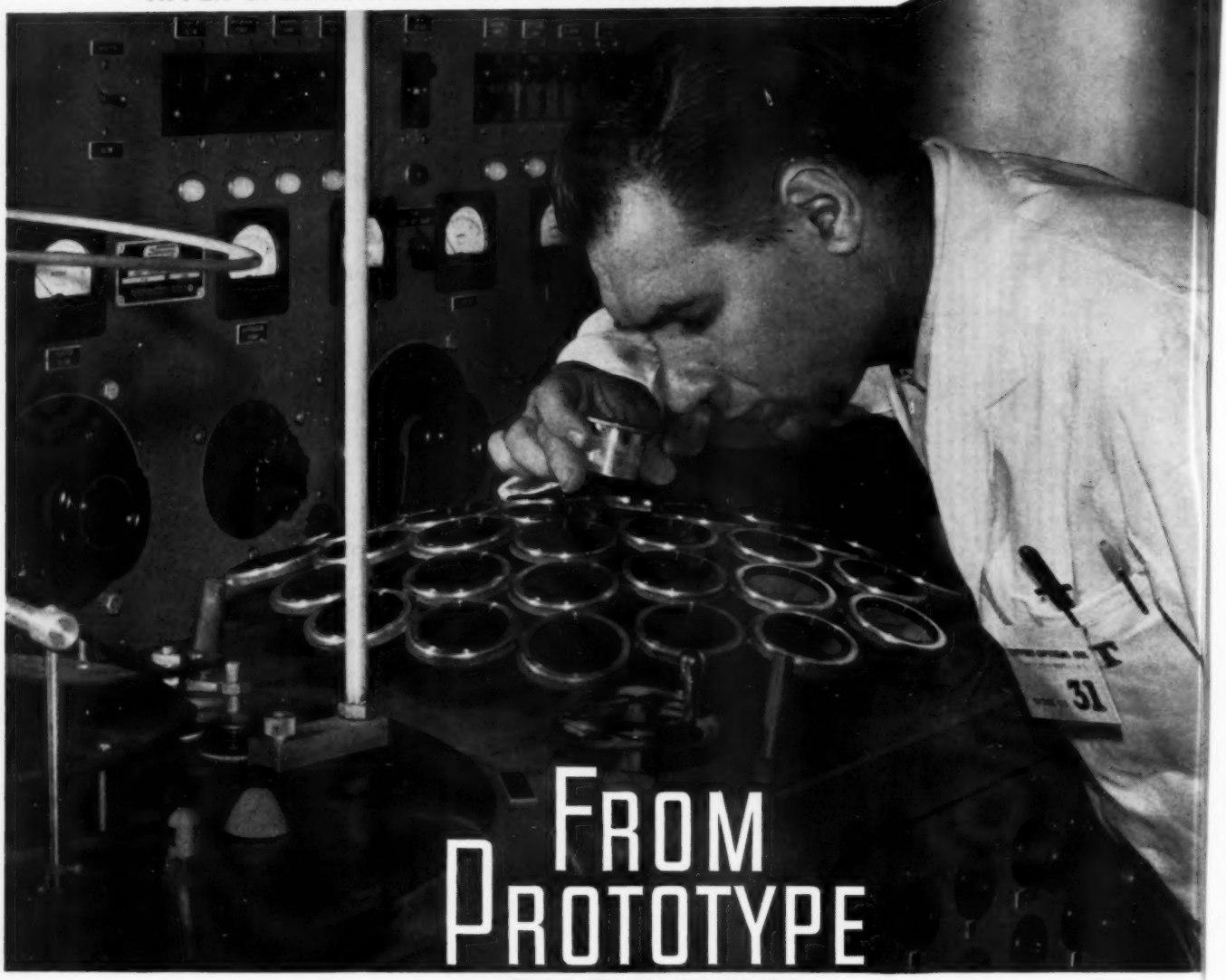

FROM PROTOTYPE THROUGH PRODUCTION

A unique integration of prototype and production facilities . . . that is TIFFEN! For over a decade, government agencies, leading industrial firms and photographic studios have turned to TIFFEN for precision photographic optical accessories.

Now, TIFFEN offers their specialized experience and greatly expanded facilities to all industry employing optics in their product. TIFFEN's major facilities are described below, and are constantly being augmented to conquer specialized problems.

BLANCHARDS ... flat grinding to .00005". Diamond grinding wheels for shaping to .0001" tolerances. Sizes to 18" dia. ***EDGING*** . . . glass and ceramics, to tolerances less than .001", up to 20" dia. Precision bevels and odd shapes ground. ***DRILLING*** . . . dia. from .010" to 12", concentric to within .0005", on glass, ceramics, silicon, germanium, etc. ***GRINDING & POLISHING*** . . . from subminiature optics 1mm dia. to mirrors 24" dia., to within 1/10 wavelength in flatness, less than 2 seconds of arc in parallel. Roof prisms to 2 seconds of accuracy. ***COATING*** . . . high vacuum deposition of all types of material. Hot and cold magnesium fluoride coating, partial coatings for beam splitters and metallic neutral density filters. Aluminizing, with silicon monoxide overcoat, for high reflection mirrors. A battery of 22" bell-jars, temperature and humidity controlled dept. ***COLOR LABORATORY*** . . . includes Densichron, Beckman Du Spectrophotometer, Weston Foot Lambert Meter, environmental test equipment, etc. ***FILTERS*** . . . laminated glass equal in environmental tests to solid glass, with superior color control. All colors and curves, .040 to 12" dia., thickness .025" to 1", resolution to 100 lines per mm. ***MACHINING*** . . . multi-spindle automatics to 4", secondary machines to 10" capacity. Thread cutting, Whitworth, English and metric, with single point tools. High precision lens barrels and metallic optical parts. ***TOOL ROOM*** . . . modern 23" swing lathes, grinders, millers. All tools and jigs manufactured internally.

Special problems? Write, call or visit: **TIFFEN OPTICAL CO.**, 86 Jane St., Roslyn Hgts., L. I., N. Y. West Coast Rep.: CRAIG CORP., 3410 So. La Cienega Blvd., Los Angeles 16, Cal.

TIFFEN DELIVERS THE GOODS!

LASER SPECIALISTS

In this modern day and age *Everyone* is a Specialist. Our experience with LASER CRYSTALS is perhaps greater than you can find anywhere in the world.

WE ARE LASER SINGLE CRYSTAL SPECIALISTS

Semi-Elements specializes in growing the largest varieties and sizes of LASER Crystals doped with rare earths and transitions elements.

*

Semi-Elements has most of the LASER Crystals of TOMORROW ready for shipment TODAY from STOCK in "As Grown" boules or finished laser rods. Single Crystal Chips are also available from stock at — $15.00 to $40.00 each.

*

Semi-Elements currently can supply such LASERS as:

CaF_2, BaF_2, CdF_2, SrF_2, CaO,
$CaWO_4$, MgO, MnF_2, Al_2O_3, TiO_2

and combinations of

$SrF_2 \cdot CaF_2$, $KMnF_2$, $SrF_2 \cdot BaF_2$,
$SrF_2 \cdot CaF_2 \cdot BaF_2$, $RbMnF_2$

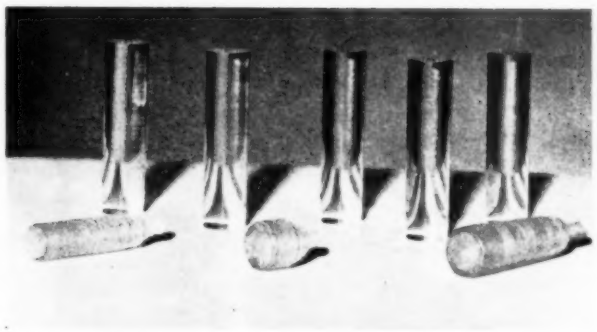

Semi-Elements is working with the following LASERS which show promise

Strontium Molybdate, Cesium Molybdate
Strontium Tungstate, Cesium Tungstate

WATCH FOR OUR ANNOUNCEMENTS ON:—
Exploratory PLASTIC LASER RODS
and Exploratory GLASS LASER RODS

Laser starting materials can be supplied for those who grow their own crystals.

If you want the latest in LASERS—write for comprehensive literature or phone
SINGLE CRYSTAL DIVISION - Dial 412 - 352 - 1548

SEMI-ELEMENTS, INC.

SAXONBURG BOULEVARD, SAXONBURG, PA. U.S.A.

OPTOVAC

HIGH QUALITY STANDARDS

. . . in Optical Crystal Blanks

CALCIUM FLUORIDE
BARIUM FLUORIDE
SODIUM CHLORIDE
POTASSIUM CHLORIDE
POTASSIUM BROMIDE

Prompt Delivery • Large Size Availability • Precision Cutting • Scattering Free • Impurity-absorption Free • Strain Free

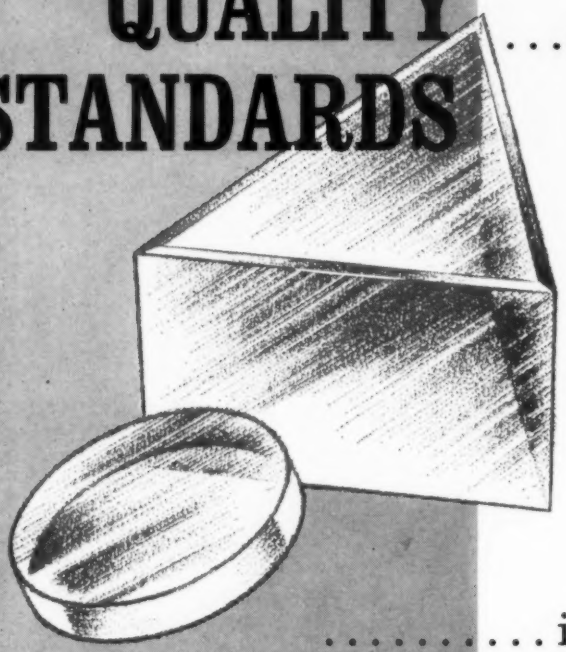

. . . . . in Optical Maser Crystals

Quality is essential in optical masers — for the development of new maser materials and to attain CW operation. Optical scattering, for example, can be the main obstacle to the successful masing of new materials. Optovac has been working with many of the research laboratories in the field with utmost emphasis on quality. Our particular interest is in the melt grown halides with rare earth and uranium dopings.

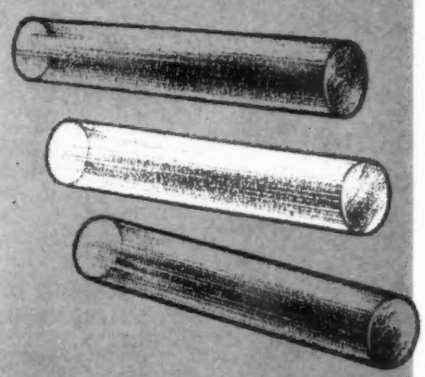

Optovac "firsts" in maser materials:

U^{+3} in CaF_2 grown for and first masedby Stevenson and Sorokin of IBM.

U^{+3} in BaF_2 first masedby Dr. Perry Miles of MIT.

Nd^{+3} in CaF_2 first masedby Bell Laboratories.

First CW operation of U^{+3} in CaF_2 by Bell Laboratories, as reported at the Phys. Soc., New York, January 24, 1962.

OPTOVAC, INC.

NORTH BROOKFIELD, MASSACHUSETTS

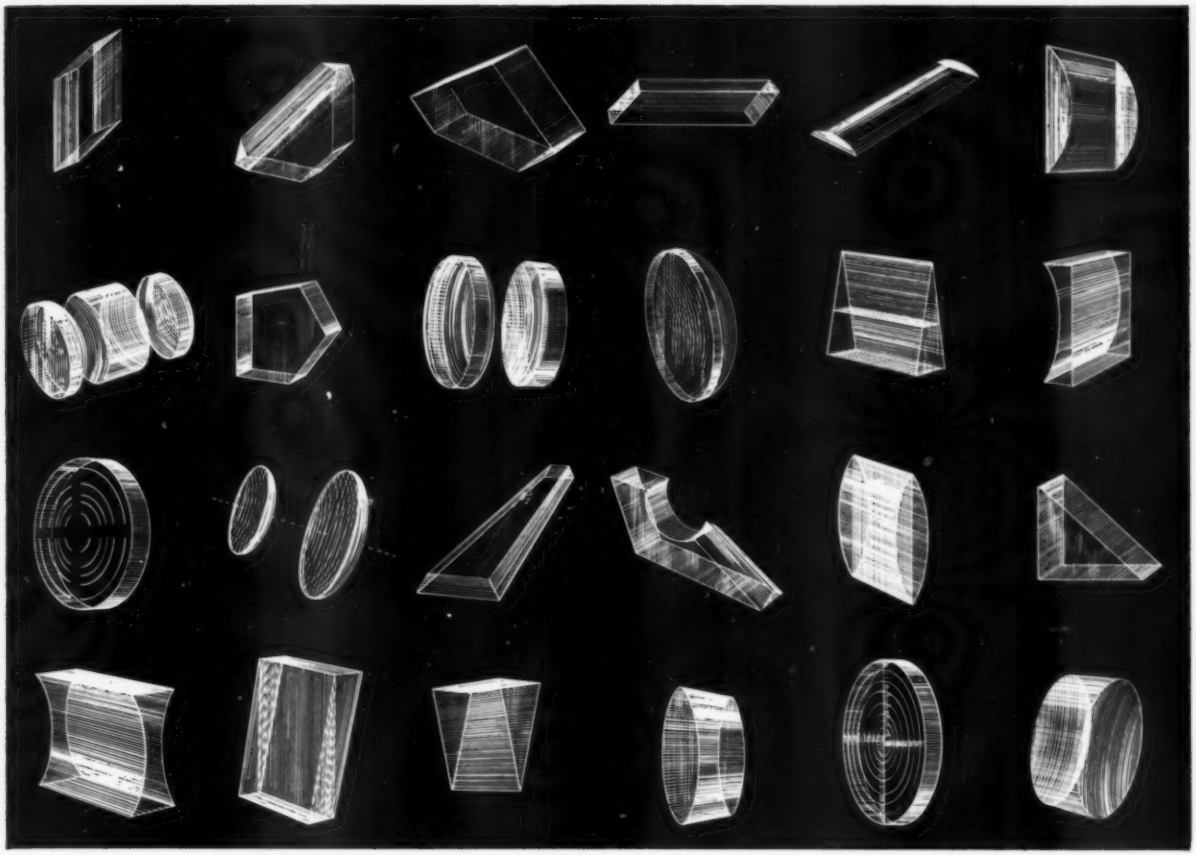

OPTICS FOR ELECTRONICS . . .

Components and systems for visible, ultraviolet, and infrared radiation. GEC's Astron-Optics Division specializes in design, development, and manufacturing of optical components and systems for the ultraviolet through infrared spectrum.

Here are a few of the optical components you can order from Astron-Optics: prisms, flats, spherical, aspherical and parabolic surfaces, reticles, information choppers, encoders, precision vacuum coating, and optically polished synthetic crystals.

Also available from Astron-Optics are infrared and optical-electronic systems.

For complete information regarding your precision optical requirements, write today to:

ASTRON OPTICS DIVISION

. . . precision optics at work

GENERAL ELECTRODYNAMICS CORPORATION

4430 FOREST LANE • GARLAND, TEXAS

capturing the spirit of research...

This is IBM's new research laboratory, dedicated in mid-1961 as the Thomas J. Watson Research Center. It is the headquarters for IBM's world-wide research activities, and is the largest laboratory in the world devoted to the growing field of computer research.

Functional design and bold use of natural materials achieve unity of site and structure in the rolling countryside of Yorktown, New York. Inside this facility, IBM scientists pursue programs in the physical sciences, including physical optics, radiometry, and electrooptical devices. The constructive thinking and the scientific achievements of our research staff will provide the basis for new and improved IBM products, and will contribute to the body of knowledge so vital to the scientific community at large.

If you sense a personal challenge to your own talents, and wish to consider joining IBM, we would like to hear from you. Write, outlining briefly your background and experience, to: John B. Farrington, Thomas J. Watson Research Center, Box 619P, Yorktown Heights, N. Y. IBM is an Equal Opportunity Employer.

OPTICS TECHNOLOGY, INC.

A New Line of Electro-Optical Components and Instruments

PULSED LASER Both coherent light source and LASER materials tester. "Zoom" telescope and transit mounting; adjustable Fabry-Perot multi-layer end reflectors for 6943Å (ruby) or other LASER wavelengths. Peak power, 1-2 Kilowatts (nominal); pulse width, 0.5 milliseconds. Two power supplies available with 400 or 800 joule capacity; variable from 0 to 1,800 volts. Price: LASER head and transit; with 400 joule power supply, $2,810.00; with 800 joule power supply, $2,965.00.

IMAGE DISSECTORS Facilitates Hypervelocity Ballistics studies; stagnation point intensity is dissected and fed to 12 photomultipliers. Useful in flash spectrographic and Doppler-Shift studies; in conjunction with a dispersing element, 12 simultaneous readings may be taken. Also useful in isolating "hot spots" in output of LASER crystal. Excellent spectral response; precision fibers transmit from 350 millimicrons through 3 microns. Price: $950.00/unit.

PHOTON COUNTERS High Quantum-efficiency Ultra-Violet photon counters with extreme sensitivity and uniform pulse height. Cs_2Te, Rb_2Te and pure metal cathodes, self-quenching or non-quenching fillings. Operating voltage, 500 to 1,000 v plateau with 50 to 100 v (non-quenching), 75 to 15 v (self-quenching); pulse height, 0.250 to 0.500 v at 750 volts; maximum counting rate, 10 Kc (self-quenched). Price: $295.00/unit.

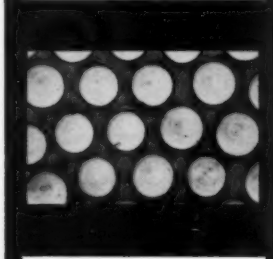

FUSED FIBER OPTICS PLATES Ideal for application in Multistage Image Intensifiers, CRT Face Plates and Field Flatteners. Vacuum tight, over 100 line pairs per mm resolution, high numerical aperture, excellent spectral transmission, non-cathode poisoning glasses. Wide variety of sealing characteristics and sizes available. Prices depend upon individual specifications. The Optics Technology Marketing Department can quickly issue quotations on face plates to meet your own unique requirements.

VACUUM DEPOSITION MONITORING SYSTEM Measure thin film thickness during vacuum deposition using optical techniques with high precision in both production and lab setups. System may be used to control thickness to ± 0.25%; accuracy is not affected by changes in filament or ambient light. Monitors metal or dielectric coatings for either reflection or transmission. The system is supplied complete with in-chamber fittings, light source, detector unit, solid state amplifier and optical components. Installation, calibration and operation is simple. Price: $2,275.00 complete.

MONOPASS INTERFERENCE FILTER SETS Available to cover the range of 400 millimicrons to 2.75 microns to meet requirements in spectral analysis. MONOPASS filter designs pass only desired wavelengths, rejecting all others from X-band to X-ray. Calibration curves, bound in a rugged volume, pinpoint individual filter accuracy. Prices from $325.00 to $450.00.

For complete information and data, contact your nearest OTI representative or write:

OPTICS TECHNOLOGY, INC

248 Harbor Boulevard, Belmont, California
LYtell 1-0359 (Area Code 415) 7617

Other exciting electro-optical instruments and components available from OTI include Industrial and Medical Microprobes, Refractometers, Fiber Optics Probe Inspection Cameras, and other Fiber Optics Devices.

New England, H. J. Schuft Co.; Metropolitan New York and Northern New Jersey, RMC Associates; Upstate New York, E. Stone & Co.; Mid-Atlantic, C. E. Snow Co.; S. California, Abbott Instrument & Engineering Co.

Scientific
Career Opportunities
for
OPTICAL SCIENTISTS

Continued rapid expansion at American Astrophysics, creator of the most advanced large automatic optical satellite tracking telescope known, has opened additional research and scientific opportunities for optical scientists and physicists.

Assignments will be with the American Astrophysics scientific and engineering team which will continue advancing the state-of-the-art on projects which include....

Large Electro-Optical-Mechanical Systems
Large Astronomical Telescopes
Optical Surveillance Systems and Telescopes
Optical Satellite and Space Probe Trackers
Cinetheodolites
Occultation Trackers
Special Purpose Spectrographs

Responsibilities require an extensive background in the research and design of large, high resolution optical systems and mirrors. Familiarity with astronomy and fiber optics is desirable. Ph.D. degree or equivalent is preferred and current security clearance is a requisite.

At American Astrophysics, professional freedom, individual initiative and creative ability are encouraged in an environment conducive to scientific accomplishment. All qualified applicants will receive consideration without regard to race, creed, color or national origin.

Please telephone or write in confidence:

Dr. Erik Ackerlind

AMERICAN ASTROPHYSICS

2000 SOUTH MYRTLE AVENUE
MONROVIA • CALIFORNIA
ELLIOTT 9-8351

WANTED: SOMEONE TO RIDE A RUNAWAY HORSE

The demand for complex new optical systems to meet military requirements is proceeding with all the speed of a runaway horse. We are seeking experienced optical people like yourself who possess the ability to contribute to this advancing technology.

Nortronics in Southern California has a number of excellent opportunities for engineers and physicists with the desire to face the challenges of some of the most advanced optical programs being undertaken anywhere. Nortronics' diversified background in optical, electronic and mechanical systems has given it the capability to tackle the complex opto-mechanical and opto-electronic systems demanded by the Armed Forces. This capability has led to the development of a 600mm, f-2 ballistic camera, articulated telescope, image display systems, and highly significant classified programs.

Under the leadership of the eminent Dr. Konstantin Pestrecov, Nortronics' activities encompass a broad spectrum of optical skills: Design of lenses and prisms for compound optical systems... studies in radiation trasmission, receiving, and absorption effects... studies in atmospheric physics... digital programming in solution of optical problems... development of methods for fabrication and test of optical components.

Nortronics is located 30 miles southeast of Los Angeles, near Disneyland in Anaheim – one of the Southland's most ideal residential areas. Career benefits are among the finest in the industry. If you feel you might qualify for a position at Nortronics, and would like to learn more about our opportunities, send your resumé to:

PROFESSIONAL PLACEMENT OFFICE
500 EAST ORANGETHORPE AVENUE
ANAHEIM, CALIFORNIA

IN ORANGE COUNTY

NORTRONICS
A DIVISION OF
NORTHROP

AN EQUAL OPPORTUNITY EMPLOYER

HARSHAW MANUFACTURES A COMPLETE LINE OF SCINTILLATION AND OPTICAL CRYSTALS

SCINTILLATION *Mounted* NaI(T1) *Crystals*

Crystal detectors designed for the most sophisticated counting problems. Our physics and engineering group are available to assist you in your special detector problems.

More detailed information is contained in our 32-page book, "Harshaw Scintillation Phosphors". We invite you to write for your free copy!

STANDARD LINE

(Hermetically Sealed Crystal Assemblies)

- The accepted standard of the industry
- Proven through years of service in research, medical and industrial applications
- unparalleled performance
- dependability
- consistent good quality

INTEGRAL LINE

(Crystal photo multiplier tube combination assembly)

- Improved resolution
- Ready to use plug-in unit
- Permanently light sealed
- Capsule design facilitates decontamination
- Close dimensional tolerances
- Harshaw guaranteed

Large Crystal MATCHED WINDOW LINE

(Designed primarily for crystals 4" dia. and larger)

- "Small crystal" performance achieved through improved optical design
- Low mass containers
- Available in standard aluminum or complete low background assemblies
- Convenient mounting flange
- Ready to use

Every Harshaw crystal is a product of our experience in crystal growing technology since 1936

Other Phosphors Available from The Harshaw Chemical Company

ROUGH CUT THALLIUM ACTIVATED SODIUM IODIDE CRYSTAL BLANKS • EUROPIUM ACTIVATED-LITHIUM IODIDE (NORMAL) • EUROPIUM ACTIVATED LITHIUM IODIDE (96% Li^6 ENRICHED) • THALLIUM ACTIVATED CESIUM IODIDE • THALLIUM ACTIVATED POTASSIUM IODIDE • ANTHRACENE • PLASTIC PHOSPHORS

OPTICAL *Crystals*

For Infrared and Ultra Violet Transmitting Optics

"HARSHAW QUALITY" INHERENT IN EACH HARSHAW-GROWN CRYSTAL GUARANTEES THE MOST EFFICIENT OPTICAL TRANSMISSION POSSIBLE THROUGH:

1) Negligible light scattering in crystals, permitting higher sensitivity and improved resolution
2) Freedom from absorptions caused by trace impurities in crystal optics
3) Minimum strain

"HARSHAW QUALITY" meets the demand for uniformity of optical properties such as dispersion and refractive index. Prices, specifications, or other information will be sent in answer to your inquiry.

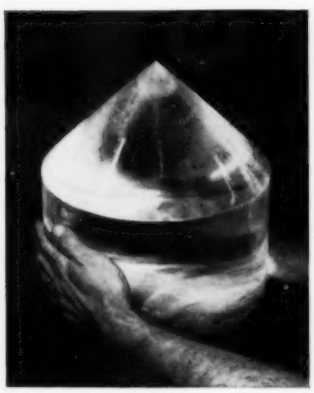

The following infrared and ultra violet transmitting crystals are available; others are in the process of development:

SODIUM CHLORIDE • SODIUM CHLORIDE MONOCHROMATOR PLATES • POTASSIUM BROMIDE • POTASSIUM BROMIDE PELLET POWDER (through 200 on 325 mesh) • POTASSIUM CHLORIDE • OPTICAL SILVER CHLORIDE • THALLIUM BROMIDE IODIDE • LITHIUM FLUORIDE • LITHIUM FLUORIDE MONOCHROMATOR PLATES • CALCIUM FLUORIDE • BARIUM FLUORIDE • CESIUM BROMIDE • CESIUM IODIDE

Additional information on the physical and optical properties of the above crystals is available in our 36-page booklet "Synthetic Optical Crystals". Send for your free copy.

HARSHAW

THE HARSHAW CHEMICAL CO.

Crystal Division • Cleveland 6, Ohio

The Radiation Environment of Interplanetary Space

John H. Shaw

A discussion of the spectral distribution and intensity of the radiation fluxes from various sources contributing to the radiation environment of interplanetary space is presented. The radiation from both the quiet and disturbed sun is described in some detail and current estimates of radiation from other sources are given.

Introduction

Prior to the rocket age our knowledge of the universe beyond the earth came predominantly from ground level observations of the radiation from extraterrestrial sources. The radiation from the stars and nebulae has given us information about the size and nature of our own galaxy and has also revealed some of the differences and the distances between still more distant agglomerations of matter. Radiation from the sun, the planets and their satellites, some of the larger asteroids, and an occasional comet has enabled us to learn about the size of our solar system and the physical properties of some of its larger constituents.

In addition to these observations, meteor trails in the atmosphere and phenomena such as the zodiacal light indicate the presence of small pieces of material ranging in size down to 10^{-4} cm in interplanetary space; the aurorae, the disturbances of the earth's magnetic field, and the flux of cosmic rays show that atomic and subatomic charged particles occur in the region surrounding the earth. These originate both from the sun and from sources outside the solar system.

However, the atmosphere is opaque in many regions of the electromagnetic spectrum and the earth's magnetic field and atmosphere interact with the particles arriving near the earth. It has long been clear that direct measurements of the near-earth environment can only be obtained from instruments outside the influence of the earth and its atmosphere. Indeed, the results already obtained from rocket and satellite experiments have confirmed previous hypotheses, refuted others, and have revealed that previously unsuspected phenomena occur in the region surrounding the earth.

Although there are still many gaps, such data have already edabled a more accurate picture of the physical environment of interplanetary space to be constructed. One of the dominating influences on this environment is the flux of electromagnetic radiation from the various sources described above. Of these the most important is the direct radiation from the sun; other contributions are made by the solar radiation scattered by the planets and by the dust and electrons in the solar system, and by the thermal radiation from these bodies and from sources outside the solar system.

In this paper the radiation from the sun is discussed in some detail and a description of some of the recent investigations of the short wavelength regions of the solar spectrum, which are inaccessible from the ground, is given. An attempt is also made to estimate the flux due to the other sources in different wavelength regions at a point about one astronomical unit (1 a.u. = the mean earth–sun distance = 1.495×10^8 km) from the sun.

Physical Description of the Sun

In the vicinity of the earth the flux of solar radiation has not only a greater intensity than that from any other source but it has been detected over a wider spectral interval extending from wavelengths in the x-ray region as short as 0.1 A to beyond 20 meters in the radio range.[1] The wealth of information carried by this radiation has enabled much to be learned about the sun and its physical characteristics.

Energy is continually being produced in the interior of the sun as a result of nuclear reactions. Throughout most of the interior this energy is conveyed outwards by radiative processes. However, there is a region, probably 50,000 km to 100,000 km thick, just below

The author is in the Department of Physics and Astronomy, The Ohio State University, Columbus 10, Ohio.

Received 13 November 1961.

This paper was prepared with support from the Geophysics Research Directorate, Air Force Cambridge Research Laboratories, and from the Aeronautical Systems Division through The Ohio State University Research Foundation.

the visible surface, where the solar gas is opaque over a wide range of wavelengths primarily because of the presence of negative hydrogen ions. In this zone energy is transported outward mainly by convection. At the outer edge of this zone the energy is radiated directly into space from a layer only a few hundred kilometers thick. This radiating layer, the photosphere, is seen in the visible as the bright disc of the sun. Its diameter is about 1.39×10^6 km and its temperature is about 6000°K. The radiation emitted contains many Fraunhofer lines caused by the absorption and re-emission of radiation by atoms and ions. These processes occur predominantly in the upper regions of the photosphere although the absorption at the centers of very weak lines and in the wings of strong lines is the result of the passage of the radiation through deep atmospheric layers.

The outer solar atmosphere is usually only seen during an eclipse of the sun. Immediately above the photosphere is a layer of glowing gas about 20,000 km thick; beyond it lies the corona which stretches far into space. The lowest solar temperatures, in the range 4000 to 4700°K, occur in a narrow region near the boundary between the photosphere and the chromosphere. Above this region the temperature in the chromosphere increases with height and reaches a value of the order of 10^6 °K somewhere between 10^4 and 10^5 km above the photosphere. These high temperatures extend for at least 4 solar radii. With increasing distance from the sun the temperature and particle density decrease but, even at the earth's distance, interplanetary space contains from 50 to 500 particles (mainly protons and electrons) per cm^3. This ionized gas is probably part of the solar atmosphere and its temperature at 1 a.u. is at least 10^4 °K[1a] and possibly an order of magnitude higher.[1b]

The various regions of the solar atmosphere described above are not always well defined since the sun is a seething mass of gas whose configuration undergoes constant change, and in which disturbances are continually present. Some of the disturbances in the photosphere and at higher levels in the atmosphere are readily detected. The most obvious signs of activity are the relatively cool dark sunspots in the photosphere. These tend to appear in groups within 40° of the solar equator and they move across the solar disc at a speed corresponding to the sun's period of rotation of about 28 days. Their numbers fluctuate in the well-known 11-year cycle and there is a general increase in the level of activity of the solar atmosphere with sunspot number. One of the effects is to cause increased emission in the x-ray and radio regions of the spectrum.

Luminescent gas clouds or prominences can also be seen in the chromosphere at the edge of the photosphere. These prominences may extend 50,000 km or more above the photosphere and can take the form of very large quiescent masses, active loops, or fast jets called surges. Incandescent matter in these surges can rise high into the corona with speeds of several hundred kilometers per second. Speeds of 1000 km sec^{-1} have been observed, much greater than the speed of 600 km sec^{-1} necessary to escape from the sun's gravitational field. When the sun is viewed in monochromatic light such as $H\alpha$ (6563 A) the prominences appear as dark clouds (flocculi) or long dark filaments projected against the solar disc. Also in monochromatic light bright areas (plages) may be seen floating in the lower atmosphere. Sunspots are usually accompanied by plage areas and occasionally a plage rapidly increases in brightness and in a few minutes spreads over a large area of the disc. Its brightness then gradually decreases in times varying from a few minutes to several hours. Such an event is called a solar flare. Observations in the visible range indicate that they are relatively flat structures extending from the chromosphere into the lower corona.

The area of a flare is used as a measure of its importance (Table I). Flares of class 3 are rare, occurring, on the average, only a few times per year, whereas flares of class 1 or less occur every few hours during periods of marked solar activity. Some data[2] on the number of flares reported during the IGY, a period of maximum solar activity, are given in Table I. While flares are associated with sunspots, and, in particular, with complicated groups, some large spots remain relatively inactive. It is not yet possible to predict when a large solar flare will occur.

Sudden ionospheric disturbances in the earth's atmosphere (SID), including short wave radio fadeouts and other effects associated with changes in the ionosphere, occur simultaneously with the appearance of intense flares. These effects are principally due to enhanced x-ray emission from the sun increasing the ionization below 100 km in the earth's atmosphere. Magnetic storms (variations of the earth's magnetic field) often commence about one day after the appearance of a flare of class 3 or 3+ and are usually most marked when the flare is near the center of the disc. These storms are caused by charged particles

Table I. Solar Flares[a]

Flare class	Mean area in 10^{-6} of sun's hemisphere	Mean duration	No. of flares reported July 1957–Dec. 1958[2]
<1	<100		835
1	100–250	20 min	5389
2	250–600	30 min	497
3	600–1200	60 min	41
3+	>1200	3 hr	

[a] M. A. Ellison, Trans. I. A. U. **9**, 146 (1957).

from the sun. Some of these particles pass close to the earth and are influenced by its magnetic field. Satellite observations indicate that one of the first effects of these particles may be to cause the outer Van Allen radiation belt to dump many of its particles into the upper atmosphere producing auroral displays. Later, the radiation belt density first increases considerably and then gradually returns to its normal value. On at least eleven occasions since 1942 showers of particles with cosmic ray energies have been associated with major flares.

At the present time our knowledge of the peak intensities of the various radiations emitted during a solar flare is incomplete. Nevertheless, from the data obtained at ground level and those being obtained from rockets and satellites, it seems improbable that the visible flares, which occur in the lower atmosphere of the sun and have temperatures of about 30,000°K, can be responsible for all of the phenomena described above. Instead, most of the effects associated with flare activity may originate in local hot spots in the corona. Observations indicate that there are regions above large sunspot groups where the coronal density may be ten or more times greater than the average density and at temperatures up to 10^7 °K as compared with the normal coronal temperatures of about 10^6 °K.

The Solar Constant

Various estimates of the solar constant, the total flux of solar radiation per unit area at 1 a.u. from the sun, range from 1.9 to 2.05 cal cm^{-2} min^{-1}. Johnson[3] has obtained a value of 2.00 ± 0.04 cal cm^{-2} min^{-1} (1.40×10^6 ergs cm^{-2} sec^{-1}). By far the greater part originates from the photosphere with relatively minor contributions from the chromosphere and corona. The spectral distribution of the radiation from the quiet sun is given in Table II, from which it is seen that about 99.8% lies between 0.2 μ and 7 μ. A more complete discussion of the solar radiation in different wavelength regions and its variation with solar activity is given below.

Infrared and Radio Emission from the Sun ($\lambda > 1\,\mu$)

Our information concerning the long wavelength solar radiation is based primarily on ground level observations which can only be made in the spectral regions where the atmosphere is relatively transparent. Between 1 μ and 14 μ there are a number of relatively transparent windows amongst bands of water vapor, carbon dioxide, ozone, methane, nitrous oxide, and carbon monoxide. From 14 μ to 1 mm the atmosphere is opaque due primarily to strong absorption by water vapor. Although there is some absorption at wavelengths shorter than about 1 cm the radio window extends from the millimeter region to about 20 meters. Longer wavelengths are absorbed or reflected by the ionosphere.

The measurements which have been made in the windows between 1 μ and 1 cm indicate that most of this solar radiation originates in the photosphere and there appears to be little variation with solar activity. It consists of a continuum although some weak solar Fraunhofer lines have been detected between 1 μ and 5 μ. The spectral brightness tem-

Table II. Spectral Distribution of Radiation from the Quiet Sun[a]

Wavelength region	% of total	Radiation Distribution ergs cm^{-2} sec^{-1} per wavelength interval at 1 a.u.	Origin	Ref.
0–1 A		$<10^{-6}$	Corona	b
1–8 A		$<10^{-5}$	Corona	b
1–100 A		<1	Corona	b
100–300 A		~0.8 (possibly high)	Corona and chromosphere	c
304 A (HeII)		0.25	Mainly from chromosphere	c
305–1000 A		0.9	Mainly from chromosphere	c
1000–1200 A		~0.4	Mainly from chromosphere	c
1216 A (Ly α)		5.1	Mainly from chromosphere	d
1218–1500 A		1.8	Chromosphere	d
1500–2000 A		200	Chromosphere and photosphere	d
0.2–0.4 μ	9	1.3×10^5	Photosphere	e
0.4–0.75 μ	44.7	6.4×10^5	Photosphere	e
0.75–2.0 μ	40.2	5.6×10^5	Photosphere	e
2.0–7.0 μ	6.0	0.8×10^5	Photosphere	e
>7 μ	0.14	<2000	Photosphere	e
>1 cm		$<10^{-5}$	Chromosphere and corona	
Total	100	1.4×10^6		

[a] The flux in the extreme ultraviolet and x-ray regions below 100 A and in the radio region at wavelengths longer than 1 cm shows great enhancements when the sun is disturbed. The flux in some regions may increase by a factor of 10^2 to 10^5 or even more above the flux from the quiet sun. Such outbursts rarely last more than a few hours.

[b] H. Friedman, *Physics of the Upper Atmosphere* (ed. J. A. Ratcliffe, Academic Press, 1960) (for 0–100 A).

[c] H. E. Hinteregger, J. Geophys. Research **66**, 2367 (1961).

[d] C. R. Detwiler, D. L. Garrett, J. D. Purcell, and R. Tousey, Ann. géophys. **17**, 9, 263 (1961) (for 1000–3000 A).

[e] F. S. Johnson, *J. Meteorol.* **11**, 431 (1954).

perature* of the sun throughout this region is close to 6000°K (see Table III) but beginning at about 1 cm it increases rapidly to of the order of 10^6 °K at 1 meter and this high value is maintained to longer wavelengths. However, the total incident flux at wavelengths longer than 1 cm, about 10^{-5} ergs cm^{-2} sec^{-1} at 1 a.u., is insignificant in terms of the total solar radiation.

Most of the emission from the quiet sun at centimeter wavelengths originates in the chromosphere; 10 cm^{-1} meter radiation comes partly from the base of the corona and partly from the outer corona; radiation of meter wavelengths is generated in the corona at distances of up to half a solar radius from the photosphere. The radiation between about 10 cm and 1 meter is correlated with the number of sunspots and the average intensity level of this radiation has been found to vary by a factor of three or more in a cycle similar to the sunspot cycle.

In addition to these long term variations at wavelengths shorter than 1 meter various types of outbursts have been detected throughout the radio window. These bursts may last from a few seconds to several minutes and may be superposed on an enhanced continuum which can persist for several hours. A series of short bursts at wavelengths longer than about one meter may continue for several days causing a noise storm. These effects appear to originate in the corona above active sunspot areas. Other types of radio noise are associated with solar flares and appear to be caused by material flowing upward through the corona. In some instances the radio emission from small areas of the sun associated with flares may be several hundred times the emission from the rest of the sun. Measurements of the dependence of the intensity of this radiation on wavelength and time give information about the regions of the sun which produce it and have helped in the construction of models of the solar atmosphere. However, a complete description of the radio emission from the sun is outside the scope of this paper. Useful descriptions of radio observations of the sun and their interpretation are found in refs. 4, 5, and 6.

The Visible and Near Visible Radiation from the Sun (0.29 $\mu<\lambda<1$ μ)

This spectral interval carries a major portion of the radiation from the sun and is also a region to which the atmosphere is relatively transparent. The results of extensive measurements throughout this spectral interval indicate that most of the radiation originates from the photosphere and that it consists of a continuum corresponding approximately to that from a blackbody near 6000°K. In the visible region, some departure from blackbody radiation arises from the fact that the radiation originates from different layers at temperatures between 4500°K and 8000°K, and the radiation curve is therefore a composite curve. Superposed on this continuum are numerous dark solar Fraunhofer lines which are more numerous and more intense than those observed in the infrared. These cause some distortion of the solar energy curve from that of a blackbody below 4000 A. No significant changes in the integrated solar radiation over this region with time have been detected.

The Ultraviolet Radiation from the Sun (100 A$<\lambda<$2900 A)

The earth's atmosphere is opaque to radiation of wavelengths shorter than 2900 A. This cutoff recedes to somewhat shorter wavelengths above the ozone layer near 30 km altitude but it is necessary to climb above 200 km before the entire x-ray and ultraviolet region becomes accessible and to still higher altitudes before the atmosphere is completely transparent. Numerous investigations of the radiation arriving at the earth in this spectral region have been carried out in recent years with a variety of rocket-borne spectrographs. These have obtained excellent spectrograms of the sun to wavelengths below 100 A. In addition, a variety of narrow-band detectors responsive to selected regions of the x-ray and ultraviolet spectrum have been used to measure the radiation flux near the earth down to 0.1 A. Much of this work has been carried out by members of the U.S. Naval Research Laboratory.

These rocket investigations have shown that the Fraunhofer lines continue to increase in number and intensity at wavelengths shorter than 2900 A so that the spectral brightness temperature of the sun drops

---

* A blackbody may be defined as a body which radiates according to Planck's Law

$$W_\lambda d\lambda = \frac{c_1}{\lambda_5} (e^{c_2/\lambda T} - 1)^{-1} d\lambda,$$

where $W_\lambda d\lambda$ (ergs cm^{-2} sec^{-1}) is the radiation emitted per square centimeter per second in all directions in the wavelength interval between λ and $\lambda + d\lambda$. If λ is measured in centimeters and T is the absolute temperature, $c_1 = 3.741 \times 10^{-5}$ ergs cm^{-2} sec^{-1}, and $c_2 = 1.439$ cm °K. The radiation emitted is therefore defined once the temperature is known. The radiation emitted by other sources in the interval between λ and $\lambda + d\lambda$ can be specified in terms of the temperature of a blackbody radiating at the same rate. If the other source is not a blackbody its equivalent blackbody temperature or spectral brightness temperature will vary with wavelength. The spectral brightness temperature can also vary over the surface of the source. In such cases, it is therefore necessary to specify whether the spectral brightness temperature refers to a specific region of the body or whether it refers to the temperature obtained by averaging the radiation over the entire area. Most of the radiation from the sun originates in the photosphere and usually the spectral brightness temperature is greatest at the center of the disc. However, limb brightening effects have been observed at some radio wavelengths and the high temperatures associated with flare activity are confined to relatively small areas on the sun.

Table III. Spectral Brightness Temperatures of the Quiet Sun from Measurements of the Continuum

Wavelength	Spectral brightness temperature (°K)	References	Wavelength	Spectral brightness temperature (°K)	References
4–100 A	7×10^5	[a]	3.5 μ	5780	[f]
1000 A	5800	[b]	5 μ	5150	[f]
1180 A	5100	[b]	11.10 μ	5036	[g]
1300–1500 A	4700	[b]	4.5 mm	6962	[h]
1750 A	4700	[b]	6 mm	4500	[i]
2080 A	5000	[b]	8 mm	8500	[h]
4300–5500 A	5800	[c]	1.5 cm	10^4	[c]
1.55 μ	6330	[d]	30 cm	$1.0\text{–}2.3 \times 10^5$	[c]
2.03 μ	6045	[d]	1.5 meters	$6\text{–}9 \times 10^5$	[c]
2.31 μ	5880	[d]	6 meters	$\sim 10^5$	[c]
1–2.5 μ	6400	[e]			

[a] H. Friedman, *Physics of the Upper Atmosphere* (ed. J. A. Ratcliffe, Academic Press, 1960).
[b] C. R. Detwiler, J. D. Purcell, and R. Tousey, Astron. J. **66,** 281 (1961).
[c] C. W. Allen, *Astrophysical Quantities* (Univ. London, 1955), p. 141.
[d] R. Peyturaux, Ann. astrophys. **15,** 302 (1952).
[e] A. K. Pierce, Astrophys J. **119,** 312 (1954).
[f] C. B. Farmer and S. J. Todd, Report No. DP 927, EMI Electronics Ltd., London, 1961.
[g] F. Saiedy and R. M. Goody, Monthly Notices Roy. Astron. Soc. **119,** 213 (1959).
[h] R. J. Coates, Astrophys. J. **128,** 83 (1958).
[i] R. N. Whitehurst, J. Copland, and F. H. Mitchell, J. Appl. Phys. **28,** 295 (1957).

to about 5000°K at 2085 A.[7] At this wavelength the ordinary Fraunhofer region appears to end abruptly and the continuum drops to almost the level of the stronger Fraunhofer lines caused by a strong continuous or quasi-continuous absorption in the outer photosphere.

Although Detwiler *et al.*[8] have observed the continuum down to approximately 1000 A no strong Fraunhofer lines are observed below 2085 A and no absorption lines at all appear below 1550 A. However, emission lines begin to occur below 1900 A. More than 200 have been reported between 500 A and 1550 A and others have been observed down to 84 A. Reference *d* of Table II presents the intensities of 36 of these lines between 835 A and 1900 A. With the exception of the Ly-α hydrogen line at 1216 A their intensities are all well below 1 erg cm^{-2} sec^{-1} at 1 a.u. Reference *c* of Table II has also evaluated the measurements in the extreme ultraviolet below 1027 A. The strongest of the emission lines at wavelengths below Ly α is that of He II at 304 A (0.25 erg cm^{-2} sec^{-1}). There is another relatively strong He I line at 584 A (0.10 erg cm^{-2} sec^{-1}).

There have been a number of investigations of the Ly α 1216 A line. Byram *et al.*[9] reported its intensity to be from 4 to 10 ergs cm^{-2} sec^{-1} at 1 a.u., and it is estimated that this line accounts for 85% of the total radiation from the sun between 1075 A and 1275 A. It is apparently little changed in intensity during periods of solar activity.[10] Purcell and Tousey[11] have found that the wings of Ly α extend one or more angstroms from the center and that there is a narrow deep absorption core at the center originating from the absorption by relatively cool neutral hydrogen atoms between the sun and the detector. It seems probable that most of this hydrogen is associated with the earth's atmosphere.[12]

Several other lines of the Lyman series have been detected. The higher members run together and appear to produce a continuum below 918 A with a maximum near 912 A. The Lyman continuum itself has been observed down to 820 A (references *c* and *d*, Table II). Although most of these emission lines must originate in the chromosphere some have been identified with very highly excited atoms. For example, a pair of Mg X lines at 625 A and 610 A must originate in the corona where the temperature is in excess of 10^6 °K.

The photospheric continuum contributes little to the radiation below 1500 A. Indeed, Detwiler, Purcell, and Tousey interpret the absence of Fraunhofer lines below 1526 A to mean that the continuum is entirely chromospheric below this wavelength. The spectral brightness temperatures of the sun, as determined from this continuum down to 880 A, are given in Table III. Measurements in the region below 1000 A are difficult to make with conventional spectrographs and the radiation from the sun at wavelengths shorter than this has not yet been completely investigated.

Solar Radiation Below 100 A

A series of measurements of the x-ray radiation from the sun have been made by Friedman and his associates at the Naval Research Laboratory.[13,14] The data

obtained with photon counters sensitive to narrow spectral regions such as 4–8 A, 8–20 A, 44–60 A, and 44–100 A indicate that the quiet sun near sunspot minimum does not emit a significant quantity of radiation at wavelengths shorter than about 8 A (less than 3×10^{-6} ergs cm^{-2} sec^{-1} at 1 a.u.); the radiation in the 8–20 A region may be as low as 1.5×10^{-3} erg cm^{-2} sec^{-1}, and the total flux in the x-ray region 0.13 ergs cm^{-2} sec^{-1}. As the sunspot maximum is reached the radiation throughout the entire x-ray region is enhanced, increasing by a factor of eight or more in the absence of flare activity. The corresponding increases in the short wavelength region (by a factor of 40) are considerably greater.

The radiation carried by emission lines is much more important than that due to a continuum in the x-ray region. However, Friedman has found that his data may be satisfactorily represented by assuming that the x-ray radiation is continuous and that it consists of two components. One component, which originates from the quiet corona, has a maximum near 60 A and drops to very small values below 20 A. Its spectral distribution corresponds to that from a gray body at from 5 to 7×10^5 °K. An emissivity of 4×10^{-16} would provide a total solar flux in the x-ray region of about 0.13 erg cm^{-2} sec^{-1} at 1 a.u. The other component probably arises from transient hot coronal condensations occupying perhaps 1% of the solar disc. If the temperature in these regions were as high as 2×10^6 °K it would greatly affect the radiation emitted below 20 A but would not contribute greatly to the longer wavelength radiation.

Since it is not possible to predict the appearance of the short-lived solar flares it is difficult to make rocket observations of the x-ray and ultraviolet flux associated with them. However, a flux of 2×10^{-2} ergs cm^{-2} sec^{-1} was observed[14] between 3 A and 8 A during a class 2 flare at an altitude of 77 km. This tremendous increase over the usual radiation from the sun in this region may be caused by the emission from regions in the solar atmosphere associated with the flare where temperatures may reach 10^7 °K.

There appears to be little solar radiation below 1 A. From one rocket flight at a time when the sun was quiet Kupperian and Friedman[15] found the total flux of x-rays at energies between 20 and 300 kev (0.6 to 0.05 A) was less than 10^{-6} ergs cm^{-2} sec^{-1} at 100 km altitude. Because of the low intensity it was not possible to be sure that the sun was the source. Observations[16] made by Sputnik III have set the upper limits given in Table IV to the short wavelength radiation from the sun both when quiet and also during a solar flare. However, Peterson and Winckler[17] have reported a flash of γ radiation of about 2×10^{-5} ergs cm^{-2} sec^{-1} peaked in the 200–500 kev region which lasted about 18 sec or less during a class 2 flare in 1958. The process leading to its production is not yet understood.

Radiation from Planets

In addition to the nine major planets and their satellites circling round the sun there are the members of the asteroidal belt, an occasional comet, and interplanetary dust. The radiative properties of this dust are discussed in a later section; the comets, usually seen by their tails of tenuous luminous gas and dust, and the individual asteroids are too small to have an appreciable effect on the interplanetary radiation environment except in their immediate vicinity. The radiation from the planets is also small compared with the direct solar radiation throughout most of interplanetary space. It consists primarily of scattered solar radiation, thermal radiation, and the probably insignificant contributions from such sources as atmospheric fluorescence and auroral emissions from those bodies with atmospheres.

The amount of scattered solar radiation received at a given distance from a planet depends on the distance of the planet from the sun, its size, scattering properties, and phase angle (the angle between the sun and the point of observation as seen by the planet). Data on the scattering properties of the planets in the visible and near visible regions are available and their values can be used to estimate the total scattered radiation flux from a planet with a fair degree of accuracy, since most of the solar radiation lies between 0.3 μ and 2 μ and most materials have a high absorptivity in the ultraviolet and infrared. Thus the radiation flux from Venus, the planet with the highest reflectivity, has fallen to less than 1 erg cm^{-2} sec^{-1} at a distance of 10^7 km.

The thermal radiation from the planets, satellites, etc., without atmospheres is close to that from a blackbody at the surface temperature. Since this temperature can vary over the surface, the radiation emitted is dependent, among other things, on phase angle. For example, the temperature of the subsolar

Table IV. Upper Limits of Extraterrestrial γ-Ray Fluxes

Photon energy (kev)	Energy flux (ergs cm^{-2} sec^{-1}) is less than	Ref.
10	1	[a]
30	10^{-4}	[a]
50	10^{-6}	[a]
20–300	Between 10^{-6} and 10^{-7}	[b]

[a] S. N. Vernov, A. E. Chudakov, E. V. Gorchakov, J. I. Lozachev, and P. V. Vakulov, paper presented at Fifth CSAGI Assembly, Moscow (1958).

[b] J. E. Kupperian, Jr. and H. Friedman, paper presented at Fifth CSAGI Assembly, Moscow (1958).

point on the planet Mercury is over 600°K while the temperature of the dark side must be less than 200°K.

The thermal radiation from bodies with atmospheres originates from different atmospheric levels and the spectral brightness temperature may depend significantly on wavelength as well as surface position. Probably the most extreme example of such a wavelength dependence is the planet Venus which has an effective blackbody temperature of 240°K near 10 μ and possibly as high as 600°K at centimeter wavelengths. A faint visible radiation has been reported from the dark side of Venus; presumably it originates in the upper atmosphere. With the exception of the earth, similar observations have not yet been made fo the other planets. The only object in the solar system, besides the sun, which is known to emit nonthermal radiation in the radio region is Jupiter.

Solar Radiation Scattered by Interplanetary Dust, Gas, and Electrons

The solar corona is visible during a solar eclipse as a luminous white halo extending for millions of miles into space. Its brightness decreases with distance from the sun. Under suitable conditions a luminous cone of light may be seen in the night sky decreasing in intensity and width in the direction away from the sun. This is the zodiacal light. It extends symmetrically along the plane of the ecliptic and at an elongation of 45° the intensity has dropped to about half its maximum value 10° from the ecliptic.[18] A slight increase in intensity, the Gegenschein, is sometimes observed in the direction opposite to the sun. It is believed that most of these phenomena are caused by the scattering of solar radiation.

Close to the photosphere the brightness of the corona is about 10^{-6} that of the solar disc, and it decreases with distance, first very rapidly and then more slowly (see Table V). Three components contribute to the corona in the visible region of the spectrum. The inner or K corona consists principally of a partially polarized white light continuum caused by electrons, moving at speeds corresponding to a temperature of about 10^6 °K, scattering light from the photosphere. The L corona, also visible close to the sun, consists of about 30 emission lines of highly ionized atoms; their presence also indicates very high coronal temperatures.

The F corona, which extends farthest from the sun, becomes predominant, according to the calculations of Ingham,[19] at between one and two solar radii from the photosphere. It consists of a white light continuum with superposed Fraunhofer lines and is slightly more red than the solar disc. It is the F corona which spreads out from the sun and becomes the zodiacal light. Van de Hulst[20] has shown that the observations of the zodiacal light agree with the assumption that sunlight is scattered by dust particles of the order

Table V. The Solar Corona and the Zodiacal Light

Elongation: Distance from sun's center in solar radii	Angle	Brightness* (10^{-12} × brightness of disc center)		Polarization[c]
1	16′	5.5×10^{6}[a]		
2	32′	2.5×10^{4}		
5	1°20′	1.4×10^{3}		
10	2°40′	2.3×10^{2}		
20	5°20′	5.8×10		
40	10°43′	1.3×10		4.0
55	14°50′	5.3		
	20°	2.4	1.3[b]**	9.7
	30°	8.8×10^{-1}	5.2×10^{-1}	21.3
	40°	4.4×10^{-1}	3.0×10^{-1}	28.7
	50°	2.6×10^{-1}	2.0×10^{-1}	31.7
	60°	1.7×10^{-1}	1.5×10^{-1}	32.9
	70°	1.2×10^{-1}	1.1×10^{-1}	33.2
	90°		7.0×10^{-2}	
	110°		5.0×10^{-2}	
	130°		4.3×10^{-2}	
	150°		4.6×10^{-2}	
	170°		5.6×10^{-2}	
	180°		6.6×10^{-2}	

* These values converted from equivalent number of tenth magnitude visual stars per square degree (S) to units of 10^{-12} times the solar disc brightness H by the formula (Roach *et al.*, Astrophys J. **119**, 253 (1954)) $\log H = \log S - 3.480$.

[a] M. F. Ingham, Monthly Notices Roy. Astron. Soc. **122**, 157 (1961).

[b] C. W. Allen, *Astrophysical Quantities* (Univ. London, 1955), p. 171.

[c] D. E. Blackwell and M. F. Ingham, Monthly Notices Roy. Astron. Soc. **122**, 113, 129, 143 (1961).

of 10^{-3} cm in size distributed throughout interplanetary space. Behr and Siedentopf[21] assumed that the polarized component of the zodiacal light is caused entirely by the scattering of free electrons in interplanetary space. On this basis they estimated an electron density of the order of 600 cm^{-3} at 1 a.u. from the sun. However, Blackwell and Ingham[18] have concluded that, from their data, the scattering is almost entirely due to dust and that it is unlikely the electron density exceeds 120 cm^{-3} at 1 a.u. Furthermore, with the improved data now available, the number of dust particles required to account for the observed scattering is appreciably less than estimated by van de Hulst and considerably closer to that predicted by observations of telescopic meteors. Blackwell and Ingham have also found that changes in brightness of the zodiacal light are correlated with geomagnetic activity, the brightness increasing by 40% when the magnetic index changed from 0 to 9. The cause of this effect is not yet definitely known. No evidence of an annual variation was observed.

In addition to measurements in the visible region,

rocket measurements[22] have shown that the entire night sky as seen from 100 km is aglow with a diffuse Ly α radiation which produces an illumination of 10^{-2} ergs cm^{-2} sec^{-1} for the entire hemisphere. The intensity drops to a minimum in the direction opposite to the sun and it is concluded that most of the radiation is solar radiation scattered by neutral hydrogen. While much of this hydrogen is probably associated with the earth,[12] part of the scattered radiation may originate from neutral atoms in interplanetary space.

Electromagnetic Radiation from Outside the Solar System

The solar system is about 30,000 light years from the center of a galaxy which has a diameter of about 10^5 light years and a thickness of about 2000 light years. The galaxy probably contains 10^{11} stars of various sorts and sizes which, together with some interstellar gas and dust, produce the greater part of the radiation flux from outside the solar system. There are also small contributions from the much more distant nebulae, most of which are too faint to be seen by the unaided eye. The greatest flux of radiation comes from directions lying close to the plane of the galaxy and from its center. This is seen as the Milky Way in the visible.

From ground level measurements through the visible and infrared windows in the earth's atmosphere it is found that many of the stars have characteristics similar to those of the sun. It is therefore to be expected that the radiation from the galaxy will span a similar broad spectral region extending from the x-ray region or even shorter wavelengths to the radio region. However, at the present time most observations have been confined to the visible and radio regions, and it is therefore only possible to give estimates of the total flux, integrated over the entire spectrum, of this radiation. There are also difficulties involved in estimating the total flux from all the extraterrestrial sources. For example, in the near visible region, the night sky is faintly luminous because of the contributions from the airglow and auroral activity in the upper atmosphere. Thus, although it is possible to measure the radiation from the brighter stars fairly accurately, the contributions from the very much larger number of fainter stars, the interstellar dust and gas, and the extragalactic nebulae are difficult to determine in the presence of the atmospheric luminescence. Sears *et al.*[23] have estimated that the starlight from the entire sky corresponds to about 1100 first magnitude visual stars ($m_v = 1$). These would give a total radiation flux of about 10^{-3} ergs cm^{-2} sec^{-1} at the earth* compared with the estimated 16×10^{-3} ergs cm^{-2} sec^{-1} from the visible airglow. The sky is not uniformly bright and Roach and Megill[24] have estimated that it varies from about 700($m_v = 10$) or 300($m_{pg} = 10$) stars per square degree in the direction of the galactic center to less than 35($m_v = 10$) or 15($m_{pg} = 10$) stars per square degree in the directions of the galactic poles.

Dunham[25] has considered the various sources which contribute to the radiation in interstellar space and has estimated a radiation density of 12×10^{-13} ergs cm^{-3}. Although this density corresponds to that in a constant temperature enclosure at about 3°K the estimated spectral distribution shown in Table VI indicates a color temperature of the radiation which increases from below 10^4 °K in the infrared to 2×10^4 °K in the ultraviolet.

In addition to their visible light, radiation has also been detected from the brighter stars in the "lead sulphide" region—from about 1 μ to 2.5 μ in the infrared—and more recently in the thermal atmospheric window from 8 μ to 14 μ, but no estimate of the total extraterrestrial flux of radiation in the infrared based on such observations has been made.

At longer wavelengths, in the radio region, there have been extensive observations of the radiation from space, and both extended and discrete sources of radiation have been detected. The discrete sources have been observed in all directions in space; some appear to be associated with objects in our galaxy and others to belong to more distant nebulae. With improved instrumental techniques it has been possible to reduce the upper limit on the solid angle subtended by these discrete sources and hence to obtain a better estimate of their spectral brightness temperatures. In the radio region of the spectrum the surface intensity I of an extended thermal source is given by $I = 3.07 \times 10^{-37}\, T\, \nu^2$ ergs cm^{-2} sec^{-1} $sterad^{-1}$ cps^{-1} where ν = frequency (cps) and T is the absolute tem-

Table VI. Spectral Distribution of Radiation Density In Interstellar Space[a]

Wavelength (microns)	0.05	0.1	0.2	0.3	0.4	0.5	0.6	0.8	1.0
Radiation density (10^{-14} ergs cm^{-2} μ^{-1})	3	11	26	34	45	62	82	121	162

[a] C. W. Allen, *Astrophysical Quantities* (Univ. London, 1955), p. 228.

* The apparent brightness of a star depends upon the intensity and spectral distribution of the radiation it emits and the spectral region over which the radiation detector (e.g., the eye, photographic plate, or photoconductive cell) is sensitive. For a given type of detector the apparent magnitude is defined as

m = -2.5 log (brightness)
m_{pg} = photographic magnitude
m_v = visual magnitude

On the visual magnitude scale
1 ($m_v = 0$) star = 2.43×10^{-6} lux outside the earth's atmosphere
$\simeq 3.1 \times 10^{-6}$ ergs cm^{-2} sec^{-1}.

perature. Leslie[26] has found that 98% of 629 discrete radio sources giving a flux density of greater than 6×10^{-23} ergs cm^{-2} (cps)$^{-1}$ had spectral brightness temperatures greater than 10^4 °K at 1.7 meters wavelength.

Radiation with a continuous spectral distribution can also be detected from the entire sky. Much of this radiation comes from the interstellar gas associated with our galaxy. It can be shown that, in comparison, the thermal radiation from stars is quite small, and indeed the sun's radiation at meter wavelengths is not too much greater than that received from an equal area of the Milky Way. Much of the radiation at wavelengths shorter than 1 meter probably comes from the thermal emission of the interstellar gas associated with our galaxy; at longer wavelengths there is probably a component due to nonthermal emission from the interstellar plasma. In addition there are also contributions from more distant sources outside the galaxy.

These various sources combine to give the celestial sphere a mean spectral brightness temperature of 700°K at 3 meters. This temperature varies both with wavelength and direction. In the direction of the galactic center it decreases from 2×10^4 °K at 30 meters to less than 10°K at 10 cm.

There have also been some measurements of the ultraviolet radiation from the sky. In the first rocket experiments[22] detectors sensitive to Ly α radiation were used. These were "blinded" by large amounts ($\sim 10^{-2}$ ergs cm^{-2} sec^{-1}) of solar radiation scattered by hydrogen atoms and no estimates of the amount of Ly α radiation coming from other sources could be made. In later experiments[27] detectors sensitive to the spectral region from 1230 A to 1350 A were used. Extended bright regions were observed centered around hot stars expected to emit large quantities of ultraviolet radiation. The brightest source, in Orion, was estimated to give a flux of 2×10^{-5} ergs cm^{-2} sec^{-1} at the top of the atmosphere, and the total flux in this spectral region due to all sources is estimated to be about 10^{-4} ergs cm^{-2} sec^{-1}. At still shorter wavelengths, less than 50 A, the influx of radiation from sources other than the sun appears to be less than 10^{-8} ergs cm^{-2} sec^{-1} A^{-1}.[14]

Although a weak flux of γ-rays in the energy range from 20 to 300 kev has been detected near 100 km altitude[15] the intensity was too low to determine whether they originated from the sun, from bremsstrahlung associated with the Van Allen radiation belts, or from a cosmic source. There has been speculation that high energy γ-rays may originate both in our galaxy and also in more distant parts of the universe. A satellite experiment with a γ-ray telescope is being developed in an attempt to detect them.[28]

Conclusions

In this survey of the electromagnetic radiation environment of interplanetary space it has been shown that the major source of radiation is the sun. There are many other fainter sources which are not expected to influence this environment to any significant degree. However, observations of these radiation fluxes made above the earth's atmosphere will greatly extend our knowledge of the external universe in the years ahead.

References

1. T. A. Chubb, H. Friedman, and R. W. Kreplin, Mém. soc. roy. sci. Liège [5] **4**, 216 (1961).
1a. J. W. Chamberlain, Astrophys. J. **131**, 47 (1960).
1b. S. Chapman, Smithsonian Inst. Publs. Contribs. Astrophys. **2**, 1 (1957).
2. H. W. Dodson and E. R. Hedeman, J. Geophys. Research **65**, 123 (1960).
3. F. S. Johnson, J. Meteorol. **11**, 431 (1954).
4. *Paris Symposium on Radio Astronomy* (ed. R. N Bracewell, Stanford Univ. Press, 1959), p. 81 ff.
5. Articles by J. H. Oort and R. H. Brown in *Handbuch der Physik* (ed. S. Flügge, Springer, Berlin, 1959), vol. 53.
6. *The Sun* (ed. G. P. Kuiper, Univ. Chicago Press, 1953).
7. R. Tousey, *Space Astrophysics* (ed. W. Liller, McGraw-Hill, New York, 1961).
8. C. R. Detwiler, J. D. Purcell, and R. Tousey, Astron. J. **66**, 281 (1961).
9. E. T. Byram, T. A. Chubb, J. E. Kupperian, Jr., and R. W. Kreplin, Astrophys. J. **128**, 738 (1958).
10. W. W. Kellogg, J. Planet. and Space Sci. **1**, 71 (1959).
11. J. D. Purcell and R. Tousey, J. Geophys. Research **65**, 370 (1960).
12. J. C. Brandt, Astrophys. J. **134**, 394 (1961).
13. H. Friedman, *Space Astrophysics* (ed. W. Liller, McGraw-Hill, New York, 1961), p. 107.
14. H. Friedman, *The Physics of the Upper Atmosphere* (ed. J. A. Ratcliffe, Academic Press, 1960), p. 133.
15. J. E. Kupperian, Jr. and H. Friedman, paper presented at Fifth CSAGI Assembly, Moscow 1958.
16. S. N. Vernov, A. E. Chudakov, E. V. Gorchakov, J. I. Lozachev, and P. V. Vakulov, paper presented at Fifth CSAGI Assembly, Moscow (1958).
17. L. Peterson and J. R. Winckler, J. Geophys. Research **64**, 697 (1959).
18. D. E. Blackwell and M. F. Ingham, Monthly Notices Roy. Astron. Soc. **122**, 113, 129, 143 (1961).
19. M. F. Ingham, Monthly Notices Roy. Astron. Soc. **122**, 157 (1961).
20. H. C. van de Hulst, Astrophys. J. **105**, 471 (1947).
21. A. Behr and H. Siedentopf, Z. Astrophys. **32**, 19 (1953).
22. J. E. Kupperian, Jr., E. T. Byram, T. A. Chubb, and H. Friedman, J. Planet. and Space Sci. **1**, 3 (1959).
23. F. H. Sears, P. J. Van Rhijn, M. C. Joyner, and M. L. Richmond, Astrophys. J. **62**, 320 (1925).
24. F. E. Roach and L. R. Megill, Astrophys. J. **133**, 228 (1961).
25. T. Dunham, Proc. Am. Phil. Soc. **81**, 277 (1939).
26. P. R. R. Leslie, Monthly Notices Roy. Astron. Soc. **122**, 51 (1961).
27. A. Boggess, III, *Space Astrophysics* (ed. W. Liller, McGraw-Hill, New York, 1961), p. 121.
28. B. Rossi, *Space Astrophysics* (ed. W. Liller, McGraw-Hill, New York, 1961), p. 96.

Applied Optics

Optical Activities in the Universities

reported by STANLEY S. BALLARD, Department of Physics, University of Florida, Gainesville, Florida. Professor Ballard hopes to receive news and comments for this column, which should be sent to him at the above address

In my January column I noted the sad state of academic optics in the U.S.A. Our situation looks even worse when compared with that in many European countries; foreign optical activities will be the subject of a future column. I mentioned that many persons are now reacting to the pitiable state of affairs in academic optics in this country, and that volunteer groups have been formulating proposals which they properly submit to the Board of Directors of the Optical Society of America. I am taking the liberty in this column of drawing rather heavily from one of these unsolicited suggestions (from "the Boston group")—it is an excellent write-up on a proposed National Institute of Modern Optics. In order to get even more people thinking along these lines, I shall sketch a possible set-up for such a national institute.

A National Institute of Modern Optics (NIMO) should be primarily concerned with fundamental or theoretical optics, and only secondarily with applied research and applications. This is not intended to suggest that applied optics is other than an important field in this country, and one that is growing rapidly due to the impetus of such national programs as space exploration and research. Rather, it implies that our weakness is on the fundamental side, and that we shall continue to grow in applications only so long as we deepen our understanding of basic principles. It is suggested, for instance, that great advances are now being made in at least two areas of modern optics: what might be called statistical optics, which includes communication and information theory and the theory of partially coherent signals and their propagation through clear and turbid media; and "optical circuitry," which is springing from recent developments in optical masers and optical fiber technology. It is not difficult to imagine the technological applications that will come from a clearer understanding of the fundamental principles in these two broad areas.

There is a good deal of research going on in fields that neighbor and even partly overlap optics, but much of this activity has been of little benefit to optics itself; I refer to microwave research, quantum electronics, linear systems analysis, etc. In microwaves and in particle physics American scientists and technologists have always been among the leaders. As a result, the industrial and engineering aspects of these fields are in a good state in this country, and research continues on a high level. Why cannot the same become true also for optics? Many of our young scientists and engineers are being trained in peripheral fields and, given the proper environment, they could become just as active and as vigorous in research fields closer-aligned to optics itself.

It is realized that some excellent optical research is being conducted in university laboratories, and perhaps an equal amount in industrial laboratories. These efforts would be strengthened by the existence of a National Institute of Modern Optics. In any case, it is certainly not proposed that financial support or scientific vigor be drained from these existing, diversified activities in order to set up a new, centralized effort. Certainly this country is able to support a greatly expanded volume of research in optics, pure and applied.

My understanding of the concept of a national institute proposed by "the Boston group" is as follows: The institute would be operated in connection with near-by universities, and there would be an intermingling of the staff of the institute with universities' faculties. Although the institute would need a permanent full-time staff as a working nucleus, there would be perhaps an equal number of visiting staff members, and professors at near-by institutions could have joint appointments and work part-time at the institute, with increased participation during the summer months. Thus graduate students in the universities could pursue their thesis or dissertation research at the institute, where presumably there would be much better facilities available for both theoretical and experimental studies. Since the university professors would also be on the institute staff there would be no question as to the propriety of the universities awarding the advanced degrees. In addition, staff members of the institute would be prepared to teach some courses at the universities, and to offer specialized, perhaps short-term courses at the request of local optical industries. Also, they would be willing to do some work of a more applied nature, but would in no case compete with the programs of established industrial laboratories. Certainly one cannot isolate "pure" optics from all applications of optical principles, and to attempt such an isolation would defeat the purpose in mind. The institute would, however, work always toward its prime objectives of research and education in optics.

It is presumed that the funding would be arranged through a prime contract with the National Science Foundation, following the pattern already established for such national research centers as the Kitt Peak Astronomical Observatory. The (nonprofit) contracting body would be made up of representatives of the associated universities, in a fashion that has worked out well not only for Kitt Peak but also for national laboratories of nuclear physics such as Brookhaven and the National Center for Atmospheric Research. For optics, it might be well to have representatives of industry and of defense agencies also on the governing board of the institute. In view of the special nature of applied optics it would be desirable to leave open the possibility of contracting with Department of Defense agencies. This, however, should be done on a broad, tri-service basis, and should be carefully coordinated with the prime contract in order to avoid conflict of interest. Contracts from industrial organizations should probably *not* be accepted—although outright grants would be welcomed! In general, the fiscal support should be of a broad-base, long-term nature so as to encourage stability of program and breadth of coverage of activity. Support made up of many small, single-purpose contracts is not an acceptable substitute since this would likely result in undue emphasis on specific items and would not provide for some of the more academic types of endeavor which cannot be justified on a short-term basis.

Will we some day have a national institute of optics, to be the intellectual center, the embryo of new ideas, the catalytic agent for applied reasearch and practical applications, the true leader in American research in optics? Only time will tell.

Infrared Satellite Radiometry

F. F. Hall, Jr. and C. V. Stanley

A 50.8 cm aperture infrared radiometer designed to detect infrared emission from satellite vehicles is described. The radiometer may be equipped with either cooled lead sulfide or indium antimonide detectors. Radiation modulation is accomplished by space filter type chopper discs enabling angular resolution of 1167 waves per radian to aid in background suppression. A nodding Newtonian folding mirror provides for scanning the $^1/_4° \times {}^1/_4°$ instantaneous field over $\pm 2.5°$ in the search-acquisition mode of operation. A memory oscilloscope is used to correlate low level signals by their ordered appearance in repeated line scans. Measurements of infrared irradiance from orbiting satellites are presented. The unfiltered PbS detector irradiance levels may be explained as being largely, if not wholly, due to reflected sunlight from the satellite. Thermal radiation from 1960 ι I (Echo I) was recorded with the InSb detector with irradiance levels on the order of 2×10^{-12} watts/cm^2 in the 2–6 μ region. A signal of this magnitude would indicate the surface temperature to be of the order of 500°K. It is shown that other satellites must have been significantly cooler than 500°K to escape detection due to their passive radiation only.

I. Introduction

The purpose of this paper is to describe the design of an infrared Satellite Tracking Radiometer and the measurement of radiation from orbiting satellites in the 1–3 μ and 2–6 μ regions. It was desired to determine whether there was anomalous infrared radiation from satellites, and to obtain information concerning their self-radiation and reflected radiation characteristics. Previous measurements with an uncooled PbS-equipped radiometer[1] indicated that near-infrared irradiance from Sputnik II was primarily due to reflected sunlight. An earlier report of anomalous radiation from Sputnik I[2] introduced some controversy on the subject, while theoretical studies[3] predicted no large sources of infrared from an orbiting object or the immediate volume of space surrounding it.

A radiometer in the form of a Newtonian telescope with a $^1/_4°$ square instantaneous field of view, together with an electrically driven modified German equatorial mount, was designed and constructed. This unit can be operated in a search or open loop track mode using either of two interchangeable infrared, cooled detectors: photoconductive lead sulfide or photovoltaic indium antimonide. Resolution of the system is 0.5 milliradians with an effective $f/1.0$ aperture for the PbS detector and $f/1.2$ for InSb. These high effective apertures are achieved by the use of radiation compression[4] after space filtering. A diagram of the radiometer is given in Fig. 1.

Numerous measurement attempts were made on orbiting vehicles, and the following satellites were tracked visually with the boresighted M-17 spotting telescope:

1959 λ	(Discoverer VIII)
1958 δ II	(Sputnik III)
1960 ζ I	(Midas II)
1960 ϵ I	(Sputnik IV)
1960 ι I	(Echo I)

Of these, infrared irradiance measurements were obtained on the last three.

II. Radiometer Design and Construction

Optics

The primary mirror has a 50.8 cm clear aperture; the focal length is 124.5 cm which gives at the optimum focus a circle of confusion of 0.6 mm. This corresponds to an angular resolution better than 0.5 mrad. Full advantage is taken of this resolution to obtain maximum space filtering. For the search mode of operation a machined brass reticle is used with spokes cut along the periphery of a 12.7 cm disc. This is rotated by a synchronous gear reduction motor to give a 1000 cps chopping rate.

The authors are with ITT Federal Laboratories, San Fernando, California.

Received 8 November 1961.

This work was supported, in part, by the Geophysics Research Directorate, Air Force Cambridge Research Laboratories.

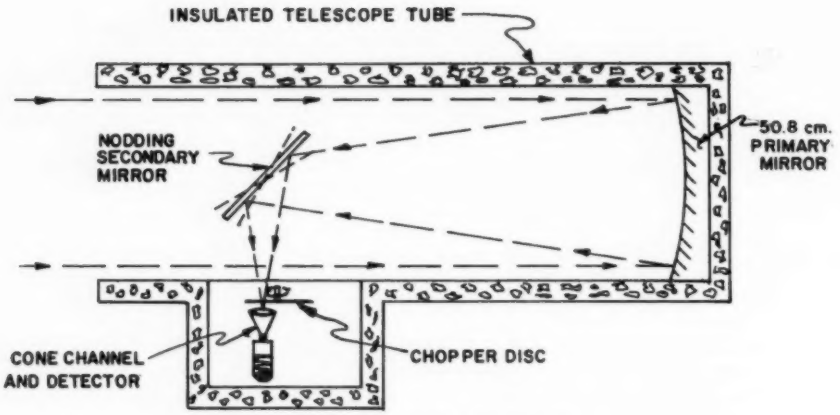

Fig. 1. Radiometer design schematic.

A nutating involute reticle is used to give a frequency modulated (FM) signal about a 1000 cps center frequency for tracking. Since the radial-spoke type of reticle provides for constant space filtering only when the spoke length is small with respect to the hub diameter,[5] an involute shape, as pictured in Fig. 2, was chosen for the track reticle because it allows constant space filtering with a relatively small size. The two reticles and their synchronous drive motors are mounted on a single movable plate inside the detector housing on the side of the telescope, to facilitate changing from search to track mode.

Radiation compression optics[4] are associated with each detector assembly. For the PbS detector, a quartz field lens and a gold plated condensing cone are used, while for the InSb, a coated germanium lens is employed. The latter system is slower than the cone channel optics, but was the only system suitable for a commercially available indium antimonide detector due to the relatively large spacing between the faceplate and the sensitive element in standard designs.

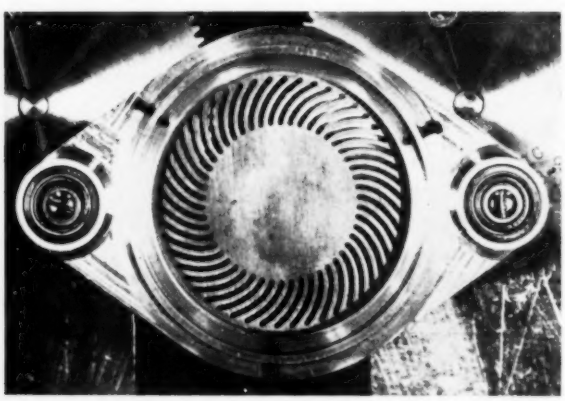

Fig. 2. Involute track reticle.

The telescope tube is welded steel structure, covered with 1.57 cm aluminum sheet, and insulated with 2.54 cm Fiberglas mats to reduce temperature variations in the wind. This tube is mounted on a counterbalanced 7.62 cm steel shaft supported by sleeve bearings on a modified milling machine table which forms the basic equatorial mount. Axes drive rates can be preset or controlled by means of slew sticks The polar axis is adjustable so that it can be set perpendicular to the predicted orbital plane of the satellite.

The Newtonian folding mirror is supported against four motor driven cams. During search operation the cam action causes the mirror to nod and simu'taneously move laterally along the axis of the telescope. This motion scans the basic $^1/_4°$ field over $\pm 2.5°$ and at the same time keeps the focal plane essentially fixed on the reticle. A detent arrangement is used to position the mirror in the center of its sweep during tracking operation. Sweep speed during search operation is variable from about one to ten scans per second.

Dowel pins are used to position accurately the detector mounts so they can be readily interchanged, and after initial alignment of the detector and compression optics they can be removed and replaced quickly without further adjustment. An impedance matching network on each detector bar allows the same preamplifier to be used for both detectors.

Small pellets (1.3 cm × 3.8 cm) of solid CO_2 are used for cooling the PbS detector, and after initial cooling will last for about thirty minutes. Pressure-fed liquid nitrogen is used to cool the InSb detector through a flexible coaxial tubing and a vacuum insulated cold finger. A quart thermos bottle is used as the supply and lasts about twenty minutes. Dry nitrogen gas circulated through the small chamber housing the lead sulfide detector prevents moisture condensation.

Electronics

The electronic design and signal processing can be best explained by referring to the block diagram, Fig. 3. Each detector has its own cell bias supply and impedance matching network so that both can be used with the same preamplifier coupled through a bandpass filter. In search operation the signal from the amplifier is fed to the bandpass filter after which it is divided. One portion is fed to the summer and the other to the quadratic detector from which it is fed to the output filter and recorder. A division of the signal is made before and after detection so that the summer receives both the modulated signal and the demodulated signal (either of which can be selected by means of a switch), and a dc signal from the counter circuit. This is added to the signal and the sum fed to the vertical input of the oscilloscope. The scanning mirror triggers the counter at each end of its sweep, and the counter supplies a dc voltage which is proportional to the count, variable from one to ten, to the summer. The storage oscilloscope can thus display up to ten scans at one time. A mirror position potentiometer supplies the horizontal sweep drive to synchronize the sweep with the mirror position. After the preset number of traces have been stored, the counter triggers the erase circuit, and a new series of sweeps can be displayed.

The search display is shown under low and high noise conditions in Figs. 4(a) and 4(b), respectively. Under the high-noise condition, it will be noted that many noise pulses are equal to or larger than the true signal, yet the eye can easily correlate the signals and pick out the simulated satellite signal with little difficulty. Since the oscilloscope sweep is synchronized with the scanning mirror, the position of the target in relationship to the axis of the telescope can also be determined by the position of the signal on the display, so that the telescope can be aligned within $\pm 1/2°$ before switching to the track mode.

During track operation, the signal from the amplifier is sent through a filter and bandpass amplifier after which it is divided, one portion proceeding as in the search mode, while the other is sent to a discriminator, buffer amplifier, and the phase detectors. Phase reference is obtained from a generator on the track reticle. From the phase detectors the signal is sent to the horizontal and vertical deflection amplifiers of the oscilloscope so that the position of the display dot is proportional to the tracking error of the telescope. Tracking may then be performed manually by observing the dot.

III. Measurement Experiments

This section will report the results of measurement

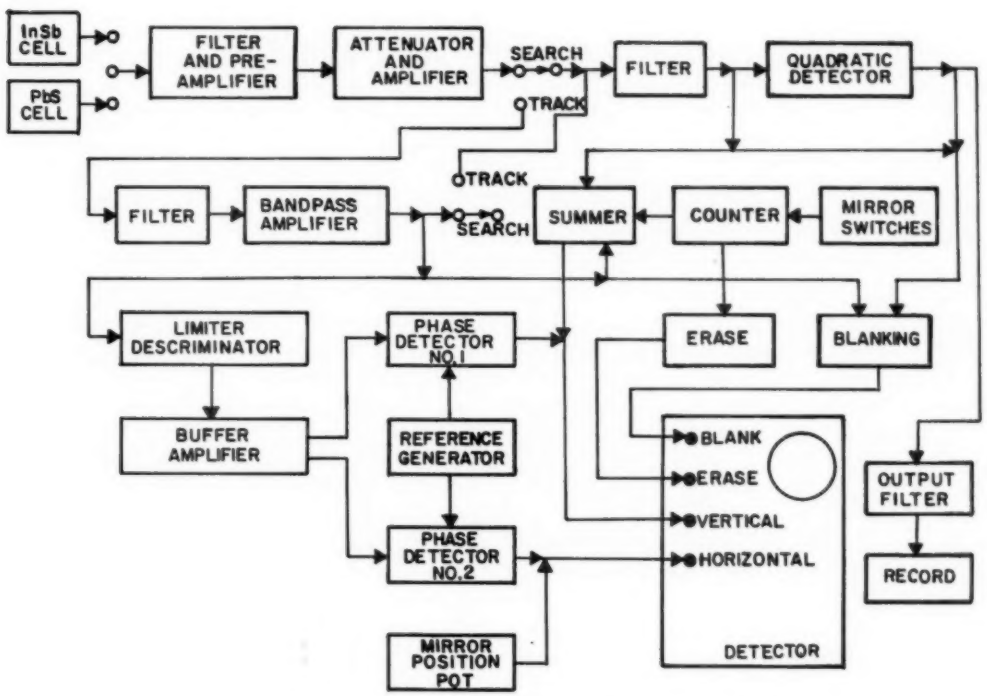

Fig. 3. Radiometer electronics block diagram.

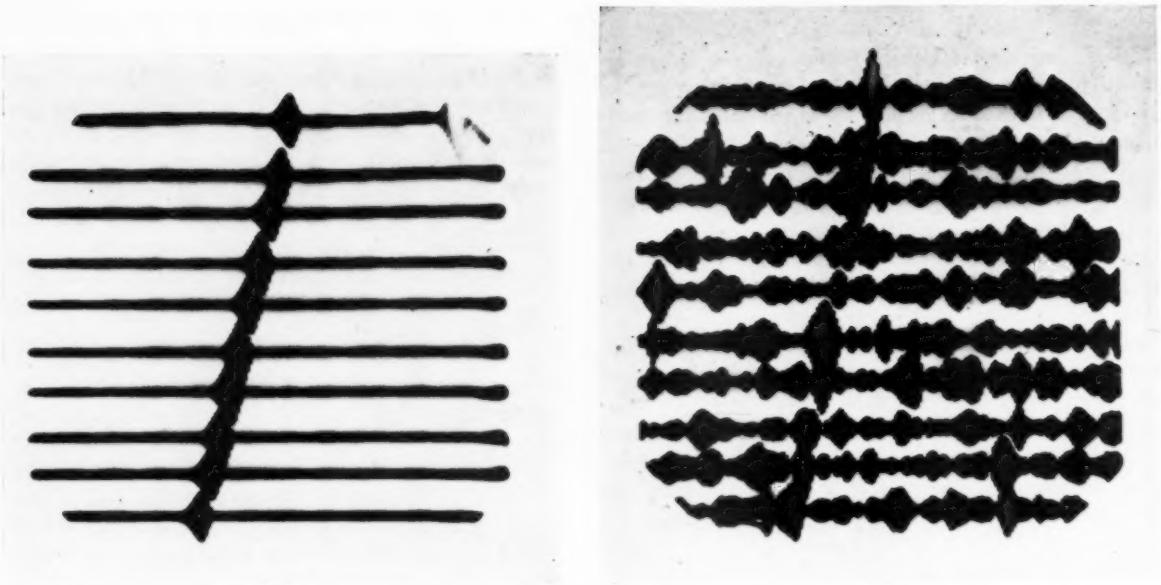

(a) (b)

Fig. 4. Memory oscilloscope search display under (a) low noise conditions and (b) high noise conditions for a given target signal.

experiments performed with the radiometer. All experiments were conducted at San Fernando, California.

Two sources of information concerning orbital elements for satellites were used during the course of this study. Information on NASA and Russian satellites was provided by the Smithsonian Astrophysical Observatory, Cambridge, Massachusetts. Orbital predictions for all known satellites were provided by the National Space Surveillance Control Center of ARDC. In addition, the Moonwatch Station at the U. S. Naval Ordnance Test Station, China Lake, California, provided on several occasions altitude, azimuth, and time predictions for various satellites. The method used to orient and slew the radiometer based on these predictions has been described previously.[6]

With the polar axis established normal to the orbital plane and having determined the maximum apparent angular velocity for a satellite as well as the time of closest approach, or culmination time, it was possible to select the slewing velocity and slew start time to insure passage of the satellite through the 5° fan over the desired portion of the observable orbit. This allowed the detection format of Fig. 4 to be used. Usually a slewing rate slower than the predicted maximum was chosen, with an early start required to "bracket" the target.

To simulate targets where some tracking noise would be expected, various stars were used as operator training aids. On several occasions, jet aircraft were acquired and tracked when at a sufficiently long range to obtain angular velocities on the order of 2° per second, or the maximum to be expected from satellites in decaying orbits.

Backgrounds

Several interesting observations on atmospheric backgrounds were made during the study. The space filtering[5] of 1167 waves per radian obtained with the instrument in the PbS region is nearly one order of magnitude higher than the 200 waves per radian reported by Eisele,[7] and it was noted that the one-dimensional angular Wiener spectrum continued to decrease at the higher frequencies at a slope of approximately -3 on the usual[5] log–log plot of (radiance)^2 per (cycle/radian) versus (cycle/radian) for clear and cloudy daytime skies. For twilight conditions, the sky background reached effective night conditions of PbS cell noise limitations over 90% of the celestial sphere when solar depression angles exceeded 9° as contrasted with the 18° depression defining the end of astronomical twilight for the visual region.

It was possible to reach a cell noise-limited operation with InSb, corresponding to an NEFD of 1.8×10^{-12} watts/cm^2 in the 2–6 μ region, only on calm, dry nights. Even then this condition was only reached when a small, 5-watt heater was optimally located in the barrel of the telescope to correct for improperly matched space filter-exit aperture geometries. A variable exit aperture as used by Moss and Brown[1] might have served as well. Winds, even as light as 5–10 mph, made it impossible to reach cell noise-limited performance, probably due to low level parcels of air with variable temperature and water content moving past the radiometer. The high emissivity of CO_2 and H_2O in parts of the 2–6 μ region probably accounts for the observed randomly-varying irradiances of the order of 2×10^{-2}

watts/cm² even with the high degree of space filtering used. Daytime backgrounds against a clear sky under calm, dry conditions (2 cm precipitable water in a vertical atmospheric column) led to NEFD's five times the cell noise-limited value, while scanning across contrails or cirrus clouds doubled the clear daytime values. At least one hour was required to reach night conditions after sunset while daytime conditions were reached one hour after sunrise.

Calibration

The radiometer was calibrated from time to time to check the detector performance and amplifier gain. An all-reflective collimator was used having a conical blackbody source, a set of carefully measured pinhole apertures, and a folded 20 cm diam $f/1$ parabolic optical system. The collimator was mounted on a wheeled base tripod with a pan-tilt head so that the exit aperture of the collimator could be made coincident with the entrance aperture of the radiometer, and the optical axes of the two instruments made to coincide. Using this technique, it was determined that the cell noise-limited NEFD of the lead sulfide-equipped radiometer was as low as 9.0×10^{-15} watts/cm² at the peak spectral response of the detector. This was determined using a 500°K calibration source. The Infrared Industries (IRI) detector used from October 1959 through early August 1960 had a peak response at slightly longer wavelength than the Eastman Kodak Ektron detector used from late August through November 1960, so that the latter yielded greater response to reflected sunlight. Both cells were always operated at dry ice temperatures.

With the indium antimonide cell, the cell noise-limited NEFD was found to be 1.8×10^{-12} watts/cm² using the 500° blackbody source and considering the effective radiation in the spectral region 1.8 through 6 μ. The electrical bandwidth for all cell calibrations was 1.0 cps.

Satellites

The initial report of the detection of artificial earth satellites with infrared equipment[2] dealt with dark passes of the satellite. Thus, it was difficult to ascertain if the target was actually in the field of view of the radiometer at the time the anomalous signals were observed. To overcome this uncertainty, attempts to measure infrared irradiance from orbiting satellites during the study were concerned first with sun illuminated satellites, so that visual correlation with any recorded signals could be made.

The NEFD of the radiometer does not reach such satisfactory values in the track mode as can be obtained with visual tracking, a stationary folding mirror, and narrow electrical bandwidths at the recorder with the search mode. Therefore, measurement attempts were made using tracking information obtained from the boresighted M-17 telescope on sunlit satellites even though sufficient irradiance to allow operation of the tracking mode was not present.

PbS Satellite Measurements

Attempts were made to detect 1959 ζ (Discoverer VI), 1959 ι (Explorer VII), and 1958 ϵ (Explorer IV) during October 1959. (Satellite identification nomenclature as given by the National Space Surveillance Control Center, L. G. Hanscom Field, Bedford, Massachusetts, is followed in this paper.) On none of the five occasions was the predicted sunlit pass observed visually in the boresighted M-17 telescope. These failures may have been due to low passes and haze on two attempts, since the China Lake, California, Moonwatch team observed the passes, and the reported magnitudes should have made the targets easily visible.[8]

1959 λ

The first satellite to be sighted visually in the M-17 spotting scope was 1959 λ (Discoverer VIII) on 5 January 1960. Although the satellite was visually tracked for approximately 20 sec, no signal was observed on the Sanborn recorder or the Memoscope display. The scan search mode of operation was used with 5 scans per second across the predicted orbit. With the bandwidth at 10 cps, the NEFD effective PbS was measured to be 4×10^{-13} watts/cm² using the IRI detector No. 1974. The visual magnitude of the satellite was estimated at no greater than +4.0 so that no reflected sunlight signal could have been detected with this NEFD,[6] but no large, anomalous radiation was present.

1958 δ *II*

The next satellite to be visually tracked was 1958 δ II (Sputnik III). The radiometer was positioned to point at the predicted orbit, but held stationary until the satellite was visually sighted. The relatively low angular velocity of 0.64°/sec allowed successful visual tracking for 58 sec, using the scanning mode of operation. Visual magnitude was estimated to be near +4.0. This estimate was later confirmed by J. G. Moore of China Lake who performed photometric measurements on 1958 δ II on 2 October 1960 and found the visual magnitude to be 4.43.[9]

No infrared irradiance was recorded from 1958 δ II although careful statistical analysis of the Sanborn record was made by determining the standard deviation of noise during a simulated satellite tracking against the sky background and comparing this information with the largest recorded pulses when the satellite was in the field of view of the radiometer. Using the χ^2 test, it was computed that the pulses measured during the time the target was in the field could be expected

in a noise distribution having the same standard deviation as obtained during the background measurements with a significance level of 70%. Since tracking was performed for only 58 sec with a coverage of approximately 30% and the bandwidth was on the order of 5 cps, there were only approximately 100 independent data points, so that for such a small population it is judged highly improbable that a significant signal was detected. With the NEFD of the system at 2×10^{-13} watts/cm^2 no reflected sunlight should have been detected,[6] and the presence of a signal would have been due to passive radiation from the satellite.

1960 ζ I

Sunlit twilight passes of 1960 ζ I (Midas II) occurred during the latter part of June 1960. The satellite was sighted on 21 June and was visually tracked for 60 sec until disappearance into the earth's shadow. The scanning search mode of operation was used with 10 scans per second, and a bandwidth of 100 cps. The estimated magnitude was +3.0 with some slight fluctuations below this value observed.

During the tracking, while the satellite was held nearly stationary in the scan field of view for over 1 sec, the Memoscope operator reported seeing correlated signals on 6 to 8 scans. The exposure from the 16 mm Memoscope recording movie camera was examined, and the correlation in the scans was indeed detectable. These pulses also were recorded on the Sanborn recorder with a probability that they were due to random noise pulses of less than 0.1%. The NEFD of the system for the 100 cps bandwidth used was 1.5×10^{-13} watts/cm^2 in the PbS region. Since the 0.21 magnitude star, Capella, of the same spectral class as the sun, yielded an irradiance of 2.8×10^{-12} effective PbS watts/cm^2 extrapolated to outside the atmosphere conditions,[6] the third magnitude satellite would be expected to yield signals near 1×10^{-13} watts/cm^2 so that the detected signals are what would be expected from reflected sunlight.

On 22 June 1960, 1960 ζ I was again detected visually and tracked for 75 sec. During this operation the Newtonian folding mirror was kept stationary so that the electrical bandwidth could be reduced to 1 cps to improve the NEFD. With the high angular velocities and the stationary $1/4°$ field of view, it was not possible to obtain better than 20% coverage of the pass. On this night the satellite brightness fluctuated more than on the previous night, and at the times of maximum brightness was not within the stationary $1/4°$ field of view. Since the magnitude was estimated to be as low as +5.0, no further information was obtained from the Sanborn recorder and reliable detection could not be proven. This experience does indicate, however, that no anomalous radiation is to be expected from such a target with irradiances greater than 1×10^{-14} watts/cm^2 in the PbS band, the effective NEFD of the radiometer on 22 June.

1960 ε I

1960 ε I (Sputnik IV) was tracked visually on 6 September 1960 for approximately 50 sec with a maximum observed irradiance of 5×10^{-14} watts/cm^2, or calculated to be 1.1×10^{-13} watts/cm^2 effective PbS outside the atmosphere. No photometric measurements of the visual magnitude of 1960 ε I are available, but it was estimated to be between third and fourth magnitude with no fluctuations observed while tracking. This would correspond approximately to the irradiance recorded in terms of reflected sunlight, so that probably no anomalous radiation or self-radiation in the PbS band was present even for this relatively low passage.

1960 ι I

The launching of 1960 ι I (Echo I) on 12 August 1960 provided a large, visually bright satellite for irradiance measurements. The radiometer was set up to detect revolution No. 10 of the satellite as calculated from Space Track Bulletin No. 1, and tracking for four minutes was accomplished. The maximum irradiance recorded with the IRI cell was 4.0×10^{-13} watts/cm^2 in the PbS region for a slant range of 1730 km. From humidity readings at the observing site and from Santa Monica weather station radiosonde data, it was calculated that there was 2.5 cm of precipitable water in the atmospheric transmission path. Using atmospheric transmission data of Howard *et al.*,[10] an effective transmittance of 0.60 was calculated. Thus, the effective PbS irradiance outside the atmosphere was calculated to be 6.7×10^{-13} watts/cm^2.

On this first pass of 1960 ι I no fluctuations in the apparent visual brightness were noticed, and it would have been interesting to have obtained entrance aperture irradiance measurements for many different zenith angles to investigate the transmittance of the atmosphere. This would have been possible for the spherical and specular satellite of these early passes, since such a source would have a constant intensity regardless of observation angle outside of the atmosphere.

Using the unfiltered EK cell No. 28, 1960 ι I was tracked and measured on the nights of 19, 24, 29, and 31 August and on 6 September 1960. All of these measurements show rapid changes in intensity which correlated with the visually observed fluctuations in the satellite brightness. These rapid intensity changes make it difficult to define the average irradiance in the PbS band. At times the signal would drop nearly to the cell noise level even when the satellite was centered in the field of view. During the brightest flashes the signal was at 100 times the noise level. This corresponds closely to brightness fluctuations observed in the visual region by Moore[9] who reported a variation

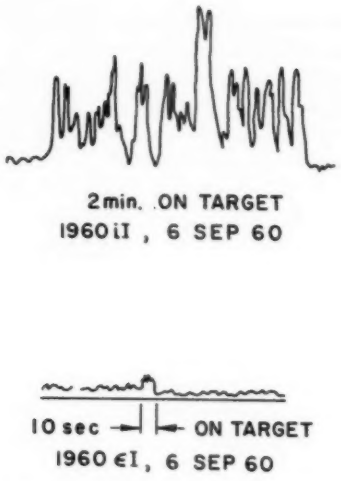

Fig. 5. Recorded PbS irradiance for two satellites.

of 5 magnitudes or 100 times as measured with his photometers.

The brightest flash observed with the unfiltered PbS Ektron Detector corresponded to an irradiance of 2×10^{-12} watts/cm² at the radiometer. Assuming an atmospheric transmittance of approximately 0.6, the irradiance outside of the atmosphere effective PbS region would have been 3.3×10^{-12} watts/cm². The more nominal bright flash would be characterized by an irradiance of 1×10^{-12} watts/cm². The average irradiance was only $^1/_3$ to $^1/_4$ of this value. As mentioned earlier, at times the signal would nearly reach the NEFD limit of the radiometer, near 10^{-14} watts/cm². A tracing of typical 1960 ι I signals is given in Fig. 5, along with signal tracings from 1960 ε I.

The extreme fluctuations of the satellite did not allow data to be gathered concerning the transmittance of the atmosphere, as would have been possible for a perfectly spherical specular target. On most of the passes the maximum intensities were observed at minimum zenith angles as would be expected for this minimum air path, but it was not possible reliably to construct an envelope to enclose these peak values.

InSb Satellite Measurements

Several attempts were made to detect 1959 ε II (Discoverer V) during February and March 1960 using the InSb cell. The satellite was never observed visually, but must have passed through the 5° search fan at a height of 250 km. It thus produced irradiances in the 2–6 μ band less than 3×10^{-12} watts/cm², the NEFD of the radiometer during these operations.

1960 ι I

The Echo balloon satellite provided a large target of low thermal capacity that could be expected to reach

Table I. Observed Infrared Irradiance at Ground Level from Orbiting Satellites

Satellite	Date	Revolution	Altitude (km)	Start range (km)	Zenith angle (deg)	Duration of track (sec)	Angular velocity (deg/sec)	Target lost due to:	Visible magnitude	Wavelength (μ)	Observed irradiance at ground level (watts/cm²)
1959 λ (Discoverer VIII)	5 Jan 60	657	196	370	57	20	1.3	Radiometer limit stops	+4	1–3	$<4 \times 10^{-12}$
1958 δ II (Sputnik III)	28 Jan 60	8958	589	690	30	58	0.64	Obscured by clouds	+4	1–3	$<2 \times 10^{-12}$
1960 ξ (Midas II)	21 June 60	434	510	580	21	60	0.74	Entered earth shadow	+3 to +4[a]	1–3	$\sim 10^{-13}$[a]
1960 ξ (Midas II)	22 June 60	449	510	590	24	75	0.74	Entered earth shadow	+4 to +5[a]	1–3	$<1 \times 10^{-14}$
1960 ε I (Sputnik IV)	6 Sept 60	1764	290	330	19	50	1.44	Inconvenient position for observer	+3 to +4	1–3	5×10^{-14}
1960 ι I (Echo I)	12 Aug 60	10	1560	1730	28	180	0.2	Obscured by trees	+1	1–3	4×10^{-13}
1960 ι I (Echo I)	19, 24, 29, 31 Aug 60	93–306	1500	1600	Varied	200 av.	0.2	Obscured by trees	+4 to 0[a]	1–3	2×10^{-14} to 2×10^{-13}
	6 Sept 60										
1959 ε II (Discoverer V)	2 Mar 60	238	286	663	65	—	0.7	Not visually observed	—	2–6	$<3 \times 10^{-12}$
1960 ι I (Echo I)	16, 29 Sept 60	435–1200	1500	1600	Varied	200 av.	0.2	Entered earth shadow, etc.	+4 to 0[a]	2–6	2.7×10^{-13}
	20, 21 Oct 60										
	12, 21, 22 Nov 60										

[a] Signal fluctuated due to tumbling.

equilibrium temperatures rapidly when in sunlight. Its low angular velocity allowed tracking with narrow bandwidths so that an NEFD of 1.8×10^{-12} watts/cm² in the 2–6 μ region could be obtained. 1960 ι I was tracked visually using the search mode of operation with stationary diagonal mirror, on seven different occasions in the autumn of 1960. A careful analysis of the recorded signals indicated an irradiance of 2.7×10^{-12} watts/cm² which did not fluctuate as did the visual brightness. The measured irradiance was so close to the NEFD of the instrument that a null hypothesis analysis was performed to test the reliability of detection. This analysis was aided by the measuring procedure of noting on the record when the target was centered in the radiometer field and when it was not. It was determined that detection was achieved with a reliability of better than 0.99 on all occasions.

IV. Conclusions

Results of the various irradiance measurements are summarized in Table I. The PbS measurements do not indicate the presence of any passive or exotic radiation from orbiting satellites. In order to be absolutely certain that the observed signals were due only to reflected sunlight, simultaneous measurements with visual region photometers would have been required; these were not made. Visual magnitude estimates by the radiometer operator and several photometric measurements performed at a remote site[9] resulted in predicted PbS irradiances, based on a 5800°K source, within 20% of the observed values.

The failure to detect radiation from 1960 ζ I when at visual magnitudes less bright than 3.0 allows the calculation of a tentative maximum satellite temperature. A sample painted panel furnished by Lockheed Missiles and Space Division, simulating the skin of the Midas vehicle, was found to have an emissivity $\epsilon = 0.5$ in the PbS region. With the instrument NEFD of 1.0×10^{-14} watts/cm², an atmospheric transmittance of 0.5, and a 5 meter² area, the satellite must have been radiating less than 4.4×10^{-3} watts/cm² below 3 μ, requiring a surface temperature below 530°K. This is a much higher value than would be expected from absorbed solar radiation alone, since the ratio of solar absorptance of the painted surface, a, to the average thermal emittance for intermediate and longer infrared, ϵ, is less than $1/4$. Hass *et al.*[11] have calculated equilibrium temperatures for massive satellites and obtain 210°K for $a/\epsilon = 1/4$, so the failure to detect passive PbS region radiation from the satellite surface is to be expected.

It should be noted that PbS measurements were made only for satellites with altitudes of 196 km or greater. The possibility that anomalous infrared radiation might exist at lower altitudes has not been disproven.

The measurement of radiation from 1960 ι I in the 2–6 μ region requires further comment. On several occasions when the satellite was observed to be visually less intense than the first magnitude star, Capella, with similar spectral characteristics to the sun, the signals were detected. Capella could not be detected with the InSb cell, and an extrapolation of PbS irradiance from this star[6] predicts 3.1×10^{-13} watts/cm² in the 2–6 μ band at the surface of the earth, nearly one order of magnitude below the NEFD of the radiometer. Thus, if the detected radiation from the satellite were reflected sunlight, the 2–6 μ reflectance of the balloon must have been at least ten times the visual reflectance, an unacceptable conclusion in light of the high visual value.

To produce the observed irradiance, it was calculated the satellite thermal radiant intensity was 180 kw/sterad. Since the softening point of the Mylar surface is 525°K, the temperature was certainly considerably less, but if the balloon diameter is assumed to be 30 meters one must conclude that the temperature was near 500°K, a temperature reached only when the solar absorptance is three to four times the thermal emissivity. These were not the design values for the surface, but perhaps sputtering or crazing had caused such changes after two months in space when the measurements were made.

The guidance of R. K. Orthuber throughout the project, the electronic designs by T. P. Dixon, and the many hours of field assistance by H. D. Coombes were important aids in this study.

References

1. T. S. Moss and D. R. Brown, Tech. Note RAD. 720, Royal Aircraft Establishment, Farnborough (September 1958).
2. Aviation Week **67**, 31 (November 4, 1957).
3. R. E. Good, Mass. Inst. Tech. A-R 517, SS-38 (April 25, 1960).
4. D. E. Williamson, J. Opt. Soc. Am. **42**, 712 (1952).
5. G. F. Aroyan, Proc. IRE **47**, 1561 (1959).
6. F. F. Hall, Jr., C. V. Stanley, and T. P. Dixon, Scientific Report No. 1, AF 19(604)-4971, AFCRL-215 (ASTIA AD257 170) (December 1960).
7. R. E. Eisele, Infrared Background Investigations, Final Report, AF 19(604)-3473, Ramo-Wooldridge Report C20-OU11 (May 1, 1960).
8. C. L. Evans, private communication.
9. J. G. Moore, private communication.
10. J. N. Howard, D. E. Burch, and D. Williams, J. Opt. Soc. Am. **46**, 186, 237, 242 (1956).
11. G. Hass, L. F. Drummeter, and M. Schach, J. Opt. Soc. Am. **49**, 918 (1959).

Infrared Spectroscopy of Planets and Stars

William M. Sinton

Infrared spectroscopy of the brighter planets and stars has been performed, and sample spectra of some objects are presented; the sensitivity limit for this purpose of scanning spectrometers is discussed. The spectrometer which has been used for three years is described. Advantages of a two-beam interferometer and its sensitivity increase are also presented.

Introduction

G. P. Kuiper has demonstrated the kind of studies that can be made of planets and stars with a near infrared spectrometer attached to a large telescope.[1-3] Near infrared spectroscopy provides the means for detecting many molecules through absorption by their vibration-rotation bands, and often these are molecules that otherwise would not be detectable by visible and near-ultraviolet spectroscopy. Kuiper used a quartz-prism spectrometer with a lead-sulfide detector attached to the McDonald 2-meter (82-in.) reflector, and with this equipment he found CO_2 in the atmosphere of Mars, showed that its polar cap is composed of ice, and detected $C^{13}O_2$ in the atmosphere of Venus.

In stellar spectra he found bands in low temperature, very red stars; these bands have not been identified. The low-temperature stars offer possibilities here because of the abundance of molecules in their atmospheres and because in this spectral region they are, for the same visual brightness, much more luminous than higher-temperature stars.

Limitations to Infrared Astronomical Spectroscopy

The primary limitation in infrared spectroscopy is the lack of sufficient energy for detection and measurement. In laboratory spectroscopy this situation can be partly alleviated by using higher-temperature sources and larger-aperture instruments. On the other hand, in astronomical work, the sources cannot be modified. One must make the optimum use of the available energy. The larger the telescope, the greater is the available energy, but practical limitations set in. For a given telescope the resolution of a conventional scanning spectrometer is set by the spectral slit width which gives sufficient energy incident on the detector to provide a satisfactory signal-to-noise ratio.

A numerical example will help here. Let us assume that we want to observe a planet or a star which has the spectral energy distribution of the sun and has a visual magnitude of -1.73; since the sun's visual magnitude is -26.73, the object is 25 magnitudes or 10^{10} times fainter than the sun. At 3 μ the sun provides 2.6×10^{-3} watts cm^{-2} μ^{-1} outside of the earth's atmosphere.[4] If we have a detector with a noise-equivalent power of 10^{-12} watts and a telescope collection area of 1.7×10^{5} cm^2 (the Hale Telescope of Mt. Palomar; 5-meter (200-in.) diam) and if we desire a signal-to-noise ratio of 100, we can obtain a resolution of $\Delta\lambda = 0.023\,\mu$, or $\lambda/\Delta\lambda = 130$, or $\Delta\nu = 25.6$ cm^{-1}. Furthermore, if the available energy is reduced by atmospheric absorption and transmission losses in the telescope and spectrometer, these figures are changed accordingly. Fortunately this resolution is sufficient for detecting strong absorption bands on the brighter planets and stars. But this resolution is not sufficient to resolve the rotational structure of these bands. Improvement of the detector sensitivity will obviously help, but the question is—what can be done with presently available detectors to obtain the greatest sensitivity?

The Present Infrared Spectrometer

With the aforementioned limitation on scanning spectrometers, there is relatively little that can be done to increase their sensitivity other than to assure that as much as possible of the light available at the focus of the telescope is imaged on a detector of the highest sensitivity obtainable. In the author's modified Perkin Elmer Model 98 spectrometer (see Fig. 1) three particular parts were treated with considerable care to maximize its efficiency.

The first area of attention is the method of chopping

The author is at The Lowell Observatory, Flagstaff, Arizona.
Received 9 November 1961.

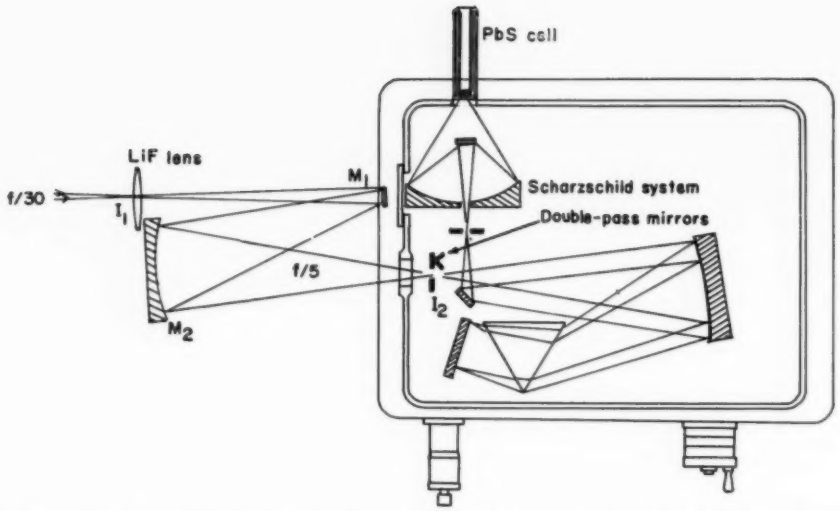

Fig. 1. Schematic diagram of the Perkin-Elmer spectrometer showing the modifications which were made for astronomical use.

to achieve ac detection. In the usual chopping technique, half of the energy is wasted with an opaque chopping blade. In the scheme utilized here the position of the image on the entrance slit is made to oscillate up and down between two discrete positions and therefore also at the exit slit, and eventually the light falls alternately on two separate detector areas. These are connected in opposition and twice the signal of half-wave chopping is obtained. Because the noise voltages from the two areas are not correlated, the total noise is increased to $2^{1/2}$ of that of one area alone and the signal-to-noise ratio is increased by $2^{1/2}$.

An additional feature of this method of chopping is obtained by imposing radiation from the sky adjacent to the planet on the second detector area when the object is on the first. In reality, because the effective temperature of the sky is much less than that of the detector, the net energy transfer is from the detector to the sky. In the usual chopping procedure, this radiation will produce a signal which confuses the desired spectrum. Of course the effect of this signal can be removed by taking a spectrum of the sky alone and extracting the difference between its spectrum and that of the desired object. This procedure, however, requires additional time.

By alternating the object and the sky adjacent to it on the detector, one obtains the signal from the object free from this interference. The time which would be spent obtaining spectra of the sky may be used for more spectra of the object. The net signal-to-noise ratio of the mean of the spectra is therefore increased by an additional $2^{1/2}$. The total gain of the two-cell chopping system is 2 in the signal-to-noise ratio.

The method of producing this chopping is illustrated in Fig. 2. A small mirror, M_1, is caused to execute rotational oscillation about an axis parallel to the plane of the mirror and produces a linear displacement of the image I_2. The image motion is nearly square-wave and is produced by the driving coil of a small loudspeaker. The mechanical system for moving the mirror is a critically-damped resonant system and is comprised of the torsional supporting wire, the moment of inertia of the mirror and its support, and the damping produced by a heavy grease encasing the driving wire in a confining hole. In order to have sufficient motion with relatively low driving power, the restoring torsional force of the wire must be relatively weak. But in order to satisfactorily execute the square-wave motion, the resonant frequency must be many times higher than the chopping frequency. The high resonant frequency with a weak restoring force is only obtained by making the moment of inertia of the mirror and its support as small as possible. In practice, a mirror, 15 mm in diameter and 2 mm thick, could be oscillated in a nearly square-wave motion of a few degrees at 45 cps with several watts of driving power. The nondamped resonant frequency of the mirror and torsional support is about 300 cps. The schematic diagram of the oscillator and amplifier for driving the mirror is given in Fig. 3. An output transformer is not used in this circuit so that the chopping frequency can be as low as 10 cps if desired. The required image motion of 2 mm was easily ob-

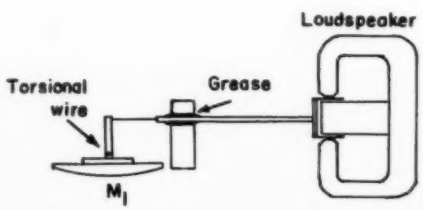

Fig. 2. The method of driving the oscillating chopper mirror.

NEW SUBSCRIPTION ORDER

APPLIED OPTICS

Please enter my/our subscription for 1962* and continue until countermanded:

- ☐ OSA member rate $6.00 per year
- ☐ Other AIP Societies' rate $8.00 per year
- ☐ Regular rate $10.00 per year
- ☐ Please send OSA membership information
- ☐ check enclosed ☐ bill me
- ☐ Single copy of issue $2.00

Name ..... Membership No. .....

Address .....

.....

*Subscriptions entered for calendar year only.

NEW SUBSCRIPTION ORDER

APPLIED OPTICS

Please enter my/our subscription for 1962* and continue until countermanded:

- ☐ OSA member rate $6.00 per year
- ☐ Other AIP Societies' rate $8.00 per year
- ☐ Regular rate $10.00 per year
- ☐ Please send OSA membership information
- ☐ check enclosed ☐ bill me
- ☐ Single copy of issue $2.00

Name ..... Membership No. .....

Address .....

.....

*Subscriptions entered for calendar year only.

FIRST CLASS
Permit No. 33649
Washington, D. C.

BUSINESS REPLY MAIL
No postage stamp necessary if mailed in the U. S. A.

POSTAGE WILL BE PAID BY

APPLIED OPTICS
Optical Society of America
1155 Sixteenth Street, N. W.
Washington 6, D. C.

FIRST CLASS
Permit No. 33649
Washington, D. C.

BUSINESS REPLY MAIL
No postage stamp necessary if mailed in the U. S. A.

POSTAGE WILL BE PAID BY

APPLIED OPTICS
Optical Society of America
1155 Sixteenth Street, N. W.
Washington 6, D. C.

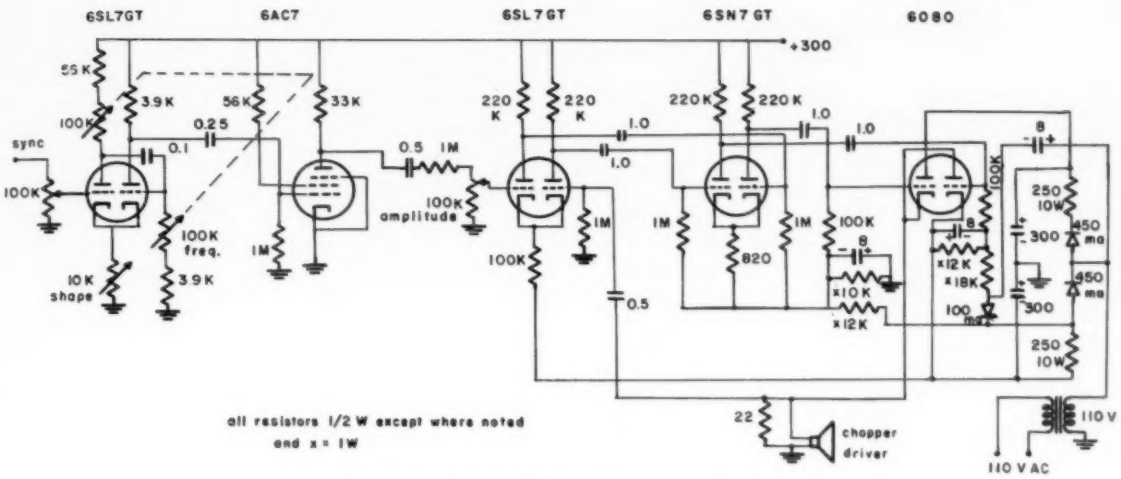

Fig. 3. Oscillator and amplifier for driving the oscillating mirror.

tained with the driving system. The optimum chopping speed for the lead-sulfide detector that was employed was near 45 cps.

The second area of attention was the condensing system lying between the exit slit and the detector. Since the noise-equivalent power of a detector is proportional to its linear size, obviously, the greater the demagnification in the condensing system, the greater can be the spectrometer sensitivity, providing that the detector size is decreased accordingly.

A Schwarzschild mirror system was designed to fit inside the housing of the Perkin-Elmer monochromator, and transferred the light from the exit slit to just outside the exit window of the monochromator. The characteristics of this system are given in Table I. Only slight modifications to the monochromator housing had to be made for it to contain these mirrors.

The last area of attention was the detector. It was selected from two custom-made lead-sulfide detectors fitted in to liquid-nitrogen dewars. These detectors each have three rectangular areas 0.15 × 0.3 mm. Two of these are used together and by rotation of the dewar cell the sensitive regions projected back to the exit slit may be either 1 mm wide by 2 mm high, or 2 mm wide by 1 mm high. The beam converging from the condenser encompassed 100° and most of the region of space surrounding the detector areas which is not utilized for this beam is shielded from room-temperature radiation by a baffle at 77°K. Tests of the entire spectrometer system, which were made by observing blackbody cavities close to room temperature, indicate that the noise-equivalent power of the cell with a final filtering time constant of 1 sec is 1×10^{-12} watts at 3.75 μ.

Other changes to the monochromator are minor. Two small mirrors were added near the lower half of the entrance slit to give double passage of the light through the monochromator. If the two beams of light from the chopper are focused at the top half of the entrance slit, the spectrum falls on the lower part of the slit plane and is returned to the prism by the double mirrors. The final spectrum falls at the top half of the exit slit and is imaged on the detector. If, on the other hand, the light is admitted at the bottom of the entrance slit, the spectrum is imaged on the top part of the exit slit and immediately goes to the detector after only one passage of the monochromator. Therefore, single- or double-pass operation is easily chosen by adjustment of M_2.

The lithium fluoride field lens images the telescope mirror 90 mm behind the entrance slit, and because of the properties of the Littrow optics, another image of the objective falls 90 mm behind the exit slit where it falls on the convex mirror of the Schwarzschild system.

All the mirrors of the system are coated with gold rather than aluminum, in order to benefit from the former's higher reflectance.

Some Spectra of Astronomical Objects

Figures 4, 5, and 6 illustrate some of the spectra that have been taken with a lithium fluoride prism. Stars of spectral class M or redder, even though they are faint visually, may be of sufficient intensity to be observed with this instrument. The long period variable star R Leonis (Fig. 5) is such an example. At the time its spectrum was taken with the 107-cm (42-in.) telescope, its visual magnitude was 5.8. As

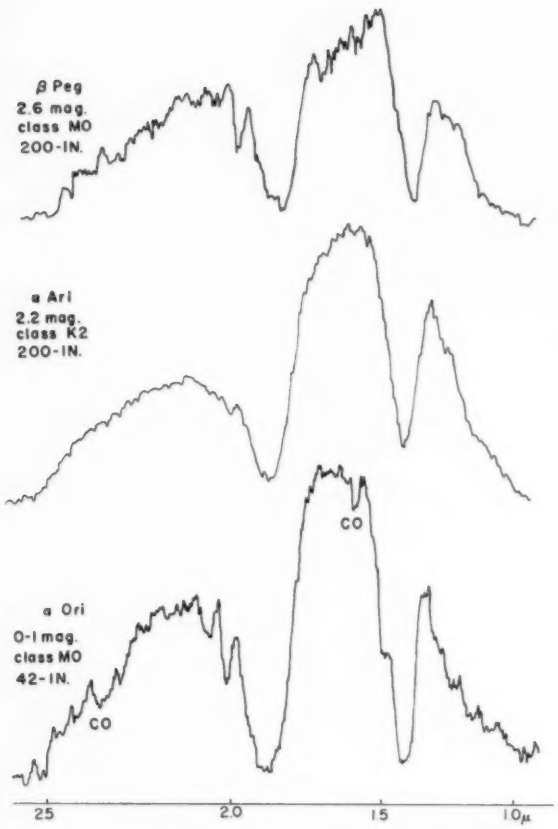

Fig. 4. Typical spectra of several stars which have been obtained with the spectrometer. Absorptions that are tentatively attributed to carbon monoxide are marked in the spectrum of α Orionis. Upper curve: β Pegasi, 2.6 magnitude, class MO, 5-meter (200-in.) telescope. Middle curve: α Aries, 2.2 magnitude, class K2, 5-meter (200-in.) telescope. Lower curve: α Orionis, 0–1 magnitude, class MO, 107-cm (42-in.) telescope.

was previously mentioned, low-temperature stars are more likely to have molecules in their atmospheres that can be observed with the spectrometer. An example is in Fig. 4 where two absorptions in α Orionis have been tentatively identified as belonging to carbon monoxide.

The possibilities inherent in planetary work are demonstrated by the discovery by the author of organic molecules in the dark regions of the Martian surface.[5] Recent spectra of Venus (Fig. 5) show the presence of carbon monoxide as well as carbon dioxide in that planet's atmosphere.

Advantage of the Interferometric Technique

As has been pointed out by Fellgett[6] a substantial gain may be obtained when the limitation is due to noise inherent in the detector by using an interferometer rather than a spectrometer. The interferogram, which is obtained by recording the detector response while varying the path difference in a two-beam interferometer, is the Fourier transform of the spectrum. The gain in sensitivity of this method is nearly $N^{1/2}$ where N is the number of resolution elements in the spectrum. If the range covered is 2 to 4 μ and the resolution is 0.02 μ, N is 100. Therefore objects which are 10 times fainter may be observed by using the interferometer rather than the spectrometer. On the other hand, if the same object is observed by the two methods and N resolution elements are obtained with the spectrometer, $N^{3/2}$ elements may be obtained with the interferometer for the same signal-to-noise ratio in the final spectrum. For our example given above, the limiting resolution width will be 0.002 μ.

The author is at present constructing an interferometer for use in the 1–4 μ region. It is hoped that with this instrument, by using the gain toward fainter objects smaller regions of Mars may be observed for studying the distribution of the organic molecules. In the spectrum of Venus, the gain in resolution may permit separation of the CO and CO_2 bands into individual rotation lines. Studies of effective rotational temperatures can then be made.

Table I. Parameters of the Schwarzschild System

Exit slit to convex mirror	78.5 mm
Radius of convex mirror	17.3
Diameter of convex mirror	20.6
Separation of mirrors	43.9[a]
Radius of concave mirror	61.2
Diameter of concave mirror	108.0
Concave mirror to final focus	75.2[a]
Exit slit to final focus	109.4[a]
Demagnification	0.146
Numerical aperture at final focus	0.78
Observed resolution at final focus	30 line pairs/mm

[a] The separation of the mirrors is adjusted for highest resolution, and the position of the final focus is changed accordingly.

References

1. G. P. Kuiper, W. Wilson, and R. J. Cashman, Astrophys. J. **106**, 243 (1947).
2. G. P. Kuiper, Astrophys. J. **106**, 251 (1947).
3. G. P. Kuiper, *The Atmospheres of the Earth and Planets* (Univ. of Chicago Press, Chicago, 1952), 2nd ed., pp. 351–365.
4. C. W. Allen, *Astrophysical Qualities* (The Athlone Press, London, 1955), p. 140.
5. W. M. Sinton, Science **130**, 1234 (1959).
6. P. Fellgett, J. phys. radium **19**, 187 (1958).

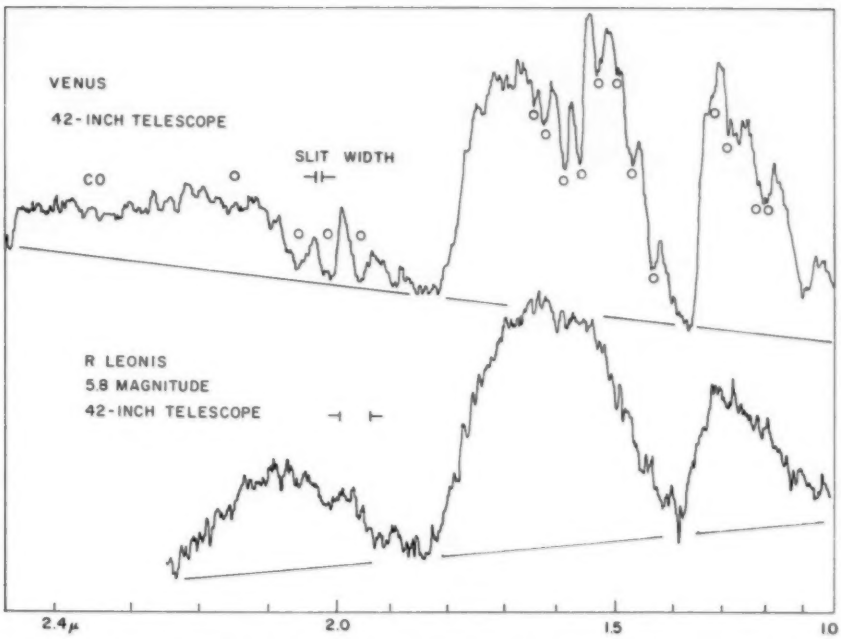

Fig. 5. Spectra of Venus and the red variable star R Leonis. Absorption peaks by CO_2 in the spectrum of Venus are marked with circles. The absorption by the 2–0 band of CO is also designated. Upper curve: Venus, 107-cm (42-in.) telescope. Lower curve: R Leonis, 5.8 magnitude, 107-cm (42-in.) telescope.

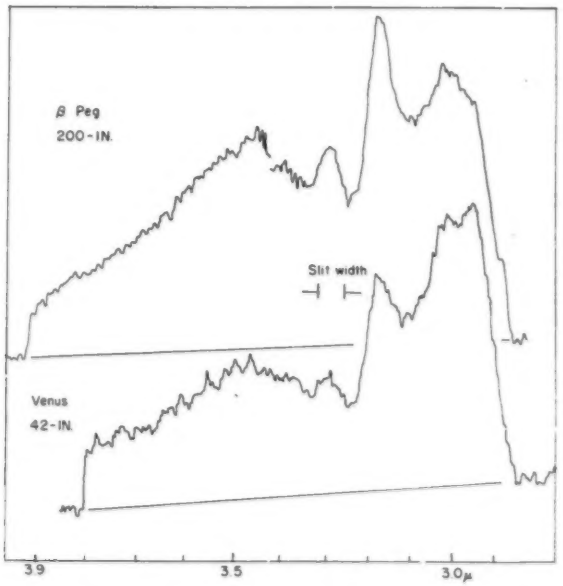

Fig. 6. Spectra obtained beyond 3 μ. The spectrum of β Pegasi is comprised of two separate spectra which individually were marred by clouds in the unshown parts on either side of the break in the middle. Upper curve: β Pegasi, 5-meter (200-in.) telescope. Lower curve: Venus, 107-cm (42-in.) telescope.

Contents of Optics and Spectroscopy

VOL. XI NOVEMBER and DECEMBER 1961 *These issues will be published in complete translation by the Optical Society of America in March 1962*

November 1961 issue

Yu. I. Ostrovskii and N. P. Penkin. Measurement of the Absolute Values of Oscillator Strengths in Atomic Spectra

F. S. Faizullov and N. N. Sobolev. Determination of the Effective Cross Section for Collisions of Excited Barium Ions with Argon Atoms

B. N. Snegirev. Vibrational Spectra of Aromatic Compounds. XI

A. N. Lazarev and T. F. Tenisheva. Vibrational Spectra of Silicates. III

T. V. Yakovleva, A. A. Petrov, and M. D. Standnichuk. Vibrational Spectra and the Structure of Enyne Silicon-Hydrocarbons

T. V. Yakovleva and A. A. Petrov. Depolarization of Multiple Bond Lines in Raman Spectra of Vinyl-Acetylene Hydrocarbons as Related to Their Structure

T. V. Ivanova and B. Ya. Sveshnikov. On the Luminescence of Alcoholic Solutions of Benzene at −196°C

R. N. Nurmukhametov, D. N. Shigorin, Yu. I. Kozlov, and V. A. Puchkov. Effect of Hydrogen Bond on the Luminescence of Oxy- and Amino- Azo Compounds

L. A. Kiyanskaya and B. Ya. Sveshnikov. On Quenching of Fluorescence in Solutions at Liquid Air Temperature by Iodides

M. D. Khalupovskii. On the Phosphorescence of Organic Molecules with Two Metastable Levels

A. M. Bonch-Bruevich, B. P. Kovalev, L. M. Belyaev, and G. S. Belikova. Study of Kinetics of the Sensitized Radiation of Certain Additions in Naphthalene Crystals

N. D. Zhevandrov, V. I. Gribkov, and I. D. Khan-Magometova. Influence of Excited Light Birefringence on the Luminescence Polarization in Molecular Crystals

A. N. Zaidel and G. S. Lazeeva. Photoluminescence of Solutions and Crystals of Gadolinium Salts

V. V. Osiko. Intercrystalline Reactions in Crystal Phosphors and the Structure of Luminescence Centres

L. Drozd and V. L. Levshin. Arrangement of Energy Levels in ZnS–CdS Phosphors

A. A. Bundel, Z. I. Guretskaya, and M. N. Noskova. Isolation of the Selenium Band in the Spectra of Sulfide-Selenide Luminors

I. N. Shklyarevskii and R. G. Yarovaya. Optical Properties of Beryllium in the Infrared Spectral Region

A. O. Sall. On the Sensibility Threshold of Optical Absorption Analysis of the Composition of Liquid or Gaseous Mixtures

A. O. Sall. On the Theory of Selectivity of Optical Absorption Analyzers of the Composition of Gaseous or Liquid Mixtures. I

I. P. Zapesochnii and A. I. Dashchenko. Oscillographic Method of Studying Optical Functions of Excitation

N. A. Pankratov. Nonselective Optico-Acoustic Radiation Receivers with Electrodynamic Microphone

K. I. Tarasov. Spectrograph with Crossed Dispersions Built after a New Optical Design

Yu. S. Varshavskii. Relation between the Frequencies of N—H Symmetric and Antisymmetric Vibrations in the Molecules of Primary Amines

S. I. Levikov and L. P. Shishatskaya. Comparison of Spectral Intensities of the Hydrogen and Deuterium Radiation

V. G. Boitsov and Yu. Ya. Gotlib. Calculation of the C—O Stretching Vibration Frequency for Cis- and Curled Isomers of Molecules of the Type $ClCH_2—C(=O)—RV$

A. S. Selivanenko. Exciton Relaxation Times in Molecular Crystals

Yu. I. Turkin and M. P. Chaika. Anomalous Ratio of the HFS Component Intensities of Indium Lines

December 1961 issue

O. P. Bochkova, L. P. Razumovskaya, and S. E. Frisch. Spectroscopic Investigations of the High Frequency Discharge in Neon

A. M. Meleshina. Application of the Metal Molecular Model to the Calculation of the Influence of Molecular Vibrations on Forbidden Transitions

K. K. Svidzinskii. Calculation of the Hyperfine Structure of Rotational Spectra of Molecules

V. M. Tatevsky, G. S. Koptev, and A. A. Maltsev. Vibrational Spectra of B_2O_3 and B_2S_2 Molecules

E. M. Popov and G. I. Kagan. Vibrational Spectra of Vinyl Alkyl Sulfides. Theoretical Analysis

G. V. Peregudov. Interpretation of the Vibrational Spectra of Naphthalene and Some of its Deuterosubstitute

M. S. Brodin and Ya. O. Dovgy. Optical Properties of Crystals with Impurities. I

N. Ya. Gorban and I. A. Shainkevich. Phase Relations for the p- and s- Components of a Reflected Light Wave Determined by Fresnel's Formulas

A. P. Ivanov. Study of the Reflection of Light in Objects Discolored

A. O. Sall. Theory of the Selectivity of Optical Absorption Analyzers for the Composition of Gas or Liquid Mixtures. II

P. P. Kasyankov. Calculation of the Aberrations of Cathode Lenses

M. S. Soskin. On the Determination of the Refractive Indices of Crystals Using a Jamin Interferometer

M. D. Borisov, I. Demidenko, and V. G. Padalka. Determination of the Electron Concentration in the Conductivity Zone at the Limit of Transition of Thin Aluminum Films in the Vacuum Ultraviolet Region

F. S. Ortenberg. On the Relative Vibrational Probabilities of Transition in the Band System $^2\Delta \rightarrow {}^2\Delta$ of the VO Molecule

L. M. Sverdlov. Calculation Formula for the Intensities of the Raman Spectra of Polyatomic Molecules

L. M. Volkova. Effective Cross Sections for Excitation of Certain Spectral Lines of Sodium

V. M. Zakharova, Yu. M. Kagan, and V. I. Perel. Spectroscopic Observation of the Rotation of a Positive Column of Discharge in a Magnetic Field

V. P. Muratov. Telecentric Optical System for Illumination of the Entrance Slit of a Spectral Instrument

M. L. Veingerov, A. A. Sivkov, and Byan Nan-khua. Incandescent Lamp with a Radiometric Modulator

The Elimination of Scattered Light in Solar Spectrographs

J. W. Evans and J. Waddell

The double pass system in the Littrow spectrograph at the Sacramento Peak Observatory is described. This system, as well as increasing the resolving power of the spectrograph, eliminates all effects of Rowland ghosts, extended instrumental profile wings, and diffuse scattered light.

Introduction

The application of a double pass or multiple pass arrangement in spectrographs for the purpose of increasing dispersion and resolution has become an accepted practice in laboratory spectroscopy. The properties of such systems were investigated in the early 1950's by Walsh,[1] Jenkins and Alvarez,[2] Fastie and Sinton,[3] and Rank and Wiggins,[4] among others. About the same time, one of the authors (Evans) included a double pass system in the design of the Sacramento Peak Observatory 13-meter Littrow spectrograph, primarily for the purpose of minimizing scattered light in photoelectric observations of Fraunhofer line profiles. The other author (Waddell) has tested the characteristics of the system and its ability to eliminate scattered light in the cores of the NaD lines. The results surpassed expectations, and the double pass arrangement is now used at the Sacramento Peak Observatory in all photoelectric observations of absorption line profiles. The purpose of this paper is to call attention to the advantages of the system for absorption line spectroscopy and to describe its rather simple principle of operation. Almost any existing large spectrograph may be easily modified to incorporate its advantages.

Principles of the Double Pass Optical System

The essentials of the double pass arrangement are shown schematically in Fig. 1 which pictures the components at the slit end of a Littrow spectrograph with dispersion in the vertical direction. In ordinary photography, light from slit s_1 is reflected by the grating to the photographic plate, f. For double pass operation, however, the grating is rotated about the vertical axis to reflect the spectrum to prism p_1, which reflects it to prism p_2 through an intermediate slit s_2. From p_2 the light passes again to the grating, back to the final defining slit, s_3, and through it to the photoelectric cell. A field lens cemented to the prism p_1 images the grating on itself. The whole double pass assembly can be mounted on a plate a few inches square. Figure 1(b) is an end view of the components, looking toward the grating to illustrate reasonable dimensions relative to the slit length to be used.

This arrangement converts the spectrograph into a powerful double monochromator, in which the same grating is used twice. It should be noted, however, that the system is incapable of suppressing undesired orders of the grating. A number of different arrangements are possible. The one shown, with one roof prism in the train, has the property of compensating both tilt and curvature in the spectral lines. Thus, s_3 and s_1 are straight and parallel at all wavelengths. Slit s_2 is generally wide enough to permit the use of a straight slit at fixed inclination, since its purpose is to isolate a fairly broad band relative to that which passes s_3. The important features are the presence of an intermediate slit smaller than the separation between the transmitted band at λ_0 and its first Rowland ghosts, and some device for inverting the spectrum in reflecting it back to the grating. The latter is the condition for the dispersions of the two passes to add rather than cancel.

The light traversing the intermediate slit contains a narrow band of the spectrum centered at wavelength λ_0, plus scattered light of other wavelengths. On the second pass, the grating dispersion separates this scattered light from the λ_0 band in the final focal plane. Thus the exit slit s_3, when properly adjusted, transmits λ_0 uncontaminated by the scattered light. Although

The authors were both at the Sacramento Peak Observatory, Sunspot, New Mexico. J. Waddell's present address is Kitt Peak National Observatory, 950 North Cherry Avenue, Tucson, Arizona.

Received 3 November 1961.

The research described here was supported by Air Force Cambridge Research Laboratories and an Air Force Contract with Geo-Science, Inc.

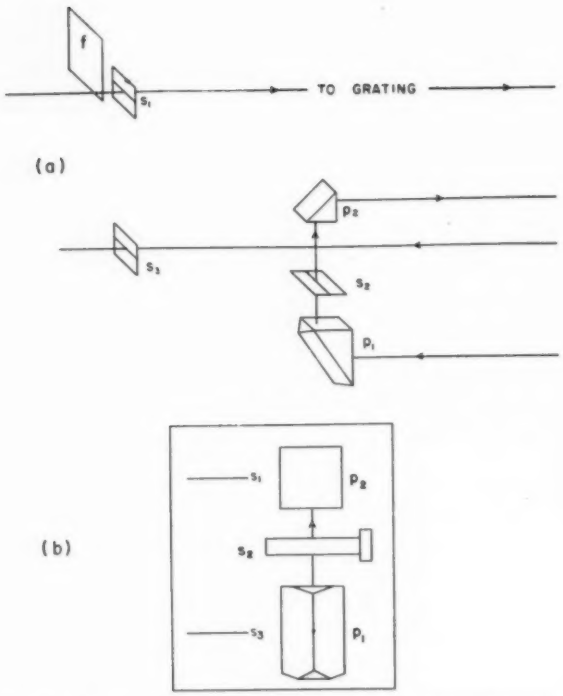

Fig. 1. Schematic diagram of the slit end of the Littrow spectrograph.

second order scatter remains, its intensity is negligible. The system eliminates the Rowland ghosts and reduces residual selective scatter to an undetectable level. When the spectrum is scanned by rotating the grating, the band transmitted by s_2 remains accurately centered on s_3. This convenient characteristic permits the isolation of a much narrower band at s_2 than would be possible in a scanning system fed by an external monochromator which must scan independently.

Figure 2 represents the distribution of light according to wavelength transmitted by the intermediate slit. The peaks labeled R are Rowland ghosts. This pattern is projected as a spectrum onto slit s_3, the width of which is represented by the dotted lines in Fig. 2. In addition to the ghosts, there is a uniform scatter background, b, due to any incomplete shielding, diffuse reflections from parts of the spectrograph, and multiple reflections between optical surfaces. Because it is quite nonselective in wavelength, this uniform background is harmless. Its effect can be removed by a zero point correction, which is readily determined by displacing s_3 to λ_1 in Fig. 2. In the Sacramento Peak instrument the intensity of the continuous background is normally about 1% of the continuum level in the solar spectrum. It varies, however, with the filtering and color sensitivity of the photo cell, and increases if the length of s_1 exceeds that of s_3.

The double pass system doubles the dispersion of the spectrum, and should ideally double the spectroscopic resolving power. Unfortunately, it also doubles any wave-front distortions introduced by aberrations or imperfections of the optical parts. Hence, the actual gain in resolving power over single pass operation has an upper limit of a factor of two, and depends entirely upon the excellence of the grating and other optics. As a rule of thumb, the double pass resolving power, R_2, is given approximately by the relation

$$R_2 = \left(1 + \frac{R_1}{R_T}\right) R_1,$$

where R_1 and R_T are the actual and theoretical resolving power in single pass.

It might be expected that double pass operation would be very costly in light efficiency. But, in fact, it is possible for the light efficiency to be increased for a given transmitted bandwidth.

In any prism or grating monochromator the light transmitted, ϵ, is

$$\epsilon = E(\lambda)\tau l_1 w_1 \frac{a_x a_y}{f^2} \delta\lambda_2. \qquad (1)$$

Here

$E(\lambda)$ = illumination of entrance slit at wavelength λ,
τ = over-all transmissions of system (including the effects of diffraction at the slits),
l_1 and w_1 = length and width of entrance slit,
a_x and a_y = dimensions of the effective aperture of the dispersing element parallel and perpendicular to the direction of dispersion,
f = focal length of the collimator,
$\delta\lambda_2$ = wavelength equivalent of the exit slit width.

The entrance slit width is related to its wavelength equivalent, $\delta\lambda_1$, by the expression

$$w_1 = f \frac{d\varphi}{d\lambda} \delta\lambda_1,$$

where $d\varphi/d\lambda$ is the angular dispersion of the system as seen from the collimator. It is a basic property of any dispersing system that $d\varphi/d\lambda = R_T/a_x$, where R_T is the

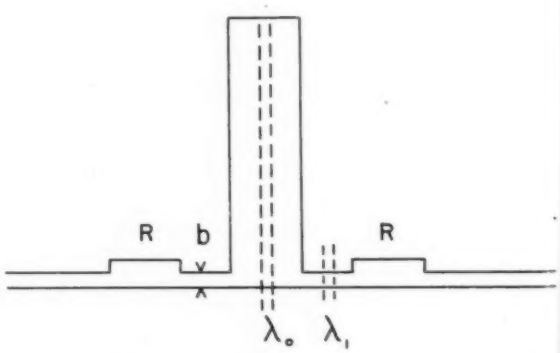

Fig. 2. The light pattern transmitted by the intermediate slit

theoretical resolving power, $\lambda/\Delta\lambda$. Hence $w_1 = (f/a_x)R_T$, and Eq. (1) can be written

$$\epsilon = E(\lambda)\tau l_1 \frac{a_y}{f} \delta\lambda_1\delta\lambda_2 R_T. \quad (2)$$

This relation is valid even when the actual resolving power is less than R_T, although this affects the useful bandwidth adversely.

Everything else being equal, then, the transmitted light is proportional to $\tau\delta\lambda_1\delta\lambda_2 R_T$.

In going from single to double pass with a fixed bandwidth, we must double the entrance and exit slit widths to keep $\delta\lambda_1$ and $\delta\lambda_2$ fixed (since the dispersion is doubled). The double use of the dispersing element doubles R_T. Hence, the ratio of double to single pass light efficiency is $2\tau_2/\tau_1$. If the transmission of the additional optics and grating on the second pass exceeds 0.5, the efficiency of the double pass system exceeds that of the single pass system. This requires a grating with an absolute efficiency around 60%. In the Sacramento Peak spectrograph $\tau_2/\tau_1 \approx 1/4$, and we suffer a loss of a factor of two. This loss is more than compensated by the enormous advantage of freedom from any detectable scattered light in the cores of the solar absorption lines.

A Comparison of the Results in the Single and Double Pass Systems

Usual external monochrometers have band passes on the order of 5 A. While this band pass is sufficiently narrow to eliminate most of the diffuse scattered light, it is too broad to eliminate the effects of the Rowland ghosts and the extended wings of the instrumental profile. The narrow intermediate band pass of the double pass system, on the order of 0.1 A, eliminates these effects as well.

The elimination of the Rowland ghosts and extended instrumental profile wings is necessary to obtain reliable central intensities of the Fraunhofer lines. Pierce[5] and Waddell[6] found that measured scattered light depended upon the width of the absorption line studied. This measured scattered light includes the effects of the Rowland ghosts. A similar result was obtained by our comparison of measurements of the central intensities of the NaD lines in the single and double pass systems at the Sacramento Peak Observatory. Table I lists the values obtained for the two systems.

Table I. Direct Central Intensities of NaD Lines

	Single pass	Double pass
NaD_1	13.6%	5.0%
NaD_2	12.0%	4.4%
Difference	1.6%	0.6%

The lowest direct central intensities heretofore obtained in a grating or prism system amount to values slightly in excess of 8%. Although the improvement in absolute values of the central intensities from single to double pass is considerable, the more important consideration is the change in the difference of the D lines on going from single to double pass. The latter effect is produced solely because the NaD_2 line, being broader, received a smaller contribution from Rowland ghosts in single pass than did the narrower NaD_1 line. The correction in double pass, therefore, diminished the Rowland ghost contribution more in the NaD_1 line than the NaD_2 line. Figure 3 illustrates the direct profiles obtained for the NaD lines in double pass.

Allen,[7] in determining the scattered light correction required for solar line profiles, used the strong atmospheric O_2 lines. He assumed that these saturated lines should have zero central intensities and that the measured departure from zero was the scattered light. Contrariwise, if observations of these lines yielded zero central intensities, we felt that the double pass system permitted the measurement of true central intensities. Figure 4 illustrates a photoelectric scan in a portion of the A band region. A precise measurement indicates a residual of some 0.3%. This residual is sufficiently close to the Planck function in the terrestrial atmosphere that it appears that all effects of scattered light and Rowland ghosts are indeed eliminated in the double pass system. We note, however, that for the accuracy of photographic observations such as Allen's, one is still justified in assuming that the central intensity of these strong atmospheric lines is zero.

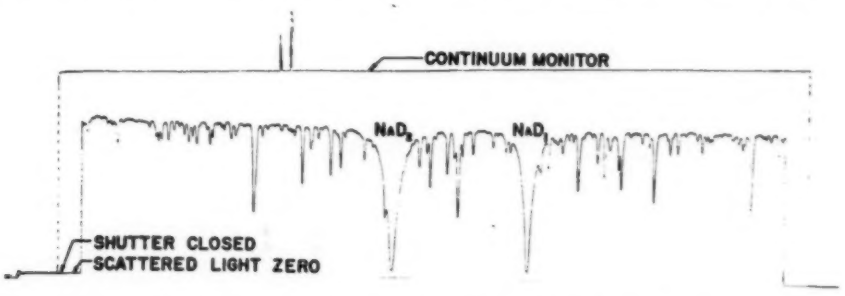

Fig. 3. Photoelectric scan of NaD lines illustrating the low central intensities obtained in the double pass system.

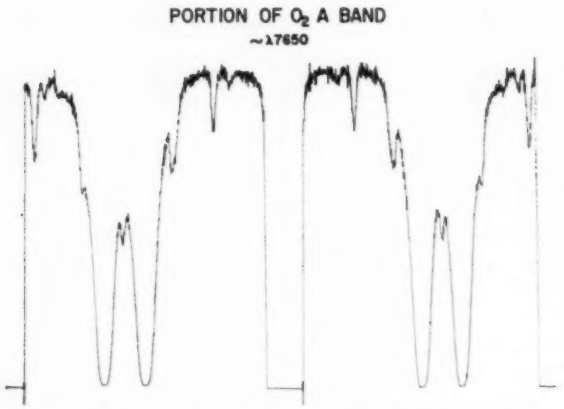

Fig. 4. Photoelectric scans of saturated O_2 lines illustrating the near zero central intensities in the double pass system.

It was also interesting to compare our results with the central intensities of lines in the Utrecht Atlas.[8] For example, the central intensity of the FeI λ 6246.333 line that measures 44% in the Utrecht Altas, in which a scattered light correction has already been included, measures 31% in the double pass system at Sacramento Peak. While neither of these measurements is given with an instrumental profile correction, it is impossible to reconcile these central intensities on the basis of the differences in instrumental profile.

Considerable effort in the past has been expended in analyzing solar line profiles. The central intensities obtained from these profiles are crucial in determining the temperature and velocity structures as well as the effects of departures from local thermodynamic equilibrium. Our results indicate that high resolution alone does not insure the reliability of observed central intensities for such work. Rather, before the character of the solar atmosphere can be inferred from the study of central intensities, it is necessary that high resolution must be coupled with a system, such as described, that eliminates the effects of Rowland ghosts, extended instrumental profile, and diffuse scattered light.

References

1. A. Walsh, Nature **167,** 810 (1951).
2. F. A. Jenkins and L. W. Alvarez, Phys. Rev. **85,** 763 (1952).
3. W. G. Fastie and W. M. Sinton, J. Opt. Soc. Am. **42,** 283 (1952).
4. D. H. Rank and T. A. Wiggins, J. Opt. Soc. Am. **42,** 983 (1952).
5. A. K. Pierce, J. Opt. Soc. Am. **47,** 6 (1957).
6. J. Waddell, Thesis, University of Michigan, 1956.
7. C. W. Allen, Astrophys. J. **85,** 165 (1937).
8. M. Minnaert, G. F. W. Mulders, and J. Houtgast, *Sterrewacht "Sonnenborgh"* (Schnabel, Kampert & Helm, Utrecht, Amsterdam, 1940).

Photo J. Allen Hawkins

A. I. Mahan *OSA Treasurer* and L. P. Bone receiving the Prize for the Best Paper Published in *J. Opt. Soc. Am.* during 1960 from Wallace R. Brode *OSA President 1961,* while Mary E. Warga *OSA Executive Secretary* and Allen Sandage, after-dinner speaker at the OSA-Los Angeles Fall Meeting 1961, applaud.

Books Received

Reviews will appear in subsequent issues of some of these titles:

Near Zero; The Physics of Low Temperature, by D. K. C. MacDonald; Anchor Books—Doubleday, New York. November 1961

Shape and Flow; The Fluid Dynamics of Drag, by Ascher H. Shapiro; Anchor Books—Doubleday, New York. November 1961

Shock Tubes, by J. K. Wright; Methuen—Wiley, New York. October 1961

Introduction to Space Dynamics, by William Tyrrell Thomson; Wiley, New York, November 1961

Tables of the Fractional Functions for the Planck Radiation Law, by M. Czerny and A. Walther; Springer-Verlag, Berlin. August 1961

Tables of Blackbody Radiation Functions, by Pivovonsky and Nagel; Macmillan, New York. June 1961

Encyclopedia of Spectroscopy, by G. Clark; Reinhold, New York. 1960

Plasma Physics, by J. E. Drummond; McGraw-Hill, New York. 1960

Encyclopedia of Microscopy, by G. Clark; Reinhold, New York May 1961

Annual Review of Nuclear Science, Vol. 10, Annual Reviews. Palo Alto. 1961.

Rocket Exhaust Radiation Measurements in the Upper Atmosphere

N. W. Rosenberg, W. M. Hamilton, and D. J. Lovell

Measurements have been made on several launches of the intensity and spectra of the visible (4000–6500 A) radiation emitted by rocket engine exhausts during powered flight at high altitudes. Two closed-circuit television cameras, mounted on a hand-tracked platform, have been used, located on Grand Bahama Island, down range from Cape Canaveral. One TV camera obtained information regarding the spatial persistence and intensity of exhaust radiation. The other employed a dispersing slit and grating and recorded spectra. In each launch, as the missile rose, a glow developed which persisted for several seconds in the wake of the missile. At higher altitudes, the glow faded in intensity but increased in diameter forming a large radiating "bow." The observed spectra have been compared with those of laboratory flames to provide identification of radiating species. These studies are useful in studying reactions in the atmosphere to heights of about 300 km.

Introduction

During the powered flight of a missile, a large quantity of radiant energy is emitted. The characteristics of this energy are a function of the type of propellant used and the interaction of the exhaust products with the atmosphere. The characteristics can be measured only during flight, as the reduced pressure, long mean free path, and ionized and dissociated state of the atmosphere cannot readily be simulated in laboratory studies. Accordingly, studies of the rocket exhaust radiations in the upper atmosphere provide useful data in understanding the physics and chemistry of this interaction.

Measurements have been made from an observation site on Grand Bahama Island. The aspect obtained from this site to a typical missile trajectory is seen in Fig. 1. The location of the site at GBI is such that a typical missile launched from Cape Canaveral remains at a relatively constant slant range throughout a good portion of its powered trajectory.

Instrumentation

The equipment used consisted of two television cameras mounted on a common hand tracked platform, as illustrated in Fig. 2. One television unit employed an image orthicon, an 875 line scan pattern, and an $f/0.85$, 150-mm focal length lens, to obtain the information regarding the spatial distribution of the exhaust emissions. This lens permits a field of view of 11° vertical and 13° horizontal. The response of the system was such that a seventh magnitude star could just be resolved in the noise. The image orthicon has an S-10 spectral response which has an effective spectral sensitivity range from about 4000–6500 A, with a peak at about 5000 A.

A combination of lens vignetting, prefogging of the photocathode, and nonuniformity of the kinescope black level combined to present a nonuniform response over the photocathode surface which amounted to a sensitivity variation of nearly an order of magnitude. Although this makes interpretation of absolute radiant intensities more difficult, it does not invalidate the main use of the television, i.e., obtaining information on the size, shape, and persistence of an expanded target of very low intensity.

The other television system employed an optical dispersing system, as shown in Fig. 3. The objective lens was an $f/1.5$, 400-mm focal length lens. The collimating lens was also $f/1.5$, and of 85 mm focal length. The grating used was a Bausch and Lomb replica blazed in the first order and of 300 lines per millimeter. The camera lens was an $f/2.5$, and of 175 mm focal length. The slit, when set in width to image onto a resolution element of the television system, permits the system to have a field of view of 0.1 × 10 milliradians.

N. W. Rosenberg and W. M. Hamilton are with the Air Force Cambridge Research Laboratories and D. J. Lovell was with the Bendix Systems Division, Ann Arbor, Michigan, but is now at the Infrared Laboratory, IST, University of Michigan.

Received 23 October 1961.

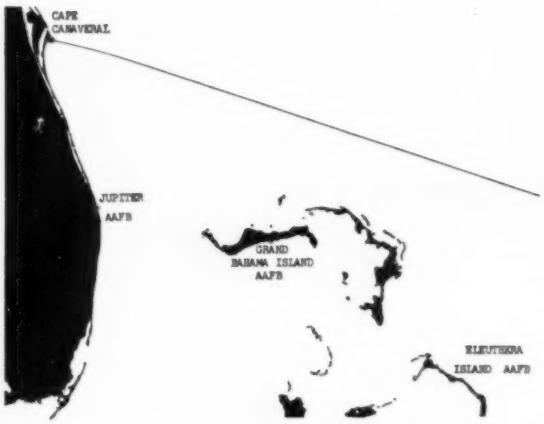

Fig. 1. Aspect of typical missile trajectory to GBI site.

The sensitive tube used in the spectral television system was an image intensifier orthicon, which represents one of the latest advances in the television state of the art. It has a high voltage intensifier section, a trialkaline (S-20) photocathode, and a MgO target. This tube has a spectral sensitivity of about 4000–6500 A, with a peak near 4500 A. The tube has a responsivity some 300–1000 times superior to that of an image orthicon, although the resolution is somewhat inferior to that of the latter.

The spectral television system used a 525 scan line noninterlaced pattern. This modification was introduced in order to increase the horizontal resolution. This increase is achieved since the product of horizontal and vertical resolutions is approximately equal to the bandwidth of the system, which in this case is 15 Mc.

Since approximately 2500 A are dispersed across the photocathode, and the system achieves a resolution of nearly 500 TV lines, or 250 optical line pairs, the resolution of the system is nearly 10 A. In fact, in the laboratory, the 5770–5791 A doublet of mercury is cleanly resolved. The field performance is somewhat less than this.

Calibration of the response, both spectrally and in amplitude, was accomplished by utilizing two reference lamps. These were a mercury arc and a ribbon tungsten filament which were focused on the upper portion of the entrance slit.

Both television units are closed circuit, and the data are presented on kinescopes in a nearby van. These kinescopes were separately photographed on 35 mm film. Although the television cameras are run at 30 ft (9 m)/sec, the recording cameras were run at 5 ft (1.5 m)/sec, to integrate effectively several TV sweeps. Densitometric traces of these films were made to facilitate analysis.

Phenomenological Description

As viewed from GBI, the missile exhaust is initially observed as a bright point of light. Subsequently, however, a number of interesting changes occur, many of which can be seen in Fig. 4—a montage of 30 missile trail photographs obtained during a night firing in which the missile never rose above the solar horizon. The photographs have been arranged in the montage to present as nearly as possible the relative appearance of the missile as seen from GBI. The general trends of the observed radiant intensity are plotted in Fig. 5. The missile rose over the northwest horizon, crossed north above the pole star, then passed due east. Of course, the angular altitude of the missile was observed to decrease as the range of the missile increases eastward, even though the vertical altitude of the missile above the earth was increasing.

Many of the characteristics of the rocket exhaust can be inferred from Fig. 4. The first event of interest is stage separation. The booster appears to fall behind the second stage rapidly accelerating away from it, when successive frames are viewed. One frame of stage separation is shown on the montage as image number 3. As the missile altitude increases, the radiant intensity begins to decrease. Upon passing through the ozone layer (35–40 km), however, an increase in intensity occurs, following which the decrease with altitude is resumed.

As the missile continues to rise, the radiant intensity is observed to increase again, and a luminous trail (rocket glow) is seen to develop in the wake of the missile. As can be seen in the sequence of frames in Fig. 6 this trail reaches considerable length. At still higher altitudes, the rocket glow fades in intensity, although it is not believed to disappear altogether. Meanwhile, another effect is becoming more noticeable, as can be seen in images 10–20 of Fig. 4 (and in greater detail in Fig. 7). The exhaust trail appears to divide in two,

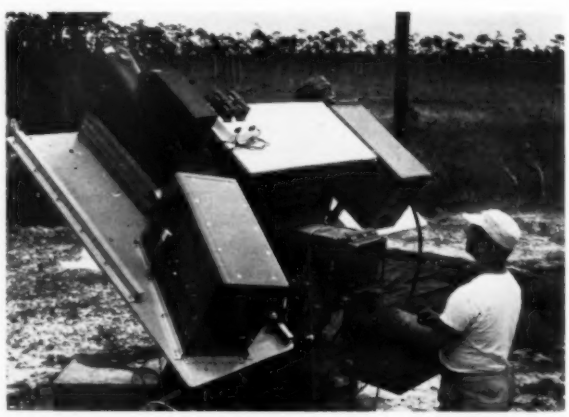

Fig. 2. Television equipment in operation at GBI site.

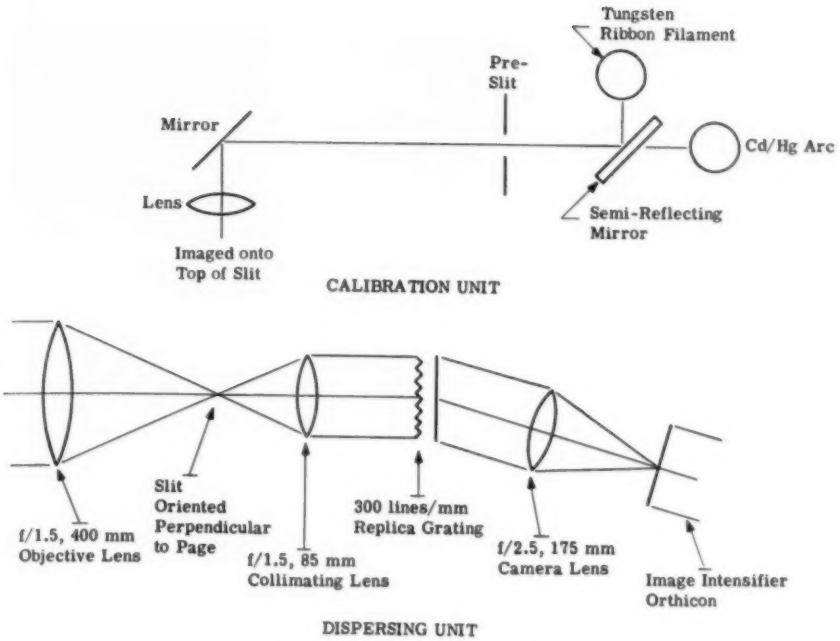

Fig. 3. Television spectrometer diagram.

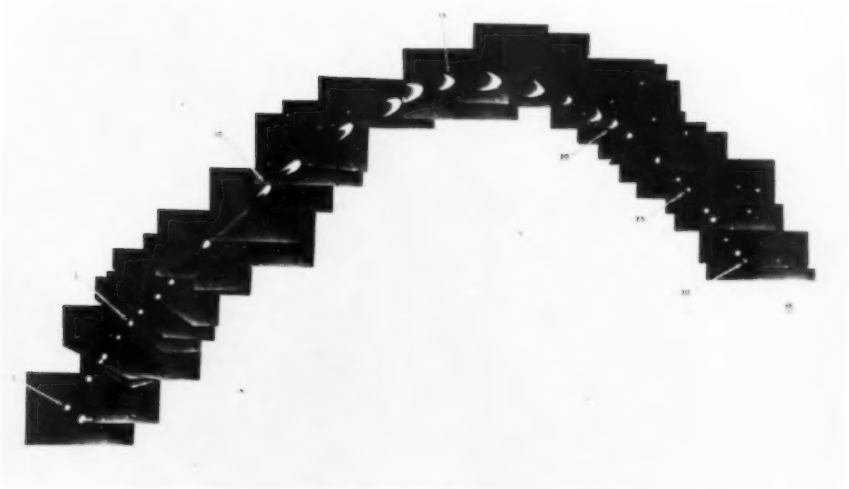

Fig. 4. Montage of missile flight as observed at GBI site.

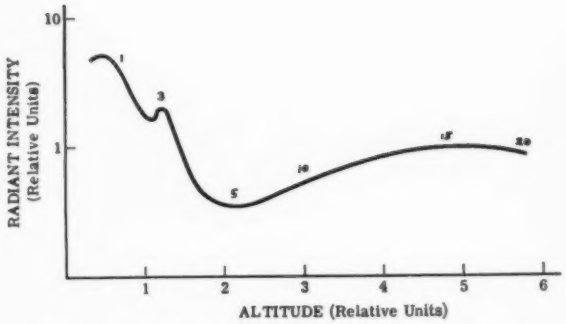

Fig. 5. Variation of observed radiant intensity of rocket exhaust. (Numbers refer to frame numbers in Fig. 4.)

presenting a "bow wave" appearance. The total radiant intensity subsequently appears to pass through a broad maximum; due to the low signal-to-noise ratio at the extreme ranges involved, however, the existence of this maximum is not certain.

Mechanism Hypothecation

The chemical reactions in the nozzle are frozen, resulting in large amounts of chemical energy in the form of free radicals being dumped into the missile trail. This energy is released during reactions at the boundary layer of the exhaust, giving rise to a luminous bow at high altitudes. At lower altitudes, the mean free time is short, and the deactivation or further reactions of species occurs within the intense radiation zone of the rocket exhaust. For example, even at 30 km altitude, the mean time between collisions is about 10^{-8} sec, which is comparable to the radiation half-life for nonmetastable excited species.

With the assumption that the chemical reactions are the most probable source of energy for the rocket glow in the trail at high altitudes, one can postulate possible mechanisms for the radiation. The species expected for a hydrocarbon liquid fuel rocket would be derived from

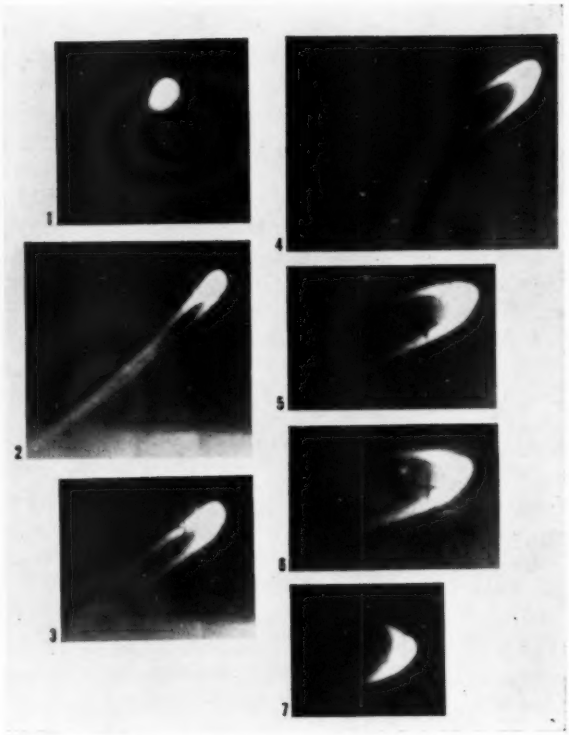

Fig. 7. Bow wave development.

a reaction of the type:

$$\text{Hydrocarbon fuel} + \text{oxidizer} \rightarrow \text{combustion products} + OH + C_2 + CH.$$

This equation is presented only as an example of the probable general reaction. The exact combustion products are a function of the specific fuel and oxidizer used. The latter three products are generally unstable, leading to afterburning reactions of the type:

$$(OH + C_2 + CH) + \text{oxygen} \rightarrow C_x + CO + OH.$$

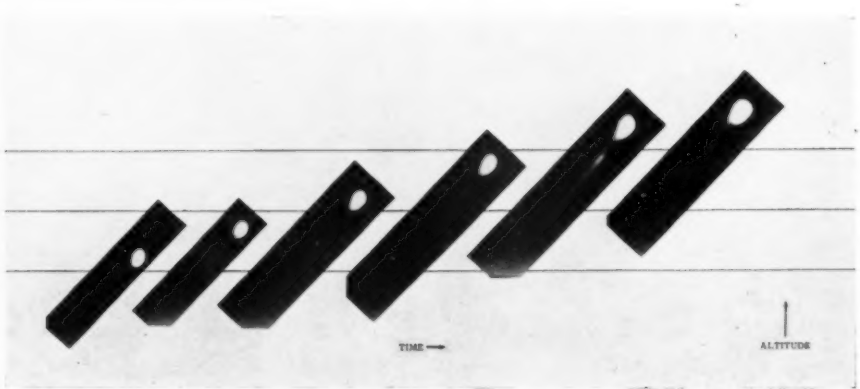

Fig. 6. Development of persistent missile rocket glow.

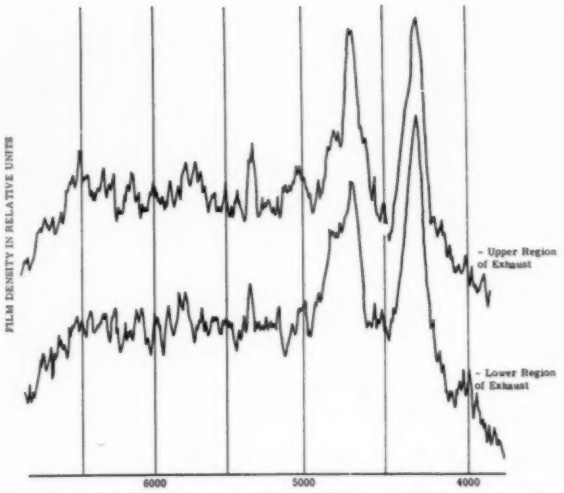

Fig. 8. Spectra of typical hydrocarbon-lox fueled rocket in two regions of exhaust (wavelength in angstroms).

Here the oxygen is obtained from the atmosphere and includes the forms O_2, O, and O_3. The term C_x is used to denote the formation of soot. The latter two compounds eventually yield stable compounds through the reaction:

$$CO + 2OH \rightarrow H_2O + CO_2.$$

It is noted that the species CO and OH are formed as afterburning products, in addition to being present as combustion products. In a solid fuel propellant, CN would probably also be present. (Although this species may also be present in the liquid fueled reaction, due to the nitrogen supplied by the atmosphere, it is not expected to be a strong source of radiation.)

The rocket glow is hypothesized to consist of a cloud of excited exhaust molecules. The low collisional probability at the altitudes at which this occurs implies that the chemical reactions listed above will take place slowly, and radiative de-excitation of the species will persist accordingly.

The spectra of the rocket glow will consist only of molecular band emissions. This is shown in Fig. 8, which presents spectra obtained from two regions in the exhaust of a kerosene-lox missile. A similar spectrum obtained on another kerosene-lox missile is shown in Fig. 9. The undisturbed cone emits a fairly continuous emission similar to that of a blackbody at nearly 2000°K. Typical of the continuous spectra observed are those exhibited in Fig. 10, obtained from the rocket exhaust at three different altitudes. The band structure seen in this emission is not a strong feature.

Confirmatory evidence has been generously supplied by Mr. James F. Baur of the Physics Department, The University of Florida. He obtained spectra of a solid fueled missile which indicated strong CN band emissions as predicted above, as well as other prominent bands.

The "bow wave" appearance which occurs at higher altitudes is attributable to the expansion of the exhaust products behind the missile in such a manner that only the outer portions of the exhaust are luminous. This implies a greater gas density in the outer regions, with the reaction concentrated in the leading edge.

In order to understand these effects we must consider the gas dynamics of the whole exhaust pattern. Rocket motors are generally designed so that the fixed exit pressure corresponds to the pressure of a given atmosphere layer about half way on its powered trajectory, subject to size and weight limitations. Therefore, the exhaust gases are normally overexpanded until the missile reaches this atmospheric layer and underexpanded above. Theoretical calculations available on these phenomena have been made only for rocket motors at rest in the ambient air. Whenever relative motion is imparted to the ambient air the constant pressure interface solution becomes incompatible with the conservation of momentum along the stream line deflected by this interface. The deflection implies a higher interface pressure than ambient.

The exhaust gas has considerable translational energy relative to the ambient at the altitudes considered by virtue of the forward motion of the missile and the vector component of the expansion into the ambient. Consequently, it seems reasonable to expect that kinetic interactions with the ambient might be responsible for some collisionally excited emissions at high altitudes.

The velocity of the exhaust relative to the ambient monotonically increases from separation until burnout.

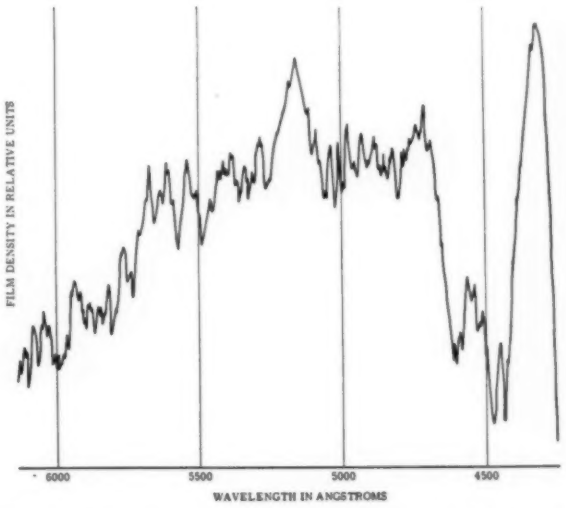

Fig. 9. Spectrum of second hydrocarbon-lox fueled rocket exhaust.

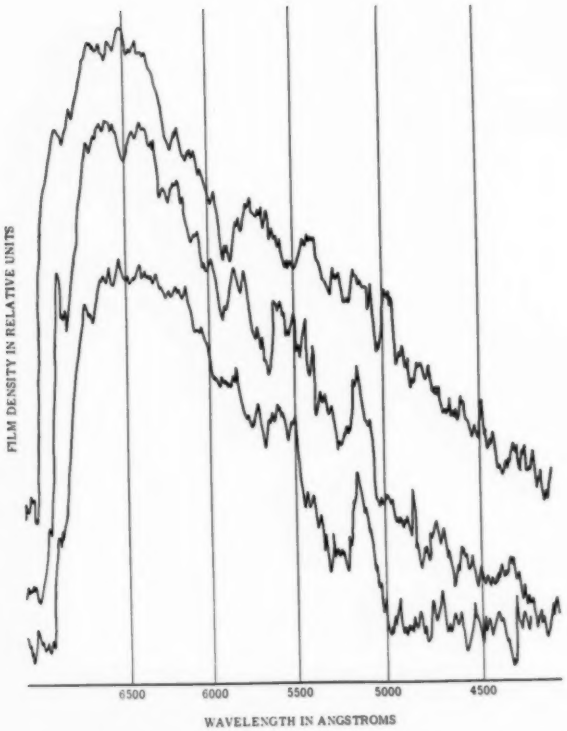

Fig. 10. Continuous emission of rocket exhaust at three altitudes.

However, while the available collisional energy is thus increasing with altitude, the collisional probability is decreasing with altitude; these two counteracting effects combine to give the broad maximum uncertainty detected at great slant ranges.

Summary

In summary, three distinct radiation mechanisms are considered, which may be responsible for the emission of rocket exhausts in the upper atmosphere. The undisturbed cone is a localized intense source of radiation approximating that of a blackbody. The rocket trail glow extends over a broad region emitting band spectra possibly arising from the deactivation of excited or metastable free radicals upon collision with air molecules. The "bow wave" represents kinetic interactions of the exhaust and ambient, the spectrum of which has not yet been fully defined (although probably characterized by a continuum). It is considered to be the source of increased emission by the exhaust at higher altitudes.

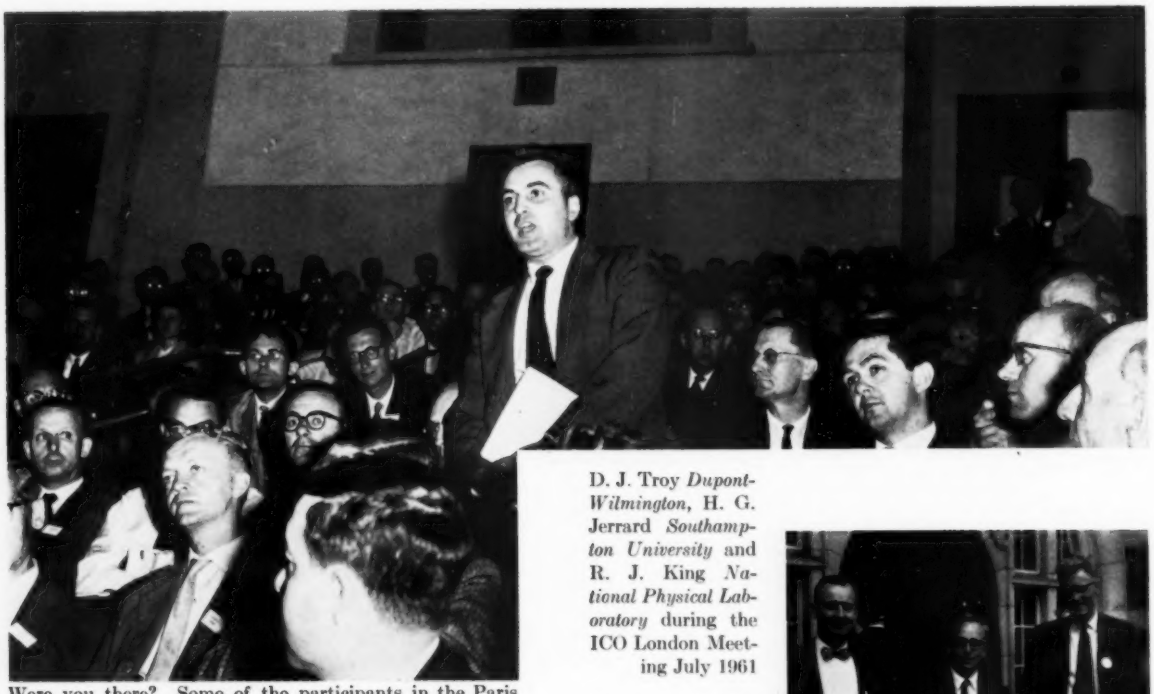

Were you there? Some of the participants in the Paris ICO Meeting July 1961 *Photo: Harand*

D. J. Troy *Dupont-Wilmington*, H. G. Jerrard *Southampton University* and R. J. King *National Physical Laboratory* during the ICO London Meeting July 1961

Photo: F. S. Harris

Optical Measurements from High Altitude Balloons

David G. Murcray, James N. Brooks, Norman J. Sible, and Herbert C. Westdal

A description is given of a system that has been constructed to make radiometric measurements from high altitude balloons. The instrumentation consists of a 20-cm aperture, 30-cm focal length radiometer that has been equipped to scan in azimuth and elevation, a filter system so that spectral data can be obtained, an onboard digital magnetic tape recording system for recording the data generated during the flight, auxiliary electronics and power supplies for operation of the equipment, and a gondola to serve as a suitable scanning platform and to protect the equipment when it is returned to the ground by parachute at the end of the flight. The results obtained on a balloon flight made with this equipment on May 8, 1959 are also presented. For this flight the radiometer was equipped with a thermistor bolometer detector with a KRS-5 window and with filters that transmitted radiation from 1 μ to 2 μ, 2 μ to 3 μ, 3 μ to 5 μ, 5 μ to 8 μ, and 8 μ to 35 μ. These results are presented in the form of isoradiance plots.

Introduction

The present study has as its objective the measurement of the spectral and spatial distribution of the radiation received from the earth and its atmosphere at high altitudes. In order to accomplish this objective a radiometer system capable of making these measurements automatically and light enough to be transported to high altitudes by means of large balloons has been constructed. A description of the equipment and the results obtained when the equipment was flown on May 8, 1959 form the body of this report.

Instrumentation

The radiometer consists of a 20-cm aperture, 30-cm focal length Cassegrainian telescope. A plane mirror which makes an angle of 50° with respect to the optical axis of the radiometer is placed at the front aperture of the radionometer. Scanning is accomplished by rotating this mirror about the optical axis of the radiometer, which is depressed 10° from the horizontal during flight. This combination of mirror angle and depression angle results in a conical scan that passes through the nadir but only within 20° of the zenith, thus missing the balloon. Azimuth scan is achieved by rotating the whole radiometer with respect to a base plate which is fixed with respect to the gondola that houses the equipment during flight. The plane mirror is rotated through 360° in 30 sec and the radiometer traverses 180° in azimuth in 5 min. The azimuth scan is limited to 180° by means of microswitches which reverse the direction of rotation of the radiometer and are activated by the radiometer motion.

The incoming radiation is interrupted 80 times per second by means of an eight-bladed chopper. The radiation also passes through openings in a filter wheel which is mounted coaxially with the chopper. The filter wheel has positions for 12 filters and is rotated through one step each time the direction of motion of the azimuth scan is changed. Thus every 5 min a scan is completed with a different filter in front of the detector.

For the flight of May 8, 1959 the radiometer was equipped with a 2.5 mm square thermistor bolometer detector equipped with a KRS-5 window. With this detector the radiometer system has a $^1/_2 \times {}^1/_2°$ square field of view. The detector is housed in a blackbody cavity and as the chopper interrupts the incoming radiation the detector gives rise to an ac voltage that is proportional to the difference between the incoming radiation and the radiation from the blackbody cavity. The blackbody is not maintained at a constant temperature but is allowed to assume ambient temperature and the temperature is monitored. The ac signal from the detector is amplified, synchronously rectified, and filtered. The details of the radiometer are shown schematically in Fig. 1.

A knowledge of the position of the scanning mirror, the orientation of the radiometer with respect to the gondola, and orientation of the gondola with respect

The authors are at the Denver Research Institute, University of Denver, Denver, Colorado.

Received 7 November 1961.

Research reported in this document has been supported by the Aeronautical Systems Division of Air Force Systems Command.

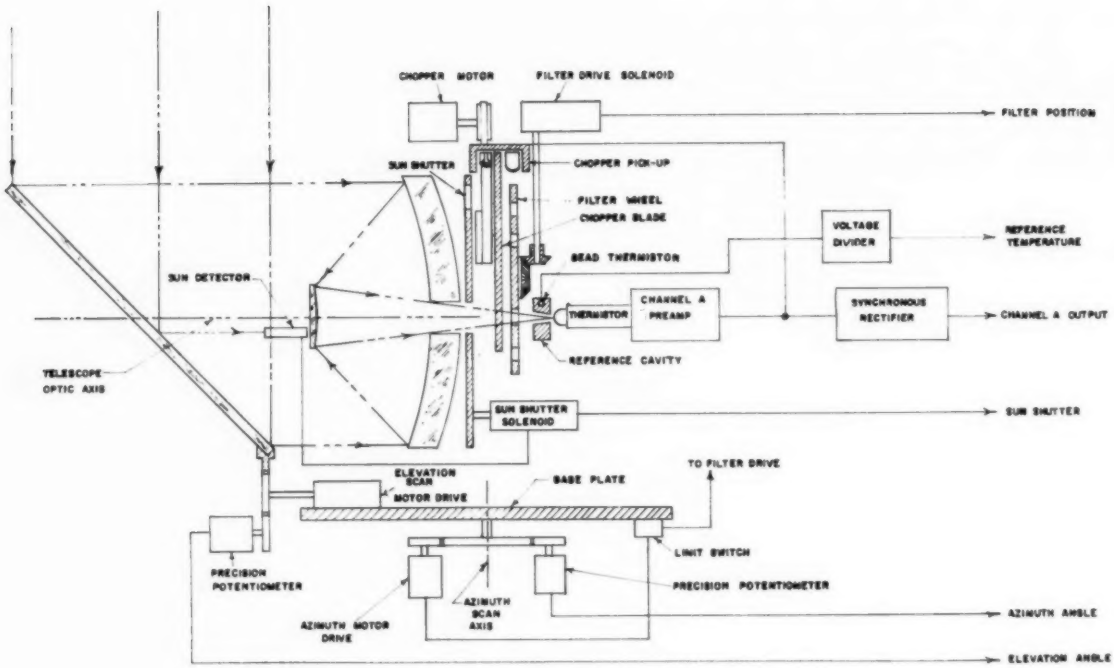

Fig. 1. Schematic diagram of balloon borne radiometer.

to the earth is required for the determination of the direction from which the radiation is being received. The position of the scanning mirror and the orientation of the radiometer with respect to the gondola are determined by monitoring the voltages across potentiometers that are coupled to the two drive systems. The orientation of the gondola with respect to the earth is determined by means of two magnetometers whose probes are placed at right angles to each other. By using two probes in this fashion it is possible uniquely to determine the position of the gondola with respect to the earth's magnetic field.

The data are recorded in digital form on magnetic tape by means of a digital tape recorder which is carried aloft with the rest of the instrumentation. The recorder consists of an analog to digital converter that converts the input voltages into a binary coded decimal suitable for recording on magnetic tape and a seven channel 12-mm tape transport. The analog to digital converter samples 10 input channels whose voltages range from 0.00 to 9.99 volts, ten times per second, with an accuracy of ± 0.01 volt. The tape transport takes the standard 27-cm magnetic tape reels. On this flight the data were recorded using a 25 mm/sec tape speed and 0.025-mm magnetic tape. This combination of tape thickness and tape speed gave an overall recording time of 12 hr.

All mechanical rotations are accomplished by means of 400 cycle, 115 volt single phase synchronous motors. The 400 cycle power is supplied by means of a sine wave inverter. The main source of power is a 28 volt lead acid battery. All other voltages except the detector bias voltage are either supplied by the 28 volt source or derived from the 400 cycle source.

The equipment is housed in a gondola which is used to provide a means of suspending the equipment from the balloon without interfering with its scanning motion and also to protect the equipment when it is returned to the ground by parachute. The gondola is constructed from electrical conduit. The radiometer system is suspended in the gondola by springs. The springs are tied with light cord so that the radiometer is supported on a rigid base during flight. Upon impact the cords break and the springs are extended beyond their elastic limit. This system reduces the forces on the radiometer during impact.

Calibration Procedures

The radiometer was calibrated using a Barnes Engineering Company 30-cm aperture blackbody source which was placed as close to the scanning mirror as possible to reduce atmospheric transmission losses. The source temperature was varied from 40 to 120°C in 10° increments and the corresponding signal voltages recorded. This calibration was performed the day before the flight using the same bias batteries and power supplies that were used during the flight.

Since the gondola is constructed of electrical conduit

it was also necessary to calibrate the magnetometers in position on the gondola. This was accomplished by orienting the gondola toward magnetic north and recording the magnetometer outputs. The gondola was then rotated through 10° and the outputs recorded. This process was continued until the gondola had been rotated through a complete circle.

Description of the Flight

The results presented in this report were obtained in a balloon flight that was made on May 8, 1959, from Holloman Air Force Base, New Mexico. The equipment was launched at 0515 and rose with an average ascent rate of 400 cm/sec. It reached a floating altitude of 26 km and was allowed to float at altitude until 1715 when it was cut down by command from the ground. The equipment impacted near Bingham, New Mexico. The sky was clear during the early morning hours but there was a slight cloud buildup by noon.

Data Reduction

The data obtained on this flight were recorded in digital form on magnetic tape. This digital tape was played back directly into the Denver University digital computer where the calculations necessary to convert the voltages into radiance versus direction were performed, and the results were printed out in the form of tables of radiance versus direction.

These tables were used to plot the results so that the isoradiance plots could be drawn. The drawing of the isoradiance lines after the values have been plotted is, to a certain extent, subjective since the information available is limited. In addition a great deal of fine structure has to be ignored in order to be able to draw the isoradiance lines at all.

No attempt is made to orient the gondola during flight. The gondola motion consists mainly of a slow rotation. This rotational motion is superposed in the azimuthal scanning motion and as a result there are occasionally gaps in the scan. Because of the placement of the filters, each hour three successive scans are made without any filter in front of the detector. The combining of the three scans makes it possible to draw a much more accurate isoradiance diagram than from a single scan. Therefore plots are presented for each hour since the background radiation was not changing rapidly with time. This is not the case for the readings taken during ascent, however; these will be presented in a separate report.

The quantity that is measured when a filter is in position in front of the detector is given by

$$K\Delta V = \Delta N = \int_0^\infty N_B(\lambda)F(\lambda)d\lambda - \int_0^\infty N_i(\lambda T)F(\lambda)d\lambda$$

where $N_B(\lambda)$ is the background radiance, $N_i(\lambda T)$ is the radiance of a blackbody at temperature T, $F(\lambda)$ is the transmission function of the filter, and K is the calibration constant for the system. Since $N_i(\lambda T)$ and $F(\lambda)$ are known functions it is possible to determine the second integral by numerical integration. This integration was performed on a digital computer for the various filters for the temperatures encountered during flight. The calibration constant K is also a function of the temperature since the sensitivity of the detector is a function of temperature. This variation of sensitivity was determined in a separate study and the calibration constant adjusted accordingly. With these quantities known it is possible to determine the value for the quantity

$$\int_0^\infty N_B(\lambda)F(\lambda)d\lambda.$$

The quantity of actual interest is $N_B(\lambda)$; however, in order to determine this quantity it is necessary to make some assumption as to the wavelength distribution of the incoming radiation. Rather than making such assumptions the isoradiance plots are given for the values of the integral and the estimate of the wavelength dependence of N is left to the discussion.

The filter functions for the various filters are given in Fig. 2. The signals obtained when filters no. 2 and 3 were in front of the detector were greater than the system noise only when the radiometer field of view was scanning close to the sun in the upper hemisphere and in the direction of maximum scattering in the lower hemisphere, so the results were not plotted.

Results and Discussion

The equipment, with the exception of one magnetometer, operated as expected and data were obtained from launch until 1100. The output of one magnetometer fluctuated rapidly about its proper value. Because of this fluctuation the orientation of the gondola had to be determined on the basis of the output of the other magnetometer using the faulty magnetometer only to determine the proper quadrant. Since the output of a single magnetometer is a function of the cosine of the angle between the magnetic field and the axis of the probe there are regions where the output voltage is insensitive to slight changes in the gondola orientation. Therefore the error in determining the gondola orientation was increased, and the values given for the azimuth angle are only accurate to within ±5°.

The data obtained without any filter in front of the detector are given in Figs. 3 through 5. Although scans were made every ten minutes without any filters in front of the detector, selected results only are presented since the radiance was changing only slowly with time. Examination of these isoradiance plots indicates that a large part of the radiation observed toward the east in the early morning is due to scattered or reflected sun-

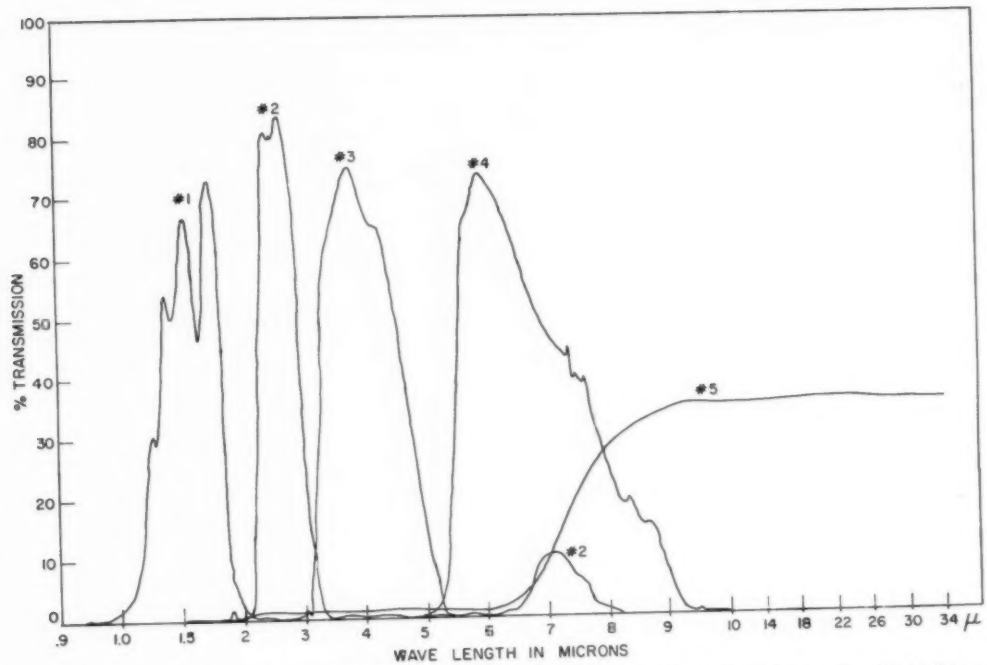

Fig. 2. Plots of transmission versus wavelength for filters no. 1 through no. 5. Numbers above the curves refer to the corresponding filter.

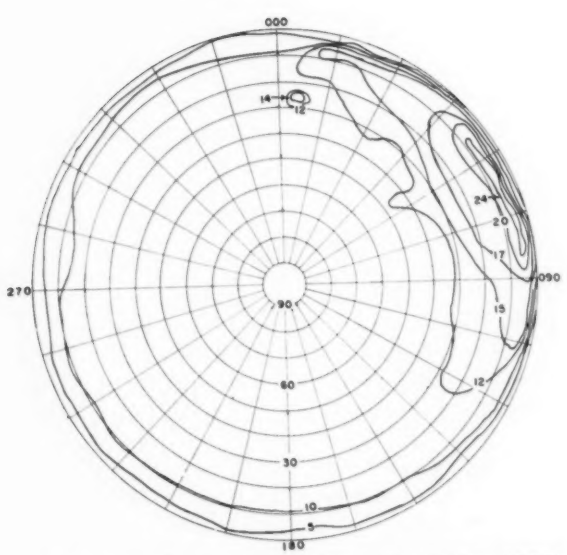

Fig. 3. Isoradiance plot open filter. 0635–0650 hr M.S.T., 8 May 1959. Isoradiance values are in mw/cm²-sterad. Azimuth values are with respect to magnetic north. 0° elevation is horizon, 90° is nadir. Solar azimuth from magnetic north 67°, solar elevation 17°.

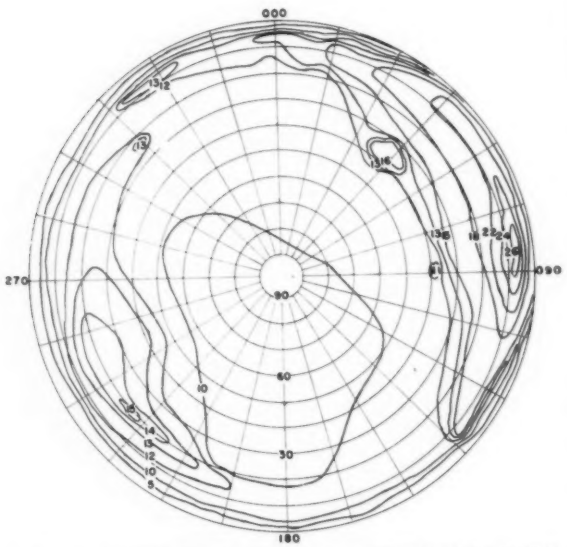

Fig. 4. Isoradiance plot open filter. 0735–0750 hr M.S.T., 8 May 1959. Isoradiance values are in mw/cm²-sterad. Azimuth values are with respect to magnetic north. 0° elevation is horizon, 90° is nadir. Solar azimuth from magnetic north 76°, solar elevation 31°.

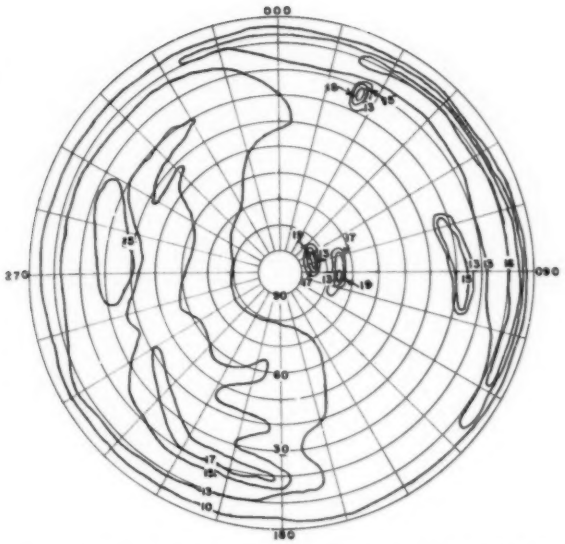

Fig. 5. Isoradiance plot open filter. 0935–0950 hr M.S.T., 8 May 1959. Isoradiance values are in mw/cm²-sterad. Azimuth values are with respect to magnetic north. 0° elevation is horizon, 90° is nadir. Solar azimuth from magnetic north 96°, solar elevation 55°.

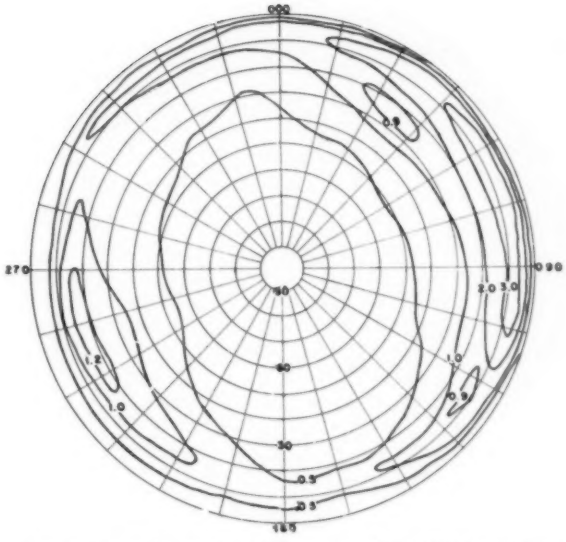

Fig. 6. Isoradiance plot filter no. 1. 0750–0755 hr M.S.T., 8 May 1959. Isoradiance values are in mw/cm²-sterad. Azimuth values are with respect to magnetic north. 0° elevation is horizon, 90° is nadir. Solar azimuth from magnetic north 77°, solar elevation 32°.

light. The strong dependence of the radiation on the angle between the sun and the viewing angle indicates that the process is probably one of scattering. Although the weather was clear at Alamogordo on the day of the flight the daily weather map for May 8, 1959 indicates the presence of a large storm over western Texas at midnight. Photos taken with a wide angle camera which was carried aloft with the equipment indicate a long thin cloud bank to the east at a depression angle of 15° from the horizontal. Between this cloud layer and the horizon there is a very bright region not associated with any visible cloud layer but which appears to be due to scattered sunlight. These photos were taken using color movie film which responds to shorter wavelength radiation than the thermistor bolometer since the KRS-5 window does not transmit below 600 mμ. On the basis of the photographs it would appear that the radiation arises from sunlight that is being scattered by something other than the tops of clouds associated with the storm.

The results obtained when filter no. 1 is in front of the detector are presented in Figs. 6 and 7. The radiation observed when this filter is in front of the detector definitely arises from scattered or reflected sunlight since the amount of radiation emitted by a blackbody at the temperature of the earth's surface in this spectral wavelength interval is considerably less than the threshold sensitivity of the instrument.

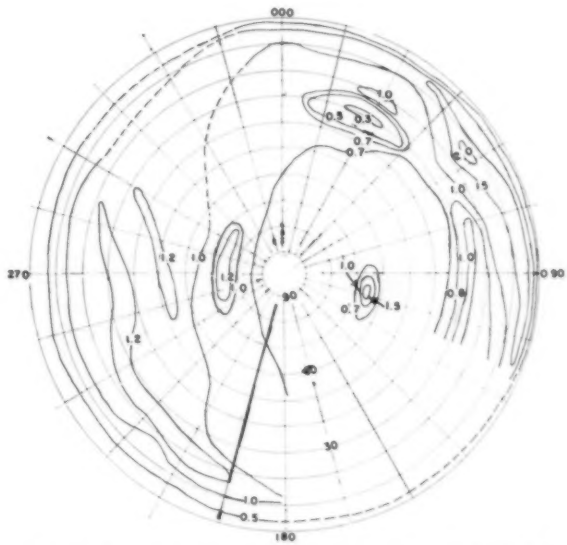

Fig. 7. Isoradiance plot filter no. 1. 0950–0955 hr M.S.T., 8 May 1959. Isoradiance values are in mw/cm²-sterad. Azimuth values are with respect to magnetic north. 0° elevation is horizon, 90° is nadir. Solar azimuth from magnetic north 99°, solar elevation 57°.

Comparison of Fig. 6 with Fig. 4 (the corresponding scan taken without any filter in front of the detector) verifies the fact that the radiation toward the horizon in the east in the early morning is due to scattered sunlight. Similar comparisons of the data taken later

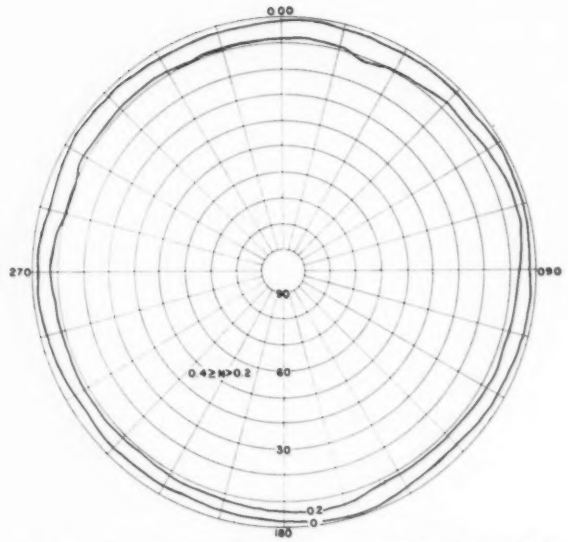

Fig. 8. Isoradiance plot filter no. 4. 0720–0725 hr M.S.T., 8 May 1959. Isoradiance values are in mw/cm²-sterad. Azimuth values are with respect to magnetic north. 0° elevation is horizon, 90° is nadir. Solar azimuth from magnetic north 74°, solar elevation 27°.

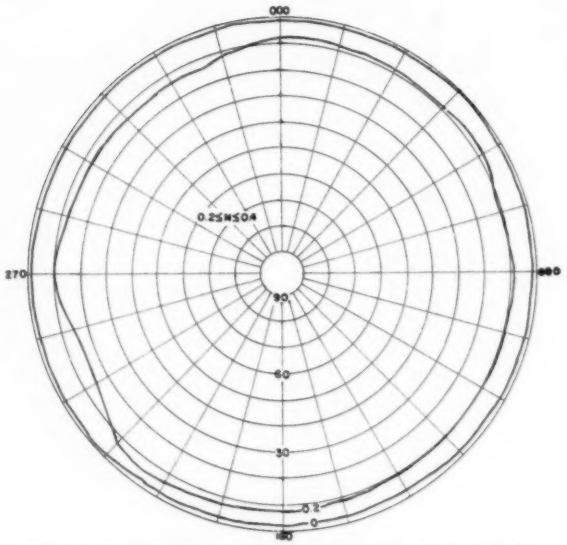

Fig. 9. Isoradiance plot filter no. 4. 0920–0925 hr M.S.T., 8 May 1959. Isoradiance values are in mw/cm²-sterad. Azimuth values are with respect to magnetic north. 0° elevation is horizon, 90° is nadir. Solar azimuth from magnetic north 92°, solar elevation 51°.

in the day fail to yield the high correlation present in the earlier data. This is not surprising since there are a number of factors such as altitude of reflecting surface, reflectivity of the surface, etc., that affect the radiation differently in different wavelength regions.

It is possible to calculate the albedo of the earth in this wavelength interval by assuming that wavelength dependence of the incoming solar radiation is similar to a 6000°K blackbody. If one makes this assumption a simple numerical integration indicates that the filter transmits 38% of the solar radiation in the 1.05 μ to 1.95 μ region. Thus all of the radiance values quoted on the plots for this filter should be multiplied by a factor 2.6 to convert them to the radiance values that one would observe without the filter if one assumes that the observed radiation has the same wavelength dependence as the incoming solar radiation. Assuming further that the solar constant is 2 cal/cm²-min then the radiance of a perfectly diffuse reflector in the wavelength interval passed by the filter would be 8.9 cos θ mw/cm²-sterad. Examination of the values obtained during the scan made at 1050(θ = 23°) gives albedo values in this wavelength region ranging from 0.32 to 0.96 with the majority of the values falling in the range between 0.32 and 0.64. These values are based on the assumption of a diffuse surface and in some cases this condition is not satisfied. It should be noted that these values represent the albedos as measured at altitude and may be quite different from the values one would obtain if the measurements were made close to the reflecting surface, since the intervening atmosphere will modify the results by scattering and absorbing the solar radiation.

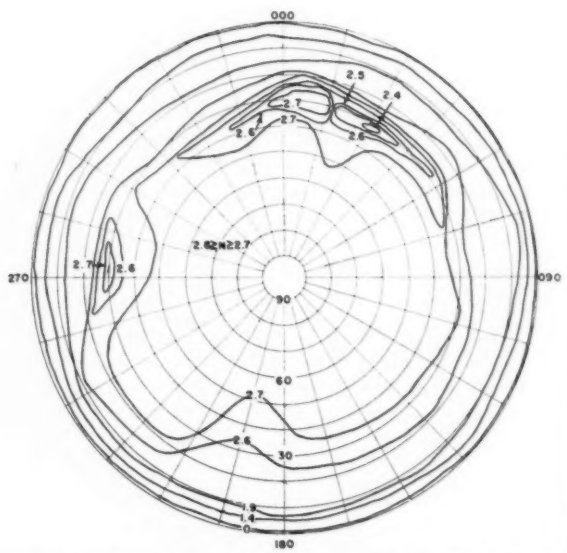

Fig. 10. Isoradiance plot filter no. 5. 0730–0735 hr M.S.T., 8 May 1959. Isoradiance values are in mw/cm²-sterad. Azimuth values are with respect to magnetic north. 0° elevation is horizon, 90° is nadir. Solar azimuth from magnetic north 74°, solar elevation 28°.

The results obtained when filters no. 2 and 3 were in front of the detector were seldom greater than the system noise so the results were not plotted.

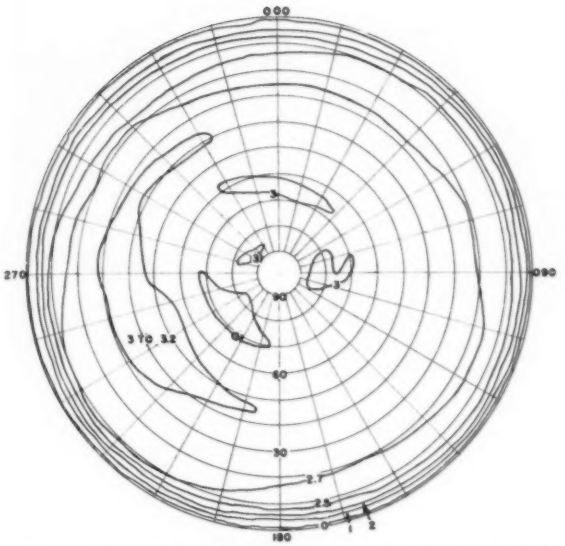

Fig. 11. Isoradiance plot filter no. 5. 0830–0835 hr M.S.T., 8 May 1959. Isoradiance values are in mw/cm²-sterad. Azimuth values are with respect to magnetic north. 0° elevation is horizon, 90° is nadir. Solar azimuth from magnetic north 84°, solar elevation 42°.

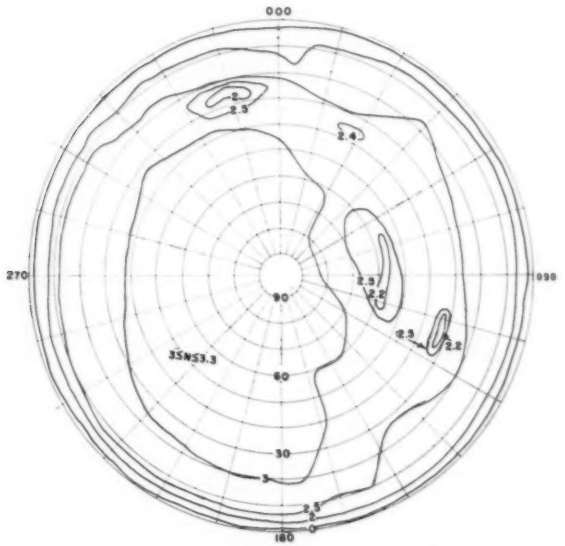

Fig. 12. Isoradiance plot filter no. 5. 1030–1035 hr M.S.T., 8 May 1959. Isoradiance values are in mw/cm²-sterad. Azimuth values are with respect to magnetic north. 0° elevation is horizon, 90° is nadir. Solar azimuth from magnetic north 111°, solar elevation 64°.

The data obtained with filter no. 4 in front of the detector are presented in Figs. 8 and 9. The wavelength region passed by this filter lies almost entirely in the 6.3 μ water vapor band. Most of the radiation reaching the radiometer in this case comes from the emission of radiation by the water vapor in the atmosphere. The only detail sufficiently gross to be drawn on the isoradiance plots is the so-called "limb-darkening" effect, the fall-off in the incoming radiation as the scan approaches the horizon.

The data obtained when filter no. 5 is in place in front of the detector are given in Figs. 10 through 12. This filter and the KRS-5 window in front of the detector pass radiation between 8 μ and 35 μ. This wavelength interval contains the so-called "window" between 8 μ and 13 μ and the intense absorption bands due to CO_2 at 15 μ, and the water vapor pure rotational band which starts at 20 μ and extends over the remainder of the interval. Since the incoming radiation is again a function of the absorption and emission of the atmospheric gases limb darkening is also observed in the isoradiance plots obtained with this filter. Some structure is observed in addition to the limb darkening. Since the CO_2 is probably uniformly distributed throughout the atmosphere this structure has to be due to variations in temperature or emissivity of the ground or else to variations in the water vapor distribution. The amount of radiation leaving the top of the atmosphere in the wavelength interval beyond 5 μ is of considerable meteorological interest and has been the subject of many theoretical studies. One of the more recent of these is the study by Hales and Zdunkowski[1] using the new Atmospheric Radiation Tables prepared by Elsasser and Culbertson.[2] These calculations are made for the total long wavelength flux leaving the earth under different meteorological conditions. In order to compare our results with these calculations it is necessary to convert our results from radiance values to flux and also remove the effect of the filter. An additional term will have to be added to correct for the radiation from 5 to 8 μ which lies outside the wavelength interval passed by the filter. Assuming that the wavelength distribution of the incoming radiation can be approximated by a blackbody of 270°K results in a multiplication by a factor of 2.8 to convert the radiance as observed through the filter into radiance at the aperture. The problem of converting the radiance values to flux values entails calculating $2\pi \times \int_0^{\pi/2} N(\theta) \cos\theta \sin\theta \, d\theta$. This could be done numerically using the data obtained during the flight. However, a rigorous comparison of the observed results data theoretical calculations would require certain with (temperature of the ground over the region observed distribution and temperature of water vapor in the region being scanned, etc.) that are not available; hence it was not considered worthwhile to perform the integration. Instead the radiation was assumed to be isotropic and the observed radiances close to the nadir are merely multiplied by π to change them to fluxes. When these corrections are made one obtains fluxes of from 242 watts/meter² to 285 watts/meter². The

theoretical flux quoted for Broken Arrow, Oklahoma, varies from 285 watts/meter^2 for a ground temperature of 40°C to 259 watts/meter^2 for a ground temperature of 15°C. The ground temperature in the vicinity of Alamogordo changes very rapidly as the sun heats it and quite often runs 15°C higher than the air temperature, and can run as high as 45°C. The Sacramento Mountains which lie to the east of Alamogordo are considerably higher and cooler than the Tularosa Basin and in addition are covered with trees, so the effective surface temperature of this region could be lower than 15°C. Thus the observed values appear reasonable in view of the many assumptions that had to be made in order to compare the results.

The authors wish to thank the personnel of the Balloon Branch at the Air Force Missile Development Center for the excellent job they did of launching and recovering the equipment.

References

1. J. V. Hales and W. G. Zdunkowski, "The long wavelength flux leaving the earth under various meteorological conditions," Scientific Report No. 1, Contract AF 19(604)-2418. Univ. Utah (1960).
2. W. M. Elsasser and M. F. Culbertson, "Atmospheric radiation tables," Final Report Contract AF 19(604)-2413. Scripps Inst. of Oceanography, Univ of Calif. (1960).

Photo D. J. Troy

Scene in London Airport on trip home from the ICO meetings—Neil Hochgraf *Rochester*, L. Mertz *Block Associates*, D. R. Herriott *Bell Telephone*, and R. Carpenter *Geophysics Corporation of America*. See page A22 for application form for 1962 group flight to Munich Meeting.

Photo D. L. MacAdam

Have you seen this one? S. Q. Duntley, who was awarded the Ives Medal at the Los Angeles Meeting, and Vern E. Hamilton, Chairman of the Program Committee for the L. A. October 1961 OSA 46th Annual Meeting.

STOP PRESS

OSA President **D.L. MacAdam** will lecture to the Local Sections as follows:

Detroit	March 26	Subject to be announced
Rochester	April 17	Color in Court
San Francisco	April 30	Subject to be announced
Los Angeles	May 2	Optical Engineering
San Diego	May 4	Optical Engineering
Sigma Xi Club		

Dates for other sections will be announced later

High Altitude Atmospheric Transmission Measurements

F. Stauffer and J. Strong

This program was designed to obtain atmospheric transmission data from high altitude, in the 1 to 12 μ region, and to measure the solar radiation spectrum in the same region. Mixing ratios, water to total atmospheric gases, at 11 km (35,000 ft) and 20 km (65,000 ft) altitude indicate a stratum of humid air above 20 km. A ground spectrum, an 11 km spectrum, and a 20 km spectrum are compared to a solar envelope constructed from available data.

Introduction

A program was carried out in Alaska in September 1960 to obtain (1) atmospheric transmission data in the 1 to 12 μ spectral region for the upper air; and (2) to measure the solar radiation spectrum over the same wavelength region, extrapolated to outside the atmosphere. The results reported here are of a preliminary nature. We plan to supplement and extend them in the future.

Experimental Program

The observations were carried out by the Lockheed Aircraft Corporation under a USAF contract.

The suntracker and all electronics were designed and built for Lockheed by Custom Instruments, Pasadena, California. These components served a spectrometer that was modified for these observations by The Johns Hopkins University.

Although it was intended that a series of spectra be obtained at various altitudes and various sun elevation angles, the only successful observations were those made at 11 km (35,000 ft) and 20 km (65,000 ft) altitude, with the sun at 20 deg elevation.

Instrumentation

The spectrometer was a Littrow instrument double-passed. It used a rock salt prism. The entrance slit was illuminated by a (f/10 beam) suntracker. A three-element thermopile was used as the detector. The spectrometer was thermally insulated from its surroundings, and provided with thermostat-controlled heating strips to maintain its temperature nearly constant.

The authors are at the Laboratory of Astrophysics and Physical Meteorology, The Johns Hopkins University, Baltimore, Maryland.

Received 2 November 1961.

The spectrometer was provided with automatic scan reversal capability; thus it was fully automatic. Three channels of a multichannel galvanometer recorder provided the data recording. One channel carried the spectral response data; a second channel carried the coarse wavelength indication—a linear voltage developed across a multiturn precision potentiometer—while a third channel carried the wavelength pip marks for more accurate wavelength monitoring.

Results

The records are represented in Fig. 1. Dr. W. S. Benedict helped us evaluate the atmospheric transmission data, yielding results summarized as follows:

(1) The observed and reduced envelope of the solar spectrum, after corrections for residual atmospheric absorption, conforms to the smooth curve of Fig. 1. This smooth curve was obtained using values of spectral brightness temperature that were found by Peyturaux[1] at 1.55 μ (6330°K), at 2.03 μ (6056°K), and at 2.31 μ (5880°K), as well as Saiedy and Goody's[2] one value at 11.1 μ (5036°K).

(2) The integrated absorptions due to water vapor yield 0.0023 cm precipitable water overhead at 11 km altitude, and 0.0013 cm precipitable water overhead at 20 km. These values give mixing ratios of H_2O to total atmospheric gases, gram for gram, of 0.9×10^{-5} at 11 km where the pressure was 240 mbar, and 2.6×10^{-5} at 20 km where the pressure was 60 mbar. Thus there appears to be a stratum of humid air above 20 km.

(3) The N_2O and CH_4 absorptions are not precise. There is no indication that the mixing ratios for these atmospheric components vary with height.

A wide variation of mixing ratio values for water vapor has been reported. The methods of measurement include: absorption spectra, frost points, and

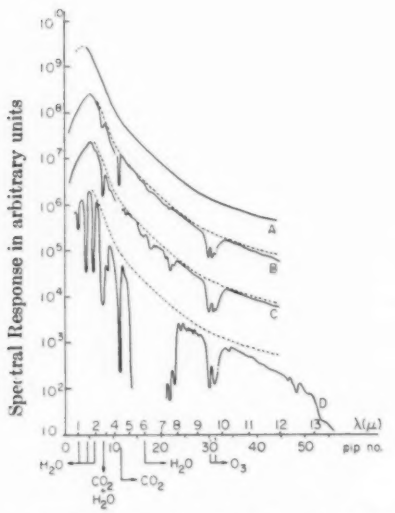

Fig. 1. Corrected solar spectra with "best" solar curve. Curve A: "best" solar curve. Curve B: solar spectrum at 20 km (65,000 ft), 20° sun elevation. Curve C: solar spectrum at 11 km (35,000 ft), 20° sun elevation. Curve D: ground run.

cooled vapor traps. Increased mixing ratio, with altitude, is reported, among others, by Murcray *et al.*[3] (absorption spectra), by Dinger and Mastenbrook[4] (frost point), and by Barclay *et al.*[5] (cooled vapor trap). Our results show a somewhat smaller mixing ratio at 11 km and a somewhat larger ratio at 20 km than these investigators. Houghton and Seeley[6] report several mixing ratio values for flights over England at 11 km. While one value for that altitude (December) coincides with the fairly constant value of 3×10^{-6} that these investigators found for the mixing ratio in the stratosphere, the other value (June) is reported as 1.5×10^{-5}. Seasonal and geographical effects, of course, cannot be ignored.

We wish to acknowledge the assistance of Mrs. Deborah Berman, of our laboratory, in the reduction of the data. We are indebted to various members of the Lockheed group, and to Mr. E. W. Silvertooth of Custom Instruments, for their part in carrying out the flight program in the field. Dr. C. H. Palmer, Jr., presently of the Electrical Engineering Department of The Johns Hopkins University, was responsible for a major part of the spectrometer modification. The suntracker, designed and built under another program, sponsored by the Office of Naval Research, was generously loaned for use during these flights. Finally, and most important, acknowledgment must be given to the Geophysics Research Directorate of the Air Force Cambridge Research Laboratories and to the Reconnaissance Laboratory, Infrared Section of the Aeronautical Systems Division, for the initiation and support of the program.

References

1. R. Peyturaux, "Contribution a l'etude du fond continu du spectre solaire dans le proche infrarouge," Ann. astrophys. **15**, 302 (1952).
2. F. Saiedy and R. M. Goody, "The solar emission intensity at 11 microns," Monthly Notices Roy. Astron. Soc. **119**, 3, 213-222 (1959).
3. D. G. Murcray, F. H. Murcray, and W. Williams, "Distribution of water vapor in the stratosphere as determined from infrared absorption measurements." Scientific Report No. 1 Contract AF 19(604)-7429, Jan. 1961. Department of Physics, University of Denver, Denver, Colorado.
4. H. J. Mastenbrook and J. E. Dinger, "The measurement of water vapor distribution in the stratosphere." Naval Research Laboratories Report 5551, Nov. 1960.
5. F. Barclay, M. Elliott, O. Goldsmith, and J. Jelley, "A direct measurement of the humidity in the stratosphere using a cooled-vapor trap," Quart. J. Roy. Meteorol. Soc. **86**, 259-264 (1960).
6. J. T. Houghton and J. S. Seeley, "Spectroscopic observations of water vapour," Quart. J. Roy. Meteorol. Soc. **86**, 358-307 (1960).

photo F. S. Harris

J. W. Larmer *Naval Weapons Plant*, A. I. Mahan *Johns-Hopkins-APL* and W. S. Rodney *AFOSR*

Ultraviolet Instrumentation for Celescope—An Astrophysical Reconnaissance Satellite

Robert J. Davis and Om P. Rustgi

Project Celescope of Smithsonian Astrophysical Observatory is designing, as part of NASA's Orbiting Astronomical Observatories program, instrumentation for mapping the sky in wavelengths between 1000 and 3000 A. The Celescope will consist of three telescopes and a slitless spectroscope. Each telescope will consist of a Schwarzschild camera with ultraviolet-sensitive television camera tube at the focus; three different wavelength bands will be covered by use of television tubes of different spectral sensitivities. The slitless spectroscope will consist of a diffraction grating ruled onto the primary of a similar Schwarzschild camera. The optical structure will be self-compensating, eliminating the need for refocusing in orbit. Calibration lamps will be carried on board the satellite to transfer the laboratory calibration to the sky. This system is scheduled to be contained in the first OAO, to be launched in late 1963 or 1964.

Introduction

Ever since the initial development of theories of the atmospheres of hot stars in the 1920's and 1930's, astronomers have needed additional observational data to support and refine those theories. However, an important portion of the spectra of these stars, that with wavelengths shorter than 2800 A, is blocked by the atmosphere and cannot reach the surface of the earth. Rocket experiments[1,2] have demonstrated that present theories do not adequately describe the appearance of the sky at wavelengths below 2000 A. However, short-duration rocket experiments cannot simultaneously have the high resolution, full sky coverage, and high sensitivity required to open this new field and pave the way for the more specialized experiments required in the future.

By its use of ultraviolet-sensitive television cameras placed in an artificial satellite, Project Celescope of the Smithsonian Astrophysical Observatory will overcome these difficulties and measure the intensity of this radiation.

Named for its pioneering use of a truly celestial telescope, Celescope is part of the Orbiting Astronomical Observatories program of the National Aeronautics and Space Administration. Other participants are the University of Wisconsin, NASA Goddard Space Flight Center, and Princeton University. Ziemer[3] describes this program more fully.

Experimental Objectives

The original and still primary objective of the Celescope program is to obtain ultraviolet maps of the sky below 3000 A to serve as the basis of further studies with more advanced satellites. This goal, as presently stated, is to obtain all-sky maps in three ultraviolet colors to a limiting magnitude of 10.0 for stars, and to a limiting sensitivity for nebulae sufficient to give rather detailed pictures of the ultraviolet nebulosities discovered by Kupperian *et al.*[1] The stellar limit should provide data on about 100,000 stars, all of which are expected to be hotter than the sun. This high, mean stellar temperature contrasts sharply with that of the visible sky, where the number of stars colder than the sun which may be observed is nearly as many as those hotter than the sun.

The nebular and stellar maps pose entirely different sets of problems. Since our stellar sensitivity requirements are relatively modest, we can concentrate on improving resolution in position and intensity measurements. The Celescope is designed to give position resolution of 30 sec, and intensity resolution of 0.1 magnitude. Our stellar information is contained in only a few points even in the most crowded picture. By disregarding any information not contained in the

The authors are at the Smithsonian Astrophysical Observatory, Cambridge, Mass.

Received 3 November 1961.

This paper is a condensation of a considerably longer and more general description of the Celescope program. The longer paper will be reproduced as a Smithsonian Special Report available from the Astrophysical Observatory in Cambridge, Massachusetts.

stellar images, and concentrating on those images, we are able to handle the stellar television photometry entirely in digital form, easily allowing us to retain the resolution capabilities of the camera tube throughout the data-handling system. These capabilities allow us 9 bits of positional accuracy in both the horizontal and the vertical directions, and 7 bits of intensity accuracy. For these stellar pictures, the satellite data-handling system treats nebulosities as "noise" that is filtered out prior to transmission to the ground, and no bandwidth is required to describe the black areas between the stars.

The nebular pictures require that we increase sensitivity at the expense of both angular and intensity resolution. Since we can make no valuable a priori assumptions regarding the information content of the picture, and since out signal transmission bandwidth is limited to 62 kc/sec, we can no longer use digital techniques. To maximize our sensitivity, we shall use the longest exposure time readily available, probably 30 sec, and an expanded scanning beam. We anticipate a resolving power of about 2 to 4 min of arc, and an intensity resolution corresponding to about 20 shades of gray. The picture will be transmitted, as in commercial television, by analog techniques.

In addition to the three broad-band photometers, we plan to install a slitless spectroscope in the Celescope. Because of the small field of view of the detector, our spectra will extend only 1.27 cm between the wavelength limits of 1100 and 2200 A. This length will allow most spectra to appear on a single picture. We have limited our spectral region to prevent interference from overlapping spectral orders. Our resolving power, limited by the scanning raster of the detector, will be about 8 A. With the stellar spectra spread out in this way, our limiting magnitude will be about 6.0, giving us an expectation of about 5000 stars. The total information content, however, as measured by the number of binary words required to describe our pictures, will be approximately the same as for one of the broad-band television photometers.

The slitless spectroscope will thus enable us to plot the spectra of the brighter stars through about 100 points, and with the broad-band equipment we may plot the spectra of a much greater number of stars through three points. The two techniques are complementary, the detailed study of individual stars supplementing a less accurate survey of a large number of stars.

Experimental Instrumentation

The entire Celescope system has been built around the television camera tube that we use as a detector. At the start of the Program in 1959, television had never been used as a true research tool in either astronomy or ultraviolet research. Our expectations for Celescope's accuracy and reliability still far exceed anything that has been done with television, even in ground-based observatories and laboratories, in either of these areas of research. Our first step was therefore to initiate the development of a suitable television camera tube, and, after this tube had been developed to essentially its final configuration, we designed an optical system around it. As the last step, we are designing the mechanical system to hold the optical elements in place, and the electronic system to operate the cameras by remote control from the ground.

Sensory System

Since optical filters alone cannot isolate the spectral regions of interest to Celescope, we require three types of television camera tubes—one for each color. The Westinghouse Research Laboratories have developed these tubes for us. Figure 1 shows preliminary spectral response curves for the three types. Type A operates at an effective wavelength of about 2200 A; Type B plus a barium-fluoride filter, at about 1500 A; and Type C, at about 1350 A. Under Celescope operating conditions, these tubes will have a threshold approximately equivalent to the radiation received from a tenth magnitude star: 3500 photons per second in a point image within the spectral pass band.

Figure 2a shows one of these television tubes and Fig. 2b how they will be placed within the optical system. Light, after being reflected from the secondary mirror, passes through the optical filter and is imaged onto the photocathode of the television tube. Since the electronic configuration of the tube requires that this photocathode have a radius of curvature of 8.00 cm concave toward the inside of the tube, the faceplate on which the photocathode is deposited takes the form of a very strong double-concave lens. The outer radius of curvature is 4.239 cm, allowing us to use a primary optical system having no curvature of field. These faceplates are ground and polished from lithium fluoride crystals, since no other known material transmits below 1200 A.

These tubes have an extreme outside diameter of 6.98 cm. The photocathode covers an area 3.56 cm in diameter on the inside of the faceplate. The scanned area is 2.54 cm square. The resolution of the best tubes approaches 250 line pairs.

We expect to use exposure times between 0.1 and 100 sec. Since these tubes can only integrate the signal from an ultraviolet image when high voltage (15,000 volts negative) is applied to their photocathodes, we have no need for a mechanical shutter. We merely turn the high voltage on and off to regulate exposure time.

The television camera tubes will be mounted, along with some of their associated electronics, in detector cases approximately 8.25 cm diam and 34.29 cm long.

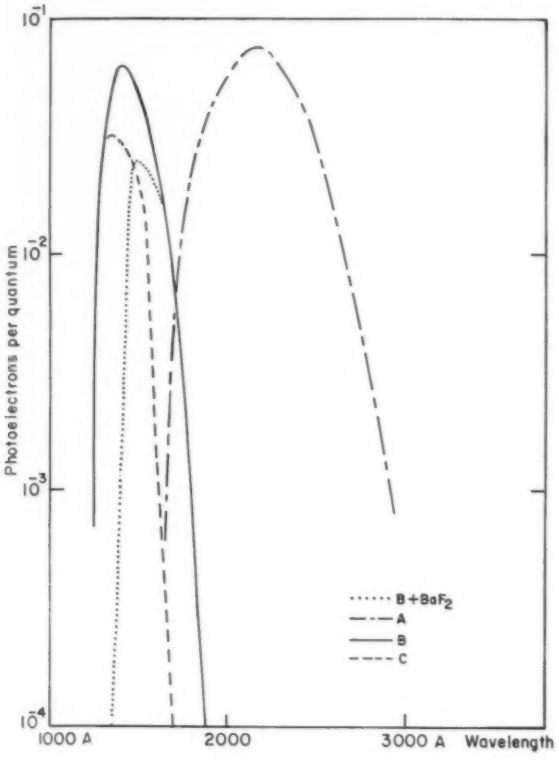

Fig. 1. Response curves of three types of ultraviolet-sensitive television camera tubes.

Optical System

The linear resolution and the field of view of the Celescope are prescribed by these detectors. The first basic parameter of the optical system, the effective focal length, must be between 40.6 and 101.6 cm. For a 101.6-cm focal length, the field of view becomes 1.5° square, thus requiring 25,000 pictures to cover the sky. We shall not have time, during the one-year expected useful life of this satellite, to take more pictures than this. For a 40.6 cm focal length, the resolving power becomes 1 min of arc. The densest star fields would in this case be expected to contain as many as 700 stars. Under such crowded conditions, we begin losing important information. In addition, it becomes very difficult to design a system of adequate aperture with so short a focal length.

The second basic parameter of the optical system, the aperture, is set by the physical dimensions of the spacecraft that NASA is supplying us. The aperture will be 30.48 cm for each of our four instruments.

Within this framework, we require the simplest system that will give adequately small aberrations throughout our field of view. Complex instruments cannot adequately survive the launch environment. We cannot allow large lenses in our system, since they are not available in materials that are useful in the far ultraviolet. We studied the properties of one-mirror systems, and found none that could meet our requirements. In two-mirror systems, the Schwarzschild camera is the simplest that fits our needs.

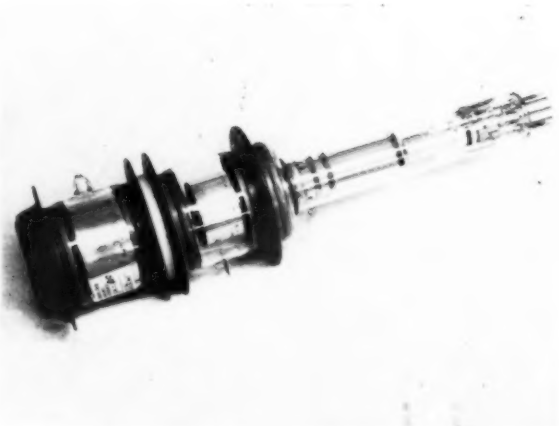

Fig. 2a. Photograph of ultraviolet-sensitive television camera tube of the ebicon type.

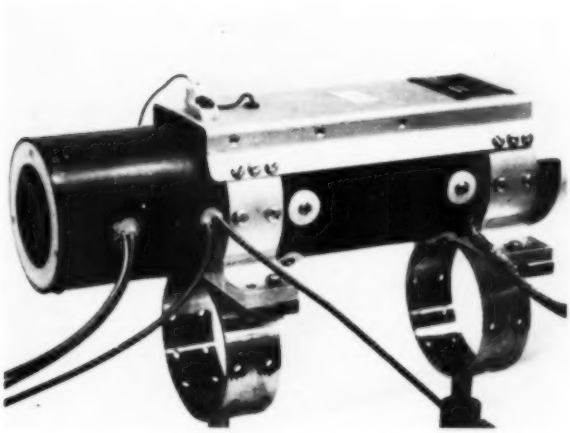

Fig. 2b. Ultraviolet-sensitive television camera tube in its mount.

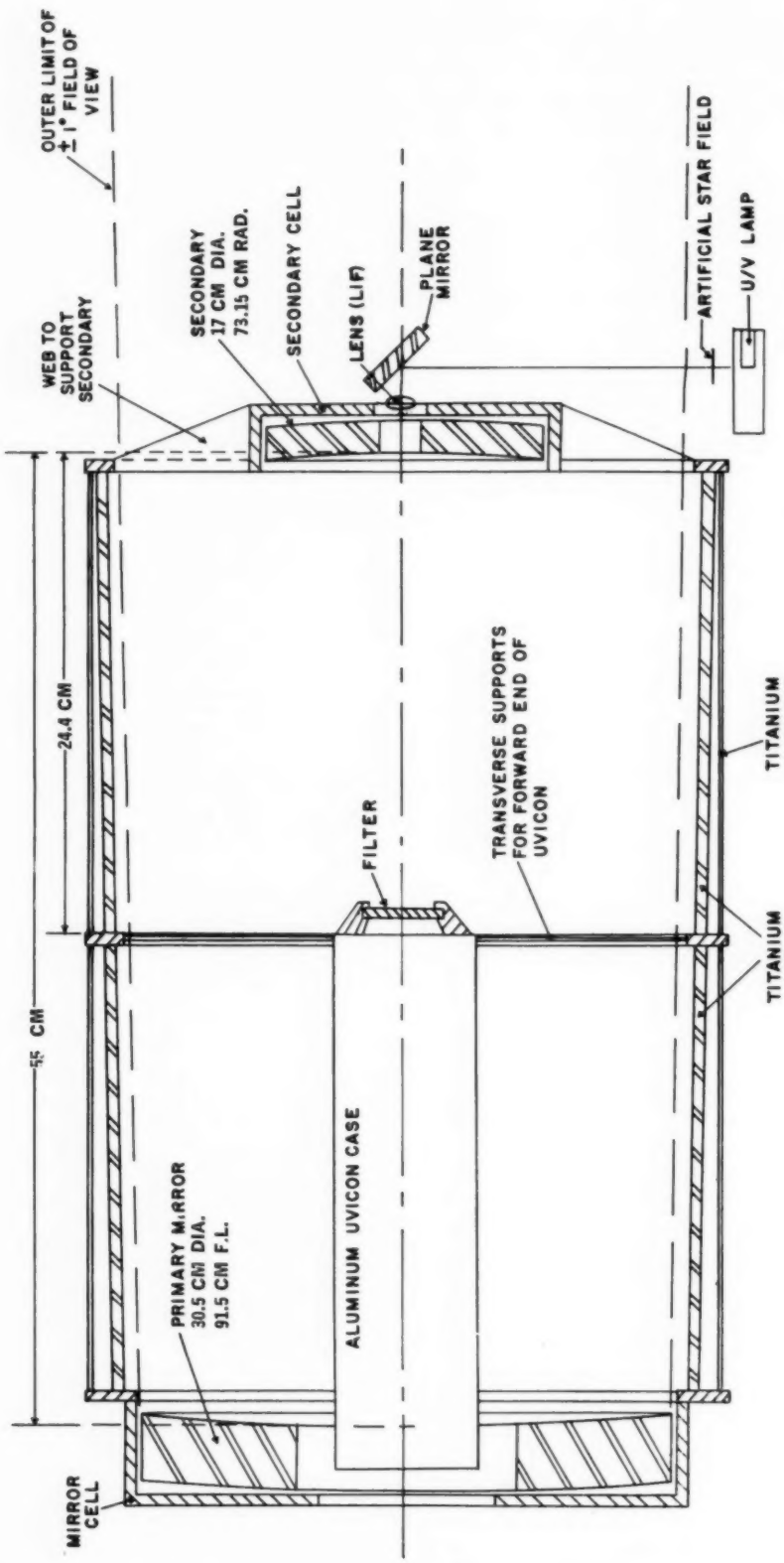

Fig. 3. Optical configuration of one of Celescope's four Schwarzschild cameras.

Schwarzschild[4] designed this family of telescopes to be free of coma, spherical aberration, and curvature of field. As applied to Celescope, this system gives nearly uniform, approximately circular star images about 50 μ in diameter, throughout a field of view 3.56 cm in diameter. Figure 3 shows the configuration.

We use a Schwarzschild camera with an effective focal length of 60.96 cm. The faceplate of the detector modifies the EFL of the system to give 63.228 cm. We have designed the system for no vignetting except in the corners of the field, since the shadow on the primary of the secondary mirror and its cell is larger than the perforation in the primary even for stars at the edges of the field of view 2.54 cm square. The reflection of this shadow by the primary mirror is, over its entire length, larger than the case containing the television camera tube. It is also larger than the perforation in the secondary mirror. Both mirrors are perforated, for structural reasons associated with the launch environment and the detector case configuration. In addition, the light path for the calibration system (to be described below) passes through the perforation in the secondary. The system thus defined has the following parameters:

Primary mirror:
- over-all diameter 31.75 cm
- clear aperture 30.48 cm
- perforation diameter 12.70 cm
- edge thickness 5.72 cm
- shape, hyperboidal, $z = h^2/182.88(1 + \sqrt{1 + 0.0001085\ h^2})$, where z is the sag and h is the height above the optic axis, both expressed in cm
- reflecting surface, aluminum + magnesium fluoride
- material, fused quartz
- weight 12.7 kg

Secondary mirror:
- over-all diameter 15.87 cm
- clear aperture 15.37 cm
- perforation diameter 2.54 cm
- outside diameter of cell 17.02 cm
- edge thickness 2.54 cm
- shape, oblate ellipsoidal, $z = h^2/146.304(1 + \sqrt{1 - 0.0018667\ h^2})$, where z is the sag and h is the height above the optic axis, both expressed in cm
- reflecting surface, aluminum + magnesium fluoride
- material, fused quartz
- weight 1.36 kg

System:
- effective focal length 63.228 cm
- total length between mirror vertices 54.86 cm
- distance between secondary mirror vertex and focal plane
- field of view, 2.54-cm square = 2.4° square
- effective focal ratio (transmission ratio), $T/3.7$, assuming 75% reflectivity
- sensory system (see above)
- image quality, 95% of light within 100 μ circle under all conditions of decentration less than 0.25 mm from optimum focus, throughout the field of view, for collimated input beam
- focal surface, plane except as modified by detector faceplate (see above)
- weight, 26.3 kg, including optics, detector, and structure

Although Schwarzschild's work was published in 1905, no Schwarzschild camera has ever been used successfully in astronomical research. Two such instruments, one at Brown University and the other at Indiana University, proved ineffective because of the difficulty of figuring the optics, and because of the inconvenient location of the focal plane. For ground-based astronomy, the Schmidt camera gives much better performance. In space, however, the Schwarzschild system is far preferable to the Schmidt. First, the Schmidt corrector plate poses great difficulties for work in the ultraviolet because of the few choices and small sizes among transmission optical materials that are available. Second, the field of view and the resolution of our television system are too poor to enable us to take advantage of the superior resolving power and field of view provided by a Schmidt system. Third, it is easier to mount small thick mirrors than large thin corrector plates for the rugged environment of launch. It is true that Schmidt systems have been designed with reflective corrector plates, but such systems must be built off-axis with consequent difficulties in figuring and mounting them.

Slitless Spectroscope

For our slitless spectroscope, we plan to use an objective grating ruled directly onto the surface of the primary mirror of a Schwarzschild camera. The region of the stellar spectrum from about 1100 to 2200 A must be spread out over approximately half the field of view. The ruling required to achieve this dispersion is 200 lines per millimeter. In order to suppress the unwanted orders and to accentuate what is expected to be the fainter end of the spectra of most stars, this grating should be blazed for Ly α (0.25° blaze angle). Since resolution is limited by the detector, we do not require a resolving power of the grating greater than 10% of the theoretical one. Our requirements cannot be met by ruling the grating onto the secondary mirror, since the best resolving power of such optics is 100 A, corresponding to 1250 μ if the spectrum is 1.27 cm long.

Several of our requirements are severe, and we are not yet assured that such a grating can be produced. The blank diameter of 31.75 cm is larger than the usual

20.3-cm maximum. We are reluctant to settle for the decreased light-gathering power that would result were we to rule only the inscribed square of side 21.57 cm, but ruling of the entire 30-cm aperture poses especially difficult problems. The central perforation is another difficulty, although probably not so serious. The rather steep curvature of the blank poses a third problem, especially in regard to blaze angle.

Mechanical System

One of the primary considerations in our design of the Schwarzschild system was the allowable decentration error. Decentration is the departure, in any dimension, of an optical element from its position of best focus. Our system will allow a decentration up to 0.25 mm for any component parallel to the optic axis. Perpendicular to the optic axis, the system will allow decentration of the primary mirror by 1.27 mm, of the secondary mirror by 0.635 mm, and of the faceplate of the television camera tube by 0.38 mm. No component may be tilted by more than 3 min of arc. Within these limits, image size throughout the field of view is less than the detector's resolution limit of 100 μ.

The temperature at which the Celescope must operate is $-30°C \pm 15$. The laboratory in which it must be adjusted prior to launch will, however, have a temperature of $+20°C \pm 10$. Since we require that the Celescope have no moving parts, we must choose structural materials that will preserve the proper dimensional relationships among the optical components over a temperature range of up to 75°C.

We have two alternatives for solving the problem of thermal expansion. The first is to build the optical components and structure from materials with the same coefficient of expansion. Unless the coefficient is negligible, this method requires that all structural elements be at the same temperature. In addition, mechanical considerations would suggest a choice of structural materials with medium or high coefficient of expansion, whereas optical considerations point toward optical materials of negligible coefficient. Although we are investigating the use of novel techniques for obtaining dimensional stability from such low-expansion materials as Pyroceram, our primary effort is now directed toward the second method, that of passive compensation.

The usual method of compensation makes use of two concentric cylinders, the shorter of which has a higher coefficient of expansion. These two cylinders are joined at one end. The distance between the free ends then remains constant regardless of temperature.

We plan to make use of the optical properties of the Schwarzschild system to simplify our compensation network. As shown in Fig. 3, the main supporting structure joining the primary and secondary mirrors will be a titanium tube approximately 63.5 cm long. The thermal expansion coefficient of titanium is about 8.5 ppm/°C, so that a drop of 75°C will cause the distance between the mirrors to decrease by 0.406 mm. Although this distance exceeds our decentration limit, we can achieve adequate focus by moving the detector faceplate 0.584 mm nearer the primary mirror. If the temperature of the television-tube support is the same as that of the titanium structure joining the two mirrors, aluminum is the correct material for joining the television-tube faceplate to the base of this titanium structure. If the heat released by the television tube cannot be removed by conduction before reaching and heating the support, the correct material is magnesium. Aluminum has a coefficient of expansion of about 21.4 ppm/°C; magnesium has a coefficient of 27.1 ppm/°C.

During launch, the Celescope will be pointed downward, a deciding factor in our mirror-cell design. Each primary mirror will be supported by padded fingers, three on the outer rim and three around the perforation. The back of this mirror will be supported by four teflon pads, and there will be three similar pads about its circumference. The 127 kg (10g) effective launch weight will be supported by the three fingers on the front side.

The support system for the secondary mirror will be similar to that of the primary. Here, however, the 13.6 kg (10g) effective launch weight will be supported by the padded back-plate.

Calibration Techniques

Proper calibration of the Celescope is so important that we anticipate spending as much as half of our entire effort to ensure calibration of adequate quality. Our techniques for the calibration of the various Celescope components are growing to keep step with the camera-tube development program. Although the spectral response and sensitivity of each tube are calibrated by the manufacturer, we recheck all tubes when we receive them, and again when they are mounted in prototype and flight equipment. Figure 4 is a photograph of our calibration equipment, labeled to illustrate the following discussion of our techniques.

We begin by calibrating a dc hydrogen glow discharge source. This lamp is placed at the entrance slit of a vacuum monochromator, and a nitric-oxide photon counter placed at the exit slit. The monochromator is set to isolate the Ly α radiation of the lamp. We know the efficiency of the counter from the absorption cross section of nitric oxide at this wavelength. This arrangement gives the absolute flux of Ly α emerging from the exit slit for our particular calibration setup.

We now replace the nitric-oxide detector with a photomultiplier tube coated with sodium salicylate. The fluorescent quantum efficiency of this material is constant over the spectral range of 1000 to 3500 Å. By scanning the monochromator through this range, we

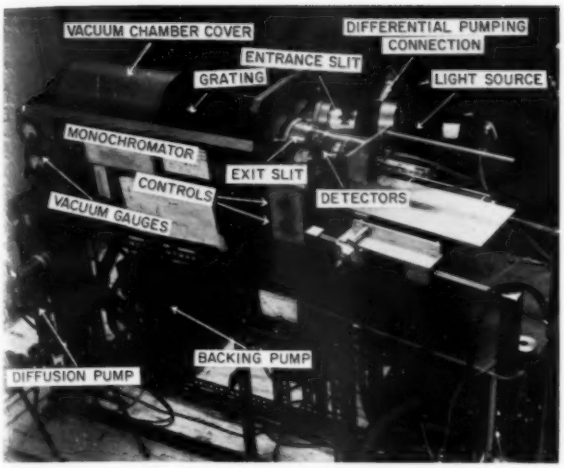

Fig. 4. Celescope spectrophotometric calibration equipment.

obtain the relative spectral output curve of the monochromator under our standard calibration-scanning conditions. The absolute output is determined from the response at Ly α.

We next check this calibration by means of a thermocouple. We first take a spectral scan using the hydrogen source and a thermocouple detector. Then we calibrate the thermocouple against a standard incandescent lamp certified by the National Bureau of Standards. We resolve any disagreement between the two independent methods of calibrating our scanned monochromator output before proceeding to the next step.

For calibrating a television camera tube, we place the tube at the exit slit of the monochromator and scan the spectrum in the standard manner. We record the video output on an oscilloscope to obtain the video output signal as a function of wavelength and position on the faceplate of the tube. Since the exit slit will be 0.10×8 mm and the photocathode is used over a 25-mm square area, this mapping of the spectral sensitivity of each tube is a time-consuming operation.

The calibration is not complete until the other elements of this system, and the assembled system itself, have been calibrated. To measure the reflectivities of our mirrors, we coat a small test plate when we coat the mirror surfaces. A special attachment at the exit slit of the monochromator allows us to measure in quick succession the direct and the reflected beam. We are thus able to determine the effect of mirror reflectivity on our system response. The same apparatus allows us to measure the transmissivity of each optical filter.

We can calibrate our video amplifiers and communications link by impressing electronically generated video signals of known amplitude at the signal input electrodes.

For the system test, we must go to the vacuum optical bench to be built at the NASA Goddard Space Flight Center for OAO use. Its ultraviolet source must be calibrated by means similar to those used on our smaller Smithsonian spectral scanning equipment. If the system calibration does not agree with the sum of the calibrations of the parts, we must again look for and remove the sources of error.

It is highly important to protect all of our optical elements, i.e., mirrors, filters, and detectors, from any environment that would tend to change the system's spectral response curve, since once the Celescope is assembled, remeasuring these quantities to the desired accuracy becomes very difficult, if not impossible. After assembly of the Celescope we will, therefore, rely on calibrated point sources to check the sensitivity calibration. Once the satellite is in orbit, it may be impossible to differentiate between sensitivity changes caused by the optics and those caused by the electronics.

Our calibrator will consist of an artificial star generator (see Fig. 3) to focus a spot of known spectrum and intensity onto the photocathode. The response of the system to this signal will enable us to determine system sensitivity changes. We have portable ultraviolet spot generators to be used as necessary during assembly of the Celescope. Once assembly is complete, we shall, of course, be able to use the ultraviolet calibrators to maintain the sensitivity calibration through subsequent fabrication, countdown, and launch. This calibration will be independently checked, in the Goddard Space Flight Center vacuum optical facility, as close as possible to final assembly of the OAO.

Each step in the calibration is performed as near as possible to the time of the first observation. By making our first observations in Orion, where a large number of stars may be expected to be bright in the ultraviolet, we hope to locate early a field suitable as a photometric standard. We shall then return to that field frequently, while we set up secondary standards in the selected areas, related back to it. A standard field will be observed at least once per day, and the internal calibration used at least twice per orbit. Thus, we shall be using our artificial standard as an aid to interpolation only, and the calibration sequence will be varied as necessary during operation.

References

1. J. E. Kupperian, Jr., A. Boggess, III, and J. E. Milligan, Astrophys. J. **128**, 453 (1958).
2. T. P. Stecher and J. E. Milligan, *Astron. J.* **66**, 296 (1961).
3. R. R. Ziemer, *Astronautics* **6**, No. 5, 36 (1961).
4. K. Schwarzschild, *Mitt. Sternwarte zu Göttingen* **9**, 1 (1905).

Meetings Calendar

1962

March

1-3 8th Scintillation and Semiconductor Counter Symposium, Hotel Shoreham, Washington, D.C. *G. A. Morton, RCA Labs, Princeton, N.J.*

5-9 13th Pittsburgh Conference on Analytical Chemistry and Applied Spectroscopy, Penn-Sheraton Hotel *L. P. Melnich, U.S. Steel Corp., Monroeville, Pa.*

12-13 Inter-Society Color Council 31st Annual Meeting, Statler Hilton Hotel, New York, N.Y. *R. M. Evans, Eastman Kodak Co., Color Tech. Div., Bldg. 65, Rochester 4, N.Y.*

14-17 **Optical Society of America Spring Meeting, Mayflower Hotel, Washington, D.C.** *K. Kessler, National Bureau of Standards, Washington, D.C.*

— American Society for Photogrammetry, Shoreham Hotel, Washington, D.C.

20 OSA Rochester Section Joint Meeting with American Chemical Society *J. L. Rood, Bausch & Lomb, Inc., Rochester, N.Y.*

26-29 IRE International Convention, New York *D. B. Sinclair, IRE H.Q. 1 E. 79th St., New York 21, N.Y.*

26-29 Instrument Society of America Meeting, Dallas *W. H. Kushnick, 312 6th Ave., Pittsburgh 27, Pa.*

28-31 Molecular Spectroscopy Conference, London *Institute of Petroleum, 61 New Cavendish St., London, W 1, England*

April

— American Astronomical Society Meeting, Cambridge, Mass.

— Symposium on the Optical Maser, New York *Office of Aerospace Research, Washington 25, D.C.*

— Association for Applied Solar Energy Symposium on Solar Science, Phoenix, Ariz.

2-13 8th Munich Photogrammetry Week *H. Bischoff, Zeiss-Aerotopograph G.M.P.H., Ismaningerstrasse 57, Munich 27, Germany*

3 OSA Rochester Section Meeting *J. L. Rood, Bausch & Lomb, Inc., Rochester, N.Y.*

3 Society for Applied Spectroscopy New York Section Atomic Absorption Spectroscopy Meeting, Statler-Hilton Hotel, New York

13-14 APS New York Section Symposium on Plasma Physics, Tarrytown, N.Y. *A. F. Turner, Bausch & Lomb, Inc., Rochester, N.Y.*

16-19 1st International Conference on Vacuum Ultraviolet Radiation Physics, Univ. So. Calif. *G. L. Weissler, Univ So Calif., Los Angeles 7, Calif.*

17 OSA Rochester Section, *J. L. Rood, Bausch & Lomb, Inc., Rochester, N.Y.*

23-26 American Physical Society, Washington, D.C. Meeting *K. K. Darrow, 538 W. 120th St., New York 27, N.Y.*

30-May 4 SMPTE Semi-Annual Convention, Los Angeles, Calif. *55 W. 42 St, New York 36, N.Y.*

30-May 3 13th Annual Mid-American Symposium, Society of Applied Spectroscopy, Hotel Conrad Hilton, Chicago, Ill. *J. R. Ferraro, Argonne Natl. Lab, Argonne, Ill.*

May

— IRE International Scientific Radio Union, Washington, D.C., Spring Meeting *IRE, 1 E. 79th St., New York 21, N.Y.*

6-10 Electrochemical Society Meeting, Statler Hilton Hotel, Los Angeles, Calif.

7-11 Society of Photographic Scientists and Engineers, Somerset Hotel, Boston, Mass. *K. Kohlman, 13712 Mariana Dr., Rockville, Md.*

8 OSA Rochester Section Annual Dinner Meeting *J. L. Rood, Bausch & Lomb, Inc., Rochester, N.Y.*

8 Society for Applied Spectroscopy New York and Philadelphia Sections Solid State Lasers Meeting

14-16 14th Annual National Aerospace Electronics Conf., Biltmore Hotel, Dayton, Ohio *G. Langston, 4745 Rean Meadow Drive, Dayton 40, Ohio*

20-23 Radiation Research Society 10th Annual Meeting, Colorado Springs

21-25 Max Planck Institute for the Advancement of Science, 13th General Assembly, Düsseldorf *J. Ammundsen, Sammenslutningen of Arbejdsgingere Indenfor den Keramiske Industri, Norrevolgade 34, Copenhagen, Denmark*

22-24 IRE National Microwave Theory and Techniques Symposium, Boulder, Colo. *R. W. Beatty, NBS, Boulder, Colo.*

28-June 2 International Optical League Berlin Congress *G. H. Giles, IOL, 65 Brook St., London, W.1, England*

29-June 19 World Meteorological Organization Congress, Geneva, Switzerland

31-June 3 German Bunsen Society for Physical Chemistry 61st General Assembly, Münster, Germany *Carl Bosch Haus, Varrentrappstr, 40-42, Frankfurt am Main, Germany*

31-June 7 International Television Conference London *Institution of Electrical Engineers, Savoy Place, London, W.C.2, England*

late Interphoto Congress, Copenhagen *International Photography and Cinematography Dealers Association, Steienvorstadt 63, Basel 10, Switzerland*

late Washington Symposium on Use of Artificial Satellites for Geodetic Purposes *International Association of Geodesy, 18 rue Auber, Paris IX, France*

June

5-8 24ème Congrès Annual du GAMS *Secretariat, 1 rue G. Boissier, Paris XV, France*

7-10 Canadian Association of Physicists 17th Annual Congress, Hamilton Ontario

11-14 Instrument Society of America Seattle, Wash., Instrument-Automation Conference and Exhibit *W. H. Kushnick, 313 6th Ave., Pittsburgh 22, Pa.*

11-15 Columbus Symposium on Molecular Structure and Spectroscopy *R. A. Oetjen, Dept. Physics, Ohio State University, Columbus 10, Ohio*

18-22 Eindhoven Congress on Magnetic and Electric Resonance and Relaxation *D. J. Kroon, Natuurkundig Laboratorium, N.V. Philips' Gloelampenfabriek, Eindhoven, Netherlands*

18-22 International Conference on Spectroscopy, Univ. of Maryland *B. F. Scribner, National Bureau of Standards, Washington 25, D.C.*

24-29 ASTM National Meeting and Apparatus Exhibit, Statler Hotel, New York *ASTM, 1916 Race St., Philadelphia 3 Pa.*

25-30 Copenhagen Symposium on Electromagnetic Theory and Antennas *H. Lottrup Knudsen, Oster Voldgade 10 G, Copenhagen K, Denmark*

July

— International Colloquium on Novae, Novoids and Supernovae, Lyons, France

— 11th International Astrophysics Symposium, Liège *P. Swings, Inst. of Astrophysics, Sciessin, Belgium*

— Munich Symposium on Crystallographic Computing *D. W. Smits, International Union of Crystallography, c/o Mathematisch Institut., Univ. of Groningen, Reitdiepskade 4, Groningen, Netherlands*

— IUPAP Conference on Paramagnetic Resonance in Crystals, Jerusalem *W. Low, Hebrew Univ., Jerusalem, Israel*

— Summer Course in Optics *Inst. of Optics, Univ. of Rochester, River Campus Station, Rochester 20, N.Y.*

9-14 6th International Commission on Glass, Washington, D.C. *C. H. Hahner, General National Committee, c/o Glass Section, National Bureau of Standards, Washington D.C.*

16-20 International Conference on the Physics of Semiconductors, Exeter *IPPS, 47 Belgrave Square, London, S.W.1, England*

24-27 Symposium in Commemoration of Fiftieth Anniversary of the Discovery of x ray Diffraction and of Crystal-structure Analysis, Munich *D. W. Smits, International Union of Crystallography, c/o Mathematisch Institut., Univ. of Groningen, Reitdiepskade 4, Groningen, Netherlands*

Optical Instrumentation for TIROS

Marvin H. Harper, Jr.

A brief description is given of the TIROS satellite* and ground equipment in order to illustrate the need for optical testing. The methods of determining resolution, distortion, and brightness response of the system are reported here, along with the instrumentation used in the measurements.

The TIROS System

The TIROS Satellite System was developed as an experiment to determine the feasibility of gathering meteorological information from an orbiting weather-observation station. The word TIROS is an acronym, derived from Television (and) Infrared Observation Satellite. This paper will deal only with the TIROS (television) cloud picture-taking subsystem and, in particular, its optics. Other papers[1,2] which have been published cover details of the infrared observation subsystem.

A satellite provides the meteorologist with an unusual vantage point from which to view the earth's cloud-cover. It frees him from the obstructions of buildings, mountains, and low-hanging clouds themselves.

At the time that the design of the TIROS satellite was begun, many effects of the space environment were unknown or unconfirmed. (The effect of cosmic rays is still being investigated.) The very low pressure experienced 640 or 800 km above the earth presented the design engineer with the problem of selecting materials that would not sublimate at these pressures. In the field of optics, it was known that many optical glasses would brown when exposed to ultraviolet radiation for long periods of time.[3] But what would cosmic and x-rays do to optical glass no longer protected by the atmosphere?

Since the TIROS satellites were not equipped with an "active" stabilization system, the satellites were given a permanent "spin" to keep them from tumbling in a haphazard fashion. Although this stabilized the spin and optic axes in space, it introduced a motion which would cause smear in a picture having any appreciable exposure time. A shutter was therefore incorporated into each camera, and the picture exposure was limited to 1.5 msec. This reduced smear, for spin rates of the order of 9 to 12 rpm, below the resolution capabilities of the subsystem.

It must be understood that the TIROS television system is not the same as commercial broadcast television, even to the point that TIROS produces "still" pictures, while commercial television generally is thought of in terms of motion pictures. However, when interest lies in the details of a picture, one generally examines a still photograph or a single frame.

A satellite in orbit does not experience any shaking or vibration. Apart from a centrifugal force caused by the satellite spin, everything will be weightless. In rude contrast to the tranquility of outer space are the conditions at launch. During this period, the satellite experiences several g's of acceleration, plus severe vibration. Consequently, the satellite structure and all components must be designed to withstand these forces. Fortunately, the launch conditions are fairly well known, and they can be considered quantitatively in both equipment design and environment simulation (tests).

The photographing of clouds from sounding rockets in space has been going on for a number of years. In preparation for the design of the TIROS optics, these pictures were analyzed at the U.S. Weather Bureau and at the RCA Space Center to determine resolution criteria for recognition of various cloud types. The rocket pictures showed that weather systems cover vast areas—no rocket picture encompassed a complete weather system. (The TIROS pictures showed that such systems cover even greater areas than those estimated from examination of the rocket pictures.) In order to have useful pictures of both weather systems and cloud detail, it was decided to equip the first TIROS satellites with two cameras, having resolutions in the ratio of 8 to 1. The lower-resolution camera used a wide-angle lens which covered an angle of 104° on the

The author is in the Astro-Electronics Division of the Radio Corporation of America, Princeton, New Jersey.

Received 1 November 1961.

* The TIROS III project is performed under the sponsorship of the National Aeronautics and Space Administration.

diagonal. The higher-resolution, narrow-angle camera covered an angle of 13°.

To minimize the complexity of the optics, and thereby retain high reliability, no provision was made for an iris diaphragm. Several studies[4-6] of the solar flux outside of the earth's atmosphere revealed data on the cloud brightness one might expect. It was thought at first that the latitude of the film used in the kinescope recorder (for the satellite-returned pictures) at the ground stations would accommodate variations in scene brightness ranging from the condition where the sun was directly over a white thunderhead (90° angle) to that where it was angled at 20° from the normal to a thin cirrus. On this assumption, the electronic equipment would require no adjustment during an orbit, once it had been properly set up. Between passes, the settings would be checked to ensure they had not changed. However, it was later found more practical to hold the photographic conditions invariant, and adjust the gamma and blacklevel of the ground electronic equipment.

Since the only objective of the television subsystem was to photograph clouds, it was desirable to obtain the best contrast between the earth's cloud-cover and its background. The first step taken was to filter out the blue end of the visible spectrum. The vidicon camera tubes used had a spectral cutoff at about 800 mμ. (Vidicons had been produced by various laboratories with a longer wavelength response, but other requirements also had to be given consideration.) The vidicons for TIROS I and II had a longer wavelength response than those for TIROS III, but the reduced response of the latter was more than compensated for by the general improvements introduced in the newer vidicons.

With the sensitivity of the cameras bracketed by the spectral limits of the vidicon and the need for a fast (1.5 msec) shutter speed, it was found desirable to hold the short-wavelength cutoff at 500 mμ. This led to the selection of a Y-10 glass filter. (Gelatin was undesirable for use in the low-pressure space environment.)

Pictures photographed by a TIROS satellite can be transmitted immediately to earth (to a Command and Data Acquisition, or CDA, ground station) while the satellite is within an approximate 2880-km range of the ground station. At greater distance, the (converted) electrical picture data are stored on a magnetic tape recorder carried in the satellite. These stored data are subsequently read out and transmitted when the satellite is within radio communications range of another CDA station.

Picture data received by a CDA station are converted to an optical image on a kinescope video display (monitor) unit, and, as it is synthesized (at a rate of 2 seconds per picture), it is photographed on 35-mm film. Additional data transmitted from the satellite and the ground-programming equipment are converted to alpha-numerical displays adjacent to the video presentation, and are photographically recorded with the cloud image.[7] This gives the picture frame number, the TV camera number, a reference angle for the sun, and whether the picture was directly-transmitted or was read out of a tape recorder. The image on the monitor display can be synthesized to produce either a film-recorded positive or a negative. Positives are used by meteorologists to make an on-the-spot analysis of the cloud-cover. Negatives are utilized as masters, from which duplicate positives can be made.

The satellite-transmitted electrical data received at the CDA station are recorded on magnetic tape (simultaneously with their display). These data can be read out for display on the video monitor between satellite passes, for the production of duplicate films.

The cloud picture, to be of maximum usefulness to a meteorologist, should have its geographical directions and location with respect to the earth identified, and should be corrected for picture-taking-angle distortion and spherical distortion (i.e., picture rectification). On the TIROS satellites, a horizon scanner was used to provide data for calculation of the spin-axis attitude, which, in turn, could be used to determine the location of the picture frame area. In practice, rather than relying on the calculated location entirely, a landmark would be used to fix the location of one or more pictures. The remaining pictures of a series can be located by using cloud formations that appear in successive pictures in order to form a running sequence. Rectification is accomplished by projecting a 35-mm film frame on a Canadian projection graph, and sketching the outline of the clouds or cloud areas.[8] This pictorial information is transferred to a rectangular plot having the latitude and longitude grid corresponding to the predetermined geographical location.

TIROS Optical Measurements

The state of the art that helped dictate the TIROS satellite design precluded the possibility of adjustments to the cameras and their optics once the satellite was in orbit. Consequently, it was necessary to establish and verify thoroughly before launch that all equipment was in optimum adjustment. Also, the conformance of the optical equipment (and its associated electronic equipment) to the established specifications must be verified before the satellite can be considered qualified for acceptance.

It must be remembered that the TIROS satellite is merely a piece of equipment required to instrument the over-all TIROS meteorological experiment. To ensure highest reliability, only proved, state-of-the-art equipment and techniques were permitted in the satellite design and operation. The application and modification of these for compatibility with the space environment did require some ingenious and novel work. In the field of optical testing, three tests were developed that are worthy of discussion, and these are presented here.

I. Resolution Measurements

Since the engineers designing the satellite's optical equipment had television backgrounds, it is not surprising to find that optical resolution for TIROS equipment was expressed in terms of television lines. This, one remembers, is double the numerical value used to express optical-line-pairs, which is the alternate acceptable definition of a black and a white TV line. The resolution values given in this paper are, to be consistent, expressed in TV lines.

The 1.27 cm vidicon used for TIROS has a nominal limiting resolution of 350 television lines. (It was scanned with a 500-line raster to ensure that the raster would not be the resolution-limiting factor.) One can calculate the ground-image resolution from the satellite altitude and the lens focal length,[9] but this information would be accurate only for pictures taken straight "down." In the laboratory, it was quite sufficient to try to visually distinguish the greatest number of television lines in a picture.

In order that resolution of the cameras could be checked frequently during the test phases of readying the satellite for launch, it was found that a test target was needed. This test target was incorporated into an optical system (which is referred to as a "collimator," although it is not an instrument like those found on a spectrometer). Due to the fact that a star pattern is not suitable to television system tune-up and camera focusing it would be desirable that the collimator have an image which covered the same angular field as the camera. In the case of the wide-angle system, this was impossible with a simple optical arrangement. A test was run with several lenses to determine the greatest field that could be covered with a single-lens collimating system. Table I gives the results. The problem that exists in this type of system can be seen from Fig. 1.

Table I. Field of View Covered with Signal-Lens Collimator for Elgeet Navitor $F = 5.33$ mm[a]

Focal length	Lens type and f/number	Front nodal point towards Elgeet lens	Rear nodal point towards Elgeet lens
50 mm	Carl Zeiss Jena Tessar $f/3.5$	15°	—
50 mm	Schneider Keuznach $f/1.9$	15°	19°
125 mm	Schneider Xenon $f/2.0$	20°	34°

[a] Angle values are "full angle," with 1 to 2 mm separation between lens cell and front-glass surface of Navitor lens. The full angular coverage is used rather than the "half angles" used in classical optical measurement.

A wide-angle collimator requires close coupling of the collimator lens and the lens under test, to prevent vignetting, or loss of the marginal pencils of light. On the wide-angle camera, it was found that approximately 30° full field was the largest practical image.

The standard RETMA TV test pattern was used in the collimator to determine resolution and general

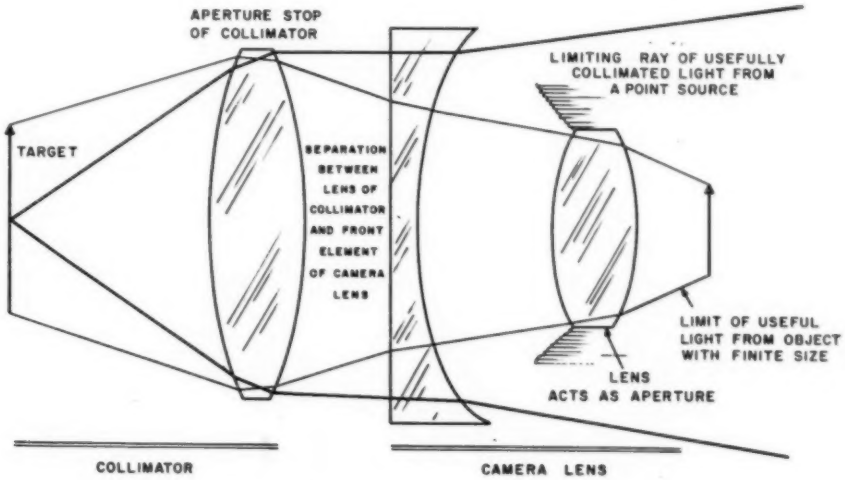
APERTURE STOP OF COLLIMATOR
LIMITING RAY OF USEFULLY COLLIMATED LIGHT FROM A POINT SOURCE
TARGET
SEPARATION BETWEEN LENS OF COLLIMATOR AND FRONT ELEMENT OF CAMERA LENS
LIMIT OF USEFUL LIGHT FROM OBJECT WITH FINITE SIZE
LENS ACTS AS APERTURE
COLLIMATOR
CAMERA LENS

Fig. 1. Useful limits of collimator system with finite size target.

picture quality. However, since only the central part of the pattern could be observed by the wide-angle lens, the gray-scale pattern was relocated to fall into that area, so that all significant characteristics of the picture could still be studied.

To assure that the cameras were focused properly, the target in the collimator then was changed to one consisting of vertical lines. (The collimator is designed to permit changing the target without affecting the focus.) The lines were grouped in triplets, with the resolution changing from about 250 television lines to more than 400 television lines. The signal generated by the scan as it swept across the picture was read out on an oscilloscope. Focusing was accomplished by alternately adjusting the electrical focus and then the optical focus of the television camera to give the maximum amplitude signal for line triplets near the limiting resolution. By using this technique, it was possible to eliminate the need for requirement of optimum focus of a monitor and the subjectiveness of a human, visual appraisal. Normally, this may not appear to be much of an advantage, but it is definitely so with a two-second sweep rate, which requires that the picture on the monitor must be photographed if it is to be analyzed. Also, the problem whether the monitor and the display-photographing (Polaroid) camera are in focus does not arise.

The collimator was focused at infinity on axis. Though theoretically this is not the most desirable distance to focus the center of the camera picture in order to get the best over-all focus, it was found that in practice this distance gives satisfactory results over the entire picture.

The standard test pattern used in the collimator was made up of the center section of the RETMA TV test pattern. A gray scale of six black levels is also included, in order to evaluate the quality of the television picture. Two of these collimators for the wide-angle cameras were mounted in the vacuum chamber at the RCA Space Center in order to evaluate the picture quality and resolution during the two week test period that the satellite operates in a near vacuum of 10^{-6} mm of Hg. Two additional collimators were designed for use on the launch-site gantry, in order to test the television cameras of the satellite when it is mounted on the rocket within a few hours of launch. The pictures taken through the system with the collimators on the gantry proved that the wide-angle camera lens was performing correctly just before launch of TIROS II. The wide-angle camera performance on that satellite was somewhat degraded during the launch.

II. Distortion Measurements

Those working with the TIROS television subsystem knew that the dimensional stability and resolution of a conventional airborne photomapping system would not be duplicated. However, it was convenient to set up a measuring system of the accuracy near that used for airborne photo-mapping measurements, and alter some of the procedures, as necessary, to obtain suitable measurements of the TV camera subsystem.

Foremost, the satellite structure was built to maintain the optical axes of the cameras parallel to the spin axis of the satellite. Then, shortly before the satellite was shipped to Cape Canaveral for launching, and when all qualifying tests were completed, the angles between the optical axes of the cameras and the spin axis were measured. Either directly before or immediately after the measurement was made to check the parallelism of the axes, a distortion test of both the electronics and the optics was performed. As one will notice when viewing a TIROS picture, there is a cross in the middle of the picture and there are four corner marks about two-thirds of the way to the corner. These are the system fiducial marks which are located on the faceplate of the vidicon.

Their relative locations can be measured with the help of a tool-maker's microscope. Since no optical distortion is introduced in the direct measurements, they provide a criterion for squaring the "aspect" of the TV picture. One is also able to set up an optimum expansion of the sweep by comparing the ratio of the scanned-raster dimensions with the area bounded by the corner marks. Unfortunately, present manufacturing technique limitations make it impossible to align the marks precisely with the center of the vidicon faceplate. This means that, although the optical axis may coincide with the axis of the vidicon, the fiducial pattern will not be symmetrical with the optical image and must therefore be calibrated in order to be useful.

In testing the distortion of a photographic camera, it is sufficient to measure along the picture diagonals.[10] These two measurements were felt to be inadequate with the television cameras, as not all the distortions that occur are symmetrical around the optical axis. A large target board was prepared for the distortion test, which consisted of concentric circles and radial lines arranged so that, viewed from 1.5 meters away, the pattern covered a field of view of 120°, full angle. The optical axis of one camera at a time is set up so that it passes normally through the center of the pattern. When this pattern is then photographed by the camera, a picture is produced that shows the relationship of the fiducial marks to the optical axis. With this picture, not only does one now have the record of the relationship of the fiducial marks but one can see the relationship of the distortion of the lens at the larger angles.

The target board was laid out so that a target line, though not quite in focus, would cover five television lines. The circles, when the front nodal point of the lens is placed at 152 cm, subtend half angles of approxi-

mately 10 through 60° in 10° increments. This value of 60° has proved a sufficiently large angle for the test. One may wonder why the target was not set sufficiently far away to ensure a sharp focus. This is due to the fact that an unwieldy-size target would be required. The present pattern is 4.9 meters in diameter. The information on distortion is then included in the Canadian Projection plots that are used to rectify the pictures.

III. Brightness Measurements

Since the exposure of the camera systems is fixed on the ground before the satellite is launched, it was necessary to determine that the exposure had been set correctly. As mentioned before, the radiation of the sun outside the atmosphere is known. In consultation with personnel of the United States Weather Bureau, the luminance of the brightest clouds that could be expected was determined to be 12.3 lamberts. With this figure as a goal, the camera electronics were adjusted so that 16 lamberts started to cause the camera system to saturate. As the average picture taken on TIROS I rarely contained any clouds as bright as this, TIROS II's wide-angle camera was set up to saturate at not under 10.8 lamberts. Because of the individual vidicon characteristics of the narrow-angle camera, it was found expedient to set this camera to saturate at about 7.5 lamberts. This latter setting proved not to be a disadvantage, as this camera took pictures of the ice breaking up in the St. Lawrence River, and the exposure was well suited to this function.

On TIROS III, it was determined to set the exposure to 9.2 ± 1.1 lamberts. This required development of a more precise method of making the measurements than that used on the previous satellites. To define fully the brightness, it was necessary to specify a color temperature of 6000°K as being equivalent to the approximate distribution of energy in sunlight. In order to provide a standard in the laboratory, it was decided to use 2854°K illumination. Some consideration was given to using filters to convert the illumination to 6000°K but it was decided, rather, to convert the results of the measurements mathematically. This required knowing the spectral response of the vidicon and the Y-10 filter, but this information was already being obtained as part of the records.

The brightness can be calculated from:

$$B_{6000} = B_{2800}\,\frac{l_{6000}\int R_\lambda N_{\lambda 2800}d\lambda \int N_{\lambda 6000}d\lambda}{l_{2800}\int N_{\lambda 2800}d\lambda \int R_\lambda N_{\lambda 6000}d\lambda}$$

where

B = scene brightness,
l = luminous efficiency,
R_λ = response of the camera including lens, filter, and vidicon at the wavelength λ,
N_λ = normalized blackbody radiation at λ.

The subscripts refer to the color temperature. The integrals are evaluated numerically as described by Engstrom.[11]

In order to provide uniform response at the high brightness levels, the 9.2 lambert response was adjusted to be within the operating limits of the system, and not at a point of actual saturation as was the case in TIROS I and II. The video signal is transmitted from the satellite by means of an FM-FM signal. In this respect, the white limit of the system is 70 kc while the black signal occurs at about 92.5 kc, but is dependent on the temperature. The sync tips (the tips of the synchronizing pulse) which appear blacker than black, and therefore require no blanking, are at 100 kc. Since it was not likely that the black level would be less than 85 kc, there would be a 15 kc (85 − 70) spread between black and white levels. It had been noted that the excursions from black to white remained constant despite the black level shifting; therefore brightness is plotted as a function of frequency deviation rather than actual frequency.

The light box that was built to provide the brightness calibration has three separate lighted areas, known as "panels." The size of this area was selected to be about 1-mm square on the 35-mm kinescope recording film. The light box was designed to be operated at a distance sufficient to allow the lighted panels to be in focus. Though the actual measurements of brightness were made by reading the demodulated signal's amplitude on an oscilloscope, one could check the reading by measuring the density of the kinescope recording film. The two side panels were operated at constant brightness levels. One was operated near the 9.2 lambert level and the other at a very low light level, just above the minimum brightness that the camera could detect. The middle panel was built to be adjustable. It could be adjusted to a brightness sufficient to cause the camera system to saturate or could be readjusted to any level below that, even to a brightness level below that which could be detected by the camera. Thus the two end panels provide constant monitoring of the bright extremes in the picture, while the center adjustable panel measures the brightness-response of the camera.

The spectral response of each camera is measured before it is installed in the satellite. A Perkin-Elmer 112-U spectrometer with supplementary optics to collimate the light emerging from the exit slit was used to provide a monochromatic light source. The camera was set up with the lens looking into the light source. The output of the camera was measured on an oscilloscope to determine its response to various wavelengths of light. As the monochromatic light was not sufficiently bright to permit operating the camera at as short as a 1.5 msec exposure, the shutter had to be removed for the test. The modulation of the light caused by the chopper in the spectrometer gave some trouble in read-

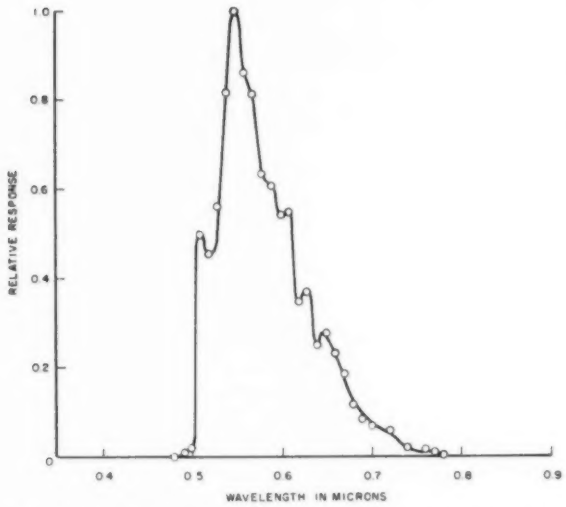

Fig. 2. Relative spectral response TIROS III Camera, system 1.

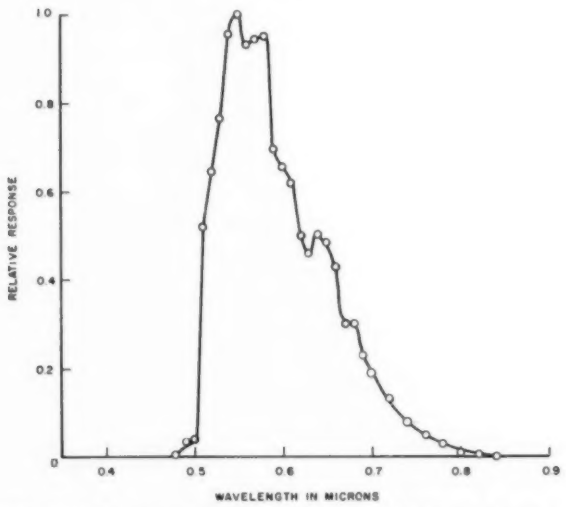

Fig. 3. Relative spectral response TIROS III camera, system 2.

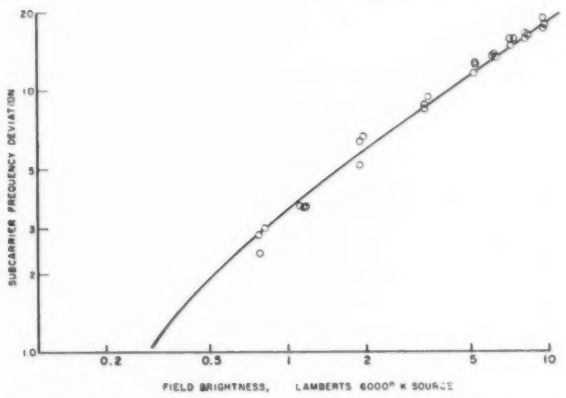

Fig. 4. Response to varying scene brightness TIROS III camera, system 1.

ing the output signal, but by using the maximum signal that was experienced in 10 to 20 seconds, reasonably consistent results were obtained. Curves of the spectral response and brightness response of the two cameras in TIROS III show the results of the above measurements in Figs. 2 through 5.

Typical data acquired with the TIROS system are presented in Figs. 6 and 7.

Conclusion

As a result of the calibration and tests, the TIROS I, II, and III satellites have proved unusually successful in obtaining pictures of weather systems. The TIROS I satellite transmitted 23,996 pictures during its three months of successful operation. At the time of writing this paper, the TIROS II satellite had taken approximately 35,000 pictures. The TIROS III satellite has taken 15,000 pictures and is continuing to add 1000 to 2000 pictures a week. The optical tests and instrumentation reported in this paper grew out of the needs that arose during tests of the payloads. It is probable that there will be additional changes in testing TIROS IV and other TIROS satellites as the information from previous satellites is evaluated.

References

1. M. Neiburger and H. Wexler, "Weather satellites," Sci. American **205**, No. 1, 80-94 (1961).
2. R. A. Hanel and W. G. Stroud, "Infrared imaging from satellites," J. Soc. Motion Picture Television Engrs. **69**, No. 1, 25-26 (1960).
3. M. Ritter and M. H. Mesner, "Image sensors and space environment," J. Soc. Motion Picture Television Engrs. **69**, No. 1 (1960).
4. R. Stair, R. G. Johnston, and T. C. Bagg, "Spectral distribution of energy from the sun," J. Research Natl. Bur. Standards **53**, 113 (1954).
5. R. Stair and R. G. Johnston, "Preliminary spectroradiometric measurements of the solar constant," J. Research Natl. Bur. Standards **57**, 205 (1956).
6. P. Moon, "Proposed standard solar radiation curves for engineering use," J. Franklin Inst. **230**, 583 (1940).
7. J. E. Keigler and C. B. Oakley, "TIROS system on the ground," Astronautics **6**, No. 6 (1960).
8. A. H. Glaser, "System for the meteorological use of satellite television observation," GRD Research Notes No. 36, Air Force Cambridge Research Laboratories, Bedford, Mass. (June 1960).
9. M. H. Mesner and J. R. Staniszewski, "Television cameras for space exploration," Astronautics (May 1960).
10. E. D. Sewell, *Manual of Photogrammetry* (2nd ed., American Society of Photogrammetry, Washington, D.C., 1952), pp. 137-176.
11. R. W. Engstrom, "Calculation of radiant photoelectric sensitivity from luminous sensitivity," RCA Rev. **16**, No. 1 (1955).

Fig.

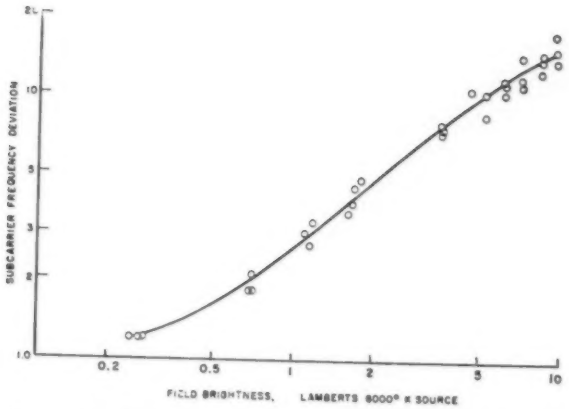

Fig. 5. Response to varying scene brightness TIROS III camera, system 2.

Figure 7 overleaf.

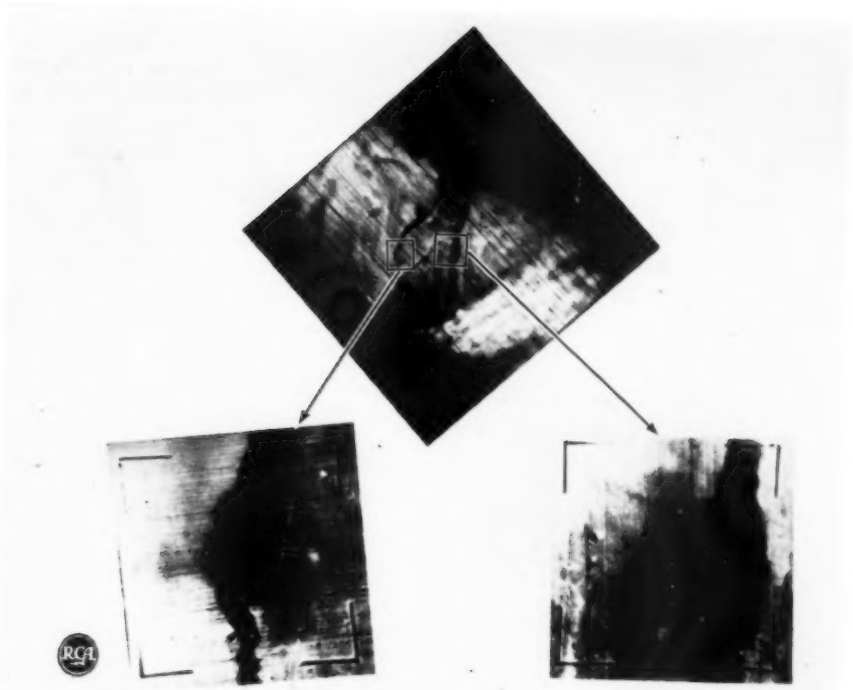

Fig. 6. Wide-angle and narrow-angle picture of Nile River and Gulf of Suez Area. The narrow-angle lens with 8 times the focal length of the wide-angle lens gives better cloud detail for the meteorologist to study.

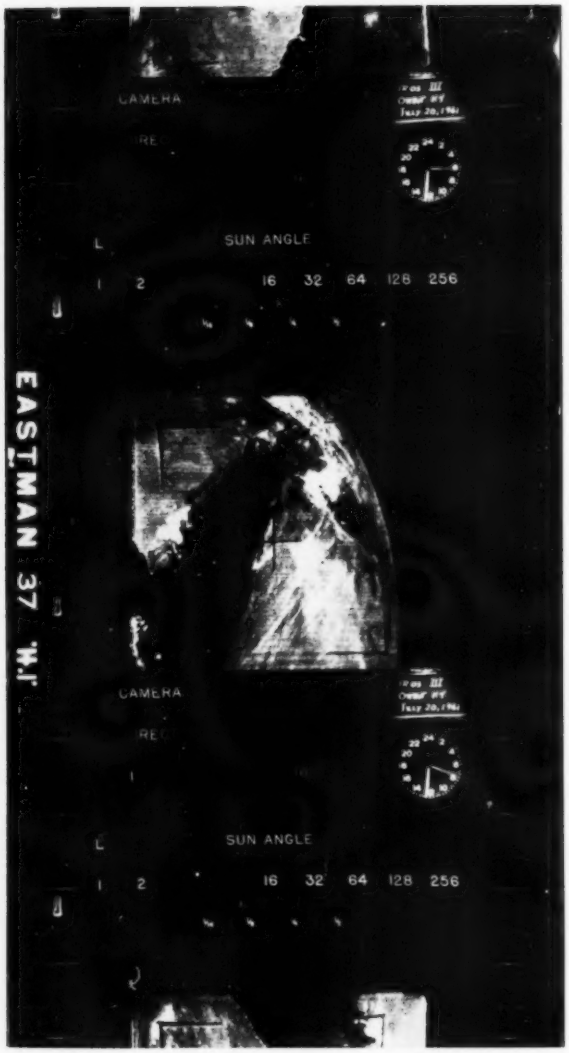

Fig. 7. TIROS pictures are photographed with associated data on 35-mm film. The clock indicates the time picture was taken by the ground station of C_1 MT.

The little boy was left alone for a few minutes in the family car. A passer-by saw him going through the motions of driving a car, making believe he was turning the wheel quickly, etc.

Said the passer-by, "At the rate of speed you seem to be going, you should put your hand out the window and signal you are making a turn."

The boy looked at him disdainfully. "Look," he said, "this is a spaceship I'm driving and if you even open the window in a spaceship it'll rip your head right off. See?"

Reproduced by kind permission of the Editor of *Current Science*

Papers to appear in subsequent issues

There have been so many papers submitted for publication since APPLIED OPTICS was announced last year that we have already built up a backlog which is as embarrassing for a new publication as it is a demonstration of the need for this journal. We are doing our best to publish papers as quickly as we can by bringing out bigger issues than had originally been intended. The Editors wish to express their sincere appreciation to all contributors who have thus demonstrated their faith in APPLIED OPTICS.

Spectroscopy for Solid State Optical Masers—*Sugano*
Inspecting Infrared Optical Materials and Systems by Means of the Evaporograph—*McDaniel and DiMattia*
Threshold Condition of Masers for Higher Frequencies—*Shimoda*
Multiple-Pinhole Multiple-Beam Interferometric Observation of Flat Surfaces—*Murty*
Optical and Cross Relaxation Maser Level Populations by Partial Distribution—*Barker and Keating*
High-Speed Sequence Photography of a Ruby Laser—*Dayhoff and Kessler*
Absorption Line Broadening in the Infrared—*Burch et al.*
Overlapping Monoculars: An Ultrawide Field Viewing System—*Shenker et al.*
Mode Control in Ruby Optical Masers by Means of Elastic Deformation—*Lipsett and Strandberg*
A Wavelength Standard for the Ultraviolet–Visible–Near Infrared *McNierny and Slavin*
High-Speed Rotating-Mirror Framing Camera—*Davis*
Negative Temperature in a Discharge in a Mixture of Two Gases—*Basov and Krokhin*
Luminescent Processes and Decay Laws in Crystalline Materials —*Pernick*
Production of Circular Disks of Known Diameter for Calibration Purposes in High Resolution Microscopy—*Charman*
Crossed-Roof Prism Interferometer—*Gould et al.*
Astronomical Refraction: Some History and Theories—*Mahan*
Durable Narrow Absorption Band Infrared Filters Utilizing Powdered Mineral Materials on Polyethylene Substrates—*Carlon*
Optical Faraday Rotation and Microwave Interactions in Paramagnetic Salts—*Chang and Burgess*
Method for Obtaining Accurate Half-Intensity Widths of Spectral Lines Photographed in the Vacuum Ultraviolet—*Jones*
Performance of the Beckman IR-7 Infrared Spectrophotometer—I. Frequency Reproducibility and Accuracy (630–4000 cm^{-1})—*Kreuger*
Refractometer Microscope—*McCutchen*
Machine-Aided Selection of Optical Glasses for Two-Element Three-Color Achromats—*Willey*
A Very High Temperature Infrared Cell for Pure Liquids or Solutions—*Fishman*
An Ultraviolet Image Tube—*Skorinko et al.*
Control of a Ruling Engine by a Modulated Interferometer—*Babcock*
Thermal Radiation from a Hemispherical Source in Contact with an Infinite Plane—*Kester and Minardi*
Influence of Scatter on Fluorescence Spectra of Dilute Solutions Obtained with the Aminco-Bowman Spectrophotofluorometer—*Price et al.*
New Backscattering Computation and Tables for Dielectric and Metal Spheres—*Adler and Johnson*
Photoelectron Energy Distribution Measurements for 10 to 50 ev Photons with a Planar Analyzer and Electron Multiplier—*Herouz and Hinteregger*
Spectral Irradiance from Stars and Planets—*Ramsey*
Thermal Imaging by Means of the Evaporograph—*McDaniel and Robinson*
An Ultraviolet-Sensitive Image Tube—*Skorinko, Doughty, and Feibelman*

Inside-Out Horizon Scanner

Joseph Killpatrick

The theory of performance for a horizon scanner with a reflecting cone and objective lens optical system is presented. The theory and equations describing the optics are given and a method of determining image plane irradiance for any object is shown. The expected performance of the device as a horizon scanner is presented. Experimental results of a horizon scanner model are presented which verify the optical calculations and theory.

Introduction

The optical-mechanical design of a horizon scanner presents many problems. When the scanner is required to operate at altitudes from 160 to 800 km above the surface of the earth, the subtended angle of the earth will vary from approximately 155° to 125°. This large subtended angle presents a problem which may be dealt with in several ways: (1) The field of view of a detector can be swept by rotating mirrors or prisms to scan alternately the various angles at which the horizon should appear. (2) Another method is to use several fixed optical systems, each looking at fields of view properly separated to achieve attitude information. (3) A simple imaging system might be used to image the entire earth image, but with conventional optics the irradiance at the edges of the earth image would be low, and the size of the earth image would be too large to be practical.

Using an inverted reflecting cone and an objective lens, the large subtended earth angle may be imaged in such a manner that the apparent earth image in the image plane of the objective lens will be located on the outside of a small dark disk representing an apparent image of space. Thus, the image might be called inside-out. If the horizon scanner's optical axis is aligned parallel with the vertical to the earth, the earth's brightness will appear on the outside of a disk whose size depends upon the cone apex angle and the subtended angle of the earth. So, a transformation is made by the optics of the large horizon angle to a small angle, forming a small angular disk which moves one degree for a one degree motion of the horizon angle.

To illustrate this imaging a photograph of a simulated earth image is shown in Fig. 1. The earth is simulated by a uniformly illuminated disk subtending an angle from the horizon scanner of 130°. The cone apex angle is 75°, and the size of the resulting dark disk in the center of the photograph is 20°. In Fig. 1, the image of a point source, simulating a small subtended angle source such as a star or the sun, is shown as an arc, the center of which is located within the dark center disk. The source is located about 4° above the simulated earth horizon.

In addition to the static case shown in Fig. 1, the consideration of the image for attitude errors when the optical axis and the earth vertical are not aligned is important. For angular errors of less than 4° the center dark disk will remain essentially circular and will move in the direction of the attitude error, an angular distance equal to the angular error. One method of reading this movement is to place four detector elements in symmetrical orthogonal positions about the optical axis. Opposite elements of the detector array are connected as the two active elements of a simple bridge which will be unbalanced by attitude errors.

The signal sensed by the detector elements arises from the brightness at many points in the object space, thereby reducing the effect of local disturbances in the radiance of the earth or the lack of a sharp discontinuity at the horizon.

Other methods of sensing this horizon position include infrared image tubes, visible image tubes for some applications, and other arrangements of detector element arrays. In practice some of the detection methods require some means for the modulation of the received energy. This modulation can be achieved by a number of methods including mechanical modulators and solid state modulators.

As an example of the use of this optical system the

The author is with the Military Products Group Research Dept. of Minneapolis-Honeywell Regulator Company, Minneapolis, Minnesota.

Received 8 November 1961.

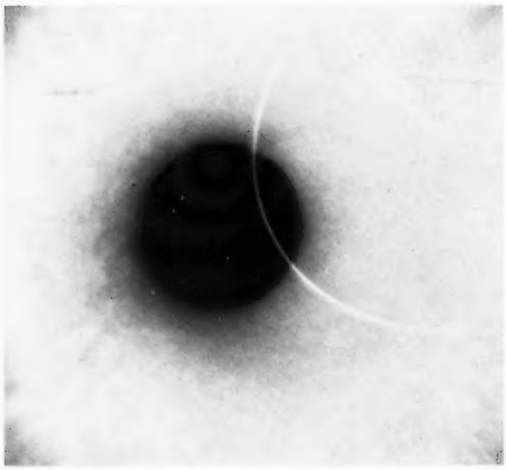

Fig. 1. Image plane photograph.

theoretical performance of a horizon scanner with the characteristics listed below would have an rms noise level equivalent to 0.03°.

Detector detectivity	$D^* = 10^8$ cm/watt
Detector element area	$A_d = 0.02$ cm^2
Bandwidth	1 cps
Source effective blackbody temperature	220°K
Wavelength band sensed	8 to 22 μ
Objective lens f-number	$F/1.0$
Objective lens diameter	1.27 cm
Optical modulation and efficiency	9%

The noise level is calculated in the following manner. The irradiance in the focal plane of a simple lens, without the cone, is calculated using an effective blackbody temperature and the wavelength band to be sensed. All irradiance values are given in terms of this objective lens, without the reflecting cone. Using this calculation, along with a curve such as shown in Fig. 9, the signal for a given attitude error can be determined. Figure 9 shows the no attitude error irradiance distribution but can be used for this calculation without introducing any first order errors. By using the area of the detectors and their detectivity, the noise level in terms of attitude error can be determined.

For example if the detector elements are placed at a position equal to $\tan^{-1} 0.3$ the change in irradiance is approximately 0.02 H_0 per degree error. Since each detector element will experience a change the total change is about 0.04 H_0 per degree error.

The radiation from the sun is distributed along an arc and is also spectrally filtered, thus reducing any errors due to the sun to low values. The effect of the sun being directly in the field of view is calculated to be less than 0.25° error under the above conditions.

Optical Analysis

In order to understand the operation of this horizon scanner, it is essential to consider the imaging of the earth, its horizon, and the star background, including the sun, by the unique optical system. It must be kept in mind that, unlike conventional optics, there does not exist a one-to-one correspondence between the image and object space.

Point to Image Plane Mapping

The mapping of a point object to the image plane of the objective lens is performed in the following manner. The equation of a cone is written as in Eq. (1).

$$x^2 + y^2 = A^2z^2. \tag{1}$$

The apex angle of the cone is θ, and the term A is defined as equal to $\tan(\theta/2)$. The reflected components, in terms of the incident ray components, are found in terms of the parameters A and X in Eqs. (2), (3), and (4). The parameter X is defined equal to x/z. The derivation of these equations is indicated in the Appendix.

$$R_x = [I_x(A^4 + A^2 - 2X^2) + I_z2A^2X][A^2(1 + A^2)]^{-1/2}, \tag{2}$$

$$R_y = [I_x(-2X) + I_z2A^2](A^2 - X^2)^{1/2}[A^2(1 + A^2)]^{-1/2}, \tag{3}$$

$$R_z = [I_z2\,XA^2 + I_xA^2(1 - A^2)][A^2(1 + A^2)]^{-1/2}. \tag{4}$$

Without loss of generality, I_y is set equal to zero in Eqs. (2), (3), and (4). This requires freedom only in selecting the coordinates of the object.

If a lens intercepts the reflected rays and the lens optical axis is the z-axis, the lens will image this reflected ray at the lens focal plane with its focal plane coordinates defined by R_x/R_z and R_y/R_z. These terms are given in Eqs. (5) and (6):

$$\frac{R_x}{R_z} = \frac{A^4 + A^2 - 2X^2 + (I_z/I_x)2A^2X}{2XA^2 + (I_z/I_x)A^2(1 - A^2)}, \tag{5}$$

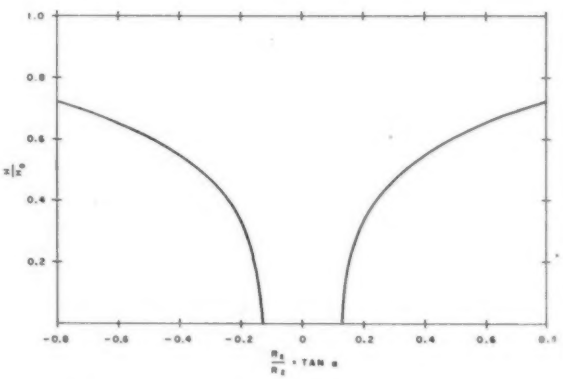

Fig. 2. Irradiance distribution in the image plane.

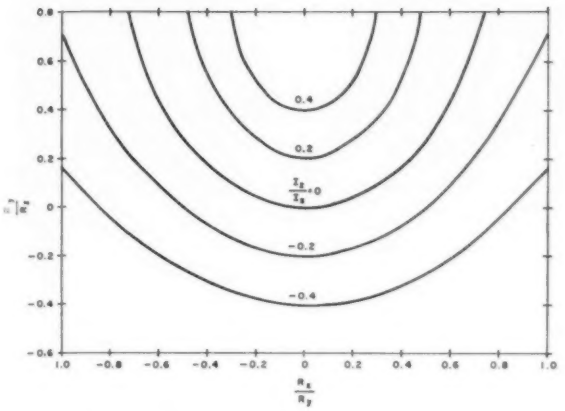

Fig. 3. Point source images for a 90° cone.

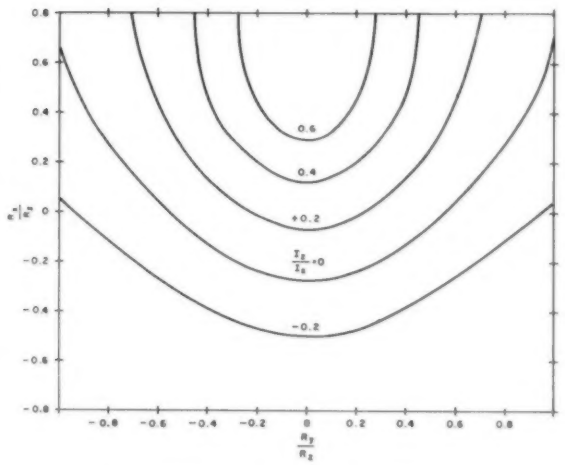

Fig. 4. Point source images for a 75° cone.

$$\frac{R_y}{R_z} = \frac{[-2X + (I_z/I_x)2A^2](A^2 - X^2)^{1/2}}{2XA^2 + (I_z/I_x)A^2(1 - A^2)}. \tag{6}$$

Equations (5) and (6) are used to show the image of a small angular object, such as the sun, in the image plane of the objective lens of the optical system, and are plotted in Figs. 3 and 4. Figure 3 presents the images of points as reflected from a 90° cone, and Fig. 4 presents the images of points as reflected from a 75° cone.

Image Point to Object Plane Mapping

The irradiance at a point in the image plane is found by first mapping the image plane points into the object plane. The mapping is done by first considering the equations for the reflected ray from the cone in terms of the incident ray. These have been shown in Eqs. (2), (3), and (4). It is convenient to write these equations in terms of R_x/R_z, X, and A, as shown in Eqs. (7), (8), and (9). The parameters R and I are interchanged so that R refers to image space and I to object space. R_y is now set equal to zero, which assumes freedom in selecting the coordinates of the image plane point.

$$\frac{A^2(1 + A^2)^{1/2}}{R_z} I_x = \frac{R_x}{R_z}(A^4 + A^2 - 2X^2) + 2A^2X, \tag{7}$$

$$\frac{A^2(1 + A^2)^{1/2}}{R_z} I_y = \frac{-2XR_x}{R_z} + 2A^2(A^2 - X^2)^{1/2}, \tag{8}$$

$$\frac{A^2(1 + A^2)^{1/2}}{R_z} I_z = \frac{R_x}{R_z}(2XA^2) + A^2(1 - A^2). \tag{9}$$

Figure 4 shows the various angles that define the rays as they pass through the cone-objective lens optical system. The angles α, γ, δ, and ϕ, are shown in Fig. 5 and are expressed in Eqs. (10)–(13).

$$\alpha = \tan^{-1}(R_x/R_z), \tag{10}$$

$$\gamma = \tan^{-1}(I_y/-I_x), \tag{11}$$

$$\delta = \tan^{-1}|I_z/(I_x^2 + I_y^2)^{1/2}|, \tag{12}$$

$$\phi = \cos^{-1}(X/A). \tag{13}$$

The angle β is then related to the other parameters and angles given in the previous equations. By simple geometry, the value of β is found to be:

$$\beta = \tan^{-1}[(A^2 - X^2)^{1/2}(X - R_x/R_z)^{-1}]. \tag{14}$$

The equations relating δ, γ, β, and R_x/R_z are then used to plot these terms as shown in Figs. 6–9. Figures 6 and 7 are graphs of δ versus γ for various values of R_x/R_z and β, respectively, for a 90° cone. Figures 8 and 9 are similar to Figs. 6 and 7, respectively, except that the cone angle is 75°.

Irradiance in the Image Plane

The irradiance at a point in the image plane is found by integrating the flux density over the objective lens. The reflecting cone is considered as a series of windows of width dx, viewing a point defined by γ and δ which, in turn, are defined by the cone angle, the value of β, and the focal plane point. The irradiance is found by integrating the source brightness, N_s, defined by γ and δ, as viewed by reflection from the cone and through the objective lens of f-number (F).

$$dH = \frac{\pi}{1 + 4(F)^2} \frac{1}{2\pi} N_s(\gamma,\delta)d\beta. \tag{15}$$

Since δ and γ are defined by β and the value of R_x/R_z, Eq. (15) can be rewritten as shown in Eq. (16):

$$H = \frac{\pi}{1 + 4(F)^2} \frac{1}{2\pi} \int_0^{2\pi} N_s(\beta, R_x/R_z)d\beta. \tag{16}$$

For convenience the irradiance in the image plane is referenced to easily found values. The irradiance in the image plane of an objective lens of f-number (F) and source brightness (N_0) is given in Eq. (17):

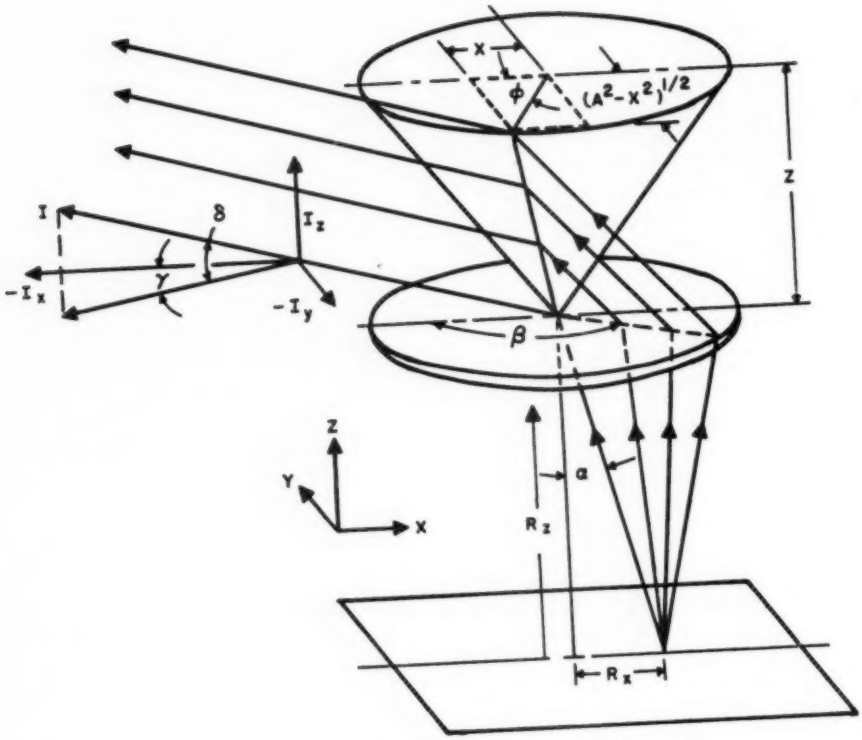

Fig. 5. Physical definition of horizon scanner optics terms.

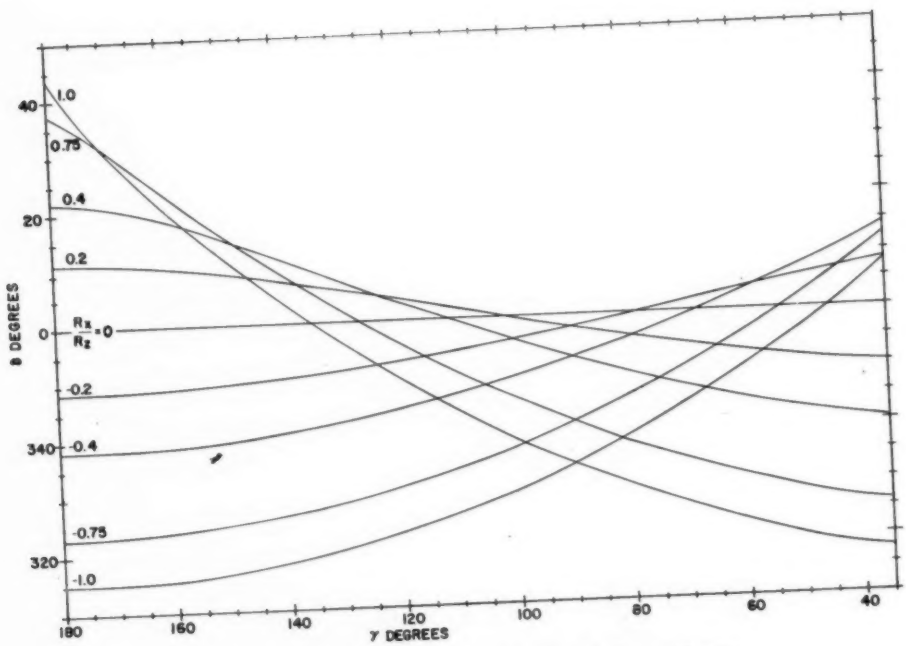

Fig. 6. Object space map of image plane points for a 90° cone.

$$H_0 = \frac{N_0\pi}{1 + 4(F)^2}. \tag{17}$$

The ratio of the value of H given in Eq. (16) to that given in Eq. (17) is shown in Eq. (18). The irradiance in the image plane is then given as a fraction of that of a simple objective lens directly imaging the source without the reflecting cone. If $N_s(\beta, R_x/R_z)$ is a constant over certain values of β, the integral given in Eq. (18) can be simplified as in Eq. (19).

$$\frac{H}{H_0} = \frac{1}{2\pi}\int_0^{2\pi} \frac{N_s(\beta, R_x/R_z)d\beta}{N_0}, \tag{18}$$

$$\frac{H}{H_0} = \frac{1}{2\pi}\sum_{K=1}^{n} \frac{N_{sK}(\beta, R_x/R_z)}{N_0}(\beta_K - \beta_{K-1}), \tag{19}$$

where

$$\beta_n - \beta_1 = 2\pi. \tag{20}$$

The case of a uniform bright source against an essentially zero background, such as earth against space, might be considered as a first approximation. Equation (19) reduces to the simple expression given in Eq. (21).

$$\frac{H}{H_0} = \frac{1}{2\pi}\frac{N_s}{N_0}(\beta_2 - \beta_1). \tag{21}$$

The values of β_1 and β_2 can be determined graphically from the curves of β versus γ and δ, and R_x/R_z versus γ and δ (Figs. 6 through 9) and from a plot of the source versus γ and δ. An equation giving the relation between the angles β, δ, and γ, the image plane point, and the cone apex angle can also be used to evaluate the values of β_1 and β_2. Therefore, given a point as defined by R_x/R_z, the limits of β are defined by the limits of β over which the source and the image of the point defined by R_x/R_z and the lens-cone optics coincide.

The graphical analysis thus provides means of defining the irradiance distribution in the focal plane for various sources. The nonuniform source can be handled in a simple manner by dividing it into n parts, as implied in Eq. (19). It is also possible to determine graphically the irradiance distribution in the focal plane for the same source in various attitudes with respect to the cone axis at an image point, defined by R_x/R_z.

As an example of an irradiance distribution calculation, consider the case of a uniform source subtending an angle of 135° oriented so that the source vertical and optical axes coincide. This source is bounded by a straight line of Figs. 6, 7, 8, or 9 at a value of δ equal to 22.5°. At a point in the image plane corresponding to a particular value of R_x/R_z, the irradiance is found by finding the limits of β over which the object plane map of this point and the source coincide. Using these values of β and Eq. (21), the irradiance at the image plane point is found. The irradiance distribution for this particular example is shown in Fig. 2.

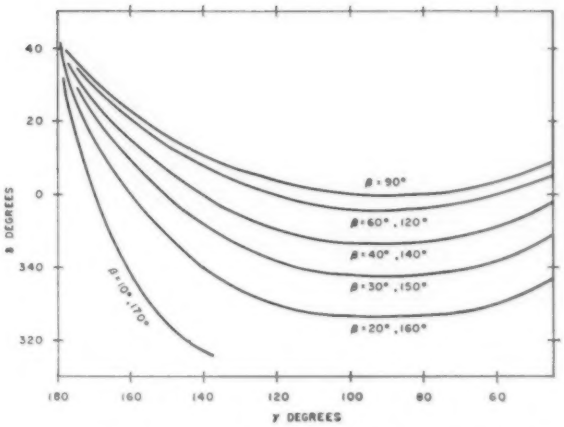

Fig. 7. Object space map of lines on objective lens for a 90° cone.

By using the procedure described above, the irradiance distribution for different angles between the source normal and the optical axis can be found. From this procedure it is seen that irradiance at image plane points located symmetrically about the line of rotation of the source about the optical axis will be equal when the source normal and optical axis coincide. For other orientations of the source, the irradiance at one symmetrical point will be greater than the other. The sign of this difference is such that the horizon scanner can acquire an attitude signal from the earth from an angle exceeding 90° from coincidence of the optical axis and the source normal when the source subtends an angle equal to or greater than approximately 120°. The irradiance difference between these symmetrical points can be made approximately linear over a range of ±10°.

It should be pointed out here that the above procedures and equations for finding the irradiance distribution in the focal plane are not exact in that they do not account for such effects as lens aberrations or the off-axis attenuation with the pie-shaped pupil. These effects can be considered as perturbations on the results obtained without considering them. It is found experimentally that these effects do not seriously alter the results obtained by not considering these effects.

Experimental Reflecting Cone-Objective Lens System

An experimental model of the reflecting cone-objective lens optics was constructed in order to demonstrate the operation of this type of scanner. Only single-axis operation was simulated in the experimental model, whereas two-axis operation will be used in the final device. The model has a cone with an apex angle of 75°; an AgCl, 13 mm-diam $F/1$ lens; and a two-element PbS detector masked to provide two active areas, each 3.5 mm off-axis. A circular diffuse surface was back-illuminated, and the output of the

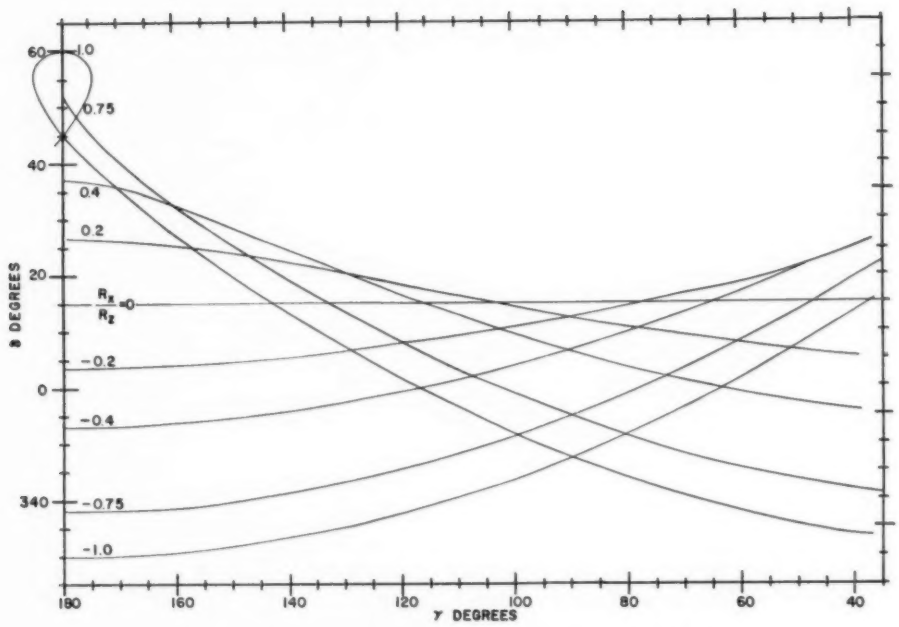

Fig. 8 Object space map of image plane points for a 75° cone.

difference signal of the two elements was read for various angles between the optical axis and the source normal.

The experimental setup is shown in Fig. 10. The output reading from the detector bridge as a function of angle is shown in Fig. 11. The curve in Fig. 11 is normalized to the signal that is obtained if a source of the same brightness as the backlighted source is imaged directly, without the reflecting cone, on only one of the two elements. From theory it is found that the relation between output signal and attitude error is expected to have a greater slope at small angles by a factor of about 2 and to be linear over a range of ±10° instead of ±20°. The reasons for this difference are

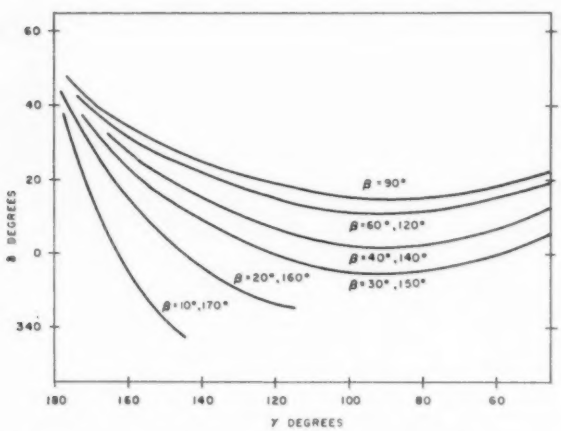

Fig. 9. Object space map of lines on objective lens for a 75° cone.

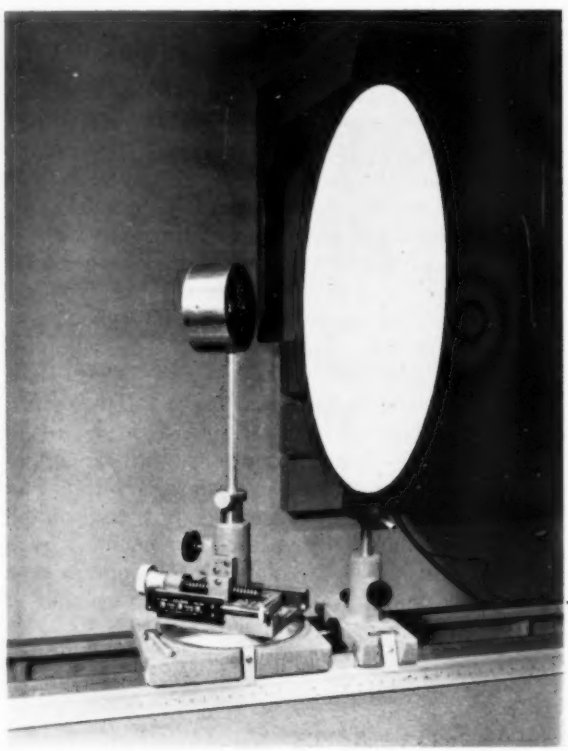

Fig. 10. Experimental setup.

many but include the fact that the experimental lens is not perfect, the simulated earth is not an ideal diffuse radiator, and a reflecting cone 20% larger than the one used is needed to avoid any uncalculated attenuations.

Conclusions

The optical system described can be used to provide a wide angle optical system which will permit the design of a simple horizon scanner. This scanner will find vertical to a spherical body whose subtended angle is in excess of 120° without the use of mechanical scanning or multiple optics with an uncertainty no greater than 0.1°. The scanner is able to acquire a signal from a large subtended angle body from any angle less than some critical angle which is typically greater than 90°. This critical angle is determined by the earth subtended angle, the cone apex angle, and the angle off-axis of the detector elements. The absence of mechanical scanning permits the construction of this type of horizon scanner with no moving parts. The scanner will operate over a range of altitudes with one optical configuration and cone angle. This range of altitudes is typically 400 km to 1280 km with the range determined by the change in the earth's subtended angle.

I wish to acknowledge the aid of J. Thomas in reviewing and commenting on the analysis of the reflecting cone optical system. Valuable extensions of some of the analyses presented here have subsequently been performed by Mr. Thomas.

Appendix A

Equations (2), (3), and (4) are obtained in the following manner:

The normal to the reflecting cone is given in (A.1) where $\mathbf{i}, \mathbf{j}$, and $\mathbf{k}$ are the x, y, and z unit vectors.

$$\mathbf{N} = 2x\mathbf{i} + 2y\mathbf{j} - 2A^2z\mathbf{k}. \tag{A.1}$$

The reflected and incident rays must satisfy the following conditions.

The incident ray, given in (A.2), and the reflected ray, given in (A.3), must make equal angles with the normal to the cone surface. This is expressed in (A.4) which equates the dot product of the normal and the incident ray with the dot product of the normal and the negative of the reflected ray.

$$\mathbf{I} = I_x\mathbf{i} + I_y\mathbf{j} + I_z\mathbf{k} \tag{A.2}$$

$$\mathbf{R} = R_x\mathbf{i} + R_y\mathbf{j} + R_z\mathbf{k} \tag{A.3}$$

$$\mathbf{N}\cdot\mathbf{I} = -\mathbf{N}\cdot\mathbf{R} \tag{A.4}$$

The incident ray and the reflected ray must be in the same plane with the normal to the cone surface. This relation is expressed in (A.5) which equates the cross products of the incident and reflected rays with the cone surface normal.

$$\mathbf{N} \times \mathbf{I} = \mathbf{N} \times \mathbf{R}. \tag{A.5}$$

In addition to these two restrictions the magnitudes of the incident and reflected rays are assumed equal. It can be shown that the combination of (A.4) and (A.5) assures this condition of equal magnitudes.

By solving (A.5) for the various vector components, two independent equations are obtained which, with (A.3), provide three equations with the three unknowns, i.e., R_x, R_y, and R_z. A solution of these three independent equations results in (2), (3), and (4) expressing the reflected ray components in terms of the incident ray components, the cone angle as given by parameter A, and the parameter X defined as x/z which defines a line on the cone surface.

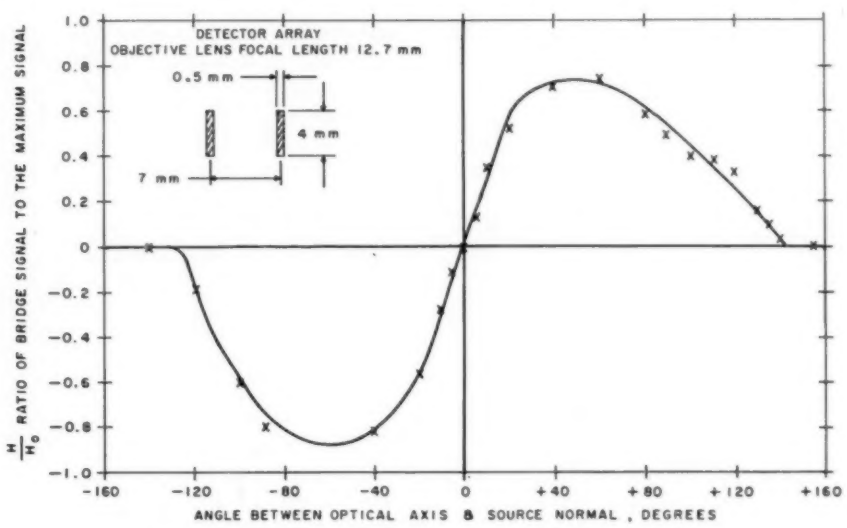

Fig. 11. Experimental results from horizon scanner optics model.

From the Editor

As we take pen in hand, the first issue has been out only two weeks. We are not yet able to assess the reaction of our audience to the journal as only a handful of comments on content and format have so far arrived. The Editor would again invite your comments.

A few comments on the editorial mechanics we can answer now: Some figures in the last issue *were* larger than necessary for their information content. There have been some raised eyebrows concerning our use of filler material, and especially on the continuation of department material from the back toward the front.

By filler material we mean the meetings calendar, book reviews, announcements, meeting reports, news columns and similar material, which, although nontechnical or semitechnical in nature, we hope is nevertheless of general interest to the optics audience. In some journals, if one article ends with more than one half of a page of space remaining, the next article is begun immediately; if there is less than one half of a page remaining, this space is left blank and the next article is begun on the following page. We are trying, as an experiment, to start each paper on the right-hand page, and any space remaining between articles contains filler. Do you care, aesthetically, whether an article is right- or left-handed? Perhaps we could offer a special inducement to authors who submit precisely one-page articles that they might not have to wait in line with everybody else but might be selected at the last minute for earlier publication on a space-available basis.

Let us consider some more serious matters concerning the content of the articles: We have had a few comments such as "These articles are too good for *Applied Optics;* they ought to be in *J. Opt. Soc. Am.*" We certainly do not wish to be thought of as a haven for rejects. One new and different thing we are doing with *Applied Optics* is to seek out those optics papers that have *not* been appearing in *J. Opt. Soc. Am.*, in an effort to persuade the authors that they should present their results to the optics audience rather than, say, to radio engineers or solid state physicists. We want it to become known that OSA has two first-class, original-content publications, not a high-class journal and a low-class magazine.

A related point is that some regrets have been voiced that our papers are "too high-brow for the average optics man to read." Optical pumping *is* a high-brow topic; we did start off by diving into the deep end of the pool. (At the risk of oversimplifying, we can define high-brow articles as those seldom understood by the audience, and sometimes not even understood by the author.) Surely the papers of this Space Optics issue are less abstruse, at least as far as integral signs are concerned. Your editor is himself a low-brow, and he always sighs with relief when he finds a paper he can understand. One must not, however, confuse low-brow with low-class: an easy-to-read article that makes a point is preferable to ten hard ones that elude us all.

At the moment we have a tremendous backlog of papers in all areas of optics, some of which were routed to us by the Editor of *J. Opt. Soc. Am.* as being more appropriate to *Applied Optics*. We hope our impatient authors will understand that this log-jam is temporary, and that we are bringing out bigger issues than we had intended in order to catch up. We obviously underestimated the need for this journal when we decided to publish as a bimonthly. Incidentally, we are happy to report that *J. Opt. Soc. Am.* appears still to be thriving in spite of our "competition." Last year *J. Opt. Soc. Am.* had a banner year, with 1440 pages of text (not counting the Directory or Minutes of the Society). This means an average of 120 pages per issue. The January and February 1962 issues comprise 236 pages, including some fine papers on optical pumping. Our readers are reminded that to keep abreast of optics they must subscribe to *both* of these journals, and to *Optics and Spectroscopy* as well.

We were remiss in the first issue in omitting to state that this new journal will receive a grant-in-aid from the National Science Foundation should we need it, during the first three years of publication. Having this grant we are able more readily to publish bigger issues and avoid large publication delays. We are grateful to NSF for this support and for the demonstration of their belief in the need for *Applied Optics*.

JOHN N. HOWARD

Information for Contributors

Scope: Papers are welcomed in the broad areas of applied optics, in disciplines related to optics and employing optical techniques. Papers should be sent to *The Editor, APPLIED OPTICS, 1155 Sixteenth St., N.W., Washington 6, D.C.* Manuscripts may be submitted in English, French, German, or Russian, and the presentation should be as succinct as comprehension will permit. In general, the metric system of units is preferred. One original and one carbon of the manuscript, with two sets of all illustrations, must be sent. Manuscripts should be typed double or triple spaced on one side of 22 × 28 cm (8½ × 11 in.) paper, leaving a 3.8 cm (1½ in.) margin all round.

An **abstract,** adequate as an index and summary, of not more than 100 words should appear at the beginning of the paper after the *title, author's name, affiliation, and address.* In the case of papers in a non-English language, they must be accompanied by an abstract in English as well as an abstract in the language of the paper.

Figures suitable for printer's use should be sent. Bear in mind that illustrations will normally be reduced to column width (8.4 cm—3⅜ in.—20 picas). *Halftones:* two sets of glossy prints are needed, which should be mailed flat, with any proportion or framing indicated on a working copy. *Line drawings* should be suitable for reproduction and be not larger than 22 × 28 cm (8½ × 11 in.). *Captions* should be listed on a separate sheet in addition to each caption appearing on each illustration.

Tables should be typed on separate sheets and the data therein be intelligible, by title, without reference to the text. Tables should include a minimum of vertical ruling.

References must be typed on a separate sheet, be numbered consecutively in the order of their appearance in the text, and follow this form:

1. F. C. Brown, Phys. Rev. **12,** 345 (1821).
2. J. Culpeper, *Space Optics* (Georgetown Institute of Technology Press, Washington, D.C., 1861) pp. 012, 345.

A list of abbreviations for the names of journals is published in the American Institute of Physics *Style Manual.* To make for uniformity of presentation generally, the *Style Manual,* second edition, should be used.

No **galley proofs** will be sent to authors; all proofreading will be done in the house. Therefore, an author will not see his paper from the time it is accepted and any alterations agreed between Editor and author, until it appears in print.

Letters to the Editor should follow the above suggestions, but no abstract is required.

Optics in the Orbiting Astronomical Observatory

Herbert B. Hallock

The NASA Orbiting Astronomical Observatory (OAO) is a precisely stabilized spacecraft designed to carry large photoelectric astronomical telescopes. General background information is presented, and the specific optical systems planned currently for the Observatory are described. The optical sensors which are required for attitude stabilization and control are emphasized in the discussion.

I. Introduction

It is intended in this paper to present a brief general description of the opto-electronic subsystems which are to be installed in the NASA Orbiting Astronomical Observatory. The basic spacecraft has been designed, and is being constructed by the Grumman Aircraft Engineering Corporation under contract to NASA Goddard Space Flight center. Grumman has no contractual obligation for scientific payload at this time. The opto-electronic equipments, including astronomical telescopes, which are to be carried by this large spacecraft cannot be described adequately in a short paper, but references are cited which will enable the interested reader to pursue some details more closely. A really complete description cannot be given for an obvious reason: namely, several of the equipments are scarcely beyond preliminary design. The opto-electronic equipments to be provided with the spacecraft by Grumman are mostly beyond the design phase but, with few exceptions, they have not yet been subjected to the gruelling testing which all spacecraft devices must undergo.

The mission of the OAO is to orbit scientific payloads designed for astronomy. The first of these payloads will be devoted to ultraviolet spectrophotometry below 3000 A extending to wavelengths shorter than Lyman alpha (1216 A). Although rocket astronomy has recently yielded, for the first time, stellar energy distributions below 3000 A,[1] it is obvious that satellite altitudes are necessary for thorough exploration in the region of Lyman alpha, because the earth's atmosphere severely absorbs and scatters light of this frequency before it can penetrate to otherwise attainable high altitudes. The spacecraft is able to carry astronomical systems to explore in other regions of the spectrum in which atmospheric attenuation may not be quite as severe, yet with considerable advantage over the ground-based telescope in respect to stability and freedom from the effects of atmospheric refraction and scintillation.[2]

One of the earlier discussions of the benefits to the study of astrophysics which could be derived from satellite observation of astronomical spectra was given by Spitzer[3] in 1956. At that time he cited the following problems which could be investigated:

(a) The detailed distribution with height of the major components of the earth's outer atmosphere.

(b) The detailed composition of the atmospheres of the moon, Venus, Mars, and the other planets.

(c) The abundance of the main atomic and molecular species in interplanetary, interstellar, and intergalactic space.

(d) The temperature and compositions of stars with high surface temperatures, and the coronae surrounding these stars.

The number and diversity of equipments actually proposed by astronomers[3-8] led to the basic spacecraft concept for a standard satellite observatory which could be used for any one of these experiments, or for others of similar caliber.

II. General Description of the OAO System

The spacecraft system which results from an implementation of this concept represents a complex of structure, power supply, data system, communications, and attitude stabilization and control. It is believed that no better example exists today of the part which optics is able to play in space technology, and it illustrates the extent to which the optical effort must be merged with the mechanical and the electronic efforts. The many interfaces between the subsystems of the basic spacecraft, plus the interfaces between the scientific payload and these subsystems, represent an inte-

The author is with Grumman Aircraft Engineering Corporation, Bethpage, N.Y.

Received 6 November 1961.

gration problem of considerable magnitude. Almost all orbital operations must be planned and programmed. Programs will be telemetered to the spacecraft for attitude control, for command sequences for the experiment, for regulation of experimental data flow, and so on. The command functions require many communication channels of narrow bandwidth, whereas the flow of experimental data over the communication link to ground during short periods of radio line-of-sight requires a wide-band capability. The commands require storage in the spacecraft, and the experimental data require many times the capacity of the command storage. The electrical power for the Observatory is furnished by silicon solar cell arrays with intermediate storage in nickel–cadmium batteries.

For those who are interested in additional details of the OAO system, reference should be made to summary papers by Ziemer[9] and by Anderton,[10] and to an article on the redundant 100,000-bit digital data storage by LaFond.[11] Early speculation on the OAO design may be found in a paper by Triplett.[12] For general interest it should be added that the first Observatory is scheduled to be launched by the Atlas Agena B rocket from the Atlantic Missile Range in late 1963. The orbit is planned to be approximately circular at 800 km altitude and 32° inclination to the equator.

The Stabilization and Control Subsystem

The stabilization and control subsystem of the OAO spacecraft is designed to rely principally upon inputs from optical sensors, both for the acquisition of attitude desired and the stabilization of pointing in this attitude. Therefore, it is a focus of optical interest in the spacecraft. The optical sensors involved are solar sensors, star trackers, and a stellar television camera. The subcontractor for the automatic stabilization and control subsystem (excluding television) is the Missile and Space Vehicle Department of the General Electric Company.

The ultimate purpose of the whole subsystem is to point the Observatory experiment axis with great accuracy and stability to the astronomer's point of observational interest—usually a star—although the interest may center in a nebulosity, or anywhere in general as in the function of sky-mapping. Since the Observatory attitude must be stabilized relative to celestial coordinates, it is logical that guide stars be used, and that star-tracking form the basis for pointing control. Also, because communication will be confined to three Minitrack stations in the Western hemisphere only, it is apparent that its most efficient and continuous use may require considerable emphasis on automation based on stored programs.

The most stringent pointing requirement which will probably be placed upon the OAO is an accuracy of 0.1 sec of arc for measurements suggested by Spitzer.[4] The sensing for this order of accuracy must be provided within the experimental optical system itself. However, as the error sensor to be provided by the experimenter has a small acquisition field (±2 min of arc, typically), means must be provided for pointing the spacecraft to within the fine sensor acquisition field with adequate stability. The desired pointing accuracy of the spacecraft in the coarse pointing mode is ±1 min of arc (one sigma value). Star trackers, other than the experiment sensor, are utilized in the automatic stabilization and control subsystem to achieve this goal.

In turn, in order to bring selected guide stars within the acquisition field of each of the star trackers, coarser acquisition devices are necessary. The system philosophy is one of wide-angle acquisition, followed by transfer of control sequentially to devices of ever-decreasing acquisition field and ever-increasing accuracy of pointing. The most obvious target for coarse pointing of the optical sensors is the sun. Accordingly, coarse solar sensors are used in conjunction with rate gyros to acquire the sun; fine solar sensors are used to point accurately at the sun; a group of gimballed star trackers is used to acquire a set of guide stars by rotating the Observatory slowly about the sun-line; the boresighted star tracker refines the accuracy of pointing, where necessary; and finally, the experiment sensor is allowed to take over control. Each of these steps involves threshold error and trigger electrical signals to enable transfer of control.

Some of the problems associated closely with the provision of a suitable optical sensing system may be mentioned briefly as follows:

1. Cyclic occultation of the sensor line of sight by the earth, which reduces the time available for use of any one sensor, introduces problems of logic and data handling, and may give rise to false attitude information. The earth is a fertile source of "synthetic stars" of any apparent magnitude because of sunlight reflected from cloud structure, and because of night light from cities and towns under clear line of sight conditions. The earth's albedo can also cause error in the pointing of coarse solar eyes.

2. Irregularity of star distribution, resulting in voids in the availability of bright stars in the celestial sphere, and many cases where otherwise desirable bright stars have neighboring weaker stars undesirably close. Double stars and stars of variable magnitude also constitute special problems.

3. The extraneous light sources which exist in a zone of the celestial sphere centered on the ecliptic, for which allowance must be made in programming the use of star trackers. These sources include the sun, the moon, and the planets, each of which has a constantly changing ephemeris.

4. The rather severe launch environment, in terms of shock and vibration, which tends to make the reten-

tion of precise alignment very difficult.

5. The severe thermal variation to which optical sensors may be subjected in orbit if alternately exposed to sunlight and to cold space. Sunlight scattered by the system parts may also be a source of optical noise.

6. The somewhat unpredictable effect of micrometeorites on optics in sensors used for precision alignment when exposed for a full year.

To complete a rough outline of the subsystem to the extent required for an understanding of the place of optics, it may be added that the sensor outputs ultimately control gas jets, inertia wheels, and magnetic coils. Optimum stabilization is accomplished by means of a fine inertia wheel system.

Structural and Thermal Design

It can be said that the Observatory is one large optical instrument (1500 kg) in which the structure is essentially part of the instrument. In the OAO design there is unusual emphasis on rigidity at minimum weight penalty, and on the provision of an isothermal enclosure for the experimental package. The preceding discussion of the stabilization and control subsystem should make it apparent that maintenance of close alignment between the axes of a number of individual optical sensors is essential to the most efficient functioning of the system, although provision has been made for operation to a required accuracy even in the event of an unexpected degree of misalignment. The exceedingly high performance goals of the scientific experiments are brought within reach by mechanical and thermal protection afforded to carefully figured large optics, and to all the mechanism which forms part of the scientific payload. The general design concept is that of a central structure that meets the requirements for mechanical strength and rigidity, which is surrounded by somewhat flexible protective skin panels exerting the least possible distorting influence on the inner structure. Figure 2, very schematically, shows the structural arrangement. The transverse cross section is that of an octagonal outer shell, to the vertices of which radiate key structural members consisting of truss beams extending from a central cylindrical core. The 122-cm central cylindrical shell surrounds the experimental package which is supported on four lugs attached to alternate trusses near the center of mass of the spacecraft. The structural material is aluminum.

Great care is being taken in the design and fabrication of precision joints of structural members, and in the relief of residual internal strains in the structure after assembly and prior to alignment of optical parts.

The solar cell arrays are built up on 2.5-cm-thick

Fig. 1. OAO mockup showing solar array paddles extended.

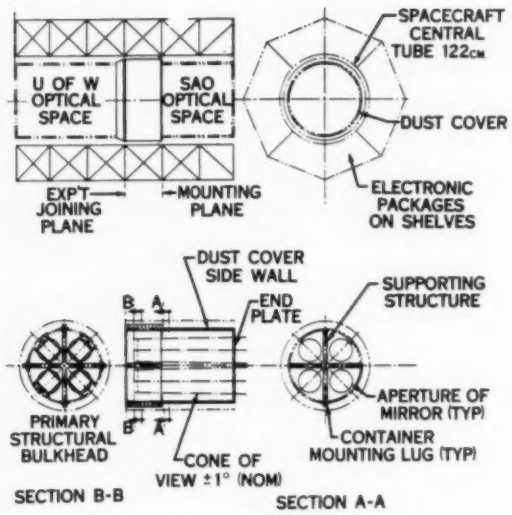

Fig. 2. OAO No. 1 structural interface with Wisconsin and Smithsonian experiments.

honeycomb panels. Four separate paddles are erected in orbit with the configuration shown in the mock-up, Fig. 1.

A large opaque sun shade is essential to protect the experiment from oblique sunlight. It is used as a cover for the optics, is opened in orbit, and thereafter is closed automatically to protect the experiment from direct sunlight in response to a protective sun sensing cell. When open (Fig. 1) it completely shades the experiment if the sun is 45°, or more, from the experiment axis, and the spacecraft is oriented favorably about this axis.

The skin panels are finished in Alcoa's Class SI Alzak* which is highly reflective in the visual but has substantial emissivity in the infrared. This skin affords protection against the severe and asymmetrical influence of sunlight, while at the same time it permits the radiation to space of internally generated heat which is deliberately radiated outward to these skin panels from the equipment bays.

III. Specific Optical Systems in the OAO

The Experiments

"Experiment" is a term officially applied to the OAO scientific payload of spectrophotometric equipment. This equipment is of the greatest optical interest. However, a detailed description of it is not appropriate here—preliminary design information is available in the literature.[13–15] Grumman's present contractual obligation extends to providing spacecraft for three experiments. A brief summary of these experiments will serve to indicate the level of opto-electronic effort involved.

* Trade mark of the Aluminum Company of America.

The first Observatory to be launched will carry two experiments designed at the University of Wisconsin[13] and the Smithsonian Astrophysical Observatory.[14] The two optical systems will face in opposite directions. Some idea of the interface with the spacecraft structure is given in Fig. 2. The Smithsonian experimental package, known as a Celescope, will consist of several ultraviolet television cameras each having its own optical system, and each optically filtered to respond to a spectral bandpass of approximately 250 A to 1000 A, centered between 1150 A and 3000 A. Schwarzschild camera optics are presently planned which will furnish imagery over approximately a 2° field of view. The television camera tube is the Uvicon developed by Westinghouse Research Laboratories. The sensor combined with an associated electronic system will be used to obtain accurate quantitative data on the ultraviolet radiance in a sky-mapping survey operation. It is planned to digitize measurements on discrete stars within the raster for transmission to the ground. Measurements will be taken and transmitted in real time while the spacecraft is within communication range of the ground station.

The other experiment in the same spacecraft will acquire data during the remainder of the orbit, which will then be placed in the OAO data storage, to be transmitted to ground once per orbit. This is the Wisconsin Experiment which is designed to determine the stellar energy distribution, and to measure the emission line intensities of diffuse nebulae in the spectral region from 3000 A to 8000 A. Compared to later experiments, such as the Goddard experiment,[15] the spectral resolution will be coarse, since the spectral bandpass of each of the photometer telescopes will be defined by a detector–filter combination rather than by a grating. The detectors will be special multiplier phototubes sensitive in the extreme ultraviolet. Four of these telescopes will utilize off-axis paraboloids, while a fifth will utilize a central on-axis paraboloid. The field stops of the off-axis telescopes will be 1′ of arc in diameter for observation, and 10′ for search, while the central on-axis telescope, used for nebular photometry, will accept a field of about 0.5° of arc. There will probably also be two objective-grating scanning spectrometers which should provide a resolution of about 10 A, but not over the extended exposures planned for later experiments.

The two experiments planned for the first Observatory launching are regarded as exploratory in nature, paving the way for detailed planning of later experiments, but the mistake should not be made of assuming that either one lacks sophistication. Both represent significant advancement in spacecraft instrumentation.

The Goddard Experimental Package,[15] designed at the Goddard Space Flight Center of NASA, will be installed in the second Observatory. It features a

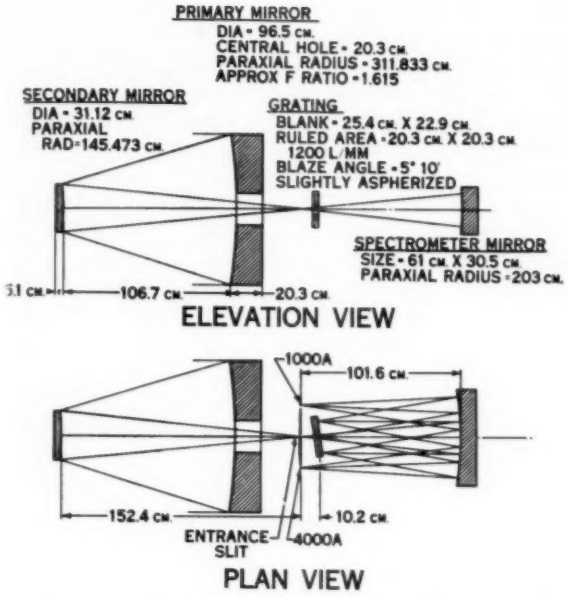

Fig. 3. General optical arrangement of Goddard Experimental Package.

91-cm spectrophotometric telescope for determination of the absolute spectral energy distribution of celestial objects, other than the sun, in the wavelength region 1050 A to 4000 A. Multiplier phototubes of special design for the ultraviolet are the sensing elements.

The demands which this experiment will make on the OAO system will be far more rigorous than the demands made by the previous experiments. The OAO must maintain a stabilized line of sight over extended exposure times while a grating is stepped sequentially through 2 A increments to cover the spectral range of interest. The field stop of the experimental apparatus will be less than 1′ of arc in diameter, and it will probably be necessary to stabilize to the order of a very few seconds of arc throughout the exposure. The expressed goal is to achieve 2 A spectral resolution. The spectrophotometric data are accumulated in the form of photon pulse counts. Either the time to accumulate a specified number of pulses, or the actual number of pulses in a standard time interval, will be determined and stored in digital form for later transmission to the ground.

As a matter of general interest, Fig. 3 has been made available by the Goddard Space Flight Center to show the present concept of the large optical system planned for the experiment. It is believed at this time that the performance specification will require a hybrid system of three aspherics. The grating recommended by Goddard is a 1200 lines/mm grating, blazed for the first order at 1200 A, with a 20-cm nominal beam size.

The Princeton experiment which has been reported to be the next OAO payload after the Goddard experiment[16] will incorporate a much smaller field stop and will have fractional-angstrom-unit resolution. As for the other experiments which have been discussed, rocket probe studies will precede the actual satellite program.[16]

The Solar Sensors

The solar sensors for the OAO stabilization and control subsystem will be furnished by the General Electric Company under its subcontract. Advantage has been taken of the availability of qualified solar sensors developed by the Ball Bros. Research Corporation of Denver, Colo. These sensors are quite similar to those described by Nidey and Stacey[17] except that the "fine eye" characteristic has been modified to that shown in Fig. 4 and a so-called "disabling eye" has been added.

The "coarse eyes" which have almost hemispherical acquisition capability are simply silicon photovoltaic cells suitably filtered and covered with a diffuser to form a cosine-law sensor. The fine eyes incorporate a small lens and a knife edge reticle as shown in Fig. 4. The disabling eye is similar to the fine eye, but has a circular aperture instead of a knife edge reticle. Initial solar acquisition to an axis parallel to the principal experiment axis, but pointed rearward, is performed with the aid of the coarse eyes. The signal from the disabling eye transfers command to the fine eye.

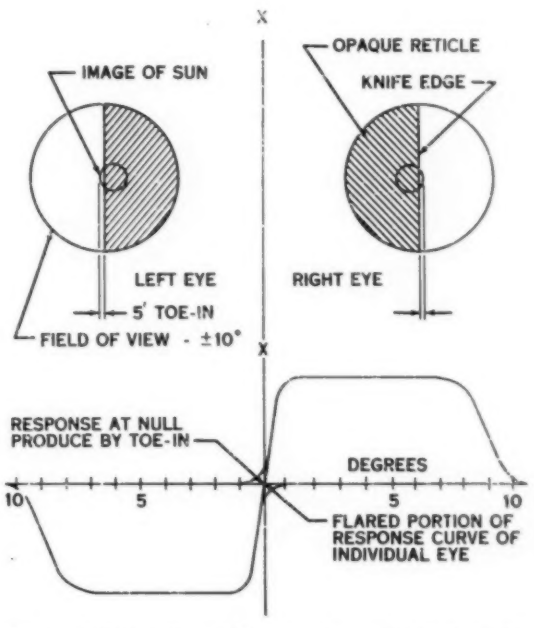

Fig. 4. Reticle pattern of fine-eye pair; sun located on axis.

The amplification of the photovoltaic cell output depends upon the use of low-impedance transistor amplifiers. The amplified error signals provide servo actuation for control of the spacecraft by the fine eyes to better than $^1/_4°$ of arc.

Problem areas in the use of the solar eyes lie in the influence of sunlight reflected from the earth and from portions of the spacecraft, as well as in shadowing by spacecraft protrusions. Locations for the eyes on the spacecraft are chosen carefully to minimize interference from solar paddles and sun shades. The earth's albedo can cause errors of up to several degrees in the pointing accuracy of the coarse eyes,[18] and this must be taken into account, system-wise, in order to guard against malfunctions.

The Gimballed Star Tracker

The gimballed OAO star tracker is being produced by a prominent manufacturer of star trackers, the Kollsman Instrument Corporation, with immediate direction of development being carried out through the major OAO subcontractor for the stabilization and control subsystem—the Missile and Space Vehicle Department of the General Electric Company.

Two of the six gimballed star trackers provided on the spacecraft are shown in Fig. 1. Each of the six is located in such a way as to minimize occultation of the line of sight by the solar array paddles, and by the sun shields, both of which extend to a considerable distance from the body. While the six star trackers provide complete coverage of the celestial sphere, emphasis in programming the attitude control will be placed on the use of stars as near as possible to gimbal field centers.

The tracker is an automatic star-seeking servo system, sensing direction by means of a telescope with a multiplier phototube at the exit pupil, using a two-axis gimbal arrangement to provide tracking freedom in a roll-pitch, $\pm 60°$ gimbal field. The telescope effective field of view is a square $1° \times 1°$ determined by the transverse oscillation of two rectangular field stops, which comprise the modulation system. These field stops are apertures in vibrating metal reeds. Both inner and outer gimbal axes are provided with angular read-out electrical transducers which can be used to indicate the direction to the star in two coordinates to external circuitry, and which can be used alternatively as feedback controls in a positional servo system by which the tracker telescope can be pointed in desired directions for star acquisition purposes. The tracker circuitry may be adjusted to recognize and acquire stars of third S-4 photoelectric magnitude and brighter, with principal emphasis on second magnitude and brighter for high accuracy.

Many of the features of this tracker are similar to those which have been described by McMorrow[19] for a $\pm 15°$ gimballed telescope to function on sixth magnitude stars. In comparison with the latter, the OAO star tracker has no self-contained search mode; has a 30-arc-sec accuracy design objective instead of 10-arc-sec; and does not incorporate variable threshold adjustment for acquisition of stars of preselected magnitudes only. The Phasolver (Trade Mark of Telecomputing Corp.) is used as a gimbal angle transducer, but in the OAO at an 18-bit rather than 19-bit level of accuracy. The Phasolver is a multipole shaft-angle-to-phase-angle electrostatic transducer. Its capacitance varies with angle and phase shifts a reference signal proportionally to shaft rotation.

While it was anticipated that development of a scanning-reed modulator such as that described by McMorrow would be completed in time to permit its use in the OAO star tracker, the required delivery schedule forced adoption of a slightly different version of the modulator. In the OAO version the two reeds operate in separate light bundles, rather than in series in the same light bundle, as described by McMorrow. The projection of the reed slots into object space, in both cases, results in an orthogonal relationship between the projected slots.

The OAO tracker optical configuration can be described by reference to the highly schematic Fig. 5. The optical design was evolved by the Kollsman Instrument Corporation to facilitate use of two reeds which did not require extremely exacting control of relative phase of vibration. In order to achieve the most compact packaging of the telescope, a prism beam divider is

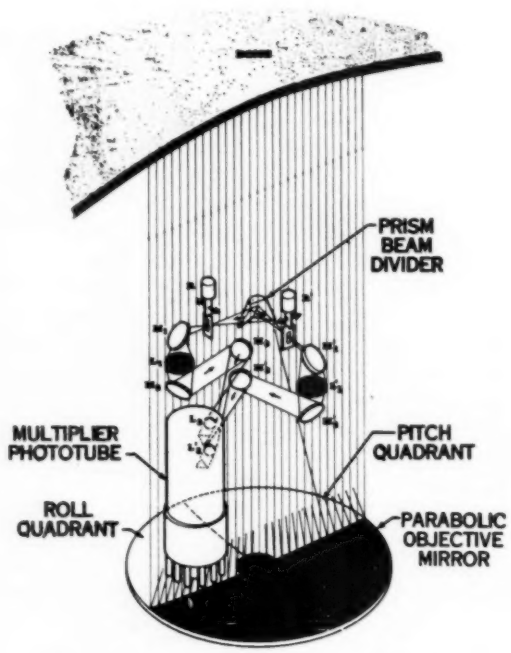

Fig. 5. OAO star tracker optical schematic.

used near the focal plane of a single parabolic objective mirror to secure two separate light bundles, one for each reed modulator. The reeds R and R^1 are driven at two different frequencies in order to make it possible to sense both modulated signals with one phototube. The reed apertures are essentially, although not exactly, in the focal plane. Folding of the bundles subsequent to the focal plane by mirrors M_1, M_1^1, etc. facilitates the imaging of the roll quadrant and the pitch quadrant of the objective mirror on the photocathode of the single phototube by a relay and collector lens system. While the spherical dome which is used to provide an hermetically sealed enclosure has minor lens power, it is not planned to use a corrector lens.

The electrical output of the multiplier phototube contains information at two different modulation frequencies plus harmonic content. Servo error signals can be derived by synchronous demodulation of the fundamental frequency content since the position of the star image relative to the null position of the reed aperture governs the phase of the fundamental. In order to derive both roll and pitch error signals from the composite signal, narrow band tuned amplifiers are used which select the fundamental signals for processing following a preamplifier. Also the second harmonic content is extracted, similarly, to provide "star presence" indication when the fundamental signal goes to zero at the null, as well as to provide continuity of AGC control.

The star tracker error indication relative to spacecraft coordinate axes is needed in digital form for telemetry, and is also needed in digital form for compatibility with the data storage which carries the commands for spacecraft control. Therefore, the analog phase shift information from the Phasolvers is digitized electronically.

The launch environment is rather severe for a precision optical instrument which is to be hard-mounted to the spacecraft structure. The mechanical design emphasizes shock and vibration resistance at the lowest penalty in weight. The center of mass is located as near as possible to the intersection of the axes of both gimbals. Careful balancing is observed. Component selection for mounting on the gimbal emphasizes low weight whenever possible. DC torque motors are used since gears are thus avoided, and the size is favorable, as well as other features, such as low power drain. The use of rotating mechanical parts for this gimballed system gives rise to bearing and lubrication problems which seem best solved at this time by hermetically enclosing the whole tracker unit and filling it with dry gas prior to launch. Careful design of the seal between the dome and the tracker body is necessary. Another feature of mechanical design which is important is the matching of thermal coefficients of expansion as closely as possible, because of distortion of critical parts which would otherwise ensue upon unavoidable rapid changes in flux input through the dome.

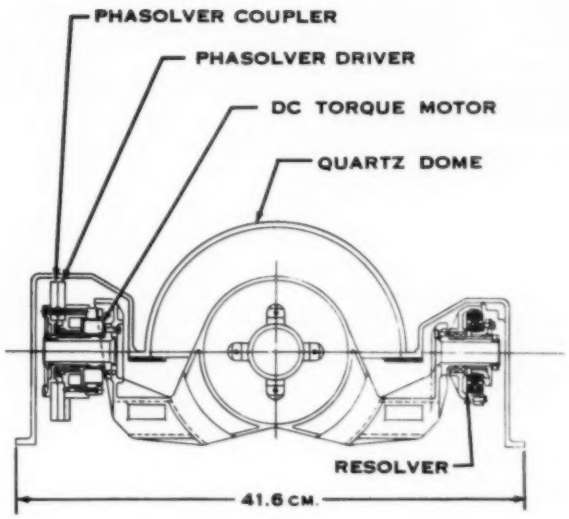

Fig. 6. OAO star tracker gimbal layout.

The star tracker is provided with an automatic sun sensor and shutter combination which cuts off direct sunlight when the tracker might be accidentally aimed close to the sun.

A resolver is provided on the outer gimbal axis to resolve the inner gimbal pick-off output to spacecraft body axis coordinates.

The general gimbal arrangement of the star tracker is illustrated in Fig. 6.

The Boresighted Star Tracker

As one of the steps in the sequential refinement of pointing accuracy from coarse acquisition to ultimate fine pointing control, it has been decided to incorporate one star tracker which is not gimballed, but is boresighted with the experiment axis. This step can be inserted when desired between the gimballed star tracker system and the fine error sensor in the experimenter's optics. For the experiments which carry no fine sensor in the first Observatory the boresighted star tracker can serve as such, in the sense of refinement of accuracy and stability of control, when desired.

By avoiding gimbals, gimbal shaft transducers, special domes or windows and the like, the accuracy, and probably the life of a star tracker, can be optimized. The ceiling on accuracy depends upon modulation errors, optical errors, and misalignment errors for the most part. The misalignment errors can be corrected in orbit by remote command, bringing the boresight tracker null into alignment with the experimenter's axis regardless of whether one or both have shifted as the result of launch and orbital environment.

By the same mechanism of remote command, alignment in orbit, a function useful to the experimenter, can be provided. This is offset guidance on a star, which makes it possible for the experimenter to examine the radiation coming from the apparent immediate vicinity of the star on the celestial sphere.

The Stellar Television Camera

The OAO stellar television camera is being produced by the Astro-Electronics Division of the Radio Corporation of America. This organization has designed and built the highly successful TIROS satellite which depends upon vidicon cameras for meteorological information.

It is believed that the feasibility of satellite television has been demonstrated beyond any question. Use of the television system in the OAO, however, is limited to radio-line-of-sight transmission ranges from the control station, whereas the automatic attitude system can be programmed for operation throughout the orbit.

Whereas the star tracker system provides automatic attitude control, the television equipment can be used for attitude sensing only. The television camera furnishes a composite video signal of 62.5 kc bandwidth to modulate the carrier of the Observatory wideband transmitter. The stellar television camera equipment will provide a real-time view of a section of the heavens centered about the small field of the experimenter's optical system. The star field is viewed on a ground monitor by an operator who can derive accurate attitude information from the picture and use it for remote control of the Observatory.

The camera will view an $8.3° \times 8.3°$ field. Accurate attitude information will be made possible by a fine-line reticle pattern generated within a special vidicon camera tube upon which the design is based. A unique feature of the OAO reticle technique is the ability to aim the system at a star with substantially less than one scan-line pointing error. The center of the reticle pattern is boresighted to a close tolerance to the experiment axis. The camera is to be hard-mounted to the spacecraft. This favors close alignment, but makes the task of providing shock and vibration resistance rather difficult.

The camera employs its special vidicon in a slow scan mode. Scanning and transmission are continuous with a frame time of 1 sec, which appears to be a suitable compromise between integration required for sensitivity, and preservation of the dynamic quality possibly required for real-time control. The 350-line scan is noninterlaced. While it has not been established definitely at this time that sixth visual magnitude stars can be seen with the camera, it is anticipated that this magnitude will be the approximate sensitivity threshold of the equipment. The average number of stars which should be seen in the field of view is at least six. By comparison with stored star patterns, or by measuring the angular separation of the stars in a display carefully designed to be as linear as practical, the star pattern can be recognized and a determination of Observatory attitude can be made at ground.

The reticle pattern is carried in the composite video signal in the form of a series of pulses. These pulses must be stripped from the composite video signal to be used at the ground control center for reconstitution of the reticle pattern. Since the reticle display is built up synthetically from these pulses, it can be rendered in any brightness or line width desired, and can be turned off completely when desired, in order to minimize obscuration of star signals. It is hoped to preserve reasonably accurate star magnitude discrimination in the whole television chain so as to provide the maximum assistance possible in recognizing star patterns and in quickly isolating stars of particular interest.

IV. Perspective

It is perhaps appropriate to remind the reader that the complex system described very generally in this paper has not yet been launched. Still, this report of the status of an essentially optical satellite is not a premature claim to success. Everyone associated with the OAO project is fully aware that many difficult problems must be solved before this revolutionary equipment begins to yield new astronomical data. However, it is believed to be a worthy objective to disseminate information during the course of the rather long development of a project such as the OAO, rather than to withhold it until completion.

It is desired to acknowledge the use of referenced documents and information conveyed in conferences with personnel of Smithsonian Astrophysical Observatory, the Space Astronomy Laboratory of the University of Wisconsin, the Goddard Space Flight Center, and the Princeton University Observatory. Acknowledgments are also due to the following subcontractors in the OAO program: General Electric Company's Missile and Space Vehicle Department, Kollsman Instrument Corporation, Radio Corporation of America, Astro-Electronics Division, and Ball Brothers Research Corporation.

Much of the system engineering information on the spacecraft has been obtained from reports prepared by the entire engineering and administrative staff of the OAO Project at Grumman. Particular thanks are due to Grumman Presentations for illustrations.

Acknowledgment is also made of the review and criticism by Mr. Robert Ziemer, NASA Project Manager for the OAO, and by Dr. James Potter of Grumman.

References

1. T. P. Stecher and J. E. Milligan, Astron. J. **66,** 296 (1961) (abstract of paper delivered June 1961, Am. Astron. Soc.).
2. A. D. Meinel, Science **134,** 1165–1171 (1961).
3. L. Spitzer, Astrophysical Research with an Artificial Satellite, Journal of the Franklin Institute Monograph No. 2, pp. 69–74 (June 1956).
4. L. Spitzer, Astron. J. **65,** 242–263 (1960).
5. F. L. Whipple and R. Davis, Astron. J. **65,** 285–290 (1960).
6. A. D. Code, Astron. J. **65,** 278–284 (1960).
7. L. Goldberg, Astron. J. **65,** 274–277 (1960).
8. N. Roman, Aerospace Eng. **19** (May 1960).
9. R. Ziemer, Astronautics, p. 36 (May 1961).
10. D. Anderton, Aviation Week and Space Technol., pp. 54–63 (Feb. 13, 1961).
11. C. D. LaFond, Missiles and Rockets, pp. 26, 27 (June 12, 1961).
12. W. Triplett, Am. Rocket Soc. Preprint 1184–60, Semi-Annual Meeting, May 1960.
13. Space Astronomy Laboratory, Univ. of Wisconsin, OAO Experiment Description Outline (February 1961).
14. Smithsonian Astrophysical Observatory, Technical Specifications for Celescope Payload and Ground Support Equipment to be used in conjunction with NASA OAO (June 15, 1961).
15. NASA Goddard Space Flight Center, Specifications for Goddard Experiment Package to be installed in the OAO (August 4, 1961).
16. C. D. LaFond, Missiles and Rockets, pp. 26, 27 (June 26, 1961).
17. R. A. Nidey and D. S. Stacey, Rev. Sci. Instr. **27,** 216–218 (1956).
18. A. J. Dennison, GE MSVD Eng. Tech. Memo 130-03-1 (May 10, 1961).
19. D. R. McMorrow *et al.*, Am. Rocket Soc. Preprint 1930-61, Guidance, Navigation, and Control Conf. August 7–9, 1961.

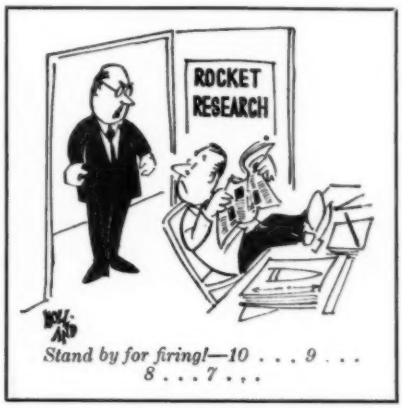

Stand by for firing!—10 . . . 9 . . . 8 . . . 7 . . .

Reproduced by kind permission of the Editor of New Scientist

Applied Optics BOOKS

Books for review should be submitted to the Managing Editor, APPLIED OPTICS, 1155 16th St., N.W., Washington 6, D.C.

Source Book in Astronomy 1900–1950. Edited by HARLOW SHAPLEY. Harvard Univ. Press, 1960. 417 pp. $10.00.

The development of scientific thought may be presented by providing a continuous narrative, or by presenting highlights with proper elaboration. The first method is apt to include details of no particular significance, although continuity is essential. The second tends to overemphasize individual achievements as the sole means for progress. Dr. Shapley has chosen to narrate the advancement of astronomy during the first half of the 20th century by following the second mode of presentation with one definite modification. Instead of providing his own narrative, he lets those who have contributed to the advancement tell their own stories. This has at least one advantage. The original narrator often records his mode of thinking by presenting the difficulties that had to be overcome and by giving the reasons for his choice of the method of approach to the problem. Such details are usually lacking in a professional journal.

We are told in the preface to this book that the collection of 69 contributions serves to illustrate the history of astronomy during this fifty-year period and that the selection was made with the general reader in mind. In each of the 23 sections we find a brief and comprehensive summary of about a page which gives in nearly every case the reasons for omitting certain significant contributions to the field under consideration. The selections in the book are almost free of mathematics; the whole book contains a dozen or so equations besides the limited mathematics needed to prove the mass-energy equivalence by Einstein. However, in spite of the efforts to present material suitable for the general reader, it is difficult to imagine the existence of such a reader. At least a first course in astronomy or its equivalent is needed to make the book meaningful and enjoyable. For the student in astronomy, the book is nearly indispensable, and reading it will prove most rewarding.

The sequence of topics and of contributors provides a rather concise exposition of the progress of astronomy and a good insight into the personalities involved. The book shows that the knack of masterly exposition among the great is not lacking. Also it shows those who are overcautious and those who are daring. But neither seem, even in this short interval of 50 years, capable of escaping the inevitable change in outlook. We call the very few who managed to escape prophetic, but their turn will come with the passage of time. This is, after all, one of the principal characteristics of the human activity that we call science. And this is one of the lessons that the student and the fortunate general reader will comprehend from this fine collection of expository material.

The success of a book of this type naturally lies in proper selection of topics. Dr. Shapley has succeeded in his selections of the highlights and guarded himself by giving reasons for obviously important omissions. This leaves little for the reviewer to do in the way of criticism but state the trivial, namely, the illustrations are poorly reproduced.

The period under review produced a number of famous debates. The inclusion of some of them would have provided an excellent way of showing that scientific progress is not a smooth-going affair and that the introduction of new concepts produces conflicting opinions. For example, he who will be writing on the progress of astronomy in the next fifty years must not neglect narrating the current debates on cosmology. Some of the debates are long and spread out in many journals and hence unsuitable for this book. But the one between Professor H. D. Curtis and Professor Shapley with reference to the extragalactic objects could have been told and would have illustrated admirably the struggle for the acquisition of new knowledge.

J. J. NASSAU

Space Astrophysics. Edited by W. LILLER. McGraw-Hill, New York, 1961. 269 pp. $10.00.

This book covers a series of lectures given at the University of Michigan by various persons active in the new field of space astronomy. The publication has been prompt, a point of importance in a rapidly developing field, but the use of photo-offset from typed copy detracts from its appearance.

The substance of the first section on experimental work is on accomplished observations of the sun and stellar sources, providing an excellent summary of both the techniques and the results. The first chapter by Tousey summarizes for the first time photographs of his many epochal observations of the solar spectrum and solar disc, although the half-tones are on a poorer quality paper than is necessary for the best reproduction of photographs. A brief section by Rossi discusses the MIT x-ray telescope, placed in orbit subsequent to the publication of the book. The second section on theory is brief with an excellent discussion of the state of knowledge of the coronal and interplanetary medium by Chapman. One is puzzled, however, by a seemingly extraneous brief discourse on "The Electric Universe" by Bondi. The third and final section in instrumentation has two good reviews of the development of stabilized platforms for both balloon and rocket astronomy and of the future requirements of space experiments. The final chapter by Namioka is a classic on the theory of the various forms of concave grating spectrometer, including his extension to ellipsoidal concave gratings.

This book is an important contribution summarizing the current state of astronomy in the far ultraviolet. As a consequence, it will not become quickly obsolete, but will be added to as space astronomy continues to expand.

A. B. MEINEL

Radiometric Standards and Measurements. Notes on Applied Science No. 23. National Physical Laboratory. By E. J. GILLHAM. D.S.I.R., London, 1961. 23 pp. ls 9d.

This short monograph describes methods used at the National Physical Laboratory for the relative and absolute measurements of both total and monochromatic radiations. Judged from precisely that viewpoint, the book meets its objectives with clarity and style. However, to a reader with expectations of finding a broad or general treatise on radiometry, the report is disappointing.

Mr. Gillham, apparently, is an experimentalist with a meticulous understanding of the radiometric methods employed at the National Physical Laboratory, and he ably describes these methods. His description of the Moll Thermopile, which he uses, is vivid regarding physical parameters such as size, shape, and resistance, but his omission of an analytical description of the process prevents one from ascertaining valid general conclusions.

The methods described will undoubtedly form useful reading to an experimentalist engaged in a radiometric standards laboratory. Because it does not treat the subject analytically, nor attempt generalizations, it will be of limited interest to radiometrists engaged in field activity and similar pursuits.

D. J. LOVELL

continued on p. 16

Threshold and Stability of a Simplified Model Optical Maser

E. J. Post

The population behavior of three level optical masers can be described by a set of four nonlinear differential equations. For practical purposes, a satisfactory analytical discussion of the stability of such a set of equations does not seem to be available in the mathematical literature. The similarity with solvable cases of the Volterra fish problem is emphasized. The equations yield the standard threshold conditions obtained by more direct physical methods when one assumes that steady state solutions exist. Instability may now occur if there is a discrepancy between the threshold power and the power needed to maintain the steady state. An extreme case, requiring infinite steady state power, is discussed.

Recent studies of modulation effects[1,2] observed in the performance of optical masers have revealed a marked similarity between the action of masers and the behavior of Volterra's famous fishes.[3] Instead of one species of fish devouring another, in the maser a population of greedy photons "devours" excited states until they have nothing left to feed on, thus causing a rapid quenching of the optical carrier. Then the population of the level of excited states has an opportunity to be replenished by the pump action until the same process starts all over again.

A detailed mathematical discussion of the maser population problem is, unfortunately, rather more involved than the Volterra fish problem. For the three-level maser one obtains a system of four nonlinear differential equations describing the following processes (the nonlinearity is caused by the induced emission and absorption terms):

1. The change of the population in the pump absorption band is determined by the pump input (dependent on the ground level population) and the excitation transfer from the absorption level to the upper maser level.

2. The change of the population of the upper maser level is dependent on three processes: (i) the photon-excitation exchange, (ii) the total spontaneous emission, and (iii) the excitation transfer from the pump absorption level.

3. The change of the photon population of the privileged modes (those selected by the Fabry-Perot) depends on (i) the excitation exchange with the maser levels, (ii) the (partial) spontaneous emission into the privileged modes, and (iii) the attenuation due to the transparency of the Fabry-Perot mirrors and the medium losses.

4. The change of the photon population in the nonprivileged modes depends on a similar set of factors as mentioned for the privileged modes. The (partial) spontaneous emission probability into the nonprivileged modes and the attenuation are larger than for the privileged modes.

A four-level maser, e.g., the uranium maser[4] (and in a sense the He–Ne maser[5]) would require a fifth equation, because the lower maser level is not coincident with the ground level.

It is a major enterprise to solve a system of four or five nonlinear differential equations, but the equations themselves can yield considerable information without one having to take recourse to explicit solutions. A point of primary importance for defining engineering parameters is the stability of the solution, i.e., whether or not the solution approaches a steady state (e.w.) in a finite interval of time. Another significant aspect is whether or not these equations have asymptotic solutions in the sense of a Poincare limit-cycle. Such solutions, similar to those in the theory of orbital motion, would correspond physically to a periodic amplitude modulation of the optical carrier. A relaxation modulation of this kind can range all the way from an almost sinusoidal to a violent pulselike modulation.

A preliminary graphical analysis (by the author) of simplified forms of the equations has established the possibility of transients (solutions spiraling in on a "focal" steady state point). The existence of asymptotic solutions has not been established with certainty,

The present article is part of an orientational study made in behalf of and supported by Diffraction Limited, Inc., Bedford, Mass. The author is now with the Air Force Cambridge Research Laboratories, Bedford, Mass.

Received July 1961.

though one would expect them on the basis of the mechanisms involved. For the three-level maser it is the sudden depopulation of the upper maser level, due to the stimulated emission, which one would suspect as a potential source of instability. For the four-level maser, in addition, one may expect a saturation of the lower maser level to have a similar effect. Unfortunately, it is misleading to draw conclusions about stability if one simplifies to less than three equations.

Let us turn to some further remarks and conclusions which have been obtained by a preliminary investigation of the equations for the three-level maser. Before doing so, however, we would like to emphasize that a population analysis, because of its very nature, cannot yield direct information about the aspects of coherence. Consequently, the concept of a masering threshold is not as clearly defined as one might be inclined to believe. Indeed, rather than speaking about a "masering threshold" one should rather refer to excitation levels at which coherent radiation becomes noticeable in the background of incoherent radiation. On the other hand, it is also appropriate to speak of an instability threshold or an instability interval. We shall not make any rigorous mathematical attempts to investigate whether or not these thresholds can be expressed analytically in the parameters of the equations, but will pursue a more intuitive line of thought which is believed to bring us close to the crucial features of the subject matter.

An investigation of the processes 3 and 4 (see Appendix) shows that a steady state photon population of the privileged modes would become extremely large with respect to the photon population of the nonprivileged modes if the population X of the upper maser level approaches

$$X \to \frac{N}{2} + \frac{\alpha}{2B}, \tag{1}$$

where

N = number of fluorescent centers in the maser medium,
α = attenuation of the privileged modes,
B = induced emission probability per incident photon, per unit time.

Note that this population level can never be reached unless

$$\frac{\alpha}{2B} < \frac{N}{2}, \tag{2}$$

because X can not exceed N.

Let us now assume that the upper maser level has reached the critical population level indicated by Eq. (1), but that the extreme photon population in the privileged modes has not yet had time to build up. The power P required to establish the level X is then primarily determined by the spontaneous emission A and becomes $AX\hbar\omega$, or

$$P = \frac{1}{2}\left(AN + \frac{\alpha A}{B}\right)\hbar\omega. \tag{3}$$

The first term in this equation is the power needed to establish the population inversion. The second term corresponds to the power mentioned by Schawlow and Townes[6] to overcome cavity losses.

Summarizing the situation we may now consider P as the effective power required to establish the system in such a state that the number of photons in the privileged modes can become extremely large with respect to the number of photons in the nonprivileged modes. There are already a considerable number of photons in the nonprivileged modes due to spontaneous emission. Hence, the number of photons generated by the regenerative stimulated emission in the privileged modes will now increase to a quite unusually high value. One would be able to maintain this dense population only if P could also supply the additional excitations. A simple calculation, however, shows that the threshold P given by Eq. (3) for the presently used ruby masers* is already so large that it can only be generated in short intense flashes. These flashes are so intense that they would be prohibitive for the crystal if they were to be sustained for longer periods of time. A dissipation in the crystal of around 100 watts/cm^3 is too high.

It is clear that the sudden energy surge into the privileged modes makes it very hard to maintain a nonintermittent behavior. However, the intensity of this surge is a favorable factor in enhancing the degree of coherence. In point of fact, a continuously pulsating maser oscillator would unquestionably be a very useful item as a highly monochromatic and coherent light source. This manner of continuous operation, according to Eq. (3), can be approached if we bring about a drastic reduction in N. The density of fluorescent centers for a 0.1% ruby is of the order of 10^{19}/cm^3. A reduction to 10^{17} or possibly 10^{16} would be necessary to lower P to a feasible value for continuous operation. A reduced value of A, of course, would have a similar effect; however, nature limits us here in our choice of metastable levels with a sufficiently long decay time. One may expect an improved A in very dilute and well annealed crystals. It has been experimentally observed that low temperature operation further reduces A.

The foregoing techniques for reducing the energy level P create some new problems which may thwart successful maser operation. First of all, a very dilute crystal makes it hard to meet the conditions of Eq. (2), which is crucial for an appreciable inversion in the photon population of the privileged and nonprivileged modes. In other words, the Q of the cavity has to be

* We are referring to ruby crystals with a chromium concentration of the order of 0.1%.

made as high as possible (low α). Secondly, a very dilute crystal may require improved pumping schemes, because of the lower effective absorption of the pump light per passage through the crystal. It is believed, however, that these requirements may be met by carefully improved engineering.

It should be of some interest to mention that the equations for the optical maser come close to reducing to the case for a microwave maser as soon as the photon population of the nonprivileged modes becomes negligible with respect to the photon population of the privileged modes. One obtains two equations of the type discussed by Statz and de Mars[7] (corresponding to processes 2 and 3 of this paper) if, in addition, the partial spontaneous emission into the privileged modes is neglected and if the pump absorption is assumed not to depend on the ground level population (constant supply of excitations for the upper maser level). Higher pumping power and smaller α should then lead to a real continuous wave optical carrier. The latter conclusion should be eyed with considerable reserve, because of the rather drastic simplifications involved. Power levels are as yet too high to test the validity of this point.

It is interesting to note that the four-level maser usually requires less power to establish the population inversion of the two maser levels. The large first term $\frac{1}{2}\,AN\hbar\omega$ in P can then be replaced by another much smaller term. Its operation, however, is rather more critical than the three-level maser. The closeness of the lower maser level to the gound level may require cryogenic conditions.

In conclusion we would like to remark that the complete population analysis of the optical maser is admittedly very complex but intermediate approaches are by no means hopeless for useful engineering information. A computer solution of a representative set of equations would certainly be helpful. A "bird's eye view" of general maser behavior, however, would benefit more from a good stability discussion for engineering purposes than from blunt computer approaches.

The author is indebted to Professor J. P. den Hartog for general information and references about the stability features of nonlinear systems, and to Dr. A. Walther for several useful discussions.

References

1. R. W. Hellworth, Phys. Rev. Letters **6**, 9 (1961).
2. J. R. Singer and S. Wang, Phys. Rev. Letters **6**, 351 (1961).
3. A. S. Andronow and C. E. Chaikin, *Theory of Oscillations* (translation from the 1937 Russian Edition, Princeton Univ. Press, 1949).
4. P. P. Sorokin and M. J. Stevenson, Phys. Rev. Letters **5**, 557 (1960).
5. A. Javan, W. R. Bennett, Jr., and D. R. Herriot, Phys. Rev. Letters **6**, 106 (1961).
6. A. L. Schawlow and C. H. Townes, Phys. Rev. **112**, 1940 (1958).
7. H. Statz and G. de Mars, *Quantum Electronics* (Columbia Univ. Press, 1960), p. 530.

Appendix

The processes 3 and 4 can be written in the following explicit forms if it is assumed that the time of residence in the absorption bands is small with respect to the time of residence in the two maser levels;

$$\frac{du_1}{dt} = (2X - N)u_1B + A_1X - \alpha_1u_1, \tag{4}$$

$$\frac{du_2}{dt} = (2X - N)u_2B + A_2X - \alpha_2u_2. \tag{5}$$

The meaning of the symbols is the same as discussed in the text, with the additional information that A_1 is the spontaneous emission probability into the privileged modes and A_2 is the same quantity for the nonprivileged modes.* The same distinction holds for the attenuation constants α_1 and α_2. The symbols u_1 and u_2 refer to the photon population in the privileged and the nonprivileged modes.

The left-hand members du_1/dt and du_2/dt are zero for steady state conditions.

The elimination of X between Eq. (4) and Eq. (5) e ds to the following relationship between u_1 and u_2

$$u_1u_2 + \frac{A_1[N + (\alpha_2/B)]}{2(\alpha_2 - \alpha_1)}\,u_2 - \frac{A_2[N + (\alpha_1/B)]}{2(\alpha_2 - \alpha_1)}\,u_1 = 0. \tag{6}$$

The hyperbola (e) is illustrated in Fig. 1 for positive values of u_1 and u_2 and for $\alpha_2 > \alpha_1$. It shows that u_2 has a positive limiting value

$$\frac{A_2[N + (\alpha_1/B)]}{2(\alpha_2 - \alpha_1)},$$

whereas u_1 can increase to arbitrarily high positive values along the vertical asymptote so that

$$u_1 >> u_2. \tag{7}$$

In order to see for what values of X the population inversion between u_1 and u_2 occurs, one solves Eq. (4) and Eq. (5) for u_1 and u_2 and one takes their ratio

$$\frac{u_1}{u_2} = \frac{A_1\,\alpha_2 + B(N - 2X)}{A_2\,\alpha_1 + B(N - 2X)}. \tag{8}$$

The ratio u_1/u_2 goes to infinity if

$$X \to \frac{N}{2} + \frac{\alpha_1}{2B},$$

thus establishing Eq. (1) mentioned in this paper.

Note that this conclusion depends on the initial assumption that the time of residence in the two maser levels prevails over the time of residence in the absorption bands.

(Figure 1 overleaf)

* A_1 is proportional to the solid angle subtended by the Fabry-Perot mirrors and A_2 is proportional to 4π minus this solid angle. Hence $A_1 + A_2 = A$.

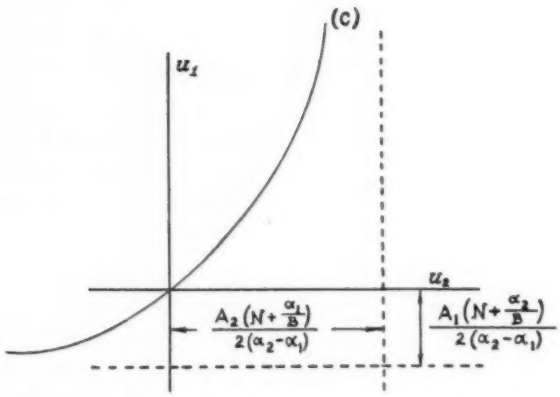

Fig 1. The photon population inversion between the privileged modes u_1 and the nonprivileged modes u_2.

Books

continued from p. 164

Tools of the Astronomer. By G. R. Miczaika and William M. Sinton. Harvard Univ. Press, Cambridge, Mass., 1961. viii + 294 pp. $7.75.

The authors, formerly of Harvard and now of Aeronutronic and Lowell Observatory, respectively, have written a new book on astronomical telescopes and techniques that is apparently intended to replace Dimitroff and Baker's *Telescopes and Accessories* (1945) in the series of Harvard Books on Astronomy. Successive chapters deal with the nature of light, photography, telescope optics and construction, photometry, spectroscopy, solar instruments, and radio telescopes. The authors' own research work has covered a considerable part of this territory and the fact is reflected in the text, although one misses the optical authority of J. G. Baker that pervaded the earlier book.

The volume is not directed to the professional, but to the amateur and the beginning student. Consequently, there is no attempt to go very deeply into any topic, and the general tone is that of a pleasant, undemanding public lecture. It is hardly the duty of a reviewer to pronounce upon what kind of book the authors ought to have written, but it is impossible not to feel some regret that they were not called upon to produce a book on the level of Danjon and Couder's *Lunettes et Télescopes*, a true classic and long in need of a replacement. *Tools of the Astronomer* is, however, well suited to the audience for which it was designed, and will undoubtedly be very favorably received. The book is beautifully produced and printed, although there are a few inaccurate diagrams.

There will be a few readers who, upon putting this book down, will be struck by the long time constant that has characterized the advance of astronomical instrumentation. Modern refractors and reflectors differ little in principle from their counterparts of 150 years ago. The number of fundamentally new instruments and techniques introduced over the past century is surprisingly small, and in recent years astronomical instrumentation has shown a considerable lag with respect to the technological level of other physical sciences. Possibly the glacial advance in telescope technology is due in some degree to the durability of a major telescope: no physicists are known to be using an accelerator built before 1900, but telescopes of even greater age are still in active service. However, the phenomenon goes deeper, because auxiliary instruments, techniques, philosophies fifty years old are common. One accustomed to the vitality and technical resources of modern physics may find the situation puzzling, but the explanation is not difficult to discover. Much of this is the physical and psychological result of the grinding poverty that enveloped astronomy as a science for generations. It is indeed remarkable that so much has been accomplished by so few, with so little, working under such handicaps.

Miczaika and Sinton have written about instruments, and little about astronomy and its problems. But it is appropriate to bring up a question that they might very well have dealt with: in which direction will the instrumentation of optical astronomy proceed next?

Today, astronomy faces the promise of financial support in an unprecedented degree, and at a time when the prospects of astronomical observations from outside the atmosphere are very bright. The question arises whether the overwhelming share of these resources should be turned to space astronomy, or whether a major effort should simultaneously be made to press earth-bound optical astronomy to its full physical limits. It is assumed, of course, that in the interim the sky can somehow be preserved for optical astronomy against the crippling effects of dipole belts and large numbers of very bright communication satellites.

Two points should be made very clear. First, let us not deceive ourselves that everything worthwhile now being done from the earth's surface can be done even better from space. As immense as the rewards of space astronomy are likely to be, there are equally significant problems to be tackled from the surface that would be foolish and inconvenient to attempt outside the atmosphere. Many of these are problems that have not been exploited through sheer lack of facilities and personnel. Second, it has not been proved that the ultimate in earth-bound optical telescopes has been reached, given today's technology and the possibility that somewhere on the planet there may exist a site where an instrument substantially larger than any now in existence could function efficiently.

This issue—in effect, whether or not support on a truly major scale should be given to earth-bound optical astronomy at the

continued on p. 183

Physical Optics of Coherent Radiation Systems

Jenny E. Rosenthal

A survey is made of physical processes which might degrade a uniphasal wavefront. Tolerances are examined for two distinct types of presentation: long-range communications and short focus, high photon concentration. The limits are found within which the perturbations can be neglected for these two applications. Conditions are formulated that must be fulfilled by the coherent light generator to make it practically useful. These include the duration of time coherence and the geometry of the uniphasal wavefronts.

The development of the ruby maser,[1] the first practical source of coherent radiation, has given new impetus to a number of optical investigations. This study is intended to ascertain whether optical systems can be designed which will take full advantage of the coherent properties of light emitted by an optical maser or similar source. Our main concern is with problems such as long-range communications by means of light beams or the interaction of light and matter under conditions when photon density becomes comparable to the density of atoms in a solid.

We will first clarify the concept of coherence and the degree of coherence required in the solution of problems, which we are considering. Waves are called spatially coherent if the wavefronts are surfaces of constant phase as well as constant amplitude. As a rule, the spatially coherent wavefronts are simple geometrical surfaces, e.g., planar or spherical. Wave trains emanating from different portions of a given wavefront can interfere with each other.

The other feature which characterizes radiation from optical masers is the high degree of their time coherence. It is well known that when a wave train entering an interferometer is divided into two wave trains, these can interfere with each other at the point of observation only if the optical path difference is sufficiently short as compared to the coherence length Δl, i.e., the length of the wave train. Otherwise, one component train will have passed the point of observation before the other one arrives. The coherence time $\Delta t = \Delta l/c$ of the wave train is connected to the bandwidth $\Delta\nu$ by the uncertainty relation[2] $\Delta t \Delta\nu \geq {}^1/_4\pi$. Thus an infinitely narrow spectral line is the only kind that can be represented by an infinitely long wave train.

While we are not primarily concerned here with different types of coherent light sources, their coherence times are of primary importance in the design of any optical system. In the ruby maser, which is a high power pulsed source, $\Delta\nu \sim 10^8$ sec^{-1} so that the coherence time is of the order of 10^{-9} sec and the coherence length of the order of 30 cm. Coherence times of this same order of magnitude can be achieved in the λ-aperture coherent generator, which is a medium power continuous wave (cw) source. This device focuses monochromatic radiation from conventional sources into a small spot, of the order of 0.2 mm diam, overlapping an aperture with a diameter of the order of the wavelength of the light focused on it. In gaseous masers, which are continuous low power sources,[3] $\Delta\nu \sim 10^3$ sec^{-1} so that the coherence time is of the order of 10^{-4} sec and the coherence length of the order of 30 km.

Optical transmission of information has the advantage that, in addition to time sequential modulation of the beam as in radio transmission, there is the possibility of the optical projection of a picture, which is equivalent to the transmission of information in parallel along a large number of channels.[4] However, an ordinary beam of light is unsuitable for this purpose because of spreading. For example, the supposedly highly parallel beam obtained with an arc lamp at the focus of a six-foot mirror still diverges by about 1°. This amount of divergence results in the spreading of a very narrow beam to a diameter of 18 meters at a distance of 1 km.

It is possible, on the other hand, to obtain a coherent light beam with a very small angle of divergence δ

The author is with Bramley Consultants, Passaic, New Jersey.
Received 12 July 1961.

given in radians by

$$\delta = 2\lambda/\sqrt{A} \tag{1}$$

where A is the radiator area. This condition is quite analogous to that encountered in the design of antenna arrays if δ is defined as the angle between the two directions of emission of radiation for which the intensity falls to zero. For a radiator area of 1 cm^2 and the 6943 A wavelength of the ruby maser, $\delta = 1.4 \times 10^{-5} = 0.4'$. While the closest experimental value so far is of the order of one magnitude higher, this discrepancy between theory and experiment is only apparent. As shown by the two-slit interference experiment of Nelson and Collins[5] and by the microsecond films of Dayhoff,[6] the ruby optical maser does not radiate as a simple unit but as a system of distinct parallel channels comprised within the crystal face. However, the evidence is that they radiate in unison.

To determine the type of optical system needed with a beam of this type where the angle of divergence, though very small, is nevertheless not zero, one must consider what resolution of the image can be retained after transmission over a distance L. If a pattern of black and white squares is impressed on the light beam, each luminous patch will act as an independent coherent source and will diverge with an angle δ given by Eq. (1). The identity of the individual patches will be recognizable only if the spread of each patch covers less than half the area of the adjoining one. For a patch of linear dimension b, the linear spread on each side is $\Delta b = {}^1/_2 L\delta$, with δ determined from Eq. (1) where the radiator area is $A = b^2$. This results in the condition

$$b > (2L\lambda)^{1/2}. \tag{2}$$

For $L = 100$ km and $\lambda = 6943$ A, $b > 40$ cm, approximately. Thus patches impressed on a beam 1 cm^2 in cross section definitely cannot retain their identity after 100 km. This can be accomplished, however, by blowing up the beam cross section from 1 cm^2 to several square meters; for example, by an adaptation of the Cassegrain two-mirror system illustrated in Fig. 1. Such an optical system will be shown not to destroy the spatial coherence of the beam. Furthermore, the increase in cross section produced by the optical system is not accompanied by a corresponding decrease in the brightness of the image viewed after 100 km. At that point the initial light beam of 1 cm^2 cross section would have spread to an area of 150 m^2 while a light beam blown up, for example, to 3 m^2 spreads to only 3.2 m^2 because of the much smaller angle of divergence for the larger source.

Another interesting utilization of coherent radiation is as a high density photon source. It has been indicated[7] that if coherent radiation from the ruby maser were focused into an area of the order of λ^2, the energy at that spot in a volume of the order of λ^3 would be 140 Mev. The condition under which this type of focusing can be realized has been evaluated both from concepts of classical optics[8] and from the uncertainty principle.[9] It has the same form as Eq. (1) for the divergence of radiation from an antenna except for a factor 2. Also since δ, which is now the angle of convergence of the focused light beam, is no longer small, it can no longer be used to replace $\sin\delta$ on the left-hand side.

The basic question that has to be answered with regard to the optics of long-range communications is whether refraction or reflection by an optical system will increase the angle of divergence of the beam by an appreciable amount from that given by Eq. (1). With regard to focusing, we have to ascertain whether coherence is retained after the cross section of the beam has been reduced to λ^2. Because of the uniphasal characteristic of spatially coherent waves, the electric and magnetic field intensities **E** and **H** combine cooperatively leading to extremely large resultants. This is impossible in the absence of coherence. However, the existence of multiple photon absorption is not predicated on cooperative action so that according to first order theory the radiation density within a volume λ^3 might collapse spontaneously with the simultaneous stripping of the atom.

As far as the exact nature of the radiation from the ruby maser is concerned, according to Haun and Ohlmann,[10] for homogeneous materials the maser tends very strongly to oscillate in a single normal mode, which produces maximum output along the axis of the structure. A different type of calculation of the amplitude and phase of the radiation in the various modes carried out by Fox and Li[11] confirms the assumption that the maser tends to radiate in the fundamental TEM_{00} mode if the mirror spacing in the Fabry-Perot interferometer is correct for resonance. In examining the action of an optical system, we are therefore justified in assuming that before entering the system the wavefront is plane, spatially coherent, and time coherent to 10^{-9} sec or longer.

We shall also assume that the optical system is aberration free since it is not the purpose of this paper to discuss the effect of various lens aberrations on the uniphasal wavefronts. Phase singularities resulting from third order aberrations have been discussed by Lee and Farnell[12] for microwave lenses.

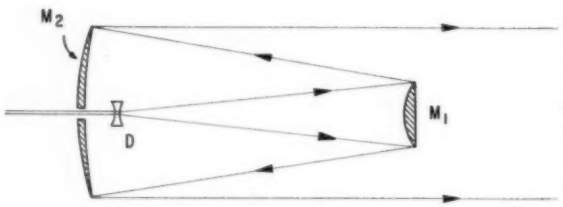

Fig. 1. Adaptation of Cassegrain optical system. M_1—convex mirror; M_2—concave mirror; D—diverging lens.

Consider the refraction of plane polarized light by an absorbing medium.[13] Denote, as usual, by A_s and A_p the components of the incident electric vector perpendicular and parallel, respectively, to the plane of incidence, and by T_s and T_p the corresponding complex amplitudes of the transmitted wave. Fresnel's formulas then take the form:[14]

$$T_s/T_p = A_s/A_p \cos(\theta - \theta_t), \tag{3}$$

where θ is the angle of incidence and

$$n(1 + i\kappa) \sin\theta_t = \sin\theta, \tag{4}$$

n being the index of refraction. The absorption index κ is related to the absorption coefficient a by

$$\kappa = a\lambda/4\pi n. \tag{5}$$

Since $\sin\theta_t$ is complex, the transmitted wave is polarized elliptically. To calculate the characteristics of this elliptic polarization, we choose $a = 0.1$ cm^{-1} as a reasonable value for a refractive medium used in lens systems. If $n \sim 1.6$, $4\pi n \sim 20$, so that $\kappa = 3.5 \times 10^{-7}$ for $\lambda = 7 \times 10^{-5}$ cm. Since the imaginary is so small as compared with the real part, we can expand T_s/T_p in powers of κ and keep only the linear term. This gives:

$$T_s/T_p = (A_s/nA_p)\{(n^2 - \sin^2\theta)^{1/2}\cos\theta + \sin^2\theta + i\kappa \sin^2\theta[(n^2 - \sin^2\theta)^{-1/2}\cos\theta - 1]\}. \tag{6}$$

Thus to this order of approximation the ratio of the amplitudes of the transmitted wave is unchanged from what it would be in the absence of absorption. If we denote by ϕ the difference in phase between T_s and T_p, we have

$$\tan\phi = \kappa \frac{\sin^2\theta[1 - (n^2 - \sin^2\theta)^{-1/2}\cos\theta]}{\sin^2\theta + (n^2 - \sin^2\theta)^{1/2}\cos\theta}. \tag{7}$$

Its maximum value, which occurs at grazing incidence, is numerically equal to κ, i.e., $\phi_{max} = 3.5 \times 10^{-7}$ rad.

Consider now the effect of a reflective system. If a linearly polarized beam of light is incident normally on a metallic reflector, the reflected light is also polarized linearly, and its change in azimuth is 180°, i.e., the azimuth remains unchanged in its absolute direction in space. If the angle of incidence is small but not zero, then according to Jenkins and White,[15] the phase difference between the parallel and perpendicular components of the electric vector in the reflected beam still remains nearly 180°. For example, the phase difference exceeds 175° for an angle of incidence up to about 10°. Thus for a beam reflected at less than 10°, the polarization, though elliptic, does not depart too far from linear.

To determine if such a change has a significant effect on the divergence angle of the beam, we have made some calculations, restricting the problem, however, to two dimensions. In the two-dimensional treatment it is, of course, not possible to take into account elliptic polarization. However, since it has been indicated that the ellipticity of polarization is completely negligible for a refractive system and quite small for a reflective system for angles of incidence below 10°, we believe that the calculations presented below are meaningful.

We computed the angle of divergence of a beam of radiation emitted by a linear antenna in the following three cases: (1) Both the phase and the amplitude of the electric vector at the antenna are constant. (2) The phase of the electric vector at the antenna is constant while its amplitude follows a cosine law. (3) The amplitude of the electric vector is constant while the phase at the ends of the linear emitter is either advanced or retarded by an angle less than π. (This is the condition found experimentally by Fox and Li[11] for an optical maser in the TEM_{00} mode.)

Let b be the length of the linear antenna, θ the angle between the emitted radiation and the normal to the antenna, λ the wavelength, ν the frequency of the radiation, and R the distance (large) from the antenna to the point at which the electric vector is being determined. Let the case under consideration be denoted by a superscript in parentheses. In cases 1 and 2 the electric vector is given by[16]

$$iE_\theta R = 1/2\ \nu\mu_0 \cos\theta\ e^{2\pi i(R/\lambda - \nu t)} \times \int_{-b/2}^{+b/2} e^{2\pi i(x/\lambda)\sin\theta}\ u(x)dx, \tag{8}$$

with $u^{(1)}(x) = K$, $u^{(2)}(x) = K\cos 2\pi(x/b)$, K being a constant. We thus obtain:

$$iE_\theta^{(1)} R = \frac{1}{2}\ \nu\mu_0 Kbe^{2\pi i(R/\lambda - \nu t)}\ \frac{\cos\theta \sin[\pi(b/\lambda)\sin\theta]}{\pi(b/\lambda)\sin\theta}, \tag{9}$$

$$iE_\theta^{(2)} R = \frac{1}{4}\ \nu\mu_0 Kbe^{2\pi i(R/\lambda - \nu t)}\left\{\frac{\sin\pi[1 - (b/\lambda)\sin\theta]}{\pi[1 - (b/\lambda)\sin\theta]} + \frac{\sin\pi[1 + (b/\lambda)\sin\theta]}{\pi[1 + (b/\lambda)\sin\theta]}\right\}. \tag{10}$$

It is of interest to note that case 1 leads to the same expression for the intensity as Fraunhoffer diffraction by a slit. The main maximum of $E_\theta^{(1)}$ occurs at $\theta = 0$, and the first minima on each side occur at

$$\sin\theta = \pm\lambda/b. \tag{11}$$

Since $\lambda \ll b$, the angle of divergence δ (comprised between the two directions for which the electric vector vanishes) is

$$\delta = 2\lambda/b. \tag{12}$$

The agreement between Eq. (1) for the two-dimensional antenna array and Eq. (12) for the linear antenna proves the validity of the approximations used.

In case 2, $E_\theta^{(2)}$ vanishes at $\theta = 0$. Its first two

minima on either side of $\theta = 0$ occur at

$$\sin\theta = \pm 2\lambda/b, \tag{13}$$

so that the angle of divergence is again given by Eq. (12).

In case 3 the electric vector is given by

$$iE_\theta^{(3)} R = 1/2\ \nu\mu_0 \cos\theta\ e^{2\pi i(R/\lambda - \nu t)} \times \left\{ \int_0^{b/2} K e^{-2\pi i x(\sin\theta - \sin\theta_0)/\lambda}\, dx + \int_{-b/2}^{0} K e^{-2\pi i x(\sin\theta + \sin\theta_0)/\lambda}\, dx \right\}. \tag{14}$$

The final expression for $E_\theta^{(3)}$ is omitted as it is rather cumbersome. It leads, however, to similar results for the angle of divergence of the emitted radiation as cases 1 and 2.

We may thus conclude that either a low absorption refractive system or a small angle reflective system can be designed to accomplish the primary objective of either increasing or decreasing the cross section of a coherent light beam by several orders of magnitude while transforming its wavefront from one simple geometrical configuration into another.

No consideration has been given so far to any possible effect on the optical medium of the extremely high energy density possible with a high power ruby maser. The conventional electromagnetic formulas used in microwaves give $E = 4 \times 10^7$ volts/cm and $H = 10^7$ amp-turns/meter at the λ^2 focus spot. These calculations presuppose that μ_0 and ϵ_0 retain their customary values in vacuo. With such high field strengths, second order Stark effects may be of significance. The calculation of the action of second order Stark effects on the complex index of refraction has not been carried out as yet. We do not know therefore whether there will be a change in the complex index of refraction sufficiently large to affect seriously the propagation of coherent wavefronts. It should be emphasized here that in any case such nonlinear effects could play a significant role only in the region of the focused spot.

Other secondary effects can also be of importance in a beam with a high photon density. Even if the wavelength of the radiation lies in the region of low absorption of the refractive material, the carriers injected by the light into the conduction band may reach sufficient concentration to put the refractive material into a state comparable to that of metallic reflection. Two parameters will determine whether or not the density of carriers in the conduction band will become sufficient to generate a condition characteristic of metallic reflection. They are the number of carriers injected into the conduction band and their lifetime. Such a process is similar to that which arises in the semiconductor light valve. In the latter case, however, the condition of metallic reflection is created not by a light beam but by a beam of electrons injecting carriers from the valence band into the conduction band.

References

1. T. H. Maiman, Nature **187,** 493 (1960).
2. M. Born and E. Wolf, *Principles of Optics* (Pergamon Press, London, England, 1959), p. 318.
3. A. Javan, W. R. Bennett, Jr., and D. R. Herriott, Phys. Rev. Letters **6,** 106 (1961).
4. J. E. Rosenthal, Bull. Am. Phys. Soc. II **6** (1), W6 (1961).
5. D. F. Nelson and R. J. Collins, J. Appl. Phys. **32,** 739 (1961).
6. E. S. Dayhoff, Bull. Am. Phys. Soc. II **6** (4), Q15 (supplementary paper) (1961).
7. J. E. Rosenthal, Bull. Am. Phys. Soc. II **6** (4), Q13 (1961).
8. M. Born and E. Wolf, loc. cit., p. 483.
9. W. Heitler, *Quantum Theory of Radiation* (Oxford Univ. Press, Oxford, England, 1954), 3rd ed., p. 65.
10. R. D. Haun, Jr., and R. C. Ohlmann, J. Opt. Soc. Am. **51,** 473 TB14 (1961).
11. A. G. Fox and T. Li, Bell System Tech. J. **40,** 453 (1961).
12. L. Lee and G. W. Farnell, J. Opt. Soc. Am. **51,** 273 (1961).
13. J. E. Rosenthal, Bull. Am. Phys. Soc. II **6** (3), U8 (1961).
14. M. Born and E. Wolf, loc. cit., pp. 39 and 614.
15. F. A. Jenkins and H. E. White, *Fundamentals of Optics* (McGraw-Hill, New York, 1957), 3rd ed., p. 513 ff.
16. J. A. Stratton, *Electromagnetic Theory* (McGraw-Hill, New York, 1941), 1st ed., p. 440.

OSA Group Flight to ICO Munich Meeting August—see page A22 for application blank.

High Efficiency Optical Maser Parameters

Stanley J. Sage

A study is made of the characteristics of an optical maser system to optimize available parameters other than the maser material itself. As each parameter is optimized a major reduction in threshold level is realized. Finally, a very lightweight optical maser unit is built and tested.

Introduction

Since the first successful demonstration of an optical maser by Maiman, the major efforts in development have proceeded toward two important goals: obtaining higher power and/or obtaining more continuous operation.

Because the development of a useful laser for applications outside a laboratory would require more efficient operation, that is, a major improvement in the ratio of output power to input power, significant effort has been expended in improving this ratio.

The development of more efficient optical maser materials has been one important approach to this problem. But in addition there are several other parameters where optimization provides important gains. These include:

(1) Improvement of the efficiency with which usable pumping energy is generated.

(2) Improvement of the resonant cavity characteristics to provide maximum utilization of the fluorescent emission to produce stimulated emission.

(3) Consideration of the characteristics of the maser material itself, to maximize the absorption of the pumping energy available to the maser.

Ruby was chosen as the material for the present study since it is readily available in the form of high quality maser crystals with relatively few flaws and a high degree of uniformity for all parameters. But many of the results reported here do not depend on the material selected and hence can be applied to improve the characteristics of any optical maser system.

I. Pumping Energy Efficiency

To provide pumping energy for systems where a short flash of power is desired, the use of xenon flash lamps now provides the best available source of power. These are presently available in either helical form, or in the form of cylindrical tubes with various electrode configurations.

The use of a helical lamp makes possible a source of high power but the amount of energy actually available to the maser crystal is relatively low, because of the inability to concentrate the energy of the lamp on the crystal effectively.

The use of cylindrical lamps provides a method for mounting the lamps in close proximity to the crystal. Edgerton and Miles recently reported the use of a number of cylindrical lamps mounted around a crystal, with this assembly in turn surrounded by a small diameter highly-reflecting chamber such as a cylinder of aluminum foil.[1] This provides a system in which a far greater percentage of the lamp energy is made available for pumping use. The threshold level immediately approaches 300 joules for a room temperature ruby crystal, compared with roughly 3000 joules for the threshold using a high power helical flash lamp at the same crystal temperature. A new series of relatively high power (100–200 watt sec) lamps has appeared on the market suitable for use in such a multiple bulb configuration. For our work we have used the Edgerton, Germeshausen, and Grier X-100 lamp which is U-shaped, and has about 6 cm active lamp length, with the electrodes mounted in the arms of the U.

Working with these lamps we found a significant difference (about 20% or more) in the effective threshold level for a given crystal depending on the number of lamps used, the value of the condenser bank storage capacity utilized, and the value of inductance present in the system.

In practice the actual lamp resistance varies widely during the period of a flash, but in an effort to gain an understanding of the principles involved, the standard equivalent circuit was utilized consisting of a series

The author is with Trident Corporation, a d.vision of Maser Optics, Inc., 89 Brighton Ave., Boston 34, Mass.

Received 18 July 1961.

L, C, R circuit with constant values to describe the time dependence of the energy dissipated in the lamp. In this equation the envelope of the power varies as the exponential of Rt/L; the damping characteristic depends on $[(R^2/4L^2) - 1/LC]^{1/2}$. The critical damping resistance R_c varies according to $R_c^2 = 4L/C$. In our particular case, $L = 368\ \mu h$; C was available in multiples of 25 μf. The lamps were always operated in series to prevent the possibility of all the power being dissipated in one lamp, so R, the average lamp resistance, could also be varied in incremental steps.

For one lamp operating, the energy in the capacitor bank $(CV^2/2)$ required to reach threshold was found to be a minimum for $C = 300\ \mu f$ so $R_{c1}^2 = 4 \times 368/300 = 4.9$, and $R_{c1}^2 = 2.21$.

For two lamps operating, the energy in the capacitor bank was least for $C = 75\ \mu f$

$$R_{c2}^2 = 4 \times 368/75 = 19.6 = 3.998 \times R_{c1}^2$$
$$R_{c2} = 2(2.21).$$

These experiments indicated that the effective resistance of a lamp was 2.21 ohms and it appeared empirically that the critical damping condition produced the optimum efficiency. Some slight reduction in threshold value was observed as the number of lamps was increased and the value of capacitance decreased in accordance with the relationship $C = 4L/n^2R_0^2$, where n is the number of lamps and $R_0^2 = 4.9 \approx 5$.

On this basis, if three lamps are used in series, $C = 4 \times 368/9 \times 4.9 = 33.3\ \mu f$. To verify this, 3 lamps were utilized using 25, 50, and 75 μf and the mimimum energy required for threshold was found to occur between 25 and 50 μf, as predicted.

For reasons discussed in Section III below, two lamps appear to be the optimum number, and a determination was made of the variation in threshold as the value of capacitance was varied from the optimum. In general, where weight is the critical parameter it has proved effective to increase the lamp resistance, i.e., the number of lamps, and reduce the value of the capacitor bank accordingly. These lamps have a minimum reliable firing voltage. Because they are in series, the minimum reliable firing voltage for n lamps $= nV_{min}$. But the value of capacitance required for critical damping varies as $1/R^2$. The minimum energy available for one lamp is

$$E_{min} = (V_{min})^2C_c/2$$

where C_c is the critical damping capacitance.

For n lamps this becomes

$$E_{min} = (nV_{min})^2C_c/2r^2 = (V_{min})^2C_c/2.$$

Hence the effective conditions remain about the same over a large range of values.

Unfortunately, low resistance inductors in the range of 0.1 to 1 mh were not readily available, and the study of the change in the envelope characteristic dependent on nRt/L was somewhat more limited. One test was made with $L = 0.125$ mh. At this level, the effective inductance of the lamp becomes important and the expected critical damping does not occur. All measurements reported here were performed with time-constant multiples of $\tau = L/R = 125\ \mu sec$.

Time study photos indicate that coherent output starts about 250 μsec after initiation of the pulse. As the power rate of the coherent output increases, relatively small spikes are observed. The spikes during this period appear to be modulation of an envelope. When the coherent energy power rate reaches its maximum the oscillations grow larger and then appear to be damped as the lamp power reaches a minimum. In one experiment, the lamp circuit was run highly under-damped so that the fluorescent output reached a minimum at about 350 μsec, which was followed by a secondary peak about $^1/_6$ the height of the initial peak at about 500 μsec. Coherent output was observed during both pulses. There was an initial delay of about 250 μsec, which corresponds in time to the negative slope of the first pulse.

The output followed the previously reported pattern of spikes until about 350 μsec, at which point coherent output ceased. However at about 500 μsec—the peak of the secondary pulse—coherent output started again and ran the usual pattern.

Interpretation, based on evaluation using the mathematics in Section II, indicates that the coherent output oscillates in accord with the G of the system.

The G of the system will depend on the difference in the number of atoms in the upper level of the fluorescent line and the number in the lower level. For the case of ruby this lower level is the ground state. The number in the upper level will depend on the integrated energy absorbed and emitted by the crystal from the start of the pulse. The number in the lower level will depend on this integrated number, but, in addition, will depend on the instantaneous power level. This will be true since the distribution of atoms between the ground state and the permitted upper levels will vary in accord with the instantaneous value of the pumping power. Hence the difference between the upper and lower fluorescent levels will depend on the instantaneous power as well as the integrated energy. This means that as the power rate is increasing, the inversion population may actually increase during coherent emission so that the coherent output duration will depend on the flatness of the surfaces. During a time period where the power rate is decreasing, the increase of atoms into the ground state will produce an increase in the lamp power utilized. This in turn will increase the rate of atoms moving into upper permitted states, and the flow of atoms into the upper fluorescent state. Hence the coherent output will increase, until the maximum coupling between lamp power and the maser is obtained.

This point will occur rapidly if the lamp power rate is decreasing; hence the coherent output will increase rapidly, until complete saturation of the pumping rate is reached. At this point the inversion population will start to decrease, and the coherent output will decrease. If all this happens very rapidly, and the time constants involved in the energy states imply that it will, a spike of energy will result when coherent emission occurs at a time when the lamp power rate is decreasing, at least in the case of ruby.

The observed spikes, therefore, may be considered to represent the oscillation of an underdamped servo, hunting for a stabilization point where the average depopulation rate matches the average inversion rate.

Schawlow has recently stated, "They (the spikes) can be eliminated by reducing the effective reflectivity of the end plates."[2] But, as indicated in Section II, such a technique will radically decrease the efficiency of the system. It seems that a more effective technique would be to control the power input to match a desired output level.

The continuous output infrared device using He–Ne reported by Javan does this. By maintaining a steady value of pumping power at a selected point above threshold, the G of the system is controlled and hence the output level is maintained. For the high efficiency ruby device reported here, the energy level required to extend the operation from 500 μsec to about 0.01 sec seems quite feasible, since useful coherent output occurs only a few percent above threshold.

Our present studies include theoretical and experimental analysis of the interaction between the input power rate and the characteristics of the maser cavity. Additional results will be reported in a later paper.

II. Resonant Cavity Effects

The design of a resonant cavity at optical wavelengths consists primarily of determining the optimum characteristics of a pair of highly reflecting plane-parallel surfaces, separated by a spacer. The characteristics of such a cavity with a passive medium in the spacer were first reported in the last century, and have become well-known, and well understood, in the form of the Fabry-Perot interferometer.[3]

The resonant cavity required for optical maser operation differs from the interferometer primarily in the fact that the passive medium is replaced by an active medium capable of re-enforcing and amplifying the electromagnetic field developed in the cavity.

The standard Fabry-Perot equation for a passive spacer is

$$\frac{I_T}{I_0} = \frac{T}{(1-R)^2} \frac{1}{1 + [4R/(1-R)^2] \sin^2 \pi x}$$

where

I_T = transmitted intensity,
I_0 = incident intensity,
R = reflectivity of the reflecting layer,
T = transmissivity of the reflecting layer,
T and R are defined by $T + R + A = 1$,
A = absorptivity of the reflecting layer,
x = phase change per unit length. It depends on optical path length and angle between the ray and the normal to the reflecting surface.

This equation, however, assumes perfect plane-parallel end-walls, and no absorption in the spacer layer. If these factors are included, the equation[4] becomes

$$\frac{I_T}{I_0} = \frac{T^2(e^{-a})}{(1-Re^{-a})^2} \frac{(1-R^m e^{-ma})^2 + 4R^m e^{-ma} \sin^2 \pi m x}{1 + [4R(e^{-a})/(1-Re^{-a})^2] \sin^2 \pi x}$$

where a represents the loss per pass due to absorption in the medium and m is the number of passes made.

From this equation, the equation for optical maser action can be deduced readily.

In the equation above, the term T^2 indicates the fact that the light passes through one reflecting film when entering the cavity and through the second reflecting film when leaving the cavity. Light generated within the cavity, however, need traverse only one reflecting film so that the value T^2 must be replaced by T, the transmissivity at the output end of the cavity. The value R actually represents $(R_1R_2)^{1/2}$, the geometric mean of reflectivities from the reflecting films at the two ends of the cavity. Furthermore, the value e^{-a}, representing the amount of light absorption per traverse, becomes e^{-a+b} where b indicates the increase per pass resulting from stimulated emission. The net gain per pass will then be $R\ (e^{b-a})$, which we shall indicate as (G).

Finally then, the general equation for the intensity at one point on the end of the cavity becomes

$$\frac{I_T}{I_0} = \frac{T}{R} = \frac{(G)}{(G-1)^2} \frac{(G^m-1)^2 + 4G^m \sin^2 \pi m x}{1 + [4(G)/(G-1)^2] \sin^2 \pi x}$$

This leaves the problem of establishing a suitable value for m.

One technique for estimating a limiting value for m is to assume the presence of local variations in refractive index or surface flatness which produce local optical path variations of magnitude λ/ρ. In this case $x = N + 1/\rho$, where N is a very large number. We choose the condition such that $m\pi/\rho = \pi/2$, or $m = \rho/2$.

At this point $\sin^2 \pi m x = \sin^2(\pi m N + \pi m/\rho)$ becomes $\cos^2 \pi \rho N/2$, representing a point after which succeeding waves are out of phase and start to subtract.

At the wavelength of maximum output $\sin \pi x \to 0$; hence for a direction normal to the reflecting surfaces

$$\frac{I_T}{I_0} \to \frac{TG}{R(G-1)^2} [(G^m-1)^2 + 4G^m] = \frac{TG}{R(G-1)^2} (G^m+1)^2.$$

Analysis shows that for $G \gg 1$ the contributions from the trigometric functions dependent on phase become negligible and the equation for any value of x resembles the equation above for the wavelength of maximum output, so that at high gain (for ruby, approaching 100% inversion) the whole system provides an output. At low gains where $G = 1 + g$, a number slightly greater than one, the value of m which is a measure of the local variations in optical path length becomes important. For those spots where the optical path approaches perfection, λ/ρ becomes small, and $m = \rho/2$ becomes large. One would predict, therefore, that, at low powers, just above threshold there would be a number of small bright emitting areas for a crystal with imperfections, and at high gain the whole surface would emit.

Since this corresponds to the actual experimental evidence, it provided an initial verification of the validity of the equation.

In addition, this equation may be interpreted as a description of the characteristics of the field amplitudes of the system during that brief period of time when amplification by stimulated emission has just become possible up to the point where coherent output is attained.

Let us first consider a point where $G = 1 - T$. Since $G < 1$ oscillation does not occur. Instead the signal is damped, and for large m, $G^m \to 0$.

$$\frac{I_T}{I_0} = \frac{T(1-T)}{RT^2} = \frac{1-T}{RT}.$$

The signal strength at this point is strongly dependent on T. Let us consider the case of a crystal with silver coated ends. At the output end $T_0 \approx 0.04$, $R_0 = 0.92$. At the reflecting end $T_1 = 0$, $R_1 \approx 0.98$; hence in our equation $T = 0.04$, $R = 0.95$.

$$I_T/I_0 = 25.$$

The amplitude of the field within such a crystal will be proportional to $1/T = 25$.

If we instead coat the crystal with multilayer dielectric films with 98.8% reflectivity, 0.01% T at either end, $I_T/I_0 = 100$, and the field will also be proportional to 100. Hence even before coherent amplification occurs, and in fact even before stimulated emission occurs, a multilayer reflector with low loss will provide a far greater stimulating electric field than a silver coated crystal.

The critical point in the equation above occurs when $G = 1$. This critical value will depend strongly on the characteristics of the reflecting films, i.e., on the loss term in the cavity. e^b depends on the inversion; at $G = 1$, $e^b = e^a/R$, $b \approx a + 1 - R$, so that the critical value for coherent output will depend strongly on R. As b grows larger $I_T/I_0 \to TG^{(2m-1)}$ and the output intensity will again depend strongly on the choice of reflecting materials.

Since a very rapid increase in output tends to deplete the inversion population, the maximum value for m can in some cases be limited by the number of atoms available, and by the instantaneous power rate discussed in Section I.

An additional factor of interest may be derived from the equation of the angular spread of the beam.

As noted earlier, under the conditions for maximum output from the cavity, which occurs in a direction parallel to the long axis of the cavity, the magnitude of the signal reaches very large values. This results from the very strong "focusing" function implicit in a high efficiency cavity with a Q of several hundreds of thousands. If this characteristic is examined, it is found that the cavity has very strong preference for oscillations in preferred directions. The solid angle between cones of adjacent maxima and minima is nearly constant and proportional to $\beta^2 = 1/N$. This solid angle provides a measure of the energy in a single mode. If the cavity were not present, the energy density in each mode would be uniformly distributed across the solid angle and normal diffraction patterns would result. However with the cavity present, half of the energy density is concentrated in a solid angle proportional to $\alpha^2 = |1 - G|/\pi NG^{1/2} = \beta^2 |1 - G|/\pi G^{1/2}$. Hence, for $G > 1$, the case of interest, we write $\alpha^2/\beta^2 = (G - 1)/\pi G^{1/2}$.

This equation describes the dependence of degree of collimation on G. For low power flashes, where the maximum value of G is small, a high degree of collimation is to be expected. For high power shots, where G is large, a wider angular divergence will be observed.

Again this prediction has been experimentally verified.

Let us next relate the angular spread to the reflectivity of the films at the ends of the crystal. For $G = Re^{b-a} \approx 1 - p + \epsilon$ ($p = 1 - R$, $\epsilon = b - a$) the $\alpha^2/\beta^2 \approx \epsilon - p/\pi$. Since p is smaller for higher reflectivity films, the degree of collimation will be higher by an appreciable amount for a crystal coated with higher efficiency reflectors. A high reflectivity multilayer coated crystal is predicted to have better collimation and higher output than the silver coated crystal under any conditions, but a limit will be reached dependent on the absorption and scattering in the crystal.

The maximum value for α^2 which is consistent with activation of a single mode occurs when $2\alpha^2 = \beta^2 = 1/N$. This provides a maximum value of G, consistent with activation of a single mode of 11.85.

For a ruby crystal 5 cm long, $N = 127{,}000$.

For the main mode, therefore, the maximum angular spread predicted is $\beta = 1/(127{,}000)^{1/2}$ rad $= 1/356$ rad. At a distance of 2.75 meters we should then expect to find a bright spot with a diameter varying from that of the emitting areas to a diameter of $2\beta \times 2.75$ meters.

plus the diameter of the emitting areas as the power in the shot is increased.

The maximum value of $2\beta \times 2.75$ meters corresponds to 1.54 cm, at $G = 11.85$. Photographs of the pattern from the crystal on a screen at 2.75 meters indicate a central bright spot of just about 1.5 cm diameter for high power shots using a flawed crystal which showed several small emitting areas at low power.

For more perfect crystals, this central spot size increases to about 2.2 cm, corresponding to emission from the whole area (0.64 cm) (i.e., 0.64 + 1.54 = 2.18 cm).

A little intuitive thought indicates that since the amplification characteristics will depend on the amplitude and direction of the stimulating field, the crystal will produce coherent output threshold values and collimations corresponding to the conditions at the point where G passes through 1.

We might guess then that a high efficiency cavity would be able to deliver high intensity, highly collimated coherent energy outputs at relatively low levels of stimulation.

Based on these predictions a number of crystals were prepared to compare the actual results obtained with films of different reflectivities.

In the following data, the energy level noted is joules in the capacitor bank, i.e., energy $= V^2C/2$. The criterion used for evaluation was the minimum energy level at which the emitted light formed a visible circle less than 1.2 cm diameter on a screen at 2.75 meters. This corresponds to about 15′ of angular divergence.

Crystal A was a ruby rod 0° orientation, 5 cm long, 6 mm diam, flatness 1 wavelength.

Crystal B was a ruby rod 0° orientation, 4.5 cm long, 6 mm diam, flatness $\lambda/10$.

Both were fine ground on the cylindrical surface.

A	$R_0 = 0.988$	$R_1 = 0.988$
B	$R_0 = 0.91$	$R_1 = 0.988$
B	$R_0 = 0.962$	$R_1 = 0.988$

A	$E_{min} = 220$ watt sec	$R = 0.988$
B	$E_{min} = 385$ watt sec	$R = 0.95$
B	$E_{min} = 210$ watt sec	$R_t = 0.975$

If we set $E_1/(1 - R_1 + k) = E_2/(1 - R_2 + k)$ where $E_1 = 385$, $R_1 = 0.95$, $E_2 = 210$, and $R_2 = 0.975$, we find k the loss factor is 0.005. This value of 0.5% represents a negligible loss resulting from diffraction and scattering. The mathematics indicate that since the "focusing" amplitude and gain depend on reflectivity, it is important to measure the loss factor in the range of R to be used. For low reflectivities (30–60%), the loss factor will be many times larger, approaching the free space scattering loss value of 25% reported[4] by Collins[5] and calculated by Fox and Li, but this does not apply to the high efficiency case.

In addition, photos were taken of the spot of light on the screen at 2.75 meters. Using crystal A, just above E_{min}, the pattern observed was a number of small spots about 1.5 mm in diameter scattered in an area about 6.5 mm wide. The spots on the screen have been interpreted as Fresnel diffraction patterns resulting from highly collimated beams originating from bright emitting spots on the surface of the crystal. Since the sizes of these spots on the crystal surface are about 1.25 mm, the corresponding angular divergence was less than 1 minute of arc.

We believe that this is the first reported case where it was possible to resolve the filamentary output using a camera focused on a screen at 3 meters.

With the system operated at maximum energy available (about 400 watt sec per pulse) the pattern observed filled about 2.5 cm circle at 2.75 cm, indicating the presence of two active modes, and a value for G in the equation relating to angular field greater than 12.

An additional experiment consisted of sending the output from the crystal into another uncoated ruby crystal which was optically pumped at the same time. This resulted in the amplification of the coherent signal and corresponded approximately to amplification expected from the equation for $R = (1.75 - 1/1.75 + 1)^2 \approx 7.5\%$. For this case, $G < 1$ unless $e^{b-a} > 133$ and since the light which is to be amplified must pass through both reflecting boundaries, the equation for the amplified output becomes $I_T/I_0 = T^2G/R(1 - G)^2$.* A number of configurations to optimize maser amplification are presently under study.

III. Optical Maser Material Characteristics

The third main area in which significant improvement was obtained was in optimizing the characteristics of the material itself.

It was found first that the use of polished sides, as opposed to fine ground sides, would increase the efficiency of the system by an appreciable extent. This occurs because the polished sides tend to cause multiple reflections, so an increase is observed analogous to the gain seen by using an integrating sphere.

Using a z-cut (0° cut) crystal 45 mm long, 6 mm in diameter, with multilayer reflectors, improvements in efficiency up to 40% were obtained, simply by polishing the sides.

Ruby provides an additional technique for improving efficiency not necessarily available with other materials, viz., use of its anisotropy. The crystal has different properties of absorption and emission in mutually perpendicular planes of polarization.

In corundum, the anisotropic properties depend on the fact that the Al atoms are asymmetrically disposed

* For the maximum power utilized $I_T/I_0 = 2$. Hence $G = 0.825$, or $e^{b-a} = 1.10$.

with respect to the oxygen atoms. Al_2O_3 has no visible absorption spectrum, but when the aluminum atoms are replaced by chromium atoms with absorption bands in the visible, anisotropic absorptivity results.

When a 0°, or z-cut crystal, is used, the axis of maximum absorption lies along the length of the crystal and hence to obtain a high inversion population it is necessary to provide illumination of high brightness along the whole periphery of the cylinder. Of this energy only light polarized with its electric vector normal to the long axis of the crystal is strongly absorbed. This effect is very apparent if a z-cut crystal with polished sides is placed in a polarized light beam. For light polarized with the electric vector parallel to the optic axis, the transmitted light is just slightly pink. For light polarized with its electric vector normal to the optic axis, the transmitted light is a deep blue-red (purple) color, indicating that most of the green and green-blue is absorbed. If however the crystal is used in a 90° (x-axis) cut, the observed effect is altered.

For an x-cut crystal, the optic axis lies in a plane normal to the long axis of the crystal. Hence, as the crystal is rotated around its long axis, the same change in color is observed *without* polarizers. For light passing through the crystal normal to the optic axis, the crystal appears to be purple in color, independent of polarization. For light passing through the crystal in a plane perpendicular to the optic axis, the crystal itself divides the light into two orthogonal components, one of which is strongly absorbed.

As stated in Section I, we found that two or three cylindrical lamps placed in close contact with the cylindrical surface of the crystal produced higher efficiency than a helical lamp. With a polished x-cut crystal, we found that we could place two such lamps on opposite sides of the crystal, and when lined up with the highly absorbing axis of the crystal an additional factor of 40% improvement was obtained. This reduces the power requirement from about 200 watt sec to 130 watt sec.

In addition, in this orientation, the heating effect was greatly reduced. As noted previously in the literature,[6] the threshold level increases with temperature and hence increases on successive repeated flashes as the crystal heats. For three z-cut crystals tested at about 240 watt sec, the average increase was about 10 joules per flash. For two x-cut crystals tested at 135 watt sec the increase averaged only $^1/_2$ joule per flash.

We found that minimum requirement for full laser operation for room temperature operation (20°C) was 128 joules. The voltage was set to provide 135 watt sec per flash. The crystal was flashed at 15 sec intervals, and on the thirteenth flash the small spot produced on the screen approached the size and intensity level of the original 128 joule flash.

The orientation of the absorbing axis with respect to the axis defined by the two lamps was important as the theory above would indicate; 20% to 30% increases in energy were required for rotations of the axis by 45° from the optimum setting.

It is interesting to note that the observed relative efficiency of x-cut or z-cut crystals will depend on the geometry of the pumping system. In a system such as the elliptical cylinder reported by Raytheon, the most efficiently focused light occurs perpendicular to the long axis of the crystal and over its whole length. For this pumping configuration a z-cut crystal should prove most efficient, since the absorbing characteristics of the crystal are optimized for the directions of maximum illumination.

For the 0° offset system proposed by Edgerton,[1] where the strongest illumination occurs in lines along the side of the crystal, the x-cut orientation will provide maximum efficiency.

Utilization of the crystal characteristics to optimize the pumping coupling efficiency between lamps and maser will, in general, prove to have important advantages.

IV. Summary

Tests were made using the techniques described above for improving the efficiency of the crystal. Within the limits available, the parameters were varied and photographs of the spot and oscillographic records of the time patterns were observed.

As each parameter was optimized a significant improvement was observed. As a result of these experiments a miniature optical maser was constructed for demonstration purposes. The unit, weighing about 30 kg, included voltage source, condenser bank, laser head, and carrying case.

This small device, with a maximum energy storage capacity of about 200 joules, has a minimum operating level around 120–130 joules. It is capable of firing a number of shots in sequence, limited only by the charging time of the capacitor bank. It will deliver up to 0.2 joules of coherent energy into a 2.5 cm circle at 3 meters.

The small size and high efficiency of this unit seem to provide experimental verification of the conclusions of the present study.

Starting with the efficient techniques specified here it seems straightforward, by the use of larger units, to build up to a high energy device of high efficiency or, by extending the pulse length, to provide longer flashes, for potential use in communication.

We plan next to study the use of a delay line for producing an extended square-pulse of energy preceded by a sharp initiating pulse. The use of an optical feedback mechanism to couple the input to the output is also within the realm of possibility.

It appears that a great amount of work is yet to be

done in understanding and utilizing the properties of coherent amplification in ruby at optical frequencies. Our plans include the development of small, high power systems, development of systems with controlled output characteristics (pulse duration and pulse height), and development of efficient multiple stage optical maser amplifiers. Developments in these areas will be reported in subsequent papers.

The author wishes to thank Dr. Perry Miles of M.I.T. for his interest and counsel in this work, and for providing invaluable aid in helping to relate the optical description of maser action reported here to the basic quantum stage physics and microwave analogies implied. However, the author takes full responsibility for all statements made.

References

1. H. E. Edgerton and P. A. Miles, "Optically efficient ruby laser pump," J. Appl. Phys. **32**, 740 (1961).
2. A. L. Schawlow, "Infrared and optical masers," Solid State J. **2**, 27 (1961).
3. See, for example, Max Born and Emil Wolf, *Principles of Optics* (Pergamon Press, New York, 1959), p. 322 ff.
4. Antonio Quesada, unpublished paper, Baird Atomic, Cambridge, Mass.
5. Paper delivered by R. J. Collins, Pittsburgh Meeting, OSA, Spring, 1961.
6. I. D. Abella and H. Z. Cummins, "Thermal tuning of ruby optical maser," J. Appl. Phys. **32**, 1176 (1961).

Applied Optics

Letters to the Editor

Letters to the Editor should be addressed to the Editor, APPLIED OPTICS, 1155 16th St., N.W., Washington 6, D.C.

More Complete Description for α/ϵ

Lucien M. Biberman

University of Chicago, Laboratories for Applied Sciences, Chicago 37, Ill.
Received 1 December 1961.

A surface property of some interest in space applications is the ratio of radiant power absorbed from solar irradiation by the surface to the power radiated to space by that surface at a given temperature.

Of late, there has been a tendency to refer to this property as

$$\frac{\text{solar absorptivity}}{\text{thermal emissivity}} = \frac{\alpha}{\epsilon}$$

and gross estimates of its value are made with the help of various arbitrary assumptions concerning temperatures and wavelength intervals.

The purpose of this letter is to propose a method for the definition and specification of this important property in a manner independent of qualitative interpretations of the terms "solar absorptivity" and "thermal emissivity."

One* criterion of surface effectiveness in maintaining a desirable heat balance is the ratio of power absorbed from solar radiation to the power radiated into space by the surface.

In free space this ratio can be approximated well by

$$\frac{\int_0^\infty \alpha(\lambda) H_s(\lambda) d\lambda}{\int_0^\infty W(\lambda,T) d\lambda}$$

or

$$\frac{\int_0^\infty \alpha(\lambda) H_s(\lambda) d\lambda}{\int_0^\infty \epsilon(\lambda) W_0(\lambda,T) d\lambda}$$

where

α = radiant absorption
H_s = solar irradiance
ϵ = radiant emissivity
W = radiant emittance of the surface
W_0 = radiant emittance of a blackbody
λ = wavelength
T = temperature

α and ϵ are numerically equivalent by definition, being the ratio of total energy radiated (or absorbed) by a given surface to that radiated (or absorbed) by a blackbody of equal area and temperature.

The radiation balance at a surface is associated with the characteristics of the surface and its absorption of the solar irradiance (with a spectral distribution related to solar temperatures) and re-radiation of power with a spectral distribution characteristic of the surface temperature and its emissivity.

Since the distribution of solar energy is fixed, and within limits the temperature of the satellite is also fixed, the control of the ratio of absorbed to radiated power is almost solely a function of the spectral radiant emissivity (or absorption) of the surface in the wave length regions about the peak of the solar curve to that in the region of the blackbody peak associated with the temperature of the space vehicle surface.

The quantities α and ϵ are often evaluated as a function of wavelength by measuring the spectral reflectances of the surface in question and simply computing the values of $\alpha_\lambda(\lambda)$ or $\epsilon_\lambda(\lambda)$ at various values of λ.

* D. Goetze, Space Aeronautics, July 1961.

Since for an opaque surface at any specified wavelength the numerical values of α and ϵ are identical, the ratio of α/ϵ without further specification gives little if any information. It would appear, therefore, that the ratio α/ϵ is a very incomplete description of the radiant properties of the surface. The surface radiant properties may be much more completely described by indicating a plot of ϵ vs λ and/or α vs λ as well as specification of the values of

$$\frac{\int_{\lambda_1}^{\lambda_2} \alpha(\lambda) H_s(\lambda) d\lambda}{\int_{\lambda_3}^{\lambda_4} \epsilon(\lambda) W(\lambda, T) d\lambda}$$

or the ratio of the two in those clearly specified wavelength regions associated with the peaks of the two radiant power distributions.

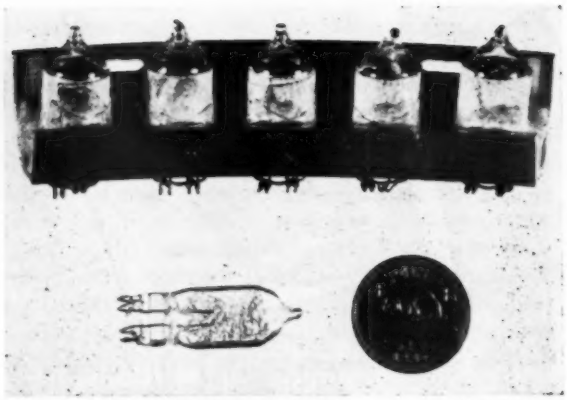

Fig. 1. AG-1 flashbulbs potted in nose cone mounting channel sector. Bulbs contain zirconium wool in an atmosphere of oxygen.

The Visibility of Flashbulbs and Their Application to Rocket Tracking

G. B. Spindler

Canadian Armament Research and Development Establishment, Valcartier, Quebec.

Received 13 November 1961.

Conventional photographic flashbulbs mounted on the base of a sounding rocket nose cone have been used successfully for visual tracking, and for determining cone trajectory from parallactic photographs of the flashes. Flash positions were determined* to ±0.3 km at a slant range of 110 km using a technique described elsewhere[1] for measuring auroral altitudes. Programming of a digital computer at CARDE to determine cone trajectories from reduced photographs is presently underway. Although originally intended only as a visual tracking aid for ground instrumentation operators, the flashbulb system has proven sufficiently reliable and accurate to serve in addition as a means of determining the trajectories of a series of chemical seeding rockets.

Forty AG-1 flashbulbs (Fig. 1) were ganged to produce 17 flashes at nominal 3-sec intervals, one bulb being fired at a time during the early part of the trajectory, and a maximum of four at a time when the cone was at a slant range of about 100 km. The apparent visual magnitude of a 4-bulb flash at 110 km is reckoned from microdensitometer traces of photographs (without taking account of the exact nose cone aspect at the time of the flash) to be between magnitudes zero and minus one.

Environmental tests carried out on the bulbs show them to be quite sturdy; they will fire after application of an acceleration of 60 g directed axially from tip to base of bulb, and at temperatures up to 270°C. The limiting accelerations and temperatures at which the bulbs fail to flash were not determined. In mounting the bulbs in close proximity in the nose cone, it was found necessary to cover most of the cylindrical surface of the bulb with metal foil to prevent the flashing of one bulb from spuriously igniting neighboring bulbs. The foil also served as a crude reflector.

The visibility of a short flash of luminous energy Q lu-sec at a slant range of R km is estimated as follows:

A scotopically-adapted observer under normally good viewing conditions can see a star of magnitude +6, corresponding to an illuminance at the cornea of 8.3×10^{-3} lu/km^2. The source flux L_T required to produce this threshold illuminance is $L_T = (4\pi R^2) \times 8.3 \times 10^{-3} = 0.1R^2$ lu, approximately, assuming the source radiates uniformly in all directions. For light pulses shorter than the retinal action time of about 100 msec (flash duration at half-peak is 20 msec) the eye integrates incoming flux, the retinal response being proportional to the luminous energy of the pulse[2] rather than the power. This considered, the threshold energy Q_T becomes $Q_T = 0.01R^2$ lu-sec.

If one assumes 200 km to be the maximum slant range attained during the flight of a typical sounding rocket, Q_T is 400 lu-sec. The smallest commercial flashbulbs (type AG-1) provide a flash of Q = 17,000 lu-sec (7000 for photopic adaptation), or about four stellar magnitudes brighter than the liminal Q_T for this range. In a more specific case—that of a rocket flight last fall—a 4-bulb flash occurred at a range of 110 km, for which Q_T = 121 lu-sec and Q/Q_T = 561, seven magnitudes brighter than the +6 limit. This estimate is borne out by the measured photographic image densities mentioned previously, which indicated a visual magnitude between zero and minus one.

Visibility calculations may be extended to include xenon discharge tube sources by assuming a scotopic luminous conversion efficiency[3] of 100 lu/electrical watt (i.e., 100 lu-sec/joule). The threshold energy input for a xenon discharge tube radiating uniformly in all directions becomes $U_T = (10^{-4})(R^2)$ joules, or 4 joules for the 200-km range. For comparison, a tube input of 170 joules would produce a flash of the same luminance as one AG-1 bulb.

No account is taken here of the effect of meteorological conditions[4] or of bulb reflectors on the visibility of the flashes. Suitable reflectors can increase on-axis flux several fold at the expense, of course, of decreasing the probability of an off-axis sighting of the bulb. To offset the R^2 fall-off of luminance, bulbs may be ganged, or larger bulbs may be chosen from the current commercial selection of bulbs, which vary in output from 7000 to 100,000 lu-sec (photopic), although from the point of view of efficiency (in lu-sec per unit bulb volume) the smaller bulbs are the better choice.

The flashbulb tracking system has several advantages over conventional discharge tubes,[5] primarily those of simplicity, a facility for ganging to offset R^2 losses, and lower cost for a given light output. Contrarily, the system is at a disadvantage if a large number of flashes is needed, as the required bulb mounting area may become prohibitively large. Also, if the nose cone is not separated from the motor, other mounting positions (e.g., fin trailing edges) less desirable than the cone base would have to be used.

* By D. McEwan, Defence Research Northern Laboratories, Fort Churchill, Manitoba.

The bulbs appear to be well suited to special applications other than rocket tracking. For example, single small bulbs of the AG-1 or M5 miniature type could be seen without optical gain at satellite altitudes, and a single large bulb of output 10^5 lu-sec could be seen with a telescope of modest aperture (15 cm) at ranges beyond the lunar orbit.

References

1. D. J. McEwan and R. Montalbetti, Can. J. Phys. **36**, 1593 (1958).
2. L. Ronchi and G. Toraldo di Francia, J. Opt. Soc. Am. **47**, 639 (1957).
3. D. E. Hudson, *Scientific Uses of Earth Satellites* (edited by J. A. Van Allen, Univ. of Michigan Press, Ann Arbor, 1956), p. 39.
4. W. E. K. Middleton, *Vision Through the Atmosphere* (Univ. of Toronto Press, Toronto, 1958).
5. A. Finlay, R. E. DeMuth, and W. D. Hall, "Tracking missiles at night by light flashes," Electronics **33**, 88 (1960).

A Continuously Operating Ruby Optical Maser

D. F. Nelson and W. S. Boyle

Bell Telephone Laboratories, Murray Hill, New Jersey.

Received 16 January 1962.

We would like to report the attainment of continuous operation of a ruby optical maser using an entirely new optical pumping arrangement. Experimental data on the nature of the output will be presented.

The first observations of maser action in crystals[1,2] were made on a pulsed basis using helical xenon flash lamps contained with a ruby crystal in a diffusely reflecting pump cavity. Continuously operating infrared masers[3,4] have been reported, one using a gaseous, the other a crystalline medium. The latter uses a specularly reflecting cylindrical ellipse to focus the light from a linear mercury arc lamp onto the sides of a rod of $CaWO_4:Nd^{3+}$. The pumping geometry that we have used in the present experiment on ruby ($Al_2O_3:Cr^{3+}$) consists of a short-arc high-pressure mercury lamp imaged upon the large end of a trumpet-shaped crystal, immersed in liquid nitrogen (Fig. 1a). This maser oscillates in the visible at 6934 A.

Fulfillment of the Schawlow-Townes criterion[5] for optical maser action requires the attainment of a critical intensity of pump radiation in the maser crystal. This intensity can be found from the following rate equation which relates the steady state population densities of the two ground state levels (n_1 and n_2) and the two metastable levels (n_3 and n_4). The effect of the pump is assumed to populate only the metastable levels, which are in thermal equilibrium with each other. For continuous pumping

$$\overline{I\sigma}\,(n_1 + n_2) = \frac{n_3 + n_4}{\tau} \tag{1}$$

where $\overline{I\sigma}$ (in photons per second) is the integral over wavelength of the product of the spectral intensity of the pump in the crystal and the cross section for absorption, and τ is the observed decay time from the metastable levels. This equation describes only the approach to the maser threshold since the stimulated emission term is neglected.

If $\Delta n = n_3 - n_2$ is the excess population required in the upper state in order to have maser action, then it can be shown that the pumping intensity must satisfy

$$\overline{I\sigma}\,\tau > \frac{(1+f)(1+2\Delta n/n_0)}{1+3f-(1+f)(1+2\Delta n/n_0)} \tag{2}$$

where $n_0 = n_1 + n_2 + n_3 + n_4$, $f = n_3/n_4 = \exp[(E_4 - E_3)/kT]$ and $n_1 = n_2$ (at our operating temperature). Thus the intensity of monochromatic pumping light at the peak of the green absorption band of ruby must be about 400 watts/cm^2 for the conditions of the present experiment. For white light considerably higher intensities are needed.

To obtain such intensities we use a short arc mercury lamp which is most effectively coupled to a narrow rod by imaging it on the rod end. This imaging is accomplished using two spherical mirrors each used at unit magnification but with one off-axis in a horizontal plane and the second off-axis in a vertical plane so that the astigmatism of the intermediate image of the arc is cancelled in the final image on the rod end.

The maser rod is trumpet-shaped having a shank of light pink ruby and a collecting cone made of sapphire. This cone is designed such that any ray entering the large end from the solid angle subtended by the spherical collecting mirror will be totally internally reflected at every encounter with the polished conical surface until it passes out of the small end of the cone. Thus the cone acts as a radiation condenser giving an intensity increase equal to the ratio of the end areas. Furthermore, the cone is terminated at such a point that all the rays leaving the small end of the cone will be totally internally reflected at every encounter with the polished sides of the ruby shank until they strike the mirror at the end of the cavity.

The dimensions of the cone are chosen consistent with

$$\frac{d}{D} = \frac{\sin\varphi + \tan\alpha\cos\varphi}{\sin\varphi_c} \tag{3}$$

where $\varphi = \sin^{-1}(\mu_2 \sin\theta/\mu_1)$ and $\varphi_c = \sin^{-1}(\mu_2/\mu_1)$ and the rest of the symbols are defined in Fig. 1(b). This formula is an approximate generalization of the Williamson formula.[6] It is most accurate for rays which intersect the cone axis and for small taper angles α.

The many reflections along the shank walls give the ray an absorption path length greater than the shank length. Since the pump intensity and the absorption length appear as a product, any increase in absorption length over the natural length is equivalent to an increase in pump intensity. After the rays reflect from the end mirror they proceed back up the ruby shank, internally reflecting from the walls once again. If only a small fraction of the intensity incident on the shank is absorbed while proceeding down and back, the double pass feature of this pump gives a factor of two in the effective pumping intensity. Thus the intensity at a given wavelength within the ruby shank is given by

$$I(\lambda) = 2\left(\frac{D}{d}\right)^2 \frac{\mu_1 \ln(\mu_1/\mu_2)}{\mu_1 - \mu_2}\,\Omega B(\lambda) R_M^2 T_G^4 T_S \tag{4}$$

where $B(\lambda)$ is the spectral brightness of the lamp, $2[\mu_1\ln(\mu_1/\mu_2)]/[\mu_1 - \mu_2]$ is an approximate expression for the average absorption length in the shank divided by the natural length of the shank, R_M is the reflectivity of a spherical collecting mirror, T_G the transmission of a glass surface of the dewar, and T_S the transmission of the sapphire surface. The latter includes the dielectric interface reflectivity and the reflectivity of the

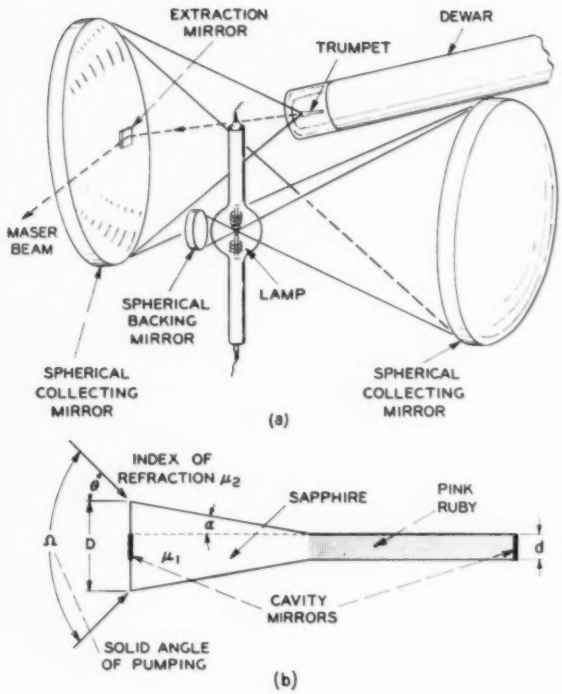

Fig. 1. (a) A schematic drawing which shows the geometrical arrangement of mirrors to image the arc lamp upon the end of the trumpet-shaped maser rod. (b) An enlarged view of the ruby-sapphire trumpet.

small cavity mirror on it.

The necessary lamp brightness can be found from (4) and (2). For a lamp emitting monochromatic light at the peak of the green band of ruby, a brightness of about 60 watts cm^{-2} $ster^{-2}$ is needed in the present geometry. For a high pressure mercury arc lamp about 400 watts cm^{-2} $ster^{-1}$ are needed in the wavelength region between 3500 A and 6000 A in spite of the fact that most of the visible mercury lines fall within the ruby absorption bands.

The attainment of the critical intensity in the rod guarantees sufficient absorption to attain an inverted population for a particular temperature. To maintain this temperature the trumpet must be designed so that the heat dissipation from the absorption process at this intensity level does not significantly heat the trumpet, that is, the trumpet surface must be capable of transferring this amount of heat to the coolant without breaking contact with it. Since the power dissipated is a volume effect and the transfer to the coolant a surface effect, the radius of the shank must be made small. The use of low concentration ruby aids this problem by reducing the total power absorbed. It also aids in realizing the factor of two in (4).

The trumpet used was cut parallel to the optic axis from a Linde disc boule such that its cone came from the 1.6 cm diameter sapphire seed and the shank from the adjoining light pink ruby which had 1.6×10^{18} Cr atoms cm^{-3}. The shank of the trumpet is 0.061 cm in diameter and 1.15 cm long while the cone has a large end diameter of 0.150 cm and a length of 1.05 cm. The entire side of the trumpet was given an optical polish. The end surfaces are parallel and flat to better than $1/10$ wavelength. Variations in the index of refraction as measured on the boule by an interferometer cause optical path differences of about $1/4$ wavelength. The latter effect plus the presence of colloidal size scattering centers in the crystal probably determine the cavity losses rather than the end reflectivity. The shank end of the trumpet is opaquely silvered while the cone end silver covering only the center 0.061 cm diameter area has a transmission of 0.05. The line width at 77°K for each of the components of the R_1 emission line is 0.2 cm^{-1}.

At threshold for this trumpet the shank must absorb about 0.3 watts from a mercury arc spectrum. Thus about 0.9 watts cm^{-2} of heat must transfer to the coolant, neglecting end effects. Liquid nitrogen at its normal boiling point can absorb almost ten times this amount before breaking contact with the rod. It is thus expected to be a satisfactory coolant and it was used in most of the experiments reported here. Liquid nitrogen a few degrees below its boiling point was also used.

The high pressure mercury-xenon lamp, designated 941B, was made especially for us by Hanovia. Its gap was made equal to the diameter of the large end of the trumpet cone. The lamp was operated on direct current. The arc light has less than 3%, 120 cps ripple. The spherical mirrors and the backing mirror collect all rays within a solid angle of 0.73 ster. The spherical collecting mirrors are used 15° off-axis. Because of reabsorption of the light by the arc, the backing mirror increases the light collection only about 50%.

Threshold for continuous maser operation was found when the 941B lamp was run at 850 watts. This is shown in Fig. 2(a) where the character of the maser output is shown for lamp powers of 1020, 930, 850 watts and lower values. The traces of Fig. 2(a), as well as longer ones obtained, have shown that there are no thermal time constants of the order of tenths of a second or longer which affect the level of the output. These traces were obtained when the trumpet was immersed in liquid nitrogen at its normal boiling point. The large width of the traces during maser action is due to noise in the maser output at frequencies between 10^2 and 10^6 cps. At an input of 930 watts the maser beam had a measured power of about 4 milliwatts. Considering that about 0.3 watt of green and violet light is absorbed to reach threshold, no more than about 16 milliwatts could be expected at this input power.

The maser power was emitted in a beam whose divergence was found to be about 0.7°, though the emission pattern was somewhat irregular. When stresses of the order of 10^3 dynes were applied transversely to the center of the shank, which is supported at each end, the emission pattern changed abruptly to less symmetric shapes. At larger stresses the output beam became so diffuse that it could not be seen or photographed with available filters in the presence of the pump light.

A striking feature of this maser at present is the continual presence of relaxation oscillations[2] in the output, shown in Fig. 2(b). This is true for operation near threshold and at 50% over threshold in lamp power. The oscillations are also present when the lamp is pulsed for a millisecond at 8 times the threshold power while also running continuously. Within this region the average height of the oscillations increases and their average spacing decreases. Using a fast sweep speed and a short detector time constant, the shape of the oscillations was found to be the same as that found for pulsed ruby optical masers.

The low frequency component of noise in the 10^2 to 10^3 cps region we believe to be due primarily to mechanical vibrations. This component of noise, as well as the relaxation oscillations, has been shown not to be due to coolant boiling (by using flowing liquid nitrogen below its boiling point) or to arc ripple. The instability giving rise to the relaxation oscillations is at present not understood.

In conclusion we would like to point out the adaptability of the trumpet geometry to solar pumping. Experiments are under way to explore this.

We would like to thank K. F. Rodgers for his technical assist-

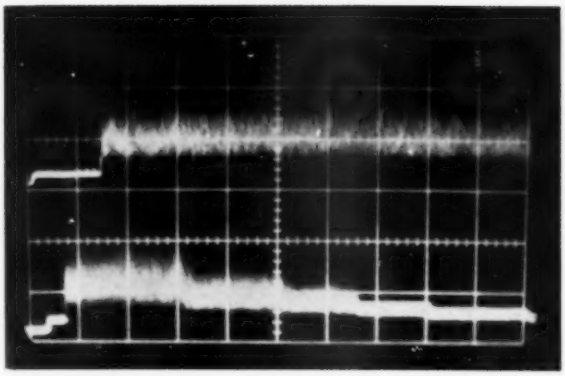

(a)

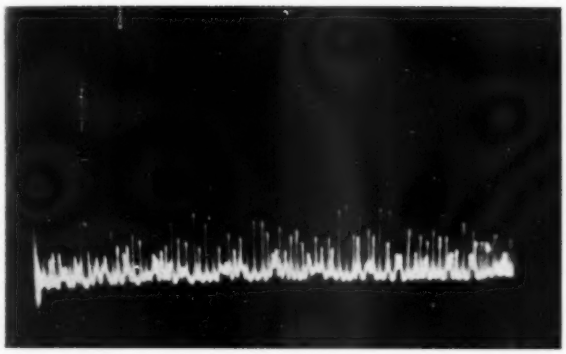

(b)

Fig. 2. (a) The maser output as measured at various power levels. The lower trace is taken at a sweep speed of 2 sec/div and the upper trace is delayed one second and expanded to 0.5 sec/div. In the lower trace the lamp power is decreased in steps of about 10% starting from 1020 watts until maser action ceases between the 6th and 7th divisions. (b) The continual high frequency relaxation oscillations in the maser output. The time scale is 50 μsec/div.

ance throughout these experiments, C. G. Bjorling for fabricating the trumpet, and C. G. B. Garrett, A. D. White, and D. R. Herriott for valuable discussions. We would also like to express our appreciation to the Hanovia Lamp Company and, in particular, to O. Lienhard for making the special lamps, and to the Linde Company for growing the special ruby-sapphire boule.

References

1. T. H. Maiman, Nature **187,** 493 (1960).
2. R. J. Collins, D. F. Nelson, A. L. Schawlow, W. Bond, C. G. B. Garrett, and W. Kaiser, Phys. Rev. Letters **5,** 303 (1960).
3. A. Javan, W. R. Bennett, Jr., and D. R. Herriott, Phys. Rev. Letters **6,** 106 (1961).
4. L. F. Johnson, G. D. Boyd, K. Nassau, and R. R. Soden, Proc. I.R.E. **50,** 213 (1962).
5. A. L. Schawlow and C. H. Townes, Phys. Rev. **112,** 1940 (1958).
6. D. E. Williamson, J. Opt. Soc. Am. **42,** 712 (1952).

Books

continued from p. 168

same time space astronomy is going forward—arises at about the same time that the future of large telescopes is being discussed for another reason: the increasing effect of atmospheric pollution and sky illumination upon some of the large observatories in the western United States, from which so many of the advances of modern astronomy have come. There is no serious plan, except in the U.S.S.R., for a still larger and more advanced telescope to extend the power of the 3 meter (120-in.) and 5 meter (200-in.) reflectors, or to replace them. The cost of such an instrument would be very large by conventional astronomical standards—about that of a large accelerator—and the continuing financial commitment would be in proportion because of the advanced technical support that the telescope would demand. But money might conceivably be found, if it were clear that such an installation would be a sound and highly desirable investment in the scientific sense.

Whether it is necessary to build a very large and very advanced U.S. telescope at the best possible site, and to back it up with the best instrumentation and personnel, is a question that deserves a considered and responsible answer. It would indeed be depressing if, in these days when there is much talk of national scientific policy and the national purpose, such a far-reaching issue were never faced squarely and decision came by default, with the great reflectors sinking quietly into a sea of mercury-illuminated smog crossed with contrails.

G. H. Herbig

The Physical Principles of Astronautics; Fundamentals of Dynamical Astronomy and Space Flight. By Arthur I. Berman. Wiley, New York, 1961. 350 pp. $9.25.

A most timely and highly acceptable book at the undergraduate and early graduate level; timely because there is no comparable text at its level and because of the explosive interest in this field, and highly acceptable because of its lucid and concise treatment of the basic principles of astronautics.

It serves to bridge the heretofore serious gap in the literature between popular and advanced writings in this field. The author has a happy capacity for coming directly to questions most troublesome to students and to those laymen who are not satisfied with merely talking about astronautics. The layout of the book is excellent for use both as a textbook and as a reference book. An excellent glossary of astronautical terms is especially useful in the latter respect. Particularly useful are the illustrative problems scattered throughout the text, plus the collected problems at the end of each chapter. The illustrative problems come to immediate grips with specific questions and are completely worked out with quantitative answers before another topic is introduced. The lead sentences of some of the illustrative problems are worth mentioning in this connection: "An ion-propulsion rocket leaves the Earth's orbit for Mars . . ."; "An object in a circular orbit attempts to reach the center of attraction by a double thrust maneuver . . ."; "Find the launching angle for maximum range . . ."; "What total escape speed is required from the Earth's surface to reach an infinite distance, taking into account the effect of solar gravitation, (a) if the Earth were stationary and (b) accounting for the Earth's orbital motion?" There are problems more elementary than indicated by these samples, and also some of greater complexity, but the clarity of treatment is maintained.

The book is divided into three fundamental but interlocking parts: principles of astronomy; foundations of mechanics; and dynamics of space flight. In the first part, the author treats the earth and moon as a dynamic system and gives a brief review

of the mechanics of the solar system and its place in the galaxy. Chapter 2, called "Physics of the Solar System," is misleading in title since physics of the solar system, as understood by the astronomer, would include a great many more topics than are here even briefly touched upon, e.g., energy generation, chemical composition, etc. This is perhaps the weakest section in the book, but understandably so since the book is not intended as a text in astronomy.

In the section on mechanics, in the remarkably short space of about 50 pages, the elements of celestial mechanics are developed in a well-rounded way, including such topics as accelerated reference frames and centrifugal and Coriolis forces, potential theory, and an instructive and usable treatment of the one-dimensional three-body problem.

In the section on dynamics of space flight, a vector treatment of orbital theory is given (there is a good basic introduction to vector calculus in an appendix) with attention to the general solution of the differential equation of motion and elliptic and hyperbolic trajectories. An instructive derivation of the universal law of gravitation from Kepler's laws adds to the general interest of this section. Transfer orbits and space navigation are treated next, and in the section on orbital perturbations the elements of classical perturbation theory are combined with the perturbative effects of solar radiation and atmospheric drag. Included in this space flight section is a clear discussion of propulsion dynamics.

Ten useful appendices (elements of vector calculus, polar coordinates, the gyroscope, the astronomical unit, summary of rocket propulsion methods, nomenclature, physical and astrophysical constants, units and conversions, glossary of astronautical terms, and bibliography) are included and constitute in themselves a very valuable reference compilation.

Naturally, in a book which attempts to survey the field, one cannot expect an exhaustive treatment of each of the many topics included. The book is definitely pitched at the undergraduate level but can, without prejudice, be used for beginning graduate students. In colleges which offer only an introductory course in astronomy, *Astronautics* could be used as a text for a second course in the department, aimed in the direction of celestial mechanics rather than astrophysics, and, indeed, the earlier portions of the book can be used as supplementary material in a solid introductory course in astronomy.

The book is remarkably free from typographical errors and the line diagrams are good and to the point. The book deserves wide adoption as a serious introductory text in astronautics and as valuable supplementary reading in engineering, physics, and astronomy, and, in addition, as general good reading in the field for serious laymen.

J. Allen Hynek

Applied Optics Patents

The Patents Panel is now forming under the chairmanship of Charles Shepard, patent attorney of Rochester and OSA member. Members of the Panel to date comprise D. L. MacAdam (colorimetry), R. Kingslake (lens design), D. Williamson (medical instrumentation and general optical design), A. Danti (chemical spectroscopy), J. Fitzmaurice (optical character recognition), G. W. Cleek (optical glass), R. K. McDonald (space optics), D. J. Lovell (general infrared instrumentation), G. W. Stroke (interferometry, gratings, opto-mechanical controls), and T. K. McCubbin (high resolution and far infrared spectroscopic instrumentation). Volunteers are urgently needed for other areas, if anything is to be made of this feature. Please let the Managing Editor know your field of interest when you write offering your services.

Meeting Reports

URSI Paris Symposium on Space Communication Research, September 18–22, 1961

Reported by V. Twersky, Sylvania E. D. L.

The Union Radio Scientifique Internationale symposium on the scientific aspects of space radio communication problems was held at the Ministère des Postes et Télecommunications, avenue de Ségur, Paris, during September 18–22, with participants from Australia, Canada, France, Germany, Japan, The Netherlands, New Zealand, Switzerland, United Kingdom, and the U.S.A. The symposium opened with brief welcoming talks by J. R. Pierce, *Bell Telephone*, H. C. van der Hulst, *Leiden*, and others, and with an introductory paper "The Scientific and Research Problems of Satellite Communication Systems" by H. Stanesby and F. J. Taylor, *United Kingdom*. Subsequent sessions covered launching, attitude control, and tracking problems; frequency and propagation problems; modulation systems in satellite communications; ground equipment; satellite equipments; satellite communication systems; and a final session on miscellaneous problems in space communications.

This report deals primarily with topics which may interest those working on scattering and long range propagation problems in optics, and touches on additional material to indicate more fully the scope of the program. The formal papers as well as the principal contributions to the discussions will be published in book form early this year under the editorship of G. M. Brown, *University College of Wales*.

Research aspects were stressed at the symposium. In addition, many papers dealt with technological features of component design; other papers emphasized economic factors; various individuals debated the merits of different modulation systems; and a small group kept reiterating that satellites would "sweep out" the Van Allen radiation belts before their function was understood, and might thereby harm life on Earth.

L. Jaffe's paper on the various satellites supported by the NASA Communications Program included descriptions of several systems based essentially on geometrical reflection of microwaves from large metalized spheres. He began with a review of communications satellite experiments to date: Project Score launched on December 18, 1959 (delayed repeater system which performed well for the 33 days of its battery life); Echo I launched August 12, 1960 (passive satellite which is still in orbit); Courier launched October 4, 1960 (complex delayed repeater which performed for 17 days). He touched on various forms of passive satellites and then reviewed results of the Echo I program. The Echo I started as a 100 ft* diameter sphere of 0.0005 inch thick Mylar plastic covered with several microns of vapor-deposited aluminum. During the first 16 days it was under positive internal pressure and performed essentially as a sphere. Since then, the shape has changed (because of punctures, solar pressure, etc.) so that its scattering characteristics are more or less those of a 70 ft wrinkled sphere. The Echo I (whose perigee ranges from 1530 to 940 km) provided the first significant data on atmospheric density at 1500 km altitude, it verified the predicted solar radiation forces, demonstrated the feasibility of passive satellite systems, and it confirmed the essential features of propagation theory and the theory for orbital behavior.

Two additional passive satellite systems are now being developed: *Echo II* uses a single 140 ft diameter sphere of a lami-

* The metric system of units is not used throughout this report, at Dr. Twersky's request.

B/A All-Dielectric INTERFERENCE FILTERS

Baird-Atomic announces the introduction of their radically improved Ultra-violet Filters and all-dielectric Visible Spectrum Interference Filters.

The new 'block shape' ⊓ passband in the Visible Spectrum Filters enables the user to obtain the greatest degree of spectral purity.

If the filter you require is not available in stock, normal delivery time is within thirty to thirty-five days.

Standard filter sizes are 1" x 1" and 2" x 2"; other sizes and shapes are available on special order. Write for your copy of our new filter brochure.

Engineers and scientists — investigate challenging opportunities with Baird-Atomic. Write Industrial Relations Department.

Visible Spectrum

- 4000Å - 8000Å
- New block shape ⊓ passband
- Absorption filters and/or evaporated blocking components provide for maximum blocking, reduced thickness, and improved signal-to-noise ratio
- Transmission outside of passband: under 0.1%
- Half bandwidths from 4.8Å to 1600Å
- Total transmission from fully blocked filter: up to 70%
- Blocking — complete on low side — high side blocking to at least 8000Å (Additional blocking at extra cost)

Ultraviolet Spectrum

- 2100Å to 3400Å and 3900Å to 3999Å

BA

BAIRD-ATOMIC, INC.

33 university road · cambridge 38, mass.

ADVANCED OPTICS AND ELECTRONICS . . . SERVING SCIENCE

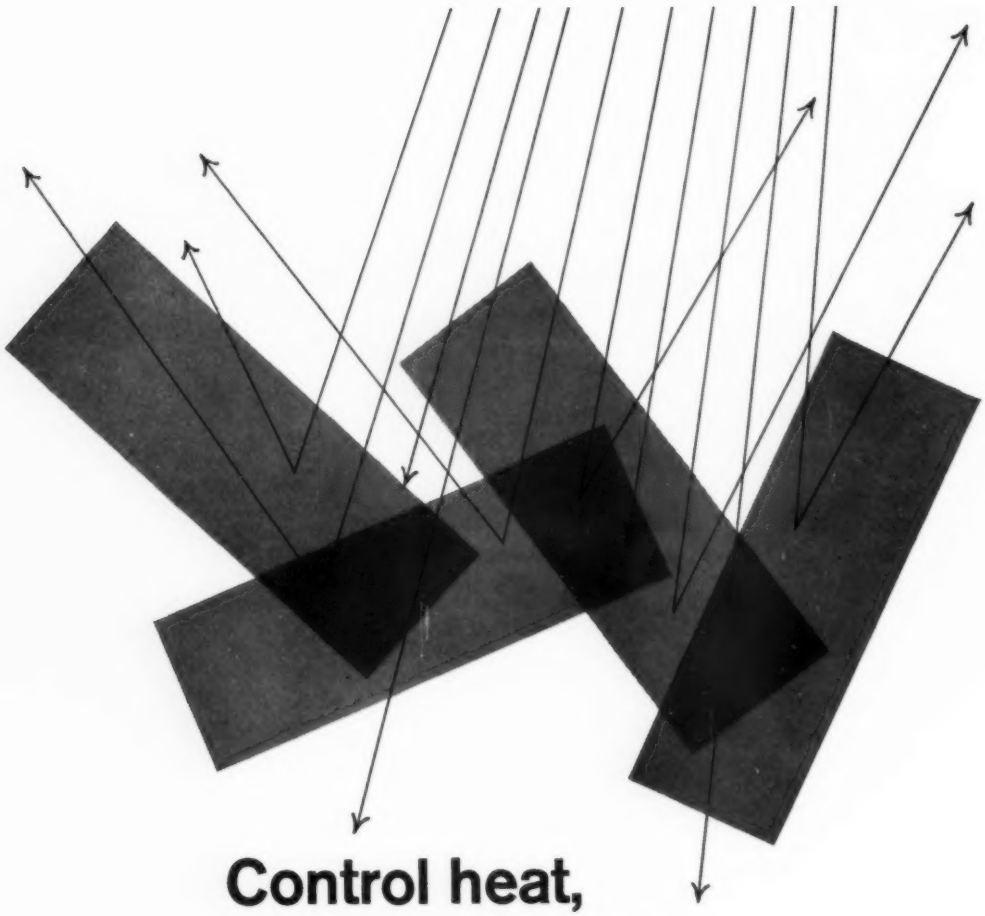

Control heat, light and color with Bausch & Lomb Multi-Films

In instrument design, a single B&L Multi-Film component—only 40 micro inches thin at the most—can replace a whole system of wavelength transmittance, reflectance and absorbance elements.

In space exploration B&L Multi-Films, by selective absorption and reflection, enable silicon solar cell power packs to achieve optimum efficiency.

And every day brings new applications, from high-efficiency reflectance to wavelength separation.

Find out more about this exciting new technique. Just mail the coupon. And if you'd like to know how Multi-Films can be put to work on your specific problem, just drop us a line.

BAUSCH & LOMB
SINCE 1853

Made in America, to the world's highest standards.

BAUSCH & LOMB INCORPORATED
77127 Bausch Street, Rochester 2, N. Y.

Please send me your new 32-page handbook on B&L Multi-Films, E-306.

NAME .....

TITLE .....

PROFESSIONAL ADDRESS .....

.....

At Optics Technology...

THE SCIENCE OF TOMORROW CAN BE YOUR CAREER

Challenging and rewarding positions are now available with Optics Technology in Belmont, California

Other excellent positions available with OTI:

Chief Instrument Engineer: 5-10 years' experience in development of complex instruments incorporating sophisticated optics, electronics and mechanical technologies. Capable of guiding a growing instrument development group.

Lens Designer: Minimum BS in Mathematics or Physics, 5-10 years' experience in geometrical optics and lens design. Excellent background in mathematics and computer programming. Knowledge of aberration theory and diffraction.

Production Manager: 7-10 years' manufacturing and product development experience in precision optical and electro-optical instruments and components.

Product Sales Manager: Minimum 3 years' experience in sales and marketing with optical or electro-optical instruments & devices. Minimum BS in Physics or Electronic Engineering.

Optics Technology is now located 20 minutes south of San Francisco. Outstanding research facilities are planned for the Fall of 1962 in new, modern laboratories.

Excellent academic atmosphere and living conditions plus cultural and climate advantages of Northern California. Generous stock participation. Professional and economic advancement commensurate with ability.

Write or phone: Dr. Narinder S. Kapany, Director of Research

OPTICS TECHNOLOGY, INC

248 Harbor Boulevard
Phone: LY 1-0358 (Area Code 415)
Belmont, California

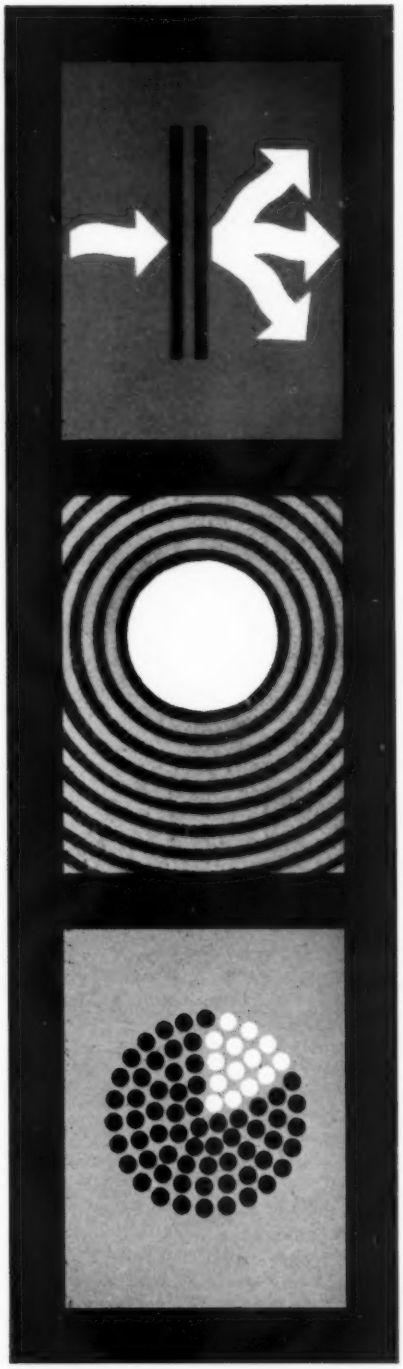

IMAGE INTENSIFIER RESEARCH AND DEVELOPMENT

Senior Scientists: PhD in Solid State Physics, Spectroscopy or Optics and 5-10 years' experience in the field. Proven record of scientific accomplishment.

Research Physicists: Minimum BS in Optics or Physics and 4-7 years' experience in Optics research & development. Capable of initiating and guiding independent research in this area.

LASER RESEARCH AND DEVELOPMENT

Senior Scientists: PhD in Solid State Physics, Spectroscopy or Optics and 5-10 years' experience in the field. Proven record of scientific accomplishment.

Research Physicists: Minimum BS in Optics or Physics and 4-7 years' experience in Optics research & development. Capable of initiating and guiding independent research in this area.

FIBER OPTICS RESEARCH AND INSTRUMENT DEVELOPMENT

Research Physicists: Minimum BS in Optics or Physics and 4-7 years' experience in Optics research & development. Capable of initiating and guiding independent research in this area.

Optical Engineers: Minimum BS in Physics and at least 5 years' experience in design and development of precision optical instruments and components.

7633

You can open new Research "Doors"

with American Optical's GLASS Maser*

Newest Advance In Maser Technology — Available Now

Under the direction of Dr. Elias Snitzer, this special glass was developed containing trivalent neodymium as the active ion. The glass optical maser material offers:

- **High intensity output at 1.06 microns.**
- **Substantially lower threshold pump power than ruby.**
- **Clad rods or fibers for concentrating pump power and improved mode selection.**
- **Variety of shapes and sizes of good optical quality.**

Production of glass laser rods has been started at our Keene, N. H. plant. Tested pre-production rods accompanied by a statement of measured characteristics are now available in limited quantity. For information write to American Optical Co., Keene, New Hampshire.

NEW POSITIONS
are now open for Solid State Physicists, Microwave Engineers, and Optical Physicists. Address Dr. S. M. MacNeille, Research Director.

** Patent Pending*

RESEARCH CENTER

American Optical

COMPANY

SOUTHBRIDGE, MASSACHUSETTS

nate of two layers of 1/4000-in. thick aluminum foil sandwiching a 1/3000-in. thick sheet of Mylar. This sphere, which is 20 times more resistant to buckling than Echo I, will be placed in a 800 mile altitude orbit early in 1962. *Project Rebound* will consist of three 140-ft spheres at a 1700 mile altitude orbit. It is expected that all three will be multiply-launched by a single rocket booster in late 1962. NASA is also studying a "wire mesh sphere," and a modified Echo II with much of the foil removed to minimize the effects of radiation pressure. They are also considering automatic attitude stabilization procedures to allow for the use of passive satellites having directional scattering characteristics.

Current plans for active communication satellites programs involve either 24-hr altitude stationary orbit systems at 19,300 nautical miles or low altitude systems of 5000 to 7000-mile altitudes. NASA is concerned with *Project Relay* (a government sponsored experimental satellite program contracted to RCA) and *Project TSX* (a joint NASA and ATT effort). Project Relay (to be placed in a 600 to 2500-mile orbit) will contain an active communication transponder, a solar cell life test, solid state component life tests, plus an environmental radiation measurement system. Project TSX will be similar to Project Relay except that different kinds of components will be used, different frequencies, and TXS will use a single transponder while Relay will use both transponders simultaneously for two-way transmission.

S. P. Brown discussed the ADVENT 24-hr military satellite program within the context of a commercial microwave communication system. The use of three equally spaced satellites over the equator at an altitude of 19,300 nautical miles will provide coverage for practically all of the inhabited Earth's surface. The satellites will serve as microwave radio relay stations which (because they revolve at the same angular velocity as the Earth) will appear to be stationary with respect to a point on the equator. It is expected that a prototype satellite will be launched in a low altitude orbit early this year. The final versions of the satellite will be launched in 1963.

W. R. Vincent's talk on the sharing of frequency channels by several satellite relays and several terrestrial systems dealt essentially with interference between several systems which overlap in "spectrum space." The paper (by W. R. Vincent and A. M. Peterson) gave families of curves which provided practical criteria for locating systems using the same microwave frequency ranges. Numerical examples were given to show that separations between 160 and 240 km will usually suffice to prevent interference between Earth terminals. (Ray Vincent of the Stanford Research Institute and Larry Hunter of the General Telephone and Electronics Research Laboratory also demonstrated a model of the joint GTE-SRI echo suppression system for satellite communication, during the course of the symposium; they used a tape recorder to insert a 0.4 second time delay in conversation between two telephones. When one of the two American telephones incorporated in the system disappeared, PTT furnished a French replacement; thus the equipment ended up with appropriate terminals for an international system.)

T. F. Rogers gave a good practical survey of propagation effects important to satellite communication, as well as to the more general problems of intercepting signals from high altitude sources by using ground based detectors. His charts, graphs, and bibliography should prove useful for many initial systems design considerations. Additional practical papers included I. M. Ross's discussion of the reliability of components used in communication satellite systems (traveling-wave tubes, transistors, diodes, polar cells, batteries, etc.), and D. G. Mazur's talk on environmental tests for such systems.

W. E. Morrow's excellent talk on communication by orbiting dipoles gave a summary of Project West Ford, a system for providing intercontinental communication developed at Lincoln Laboratory. This system has received much discussion in the newspapers (even the Russians came out against it in the Paris newspapers on the very morning of Morrow's talk), and its technical, political, metaphysical, and even theological aspects are now well known. Its essential features are two orbital belts (polar and equatorial) of metal "needles" 2 cm in length and 0.0025 cm in diameter which serve essentially as "half-wave" resonators for wavelengths near 4 cm. At the time of the meeting, it was planned to launch a test belt (as a side experiment for a programmed satellite launching) at a high-latitude inclination near-circular orbit at an altitude of several thousand kilometers. The dipoles were to be released from a rotating dispenser with velocities ranging from 0.8 to 3.0 meters/sec. The resulting cloud of dipoles was to spread along the orbit behind and ahead of the dispenser to yield a daily increase of 2000 km in length; after 30 days, the belt would close on itself to provide a "torroid" of dipoles.

Morrow's communication system was based on incoherent scattering by the needle-shaped objects. More generally, both coherent and incoherent effects may arise. In particular, for relatively high concentrations of scatterers the special torroidal geometry may focus the coherent scattered field to provide high field strengths at selected locations. (The coherent intensity on the caustic and its cusps would be greater by $(R/\lambda)^{1/3}$ and $(R/\lambda)^{1/2}$ respectively, where R is of the order of the earth's radius and λ is the wavelength.)

While I was in Paris, I called at the Institut d'Optique Théorique et Appliquée. André Maréchal spoke of the current work on the formation and structure of optical images, instrument quality, the perception of images, thin films, microscopy, photometry, spectrometry, colorimetry, interferometry, etceterametry. Excluding mathematical analysis of optical problems based on Maxwell's equations, the Institut has a comprehensive program in optics.*

Unfortunately, neither V. Siforov, the official USSR representative to the organizing committee, nor any of the invited Russian participants, appeared at the URSI Symposium. However, his country contributed to the technical background for the meeting in that the spectacular Soviet Exhibition was on in Paris at the same time. The exhibits included nose cones, models of nuclear fission power plants, automobiles (resembling USA 1958 models), fashions, foods, beautiful miniature abstract stage settings and puppets, and one could buy books, records, signed photographs of Gagarin and Titov, etc. There also was a specialty restaurant in operation, and their ballet performed nightly in a neighboring auditorium. Demonstration techniques were good, individual exhibits were tasteful, and the over-all impact (particularly on the nonscientific visitor) was quite strong.

Another outstanding attraction in Paris during the symposium, and one of optical interest (particularly colorimetry), was the Chagall exhibition of abstract stained glass windows. The twelve masterpieces (each taking one of the tribes of Israel as its theme) formed one wall of a detached building on the grounds of the Louvre.

* Professor Maréchal and his colleagues will be writing more about their work in the May issue—Ed.

James L. Jones *Applied Research Laboratories*, Gene Soltys *Soltys Associates*, and Clifford Thomas *Autotechnics* of the OSA-Los Angeles Fall Meeting 1961 Program Committee

photo R. S. Hawes

OSA Fall Meeting, Los Angeles, October 18–20, 1961

Reported by Roland C. Hawes, Applied Physics Corporation

The forty-sixth annual meeting of the Optical Society of America, held in the Biltmore Hotel in Los Angeles, California, on October 18 to 20, 1961, was remarkably successful for its large attendance of 772 persons, and for the variety and interest shown in the technical sessions. With 121 papers on the program, one of the sessions, on Thursday afternoon, had to be held in triplicate.

The host section was the Optical Society of Southern California, with Wilbur Kaye as its president. Credit for the success of the program goes to the program committee headed by Vern Hamilton, with special recognition due James Jones, the arrangements chairman, for an extremely smoothly-run operation. Willard Perkins, as field trip chairman, arranged trips to Mt. Palomar Observatory and to the Michelson Laboratory at the Naval Ordnance Test Station at China Lake, which were well attended, and a successful ladies' program, which included tours through Hollywood and to other California tourist attractions.

Each morning and afternoon session began with an invited review paper of about 40 minutes duration on some currently interesting topic. Immediately thereafter, the meeting split up into smaller groups for the contributed papers. Skillful arrangement of the program material by Vern Hamilton, S. Q. Duntley, James Jones, and Mary Warga resulted in few conflicts of interest between the simultaneous papers and in good continuity of interest.

In the first paper on "Astronomical Optics and Instrumentation in the Modern Observatory," A. E. Whitford, Director of Lick Observatory, Mt. Hamilton, California, described the observatory program of photographing the available sky with the J. G. Baker astrographic 51-cm refractor, on high-resolution plates. Positions are determined by reference to the most remote external galaxies. These, of course, regardless of proper motion, are so distant that in many 20-year intervals they will show no apparent motion. In fact, the precision with which positions may be established is limited principally by drift of emulsion material on the glass plates during processing. Positions can be reproduced to about 0.005 sec. The first duplicate set of plates after a 20-year interval is just now in preparation. Dr. Whitford also reported success with the use of the Lallemand photoelectric image tubes. They give improvements in real speed of about 25-fold and occasionally as much as 45 times. Such increases may make it unnecessary ever to construct larger telescopes than those presently available, for earth-bound astronomy, since in a comparatively short exposure time the limitation set by the radiant emission from the night sky can be reached.

D. R. Craig described an interesting photoelectric focus-indicating device, which was also on display in the LogEtronics booth. It depends for its success on the nonlinear response of a cadmium sulfide photoconductor. Two detectors of extended area are exposed in the desired focal plane. One is covered with a diffusing screen so that its response is proportional to the average energy. The uncovered one is exposed to any pattern it is desired to focus, and due to its nonlinearity has a lower output. The detectors are in a bridge circuit with a meter to indicate their difference. For sharp black and white patterns, the device has considerably higher sensitivity to small misadjustments of focus than the unaided eye.

R. Clark Jones of the Polaroid Corporation, using a somewhat idealized model of an optical communication channel, showed that it is possible, under favorable conditions, to transmit more than one "bit" of information per photon. The necessary conditions make it somewhat unlikely that this will ever be utilized in practice: the probability of transmitting a pulse must be a very small fraction. Results of greater practical utility were shown, however, for cases where the information is diluted by substantial amounts of ambient radiation. Although it may be argued that this is not primarily optics, and is also of doubtful applicability, the prospect of using lasers in communication channels seems sufficiently imminent and practical to warrant some emphasis on the limitations of what they can do for us.

Lasers represent one of the most exciting current developments in optics, and several working models were on display, including one setup which punched holes in aluminum foil with a focused beam. An interesting paper on the subject was presented by G. L. Clark, R. F. Wuerker, and C. M. York of Space Technology Laboratories. The STL image converter camera, which has a capacity to take 20 million frames per second, and can also be used in a streak camera mode, was used to study the time-resolved behavior of a ruby laser. Dr. Clark's photographs demonstrated the existence of spots of preferred emission which are obviously oriented in relation to the geometrical axes of the crystal. Each discharge, excited by the xenon pumping radiation and lasting in the order of a millisecond, has a fine structure consisting of many pulses of about a microsecond duration. The "sub-pulses" in turn vary in a characteristic manner, some of the preferred spots winking simultaneously, others appearing to have independently timed output. Streak photographs demonstrated that in some instances a series of illuminated dots moved by several times their diameter across the face of the crystal. No explanation was suggested for this behavior. It is interesting and possibly significant that the cycle time of these processes is of the order of magnitude of the reciprocal of the bandwidth of the emitted light.

In a remarkable series of papers, Lawrence Dunkelman and his co-workers at Goddard Space Flight Center, NASA and ASCOP Division, Electromechanical Research, Inc., showed that the wavelength range over which a quantum efficiency of 10% or more can be attained by detectors extends now from the visible and near ultraviolet through the vacuum ultraviolet to 1050 A. Furthermore, many of the new photomultiplier and photoionization detectors discriminate strongly against radiation of longer wavelengths and thus permit new orders of accuracy for photometry in the vacuum ultraviolet.

Shafer, Megil, and Droppleman of the NBS Boulder Laboratories again showed the power of modern computational techniques using large scale digital computers to optimize designs. In a study of monochromator variations, major improvements in imaging by introducing controlled degrees of dissymmetry were achieved for the Fastie-Ebert, as well as other arrangements.

In a short report, only a few of the most interesting topics can be touched upon. Furthermore, no one person may hope to take in all of the valuable things that are going on simultaneously at the three-ring circus which an Optical Society meeting has become. There is no substitute for attending a national meeting in person.

Stanton Cushner *Bissett Berman Corporation* and E. D. McAlister *Scripps* during the OSA - Los Angeles Fall Meeting

photo R. S. Hawes

Joint Fall Meeting of URSI and Certain Professional Groups of IRE, October 1961

Reported by Charles S. Williams, Texas Instruments, Inc.

The Fall Meeting of several Commissions of the International Scientific Radio Union was held jointly with certain professional groups of the IRE in Austin, Texas, on October 23, 24, 25, 1961. A Conference on Telluric and Geomagnetic Field Variations co-sponsored by the U.S.A. National Committee of URSI, the Office of Naval Research, and The University of Texas was held on October 20 and 21, 1961. Technical sessions of both were held in the Student Union Building of The University of Texas, with many of the 340 participants attending both.

The Geomagnetic Conference was primarily concerned with geomagnetic and telluric phenomena in the frequency range from 0.001 to 30 cps. One may generalize as follows, and also be guilty of being too brief. The papers discussed measuring and recording techniques and equipments, experimental results obtained, and data interpretation and analysis. Typical signals are 5×10^{-9} gauss for the magnetic field and 3×10^{-6} volts per foot for the electric field, peak to peak. The exact sources of the signal have not been determined, but seem to be associated with events on the sun.

This meeting of URSI was the first following a redefinition of its commissions. Three of the current 7 commissions (2, 3, and 4) were each defined by a particular region of the atmosphere, a region with which is associated a wavelength range of radio waves most effected by phenomena in the region. Commissions 3 and 4 were redivided into ionosphere and magnetosphere. The ionosphere, which in the main controls propagation of terrestrial radio waves, reaches into the region of maximum electron density and includes the regions below. It is the region where collisions are important and where local thermodynamic equilibrium may be said to exist. The magnetosphere starts in the region of maximum electron density and is the geocentric region beyond. It is the region where charged particles travel in long trajectories controlled by magnetic fields. Commission 2 is the troposphere. Commission 5 on radio astronomy did not participate in the fall meeting.

OSA members will be interested in the outcome of several investigations being conducted by Commissions 2, 3, and 4. For example, there seems to be some evidence that helium nuclei are present in the upper atmosphere. We shall be interested to learn, when other data are available, if additional evidence to support the presence of helium is obtained. Another interesting phenomenon, which is not yet satisfactorily explained, is the propagation of short wavelength radio waves around the surface of the earth to greater distances than accepted theories will explain. Opticists will be interested in the solution of problems like this concerning the transmission of an electromagnetic wave through an inhomogeneous and time varying medium. The radio engineers have the difficult challenge of explaining the atmospheric inhomogeneities and time variations from data obtained at only the transmitting and receiving points.

A joint session of all participating commissions consisted of reports on the September 1961 URSI Paris Symposium on Space Communications. The following are a few brief notes from the reports: The significance of practical uses, such as communication and weather observations, for satellites should be emphasized. This is in sharp conflict with the popular demand for us to be the "first to hit the moon." There definitely will be satellites used for communication purposes although the "form" of the satellite is not determined. In the near future, efforts will concentrate on the solutions of three main problems: station keeping—maintaining the satellite in a fixed position relative to the earth, altitude control, and modulation techniques for communication.

The level of the papers was good, and the sessions seemed to be well organized and well run. There were 21 papers given at the Conference on Telluric and Geomagnetic Field Variations and 69 at the URSI-IRE meeting. Most of the 90 papers originated in universities and their associated research laboratories coming from as far away as the University of Natal in South Africa and the University of Alaska. Stanford was well represented with some 9 papers. Government laboratories were also well represented, the NBS contributing some 13 papers. An international flavor is shown by the following by-lines: Nuffield Radio Astronomy Laboratories, Jodrell Bank, England; Ionosphären Institut, Breisach/Rhein, Germany; and Defence Research Telecommunications Establishment, Ottawa, Canada. A few industries were represented—the Lockheed Missile and Space Company in particular, which presented 5 papers.

Future Issues

Each issue will specially feature one area of applied optics in addition to the usual contributed papers, shop and technical notes, reports of Meetings, Letters to the Editor, book reviews, Meetings Calendar, and special columns. The feature subject of each issue will be the responsibility of one editor.

1962	May	**Foreign Optics**	David Z. Robinson
	July	**Optical Engineering**	Roderic M. Scott
	September	**Infrared**	John N. Howard
	November	**Information Theory**	F. Dow Smith
1963	January	**Astrometric Astronomy**	James G. Baker
	March	**Instrumentation**	W. L. Hyde
	May	**Interferometry**	R. A. Woodson
	July	**Spectroscopy**	Mary E. Warga
	September	**Lens Design and Computers**	Editor invited

Applied Optics Reporters

These reporters submit information from which are compiled in part the news columns of APPLIED OPTICS. They have a rather thankless and seldom properly recognized task, and the APPLIED OPTICS editors are very grateful to them.

L. H. Chasson, *San Francisco*
T. K. McCubbin, *Pennsylvania*
Stanley S. Ballard, *Florida*
E. Scott Barr, *South East*
J. L. Rood, *Rochester*
E. M. Wormser, *Connecticut*
R. A. Oetjen, *Ohio*
L. E. Bergstein, *New York City*
D. J. Lovell, *Michigan*
R. Kraushaar, *New Jersey*
Mary E. Warga, *D.C. and Baltimore*
R. K. McDonald, *North West*
M. Kent Wilson, *Boston*
David M. Gates, *Denver*
K. M. Baird, *Canada*
C. S. Williams, *Texas*
A. J. Cussen, *Los Angeles*
H. McAllister, *Hawaii*
A. Cox, *Chicago*
A. Walsh, *Australia*

Applied Optics — Of Optics and Opticists

This column is compiled partly from information sent by our Reporters in various centers of optics across the continent, but the Managing Editor welcomes news from any source

I keep six honest serving men
(They taught me all I knew);
Their names are What and Why and When
And How and Where and Who. *Rudyard Kipling*

Five electric quadrupole transitions in the near infrared vibration-rotational spectrum of molecular hydrogen were observed for the first time by **D. H. Rank** at the Pennsylvania State University in December. H_2, a symmetrical diatomic molecule, does not, to the electric dipole approximation, have an infrared absorption spectrum. The absorption lines, discovered with a White multiple pass cell and a high resolution echelle grating spectrometer using a lead sulfide cell, are remarkable in that they exhibit no appreciable pressure broadening even at a pressure of 12 atm. The quadrupole spectrum is many times as intense as has been calculated by James and Coolidge. The lines are so strong that, with extremely high spectral resolution, it is possible to detect as little as 30 meter atm of molecular hydrogen. Several of the strongest lines occur in regions of atmospheric transparency, and thus an investigation of atmospheric and possibly extraterrestrial hydrogen will be possible.

The **National Bureau of Standards** has developed and calibrated an ionization chamber for the determination of total betatron and synchrotron x-ray beam energies from 6 to 170 Mev. After calibration with an absolute device, such as a scintillation spectrometer or a calorimeter, the ionization chamber can be used to calibrate other monitors, or to measure beam energy directly. For further technical details, see "Determination of Total X-Ray Beam Energy with a Calibrated Ionization Chamber," by **J. S. Pruitt** and **S. R. Domen,** to appear as a *Natl. Bur. Standards (U.S.) Monograph*. . . .**William B. Olson** has been appointed to the NBS Infrared Spectroscopy Section of the Atomic Physics Division. He will investigate the vibration-rotation analysis of mono- and dideutero-methane and study molecular structure by means of high resolution infrared spectroscopy; he will develop high resolution instrumentation and techniques for the object of obtaining better spectral data and the establishment of standards in the infrared region of the spectra. . . .The dominant isotope of carbon—carbon 12—with the exact number 12 as its assigned atomic(nuclidic) mass, has been chosen by IUPAC as the **new reference species for the scale of atomic weights.** This action follows a similar adoption of carbon 12 as the basis for the scale of nuclidic masses by IUPAP, and provides chemists and physicists with a common scale for the first time in 30 years.

Gerhard Herzberg, Director of the Division of Pure Physics of the National Research Council of Canada, has been selected as the recipient of the 1962 Award of the Spectroscopy Society of Pittsburgh. The award is given annually for pioneering research in one of the branches of spectroscopy. Dr. Herzberg's field of interest is the study of molecular spectra in the vacuum ultraviolet region, and his talk on this subject will be given on March 7 at the 1962 Pittsburgh Conference on Analytical Chemistry and Applied Spectroscopy. . . .**Stanley S. Ballard,** OSA President-Elect, has been elected by the Council of the American Association for the Advancement of Science to its Committee on Council Affairs. . . .**Henry H. Blau** has transferred to the new west coast office of the A. D. Little Company in San Francisco.

Education Members of the OSA Rochester Section met last September with representatives of nearby schools and industries to discuss the need for people trained in optics and the educational programs serving these needs. There was general agreement that, while present day physics courses are being refined away from optics, resulting in fewer enlightened graduates, industrial and government programs in optics are expanding rapidly, creating a greater demand for optical physicists and optical engineers.* Considerable discussion led to no conclusions on the causes of this odd mismatch or, indeed, on its magnitude, and a set of questions was framed in the belief that the answers would establish the magnitude of the problem and point the way to its solution. The Rochester Section arranged a symposium during the OSA Los Angeles meeting with representatives of the OSA Corporation Members to discuss these questions and ways for obtaining answers. It was a lively day during which three attitudes were established as follows: (1) Research, development, and production relating to optics are in good shape in America. So why tinker with a running watch? (2) Industry and government need physicists who have specialized in optics. Physics departments should be encouraged to revitalize optics courses. (3) A new discipline, Optical Engineering, is at hand. Guidance and aid should be given to its creation and development. Subsequently a request went to the OSA Board of Directors that the Society implement a study of the manpower problem in optics as defined by these questions: What is the present and projected national need for men trained in optics? What are the detailed requirements in terms of character and extent of education, student motivation, etc.? What programs (and facilities) now exist for providing such education? Are existing programs adequate, or would they be adequate with a modification of present curricula? Are existing educational facilities limited by availability of qualified students, availability of qualified instructors, availability of financial support, or by demand for graduates with such training? Assuming that there is a demonstrable need for an expansion of education in optics, what would such an expansion require in terms of students (undergraduate and graduate), instructors, and facilities? The faculty of the Institute of Optics of the University of Rochester has contributed to the planning of these meetings and is vitally interested in the outcome of the proposed study, mainly because the Institute was recently made a department of the College of Engineering and, with a few exceptions, the Institute believes it plays a losing game with industry. While students cross the university–industry barrier, reciprocal support is less successful. This has led to a serious reduction in the

* At the request of Hal Stewart the word "opticists" is not used as a generic noun covering both these groups.

Institute's teaching facilities, in support for students, and now in the numbers of undergraduate students.

Summer School Course in Optics. . . .The Institute of Optics is planning a two week course in optics in early July. The course is designed to acquaint physicists and electrical and mechanical engineers with modern methods in optical design and the analysis of optical systems. The information in the course should have direct application to problems encountered in integrating optical systems into modern detection, guidance, and information handling systems. At intervals during the course specialists in the field will give lectures on their research. At other times, small groups of students will have the opportunity to perform optical computations on digital computers such as the IBM 7070 or the Royal McBee LGP 30. The number of groups which may be accommodated will limit the size of the enrollment. Further details may be obtained from the Institute of Optics, University of Rochester, River Campus Station, Rochester 20, N.Y.

A successful academic-industrial relationship has been worked out in Orlando, Fla., between **Rollins College** and the **Martin Company.** Under this program, scientists and engineers in the Martin plant may work at Rollins College towards the Master of Science degree in Physics or Engineering Physics. Some of the instructors are Rollins professors and some are Martin scientists. This is typical of arrangements that are now being made in many parts of the country and is a new and burgeoning aspect of graduate education in the sciences and engineering.

The Chemical Physics Laboratory of **The Dow Chemical Company,** Midland, Michigan, will move into a new building, presently under construction and scheduled to be ready for occupancy in the late spring, which will nearly double the space available to this research group, and provide improved conditions for undertaking research activity. The laboratory, under the direction of **Norman Wright,** is engaged in varied chemical researches in an effort to develop new products and to improve currently used processes. Optical techniques play an important role in these investigations. The methods used in the laboratory include emission spectroscopy; infrared, ultraviolet, and microwave absorption; Raman effect; mass spectrometry; color measurement; vapor phase chromatography; and nuclear magnetic resonance. At present the group numbers about 100, of whom approximately half are professionally skilled. The skills displayed represent an interdisciplinary effort, with chemists feeling as "at home" with electronic and spectrometric devices as with beakers and test tubes. The diversity of capability is evident in the varied activities of the group. In one part of the laboratory, **L. W. Herscher** undertakes the development of infrared spectroscopic equipment which can be installed to aid the various plants to automatically monitor or control processes. In another area, **T. M. Hess** undertakes research activity in emission spectroscopy. A library containing infrared spectrograms of over 15,000 compounds is maintained to aid spectroscopic identifications of unknowns. A collection of sort cards can also be used in conjunction with an IBM collator to aid species identifications. . . .**Infrared Industries Inc.** of Waltham, Mass., has acquired **Simpson Optical Manufacturing Company** of Chicago. The 35-year old precision optics firm will be operated as the Simpson Optical Company, a Division of Infrared Industries, Inc., with a continuance of its present management. Both Infrared Industries and Simpson Optical are contractors on the Sidewinder missile, MIDAS satellite, and other aerospace infrared programs. . . .News from Connecticut is that two of the major companies working in applied optics there are significantly expanding their facilities. . . .The Electro-Optical Division of **The Perkin-Elmer Corporation** is in the process of moving into a new modern 9900 square-meter facility located on Route 7 in Wilton, Connecticut, a short distance north of its main headquarters. This new building will house the Engineering and Advanced Research and Development Departments of the division. . . .**Barnes Engineering Company** has begun operations in a new plant to house the Engineering Division adjacent to its original building on Commerce Road in Stamford, Connecticut. This two-story facility will add 3400 square-meter of engineering office and laboratory space—almost doubling the Company's present 4000 square-meter facility. The building is equipped with extensive specialized facilities for design, development, and fabrication of infrared and optical-electronic instruments needed to meet military, space, and industrial requirements. An environmental test facility includes shock testing equipment, sine and random vibration testing, an environmental chamber for simulating temperatures and atmospheric pressures up to an altitude of 60,000 meters, and a test chamber for simulating the vacuum conditions of space. A 7.5 by 7.5-m roof platform has been installed and is capable of supporting tracking pedestals and optical equipment mounts so that outdoor tests with real space and atmospheric targets can be conducted. Other special facilities include a 5-m and a 53-m dark tunnel for optical alignment and testing, and a 6 by 12-m clean room for precision assembly of space instrumentation. The entire building has been designed to permit maximum flexibility in converting any area to either laboratory or office space and in providing precise temperature and humidity control in any of its areas. A germanium meniscus lens—2.54 cm in diameter, yet requiring spherical surfaces accurate to within a few thousandths of a millimeter—was recently installed in an artificial planet simulator, built by Barnes. This piece of equipment is designed to test the company's infrared horizon and guidance sensors, similar to those used in the Project Mercury spacecraft and the several TIROS weather satellites. This size diameter was necessary because a wide field of view is required of the sensors to be tested in this simulator. In its completed form, weighing little more than 22 kg, it is almost worth its weight in gold. And, of the nearly $4000 it cost to produce, almost 75 per cent represents the cost of the germanium blank itself; for most conventional lenses, time and labor require a much greater investment than the lens material. The lens was ground from a 44-kg blank of high-purity germanium, cast by Sylvania Electric Products, Inc. Although more difficult to work with than glass, this material was selected by Barnes for the artificial planet simulator because it is transparent to radiation in the far infrared region, because it has a high index of refraction which affords a high degree of image perfection, and because it has low optical dispersion. The expansion in building space and personnel of both Perkin Elmer and Barnes is mainly to meet the increased demands for development and fabrication of complex optical-infrared instruments for use in connection with the space program. . . .On the 25th anniversary of the founding of his company **Walter Baird,** the Chairman of Baird-Atomic, was presented with a facsimile model of his first spectrograph. . . .**Photomechanisms'** high speed streak camera was designed and built to record the pinch flash to Republic Aviation Corporation's plasma engine. A special mirror system is incorporated to permit the recording of single or compound images. The primary optical system records the pinch flash as a long modulated streak on a 25.4 cm length of 16 mm film moving at 127 meters/sec. A secondary optical system projects precise, synchronized time marks at 10 μsec/intervals, on the edge of the film from an electronic timing mark generator within the camera body. Thus, in a playback or under a microscope the discharge flash may be studied to determine its energy variation with time.

Missile accuracy USSR. . . .*Current Review of the Soviet Technical Press* distributed by the Department of Commerce reports

that the commander of the Soviet observation ships sent to the impact area of the rockets tested last year in the Pacific termed the accuracy of the rockets "really fantastic." Visual observations supported by the most delicate instruments testified to the fact that "all the rockets, after a flight of more than 12,000 km, landed exactly at the predesignated point."

An electromechanical shutter with submillisecond open time, designed to control the recording period of a medium quartz spectrograph, has been built at the **Naval Ordnance Laboratory.** The time involved is "about 15 μsec after the shutter is triggered." The NOL Rept. AD 260 765 on this—*A High-Speed Electromechanical Shutter*—is available from the OTS, Department of Commerce, Washington 25, D.C.

Readers' attention is drawn to. . . .*International Aerospace Abstracts*, a monthly IAS service, and to the annual *Index* which will be issued in book form early this year. Covering more than 10,000 documents selected for their scientific importance and research value, this index is designed to expedite the flow of information to scientists and engineers working in the space and missile program. . . .An 1150-page bibliography of abstracts of Air Force-supported basic research projects valued at $60,000,000 and accomplished during 1950–56. This unique collection of over 4000 basic research summaries is the result of a search of technical libraries, government repositories, and leading professional journals (domestic and foreign). This search rediscovered some 3000 technical and scientific reports and this *Air Force Scientific Bibliography*, Volume 1, makes them available to the scientific community for the first time. Volume 2, to appear later in the year, will cover 1957 and 1958. When volumes covering research up to 1960 have been published, further bibliographies will be accomplished by ASTIA. Current volumes may be obtained from the Government Printing Office for $6.75. . . .*Research Highlights of the National Bureau of Standards*, (annual report for fiscal 1961, NBS Miscellaneous Publ. 242, available from the Government Printing Office, $0.75, 204 pp.) reviews the Bureau's research activities in developing, maintaining, and extending standards of physical measurement, and in investigating the physical constants and basic properties of materials. It is directed to research and industrial management, as well as to engineers and scientists. Among the topics covered are the Bureau's program in plasma physics and laboratory astrophysics. Lack of precise measurement techniques in this field have been delaying progress in such areas as space exploration and astronomy, and ballistic missile defense systems. . . .The published lectures of the International Mathematical Summer Center's course on *Electromagnetic Surface Waves* (September 1961), which include introductions to the theories behind dielectric fibers and Wood's grating anomalies, may be ordered from Prof. G. Toraldo di Francia, Istituto di Fisica della Radiazione, Via Panciatichi 56, Florence, Italy. Principal authors are: H. Bremmer (Netherlands), F. J. Zucker (USA), M. A. Miller (USSR).

The following are some of the recent contracts and grants awarded by the **Air Force Office of Scientific Research**. Univ. of Oklahoma Research Institute, Chun C. Lin, *Theoretical Determination of Optical Excitation Cross Sections in Atomic Gases*, $11,293, and R. M. St. John, *Experimental Research on Optical Excitation Cross Sections in Atomic Collisions*, $20,780; Johns Hopkins Univ., J. Strong, *Far Infrared Spectroscopy*, $15,000; and Warner and Swasey Company Control Instrument Division, R. H. Tourin, *Infrared Temperature Distribution in Combustion Gases*, $42,000.

During 1962, American, Canadian and British scientists will cooperate in two experiments which, it is hoped, will shed more light on the mysteries of the ionosphere. Under NASA direction, two **Topside Sounder** satellites—one American and one Canadian—will be placed in orbit to examine the ionosphere from above. The Canadian satellite is being developed by the Defence Research Telecommunications Establishment, Ottawa, while the U.S. device is designed by the Airborne Instruments Laboratory. The British Central Radio Propagation Laboratory is providing scientific supervision and analysis of the material. The Radio Research Station at Slough, England in the United Kingdom regularly exchanges information with NASA and DRTE. Slough, with its new Minitrack interferometer unit, constitutes an invaluable link in the chain of fourteen NASA satellite tracking and telemetry stations throughout the world. The first British satellite, **Scout I** is to be launched from an American rocket this year.

Thorne Shipkey, of the Department of Ophthalmology of the University of Miami (Fla.) Medical School, is the senior editor of a new publication *Vision Research* and OSA President **David L. MacAdam** serves on its honorary editorial advisory board. This is a bimonthly international journal published by the Pergamon Press, the first number of which appeared in June 1961.

The theme of the 91st Los Angeles convention of the Society of Motion Picture and Television Engineers, April 29–May 4, will be *Advances in Color Motion Pictures and Color Television*.

Miscellania. . . .horse-loving opticists' attention is drawn to the four-year-old colt which raced in New England last season rejoicing in the name of *Optics*. . . .Readers who do not see the *New York Times* may like to know that it reports the addition of another letter to the permanent White House memorabilia collection. It comes from a Taiwan teacher and is addressed to President Kennedy "care of Mr. Nathan M. Pusey, President of Harvard University."

ANNUAL SUBSCRIPTIONS

Per volume of six issues per year

OSA members	$ 6.00
Other AIP societies' members	$ 8.00
Non-members and libraries	$10.00
Single copies	$ 2.00

Subscriptions should be addressed to APPLIED OPTICS Subscription Handling, American Institute of Physics, 335 East 45th Street, New York, New York.

ADVERTISING

Advertising Agent	ALFRED P. OPPENHEIM
Assistant	RUTH STEGER

Advertising inquiries, orders, plates, and correspondence should be addressed to the APPLIED OPTICS Advertising Office, 55 West 16th Street, New York 11, New York. CHELSEA 2-1311

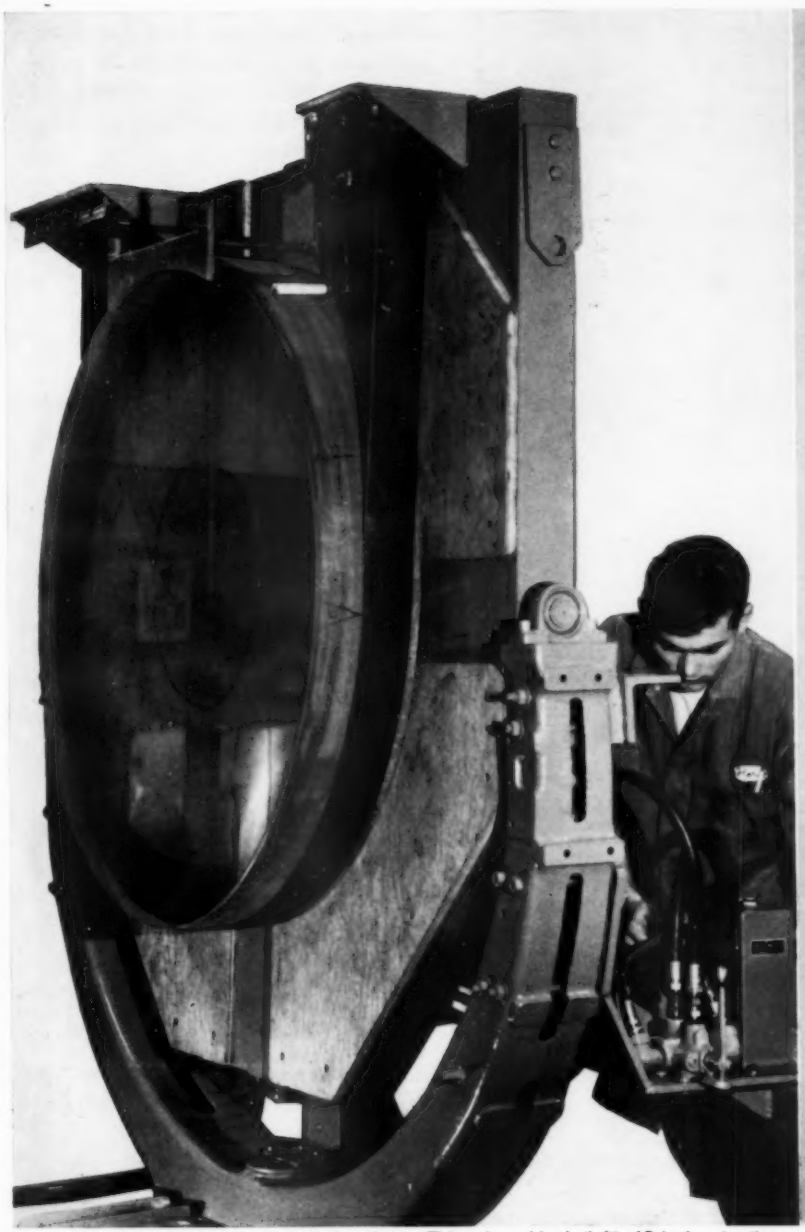

The 48-inch mirror blank and the tiny 4-sided pyramid are both within 1/10 wave length of perfection. They are examples of the extraordinary capabilities of Tinsley Laboratories, where unusual optical pieces, extremely precise, are in almost constant production. More conventional products, quite naturally, benefit from this sort of operation. A careful examination of any Tinsley telescope will lead you to the same conclusion.

This mirror blank (left), 48 inches in diameter, is being prepared for surface accuracy test. A nylon strap supports the 1500 pound piece free of strain during testing. Hydraulic controls allow the Tinsley-designed testing cradle to be tilted from horizontal to vertical. The Pyrex mirror blank will be coated with a vacuum-deposited layer of aluminum, with a protective layer of silicon monoxide. Tinsley is capable of coating surfaces up to 72 inches in diameter.

The four pyramidal faces and the base of this prism (right) are polished to 1/10 wave length flatness, and the relative perfection of the faces to that of a true pyramid is better than 4 seconds of angular accuracy. The polished base (not shown) is equally accurate in its relationship to the sides. The pyramid in function will rotate at approximately four thousand revolutions per minute about an axis perpendicular to the base and passing through the apex.

what they have in common is TINSLEY precision

For a folder describing Tinsley's optical capabilities, write TINSLEY LABORATORIES, INC., 2448 Sixth Street, Berkeley 10, California

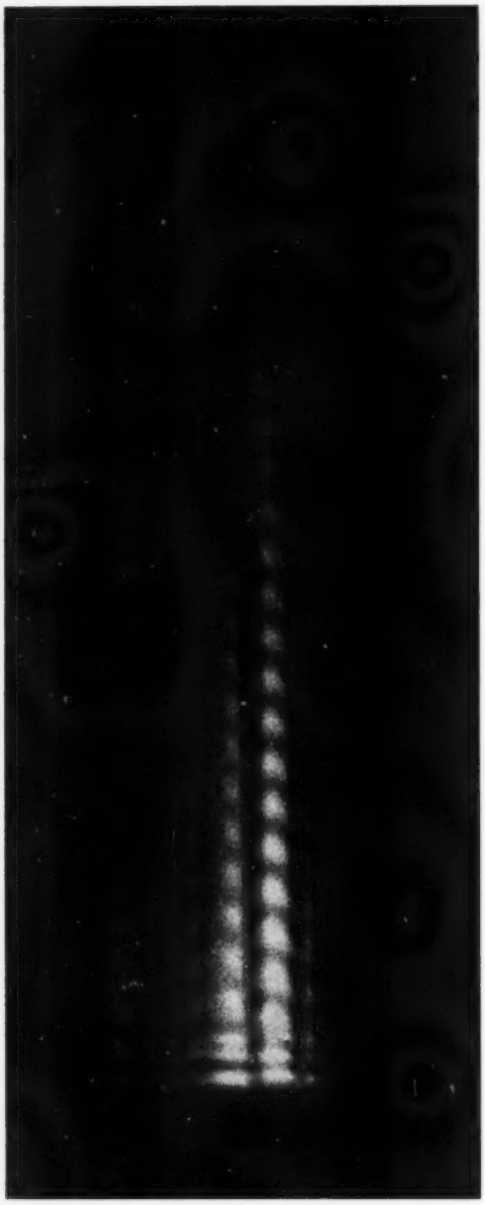

LASER PHENOMENON REVEALED BY STL IMAGE CONVERTER CAMERA

Self modulation of the output intensity of a ruby laser can be clearly seen in this 0.5 microsecond streak photograph of a single burst. Measurement of the spacing between the dark bands indicates that the emission is periodic at a frequency of approximately 40 Mc. This value corresponds with the estimated Q of the ruby when it is considered as a resonant cavity, thus suggesting a possible explanation of the self modulation phenomenon. To the best of our knowledge the STL image converter camera is the first to photographically record this phenomenon.

Because the time of occurrence of a single burst is not predictable, it was necessary that the burst being photographed trigger the camera. This was accomplished by coupling the STL Trigger Generator to the camera as shown in the diagram. This technique allowed photographing all but the first 30 nanoseconds of the burst.

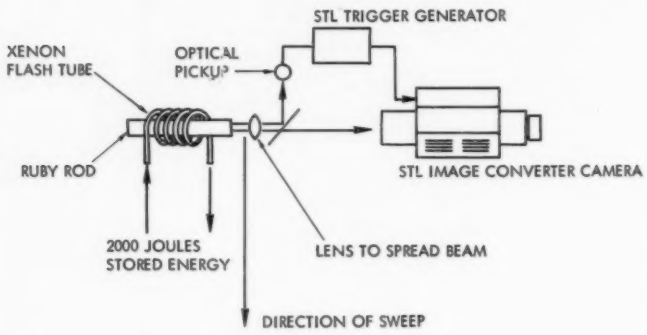

The results of a photographic study of a laser, utilizing both the framing and streak capability of the STL image converter camera, were presented at the 46th Annual Meeting of the American Optical Society. Copies of this paper are available on request.

The STL image converter camera provides scientists a highly flexible diagnostic tool wherever high speed luminous transients are being studied. The image converter tube, in conjunction with STL's new concepts for generating fast rising precision voltage pulses, provides the following specifications:

FRAMING OPERATION — exposure times from 5 to 200 nanoseconds. Independently adjustable exposure intervals from 50 nanoseconds to 10 microseconds.

STREAK OPERATION — writing times from 50 nanoseconds to 10 microseconds.

LIGHT GAIN — 50 X

PRICE — $20,000 F.O.B. Los Angeles.

A demonstration of the STL image converter camera at your facility may be arranged by writing David Fladlien at P.O. Box 45738, Westchester Station, Los Angeles 45, California.

STL PRODUCTS

A DIVISION OF SPACE TECHNOLOGY LABORATORIES, INC.

WEST COAST: P. O. BOX 45738F, WESTCHESTER STATION • LOS ANGELES 45, CALIFORNIA

EAST COAST: 515 HERRICKS ROAD, NEW HYDE PARK, NEW YORK

Space Technology Laboratories, Inc. is a subsidiary of Thompson Ramo Wooldridge Inc.

THOSE ATTENDING IRE INTERNATIONAL CONVENTION ARE INVITED TO VISIT STL BOOTH 1435.

FACTS FOR INFRAREDMEN ABOUT KODAK'S RUGGED POLYCRYSTALLINE OPTICS

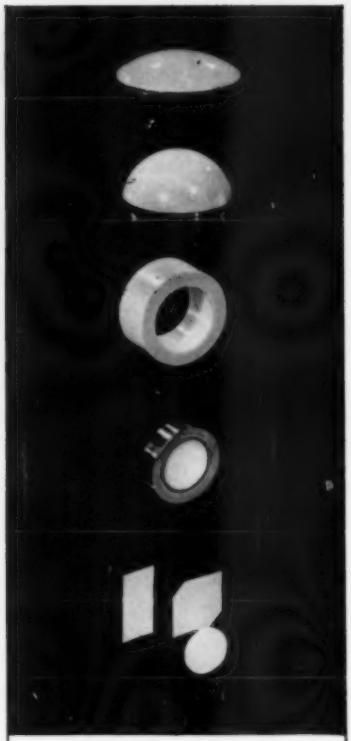

	IRTRAN-1	IRTRAN-2
RANGE:	2μ to 8μ.	1μ to 14μ.
REFRACTIVE INDEX:	1.37 to 1.31. Anti-reflection coating unnecessary and impossible. What would you use?	2.29 to 2.14. For lens power, deviation power, even a little dispersion power. Glad to coat.
MAXIMUM SIZE:	7-inch hemispheres. Other forms to 6½-inch diameter x 1 inch. Fusing extends possibilities.	6½-inch diameter x 1 inch. Stainless steel mounts can stand 600°C.
KNOOP HARDNESS:	576.	354.
ABRASION RESISTANCE:	Better than most conventional optical glasses.	Not quite as good as Irtran-1 but still better than many glasses.
THERMAL SHOCK RESISTANCE:	Survives quench from boiling water to 23°C. Good microwave characteristics.	Almost as good as Irtran-1. Resists more solvents than anything else we know for this transmittance band.

A big point of pride is the low emissivity. To achieve this relative immunity from blinding by high temperature, we have worked like galley slaves to get the absorption out. Lenses, domes, prisms, flats, filters. Some can even be shipped from stock. To get on the list of people we keep informed, write:

EASTMAN KODAK COMPANY
Apparatus and Optical Division
Rochester 4, N. Y.

Kodak
TRADE MARK

*Metallic plasma jet produced by a concentrated laser beam. (Trion Instruments, Inc., LS-2 System). Unretouched photo.

A LASER AT WORK*

laboratory curiosity?
no longer... now it is part of
a new technology!

As a qualified producer
of laser systems, components,
and accessories,
Trion Instruments, Inc., is
ready to assist you in
your laser research projects.

For detailed information write:

TRION INSTRUMENTS, INC.

1200 N. Main Street
In Ann Arbor, Michigan
"Research Center of the Midwest"

Booth No. 6
O.S.A. Instrument Exhibit

REFEREES

The following people referee papers submitted to ***APPLIED OPTICS*** *from time to time, and the Editors wish to acknowledge this service with gratitude:*

H. H. Allen, Jr., G. F. Aroyan, A. V. Baez, J. G. Baker, S. S. Ballard, R. Barakat, R. B. Barnes, E. Barr, E. S. Barr, A. M. Bass, J. R. Benford, L. E. Bergstein, B. H. Billings, L. S. Birks, F. F. Byrne, H. Cary, R. M. Chapman, L. H. Chasson, K. C. Clark, G. W. Cleek, V. J. Coates, R. J. Collins, W. A. Craven, Jr., A. Danti, J. A. Dobrowolski, K. Dressler, W. G. Driscoll, S. Q. Duntley, D. F. Eggers, Jr., R. S. Estey, W. Fastie, D. P. Feder, S. Fritz, A. G. Fox, J. S. Garing, N. Ginsburg, M. Parker Givens, G. E. Gross, F. F. Hall, Jr., L. W. Herscher, M. Herzberger, I. C. Hisatsune, R. E. Hopkins, G. A. Hornbeck, E. O. Hulburt, R. S. Hunter, W. L. Hyde, J. A. Hynek, S. S. Impiombato, R. C. Jones, K. Innes, J. A. Jamieson, L. D. Kaplan, S. Katz, J. W. Kemp, K. G. Kessler, J. I. F. King, R. Kingslake, W. F. Koehler, N. Kriedl, E. W. Kutzscher, T. Li, J. Lambe, E. V. Lowenstein, D. J. Lovell, T. K. McCubbin, R. K. McDonald, R. H. McFee, J. R. McNally, Jr., R. P. Madden, A. B. Meinel, P. E. Mengers, L. H. Meuser, P. Nolan, R. A. Oetjen, J. Parsons, F. H. Perrin, G. N. Plass, E. K. Plyler, H. D. Polster, R. Potter, R. W. Powell, D. Richardson, D. W. Robinson, D. Z. Robinson, N. Rosenberg, J. A. Sanderson, A. L. Schawlow, B. F. Scribner, J. H. Shaw, W. Sinton, F. S. Smith, V. J. Stakutis, O. N. Stavroudis, S. Sternberg, H. S. Stewart, B. Stoicheff, G. W. Stroke, R. E. Stroup, R. Tabeling, R. M. Talley, Y. Tanaka, R. Tousey, A. F. Turner, G. A. Vanasse, M. E. Warga, J. U. White, B. W. Wild, P. A. Wilks, Jr., V. Z. Williams, M. K. Wilson, W. Wolfe, E. M. Wormser, N. Wright, H. W. Yates, M. Zelikoff, and G. J. Zissis.

APPLIED OPTICS

Subscription Order

☐ 1 year, at OSA member rate of $6.00

☐ 1 year, at special rate, to other AIP Societies members, of $8.00

☐ 1 year, at non-member rate of $10.00

☐ Please send OSA membership information

Membership No.....

Name.....

Address.....

.....

.....

WITH ZOOMAR

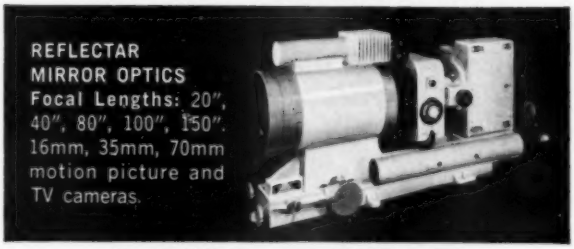

LONG RANGE

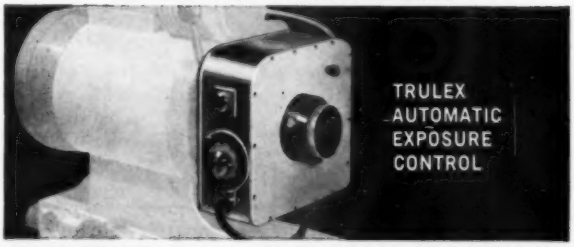

OPTICAL EQUIPMENT

Write or call for literature
Dept. AO 362.

ZOOMAR

ZOOMAR, INC.
GLEN COVE, L. I., N. Y. • HOLLYWOOD 28, CALIF.

OPTICS

Ph.D. or M.S. with demonstrated ability is needed for theoretical and experimental studies of optical components and systems.
(UV through IR Optics.)

Immediate application to space systems and tactical missile contracts.

Independent basic and/or applied research experience and capabilities highly desirable.

Positions are available in I.R. Systems and I.R. Information Processing.

Send resume to:
B. L. DIXON
Industrial Relations Administrator
Engineering - Department 110
General Dynamics Pomona
Pomona, California

GENERAL DYNAMICS POMONA

(Formerly Convair-Pomona)

"An Equal Opportunity Employer"

OSA Group Flight to Europe

AUGUST, 1962

OSA has arranged a group flight with SWISSAIR, for members attending the *Munich ICO Meeting on Image Formation and Vision*, August 20–25. Fare $353 round trip plus $7 organizing fee—$360.

The flight will leave New York (Idlewild) on Monday, 30th July at 6:40 p.m. for *Zurich* by a SWISSAIR DC8 jet, arriving there at 7:05 a.m. 31st July. We shall return from *Munich* Airport on August 27th, at a time to be announced later which will bring us back to Idlewild in the late afternoon of 27th August. Fifty seats have been tentatively reserved and we need your deposits ($50 per seat) **now**; the balance of the charge ($310) must be paid by 30th May.

Members who have already expressed interest have heard from OSA. Others are asked to send in their reservation and deposit at once. This flight is open to members and their immediate families.

* If a minimum of 25 members are interested, it will be possible for members to travel between Zurich and Munich at *no extra* cost. **But participants must travel as a group,** and it is not possible to obtain a rebate on that part of the flight coupon if it is not used. This flight would be on August 19th at about 4 p.m.

REPLY

Assistant Secretary
OPTICAL SOCIETY OF AMERICA
1155 Sixteenth Street, N.W.
Washington 6, D. C.

GROUP FLIGHT AUGUST, 1962

I wish to reserve ( ) seats on the OSA GROUP FLIGHT N. Y.-Zurich, July 30, 1962, returning Munich-N. Y. August 27, 1962

( ) I am a member of OSA ( ) I enclose a check for $_____

( ) I wish to travel as part of the group between Zurich and Munich on August 19th.*

( ) I shall be accompanied by ( ) my wife ( ) my children *state number*

Name_____Membership No._____

Address_____

_____

ELECTRODELESS DISCHARGE LAMPS

for calibration purposes and fundamental wavelength studies

For INTERFEROMETRY — the Hg 198 lamp

For SPECTROSCOPY — the noble gas lamp . . . or a metallic halide lamp

or

STATE YOUR SPECIFICATIONS

We Design Special Lamps and Cells and Fill Them To Your Needs

Resonance Cells for Optical Pumping

Resonant Cavities for 2450 mc RF Generators

OPHTHOS INSTRUMENT CO.

9600 Overlea Drive Rockville, Maryland

FUTURE MEETINGS

ROCHESTER, NEW YORK
October 3, 4, 5, 6, 1962

MANGER HOTEL
Details to be announced.

Information about later meetings will be announced shortly.

OPTICAL SOCIETY OF AMERICA
Executive Office
1155 16th Street N.W.
Washington 6, D.C.

THIN FILM (8μ) BEAM SPLITTERS

NO GHOSTS! NO REFRACTIVE ERRORS!

NOW!

- Flatness to 1/20 wave and parallelism to less than 1 fringe per inch; on order.
- Sizes up to 12" diameter
- Large coating selection, including dichroics.

FOR FURTHER INFORMATION ON NPC PELLICLES, SEND FOR BROCHURE AO

NATIONAL PHOTOCOLOR CORP.

225 EAST 44TH STREET NEW YORK 17, NEW YORK

Optics and Spectroscopy

OiS Club The Optical Society of America has been translating *Optika i Spektroskopiya* and distributing this monthly journal free—thanks to an NSF grant—to all OSA members and subscribers to the *Journal of the Optical Society of America*. This free distribution has been an experiment for three years, so that the individual reader might become accustomed to reading a translation journal not as an oddity but as a publication that is looked for each month in the same manner as is *J. Chem. Phys.*, *J. Am. Chem. Soc.*, etc. In December 1961 the NSF grant ended, but the interest in *Optics and Spectroscopy* is now too lively for OSA to discontinue the translation, so the OiS CLUB has been evolved, a group of some twenty-four Societies whose members may subscribe to *OiS* at a reduced rate, viz: *ASA, AAPT, ACS, ACA, AOCS, APS, ASTM, Electrochemical Soc., IRDG-UK, IRIS, Inst. Chemists-India, Inst. Physics and Physical Soc-UK, ISA, I-SCC, Netherlands Chemical Soc., SAS, SSP, Soc. for Chem. Ind. UK, Chem. Inst. Canada, SPSE, PES Group-UK, Soc. Anal. Chem.-UK, Can. Ass. Phys., Ass. Tech. Phys.—Sweden.*

OPTICS AND SPECTROSCOPY is the leading Russian journal in the field, its coverage corresponding in part to that of the *J. Opt. Soc. Am.*, although the spectroscopy papers are more theoretical than analytical or instrumental. Luminescence and optical properties of materials are fully represented, instrumental optics, diffraction and coherence problems less so.

OPTICS AND SPECTROSCOPY is published *monthly* in English translation 3 months after the Russian original e.g. the January 1962 issue will appear in March/April.

Send in your subscription for 1962 now

----------ORDER FORM----------

To: OPTICS AND SPECTROSCOPY
Optical Society of America
1155 Sixteenth St. N.W.
Washington 6, D.C.

Please enter my/our subscription to **OPTICS AND SPECTROSCOPY** 1962 issues (Vol. XII and XIII) and continue until countermanded.

☐ ***Special OSA member rate*** $ 7.50
☐ ***Special rate to members of Societies cooperating in OiS Club*** (see above) $11.00

Name of your Society.....
☐ ***Non-members rate*** $15.00
☐ Please send OSA membership information

Membership no.....

Name.....

Address.....

.....

FLASH TUBES

for **LASER** applications...
LARGEST VARIETY and RANGE of Sizes Available Today!

KEMLITE
LABORATORIES, INC.
1819 W. Grand Ave., Chicago 22, Ill.

SUPPLEMENT ON OPTICAL PUMPING AND MASERS

It is hoped to publish an *Applied Optics* **Supplement** in December 1962 on the subject of Optical Pumping and Masers. This special edition will gather together all the papers in that area of activity published in *Applied Optics* during the first year of publication and may possibly include articles not previously published. In addition, a 15,000 word review will be written by a leader in this fast-growing area of scientific knowledge, which will not only survey the present state of the art and give fundamental theories but will integrate all the papers published in the **Supplement.** This **Supplement** will be sold at not more than $5.00 a copy.

ORDER FORM

Please enter my/our order for the **APPLIED OPTICS FIRST SUPPLEMENT—OPTICAL MASERS,** to be published in December 1962 at a cost of not more than $5.00 a copy

Name.....

Address.....

.....

.....

MULTI-LAYER INTERFERENCE FILMS

High-efficiency type. Transmission and reflection over 90%. For dichroic and achromatic beam splitters, including:

XUR-96. Reflects substantial portion of infrared; transmits nearly all visible.
6143. Completely removes ultraviolet and reflects infrared; transmits nearly all visible.
IRT-211. Cold mirror. Reflects visible from 400–700 mμ; transmits from 725 mμ and longer.

For lasers and masers:
3132-N. Multi-layer high reflection coating; 98–99% reflectivity up to about 850 mμ.

•

SCHOTT OPTICAL RAW GLASS
by
JENAer Glaswerk Schott & Gen.
Mainz, West Germany

Available in about 300 varieties, including 160 standard glasses, 35 rare-earth types and 75 special types.

•

SCHOTT COLORED OPTICAL FILTER GLASS

Available in about 100 types for ultraviolet, visible and infrared spectral regions, including absorption filters containing neodymium for use in lasers and masers.

•

SCHOTT NARROW BAND INTERFERENCE FILTERS

300 to 2000 mμ. Transmission up to 60%. Half-width down to 5 mμ. Available as line filters, line double filters, band filters, band double filters, wedge filters, broad-band filters, spectral band filters.

Visit us at the OSA Instrument Exhibit

March 14–17 Booths 31 and 32
Mayflower Hotel, Washington, D.C.

FISH-SCHURMAN CORPORATION
90 Portman Road, New Rochelle, N.Y.

WHAT'S NEW!

Our Optical Bench Catalog! And why not: The optical bench business is booming. For the past several months demand has kept ahead of mounting production. It is temerity indeed to further spur things on with a new catalog. Yet we've done it, we're glad, and we hope you'll not waste a minute writing for your free copy.

In addition to our seasoned favorites, the sturdy triangular "Zeiss" form and the magnificent Beck Precision Research Bench, three new benches of intermediate price have been added.

First is the 22-950, a 2 meter lathe bed bench of heavy cast iron, flat over its length to about 0.003–0.005 inch and priced at $395. *That* is real value.

Next comes a similar 2 meter lathe bed bench of better quality cast in stress-free Meehanite, and guaranteed flat to 0.0025 inch. This bench is the 22-965 priced at $990. How does that smack you?

The third is a real bombshell. Our newest Research Lathe Bed Optical Bench, the 22-990, is a massive 8 ft. Meehanite stress-free casting, machined to a guaranteed accuracy of at least 0.001 inch over its entire length—and it is priced at just $3,400.

If the truth be known, this bench is a close relative of the 23-000 Beck Precision Research Bench, differing (apart from price) only in the absence of side slide carriers and a slightly lower guarantee of precision on flatness, the Beck 23-000 being guaranteed flat to 0.0005 inch and costing an appropriate $6,350.

Needless to say, over 50 accessories including Nodal Slides are available and interchangeable for all benches except for the two Research Benches which share their magnificent goodies compatibly.

Should these few modest lines start a stampede of unforseen dimension, we'll take our chances with phlegmatic poise. Foresightedly we have placed large orders with the manufacturers. If you are seriously considering one of these new benches, give me a ring. It's Frank Ferguson, Sales Manager, at the number listed below. Let's talk about it. In the meantime send for the new catalog.

THE **Ealing** CORPORATION

33 University Road,
Cambridge 38, Massachusetts

Telephone: 617 — KI 7-5760
Cable: Ealing

Engineers and Scientists

Make '62 a Year of Achievement

TECHNOLOGY AND SCIENCE, like the calendar, moves on...Did '61 see you, the engineer or scientist, move a step further toward your professional goals. If not...'62 is here...with new vistas beckoning, particularly in the interrelated world of space and electronics.

Grumman's steady advance in these areas has been sparked by the engineers and scientists who spearhead our company. Our design, development and study activities include vehicles and systems for programs ranging from submarine searching to space stations.

We cordially invite those engineers and scientists with kindred experience, who are determined to make '62 a year of achievement, to immediately explore positions in the following areas:

- **Digital Computer Systems**
- **Radar Systems Development**
- **Data Processing**
- **Electronic Displays**
- **Counter-measures**
- **Communication Systems**
- **Radome/Antenna Design**
- **Programming & Systems Analysis**
- **ASW Development**
- **Systems Engineering**
- **Reliability Control**

To arrange an immediate interview send your resume to Mr. W. Brown, Manager Engineering Employment Dept. GR-94 (U. S. citizenship required)

Grumman

GRUMMAN
AIRCRAFT ENGINEERING CORPORATION
Bethpage · Long Island · New York
An Equal Opportunity Employer

LASER OPTICS

Extend your capabilities for laser investigations by utilizing ISOMET's extensive crystal growing and precision crystal finishing facilities.

LASER CRYSTALS

Forms Available: Boules or fabricated rods with end polished optically flat and parallel.

Reflective Surfaces: Evaporated metallic coatings or multiple dielectric layers.

Types Stocked: CaF_2 doped with divalent samarium or trivalent uranium; ruby.

Types Custom Grown: Host crystals such as CaF_2, CdF_2, BaF_2, MgF_2. Activators such as the rare earths and transition elements.

OPTICAL COMPONENTS

Optically flat windows of quartz or various optical crystals.

Interferometer flats — Special reflective cavities

for prompt attention to your needs call Windsor 4-4100.

ISOMET CORPORATION

434 COMMERCIAL AVE., PALISADES PARK, N. J.

INSTRUMENTS FOR THE FAR ULTRAVIOLET

Model N-1	Ultraviolet Grating Monochromator
Model BNH-1	Hydrogen or Helium Discharge Lamp
Model P-2	D.C. High Voltage Power Supply
Model S-1	Transmission-Reflection Attachment

Special Instruments for Rocket and Satellite Spectroscopy

TROPEL, INC., 52 WEST AVE., FAIRPORT, N. Y.

CONSULTANTS AND DESIGNERS OF OPTICAL SYSTEMS
MANUFACTURERS OF PROTOTYPE LENSES AND INSTRUMENTS

MELLER RUBY LASERS

New Flatness and Parallelism! No Increase in Price!

With new manufacturing processes which produce Ruby Lasers in 32-unit lots, Meller can now guarantee flatness and parallelism to 2 millionths (1.25 sec. of arc) or better AT NO INCREASE IN PRICE. Two sizes are available with this guarantee — ¼" x 2" and ¼" x 3" with either 0° or 90° orientation. Surface finishes are superior, too.

Meller Ruby Lasers (all guaranteed to laser) are very slow grown and annealed . . . doped .04% chrome by weight . . . with orientation within 1°. Meller also offers ¼" x 1½", ¼" x 2½", and .200" x 2" sizes with flatness ¼ wave, parallelism 6 secs. of arc . . . with either 0° or 90° orientation.

ALL SIZES LAPPED . . . IN STOCK . . . READY TO SHIP!

Details and prices? Contact Adolf Meller Co., Box 6001, Providence, R. I. Phone 401 DExter 1-3717.

MELLER SAPPHIRE PRODUCTS

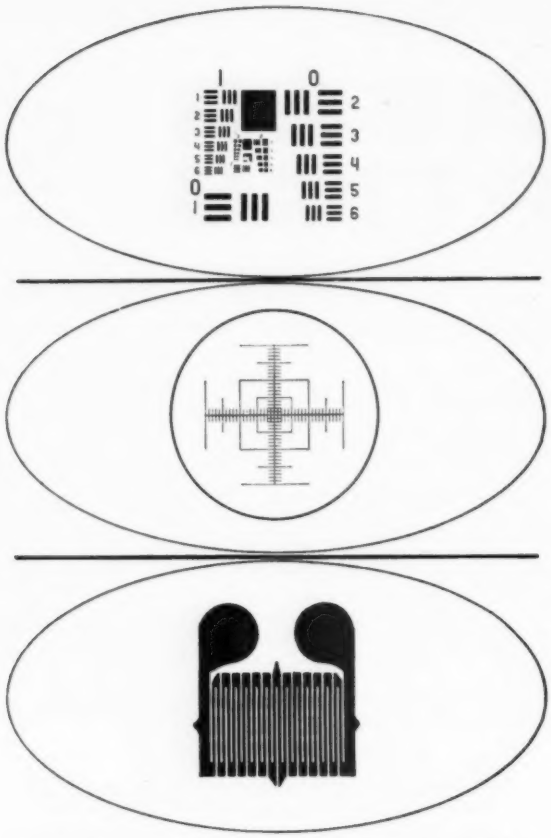

PRECISION TEST PATTERNS

for

- Photo-optical Evaluation
- Dynamic Simulation
- Electro-optical Evaluation

Resolving power targets are a simple and effective tool for the quantitative evaluation of photo-optical and electro-optical systems. Targets are available on film which cover the range from 1 to 228 lines/mm. The targets conform to the MIL STD 150-A configuration and can be supplied in negative or positive form at high, medium, or low contrast. Single or multiple arrays on special widths can be supplied on order. Single targets are available as stock items in 70 mm film widths. Also strips of targets on centers spaced 1½ inches apart on 35 mm film can be obtained.

MICRO-IMAGES

A custom capability is available for the design, drawing, and production of single or multiple micro-images on film, glass, or metal. Dimensions and position can be held to tolerances in the order of 0.0005 inch. Itek can supply precision masks for vacuum deposition, reticles, and other special micro-images to customer specifications.

For further information, please call our Photographic Technology Department, or write Department A-120.

Itek

Itek Laboratories

A Division of Itek Corporation

10 Maguire Road, Lexington 73, Massachusetts

This reticle, bearing a special resolution test pattern, was produced by the Optics & Metrology Division of K&E for precision photographic equipment.

The finest lines and the smallest spaces between the lines in this pattern are 20 microns (.020mm) wide. Photographically reduced from a master 50 times larger than the actual reticle, the finished test pattern was formed by vacuum deposition of chromium on glass.

Flawless lines, circular or straight, can be combined to form any pattern . . . placement of these lines can be held to accuracies approaching 1 micron . . . line widths can be controlled to accuracies approaching 2 microns.

This reticle shows the scope of K&E capability in optics and metrology. Similar ingenuity and skill can be brought to bear on any problem involving optical components.

Facilities brochure on request.

OPTICS AND METROLOGY DIVISION

K+E

KEUFFEL & ESSER CO.
Hoboken, N. J.

OPTICAL COMPONENTS: Prisms • Le nses • Mirrors • Coatings and Filters • Targets and Reticles • Graduations, angular and linear

ELECTRO-OPTICAL SYSTEMS: Angle Transducers • Auto Collimators • Photo-Electric Devices

OPTICAL SYSTEMS: Telescopes • Periscopes • Range-Finders • Collimators • Theodolites

Optical Tooling and Industrial Alignment Equipment
Radar and Missile Alignment Systems

2643

SCIENTIFIC INSTRUMENTS

HILGER & WATTS

FOR RESEARCH, PRODUCTION, ENGINEERING SINCE 1856

- Atomic Absorption Equipment
- Auto-Collimators
- Clinometers
- Crystals, Synthetic
- Diffractometers
- Digitizers (Optical, Mechanical)
- Etalons
- Goniometers
- Hollow Cathode Lamps and other Light Sources
- Interferometers
- Measuring Microscopes
- Microwave Components
- Microphotometers
- Microptic Levels
- Monochromators
- Optics (Prisms, Lenses, Flats, Polygons)
- Photoconductive Cells
- Polarimeters
- Refractometers
- Seismometers
- Spectrographs
- Spectrometers
- Theodolites
- Thermopiles
- X-ray Equipment

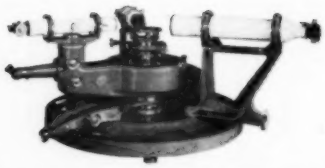

SPECTROMETER C-20 For research refractometry and highest class goniometric work. Refractive index measurement to sixth decimal can be obtained; micrometer scale divided at 0.1 second intervals.

MONOCHROMATOR D-290 Small, compact, low cost; utilizes a 15,000 lines/in. plane grating with special range of 2000A to 10,000A and dispersion of 70A/mm. Easily combines with other optical systems.

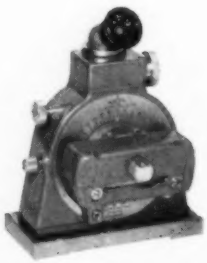

PRECISION CLINOMETER TB-95 Reads angles and circular spacing direct to 1 second; by estimation to 0.5 second—through 360°. Accessories permit use in horizontal position as rotary table or dividing head for light work.

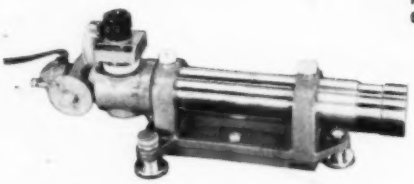

UNIVERSAL AUTO-COLLIMATOR TA-51 The master instrument for angle measurement. Reads in both planes simultaneously. Range 10 minutes of arc; direct reading to 0.1 second; straight or right angle viewing.

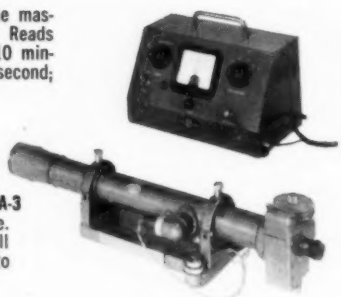

PHOTO-ELECTRIC AUTO-COLLIMATOR TA-3 Eliminates human factor — fatigue. Adjustable sensitivity and range; full visual optics. Setting accuracy to 0.05 second.

New

HILGER PRECISION OPTICAL BENCH Massive Meehanite casting holds heavy instruments with no flexing; supported at three points for precise levelling. Flat ways are hard chrome plated for long life; absolutely rust proof. Designed for convenient, universal mounting of accessories.

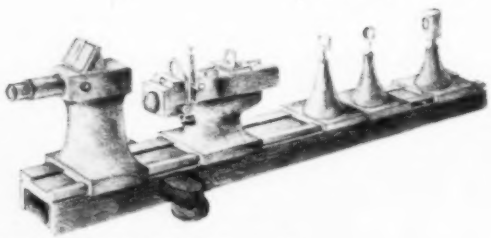

Write for complete descriptive literature of these and other Hilger & Watts instruments

HILGER & WATTS, INC.
431 SOUTH DEARBORN ST. CHICAGO 5, ILL.

Sales, Service, Parts by
ENGIS EQUIPMENT COMPANY
CHICAGO 5, ILL.